

# COORDINATIVE PEPTIDE RECOGNITION

## Making Intermolecular Processes Intramolecular

### Dissertation

Zur Erlangung des Doktorgrades der Naturwissenschaften  
(Dr. rer. nat.)  
der naturwissenschaftlichen Fakultät IV  
– Chemie und Pharmazie –  
der Universität Regensburg

vorgelegt von  
**Michael Kruppa**  
aus Erlangen

**2005**





# **Coordinative Peptide Recognition**

## **Making Intermolecular Processes Intramolecular**

### **Dissertation**

Zur Erlangung des Doktorgrades der Naturwissenschaften

(Dr. rer. nat.)

der naturwissenschaftlichen Fakultät IV

– Chemie und Pharmazie –

der Universität Regensburg



vorgelegt von  
**Michael Kruppa**  
aus Erlangen

**2005**

The experimental part of this work was carried out between October 2002 and April 2005 at the Institute for Organic Chemistry at the University of Regensburg, under the supervision of *Prof. Dr. B. König*.

The PhD thesis was submitted on: 31.05.2005

The colloquium took place on: 24.06.2005

Board of Examiners: Prof. Dr. R. Gschwind	(Chairman)
Prof. Dr. B. König	(1st Referee)
Prof. Dr. O. Reiser	(2nd Referee)
Prof. Dr. A. Pfitzner	(Examiner)



**Für meine geliebten Eltern**

## Acknowledgements

I would like to express my sincere gratitude to Prof. Dr. B. König, for his continued guidance, advice and encouragement throughout this work.

Thanks are extended to the analytical departments of the University of Regensburg for the prompt and accurate measurement of my numerous, often difficult samples. Special thanks to Dr. T. Burgemeister, Mr. F. Kastner, Ms. N. Pustet, Ms. A. Schramm and Ms. G. Stühler (NMR), Dr. K. K. Mayer, Mr. J. Kiermaier and Mr. W. Söllner (MS), Mr. G. Wandinger, Ms. S. Stempfhuber and Mr. H. Schüller (elemental analysis), Dr. M. Zabel (X-ray crystallography) and Dr. R. Vasold (HPLC).

My special thanks go to:

All colleagues, past and present at the University of Regensburg, for making the working environment positive, constructive, as well as relaxed.

Daniel Vomasta, Andreas Grauer and Nicole Holub for their efforts during their research period in my laboratory.

Daniel Frank for his work during his Zulassungsarbeit.

Mrs. Helga Leffler-Schuster for the potentiometric titrations and here marvellous reports about foreign countries.

Dr. Thomas Walenzyk, Daniel Vomasta, Eva Engel, Michael Egger and Stefan Ritter for their corrections of this work.

Dr. Maria Teresa Hechavarria Fonseca and Thomas Suhs for the fabulous time in laboratory.

My very special thanks go to:

Stefan Ritter for the wonderful time in China, the very delicious dinners and his infectious laughter.

Eva Engel for all the tasty cakes and sweets. Thanks also for the time at Tai-Bo lessons and all the climbing trips to Schönhofen.

Stefan Miltschitzky for his fabulous cooking and the perfect time in Italy. Thank you for your tireless microcalorimetical titrations.

Giovanni Imperato for making live better since he appeared in our working group. Thanks Gio for all your Italian dishes and showing me how to climb up mountains. Thank you also for one unforgettable week in my life staying in Italy.

Dr. Christian Mandl and Dr. Christoph Bonauer for cooperation in two great projects and all the great ideas. Thank you also for all the private discussions until the early mornings. I am not able to say how much they influenced my life.

Dr. Thomas Walenzyk for showing up in my life. Thanks Thomas for all the evenings, discussions, and support in any situations of my life.

Christian Geiger for three wonderful years in our apartment.

Doris Huber for showing me that there is still a lot more in life than chemistry and working. Thanks for your patience and your love.

My parents for all their support and love.

# Content

	Page
<b>A. Introduction</b>	<b>1</b>
1. Iminodiacetato (IDA) Complexes	4
2. Nitrilotriacetato (NTA) Complexes	36
3. Bis-(2-pyridylmethyl)-amine (BPA) Complexes	61
4. Tris-(2-pyridylmethyl)-amine (TPA) Complexes	87
<b>B. Main Part</b>	<b>117</b>
1. Investigation of Metal Complex – Amino Acid Side Chain Interactions by Potentiometric Titration	117
1.1 Introduction	118
1.2 Results and Discussion	120
1.3 Conclusion	129
1.4 Experimental Section	131
2. Molecular Recognition using Modular Receptor Synthesis	137
2.1 Terminal Receptor Building Blocks	139
2.1.1 N-terminal Receptor Building Blocks	139
2.1.2 C-terminal Receptor Building Blocks	143
2.1.3 Terminal Recognition Units with two Chelating Sites	148
2.1.4 SPRS (Solid Phase Receptor Synthesis)	152
2.2 Receptors as Side Chains of Amino Acids	156
2.2.1 Tyrosine based Receptor	156
2.2.2 Phenylalanine based Receptors	157
2.3 Conclusion	160
2.4 Experimental Section	163
3. Enhanced Peptide $\beta$ -Sheet Affinity by Metal to Ligand Coordination	202
3.1 Introduction	203
3.2 Results and Discussion	204
3.3 Conclusion	208
3.4 Experimental Section	211

4. A Luminescent Receptor with Imidazole and Ammonium Ion Affinity for Peptide Binding in Aqueous Solution	224
4.1 Introduction	225
4.2 Results and Discussion	225
4.3 Conclusion	231
4.4 Experimental Section	234
5. Receptor for Protein Surfaces with Affinity to Histidine and phosphorylated Amino Acids	242
5.1 Experimental Section	244
<b>C. Appendix</b>	<b>247</b>



## A. Introduction\*

Metal complexes with open coordination sites have found wide use in molecular recognition. They serve as binding sites in the development of chemosensors,<sup>1</sup> to study metalloenzyme function in bioinorganic chemistry<sup>2</sup> or direct supramolecular self-assembly.<sup>3</sup> Lewis-acidic metal complexes can target a large variety of Lewis-basic functional groups, which makes them very suitable for the design of synthetic receptors. Coordination to metal ions occurs typically with large enthalpies compared to hydrogen bond formation, salt-bridges or dipole-dipole interactions. This gives the opportunity to study molecular recognition and self-assembly in solvents competing for binding, such as water, using coordinatively unsaturated metal complexes as binding sites. A single coordinative bond from a guest to a metal-complex host may provide sufficient binding energy to result in stable and defined aggregates at micromolar concentrations in water. Typically, to achieve tight binding in such environment using weaker intermolecular interactions, multiple interactions and large receptor structures are necessary to exclude competing solvents.<sup>4</sup> However, not all coordinatively unsaturated metal complexes are suitable binding sites for molecular recognition of guest molecules. The coordinative bond between metal complex and bound guest should be strong, but not too tight. Binding affinity and binding kinetics, the on- and off-rates of the ligand, should still allow reversibility to keep the important features of molecular recognition, such as self-assembly to the thermodynamically most favored structure, dynamic of supramolecular aggregates and displacement of a bound guest by a better ligand. Metal complexes, which bind ligands at their open coordination sites with milli- to micromolar affinity and rates in the millisecond time range or faster are most suitable for self-assembly and molecular recognition processes at the laboratory time scale.

The complementarity of shape and binding sites usually determines the binding selectivity of host molecules using hydrogen bonds or electrostatic interactions. This applies equally to the small number of oligonuclear metal complex receptors reported until now. However, even a single reversible bond between metal complex and ligand shows intrinsic selectivity towards the nature of the ligand exceeding its simple Lewis-basicity. The Lewis-basicity of a ligand correlates to the hydrogen bond donor or acceptor ability in hydrogen bond

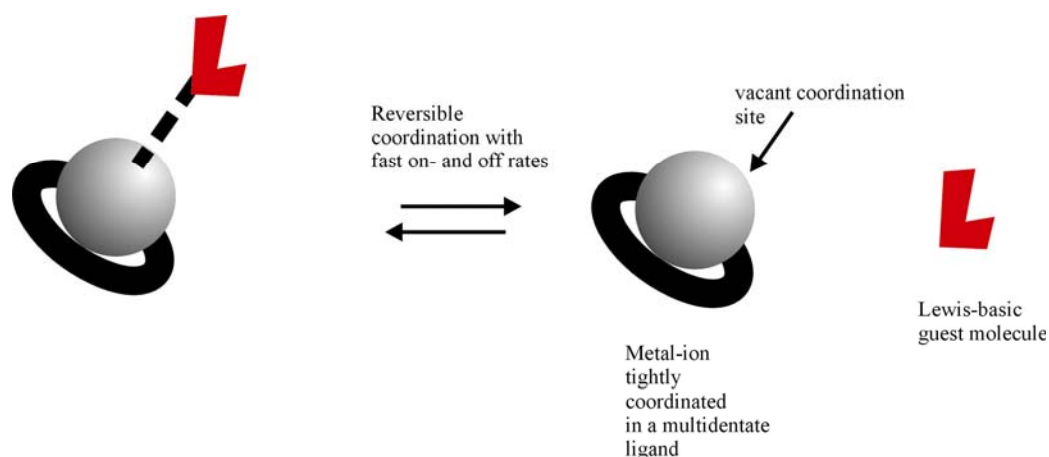
---

\* This introduction is part of a published review: Kruppa, M.; Walenzyk, T.; König, B. *Chem. Rev.* **2005**, *under revision*.

receptor binding. The strength of the coordinative bond depends additionally on the nature of the metal ion and the Lewis basic ligand atom as predicted by the HSAB principle. Such selectivity is well documented in metal ion complexation, e.g. by the preferential binding of imidodiacetato transition metal complexes to imidazole or pyridine nitrogen atoms. The selectivity is useful for receptor design in molecular recognition.

An obvious prerequisite for a metal complex to serve as binding site is its stability. The metal ion should be coordinated thermodynamically and kinetically tight. A reversibly bound Lewis-basic guest should not displace the original ligand from the metal ion. This calls for multidentate and/or macrocyclic primary ligands for metal ion binding, and indeed all reported examples of reversible coordination of a guest to a metal ion-binding site in molecular recognition use such ligands.

**Scheme 1.** Principle of a coordinatively unsaturated metal complex as binding site for the reversible coordination of a Lewis-basic guest molecule



## Scope and Limitations

This introduction will summarise the use of reversible coordination to metal complexes in molecular recognition. To be included, the stable metal complex of a primary ligand and a transition metal ion must possess unoccupied coordination sites and bind reversibly to a complex Lewis-basic guest. The primary ligands at the unsaturated metal complex used as binding sites define the scope of this survey. Figure 1 gives the general ligand types that are discussed. For each ligand type the discussion is about

- the typical stability constants of their transition metal complexes,
- solid state structures from the Cambridge structural data base, in which the primary ligand-metal complex coordinates an additional complex ligand,
- reversible guest binding of the metal complex in homogeneous solution, and



- binding processes of metal complexes immobilised on solid supports, such as polymers or gold.

The discussion excludes the solid-state structures and reversible coordination in solution the binding of simple inorganic ligands, such a halides or sulfate ions. The purpose of this introduction is to provide material supporting the design of functionalised metal complexes as synthetic receptors for complex guests, such as peptides, amino acids, heterocycles or nucleobases. The range of functional groups covered, which interact with metal complexes, is therefore limited to relevant ones for this purpose, such as carboxylate, phosphate, aromatic amines, diamines, imines or thiols.

In addition, complexes with bipyridines or terpyridines as primary ligand are excluded from this introduction, because the few examples in which such complexes are solely used as metallo-binding sites are difficult to distinguish from the vast majority of applications of this complexes in photochemistry and photophysics. The key references for the use of bipyridine and terpyridine complexes as binding sites in molecular recognition by *Anslyn*<sup>5</sup>,<sup>6</sup> and others<sup>7</sup> are given.

Porphyrin metal complexes as host binding sites are not covered in this introduction. *Hamilton*<sup>8</sup> very successfully used them for protein surface binding. *Kral and Schmidtchen*<sup>9</sup> reported sugar binding by porphyrin sandwich complexes. In these examples, the large hydrophobic porphyrin surface is significant for the binding process in water. The formation of a reversible coordinative bond to the central metal ion of the porphyrin ligand is ineffectual for the process. Functionalised porphyrin hosts were widely used for guest binding. *Sanders* reported macrocyclic zinc(II) porphyrins and their use as synthetic enzymes directing and catalyzing Diels Alder reactions.<sup>10</sup> Neutral zinc(II) porphyrin reversibly coordinates pyridine derivatives as additional ligand in dichloromethane solution. Synthetic porphyrin-based receptors for amino acids<sup>11</sup> or nucleobases<sup>12</sup> are known, but their binding ability is usually restricted to non-competing solvents, such as dichloromethane or chloroform. Neutral porphyrin complexes of divalent metal ions, such as zinc(II), show only little Lewis-acidity and therefore weak coordination ability of additional ligands. Studies using trivalent porphyrin metal complexes as defined hosts reversibly coordinating guest molecules are limited.<sup>13</sup> The use of porphyrin complexes in composite materials or self-assembled aggregates in material science is well documented,<sup>14</sup> but outside the scope of this introduction.

Overall, this introduction<sup>†</sup> provides a survey of reversible coordination to unsaturated metal complexes used in molecular recognition limited to the most important ligand classes used so far. The selection of the ligands is defined by the ability of their corresponding transition metal complexes to reversibly and tightly bind Lewis-basic guest molecules in competing solvents, such as water. This renders the selected complexes suitable as potential metal binding sites for synthetic receptors applicable in chemical biology or biotechnology, where their use would be most advantageous.

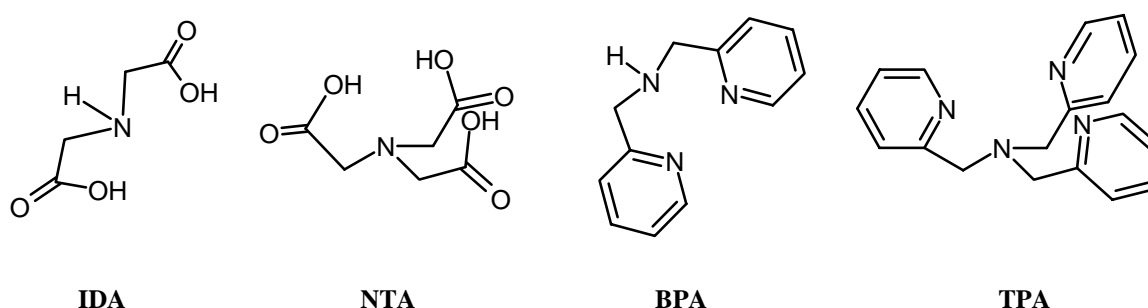


**Figure 1.** Acyclic general ligand types of transition metal binding sites for molecular recognition covered in this introduction.

## 1. Iminodiacetato (IDA) Complexes

Heintz first reported the iminodiacetato ligand (IDA)<sup>15</sup> in 1862. Since then it has been widely used as a chelating ligand for various metal ions, e.g. Cu(II), Ni(II), Zn(II), Co(III), Fe(III), Al(III) and Cr(III).<sup>16,17,18,19,20,21</sup> Table 1 summarises the metal ion binding constants of some typical complexes. Complexes with ligand to transition metal ion stoichiometries of 1:1 and 2:1 are typical. Metal ion binding constants, thermodynamic and kinetic stability are usually very high. Depending on the coordination number of the transition metal ion, complexation with the tridentate IDA ligand leaves coordination sites open for reversible ligand binding. Therefore, unsaturated IDA complexes qualify perfectly as binding sites for molecular recognition of Lewis-basic guests.

---

<sup>†</sup> The chapter about azamacrocycles (contained in the published review) can be found in the dissertation of Dr. T. Walenzyk

**Table 1.** Overview of binding constants of different metal ions to IDA<sup>22</sup>

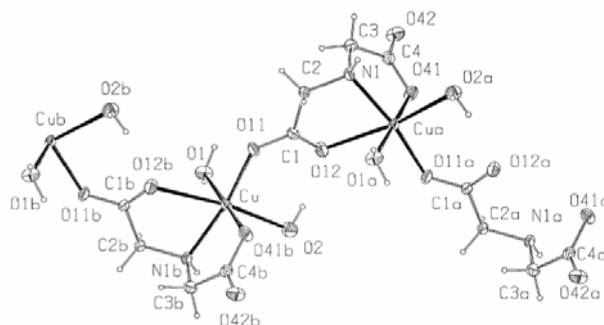
Ion	Equilibrium	log K
Cr <sup>3+</sup>	ML/M.L	10.9
	ML <sub>2</sub> /M.L <sup>2</sup>	21.4
Co <sup>2+</sup>	ML/M.L	6.54
	ML <sub>2</sub> /M.L <sup>2</sup>	11.95
Ni <sup>2+</sup>	ML/M.L	8.3
	ML <sub>2</sub> /M.L <sup>2</sup>	14.5
Cu <sup>2+</sup>	ML/M.L	10.56
	ML <sub>2</sub> /M.L <sup>2</sup>	16.4
Fe <sup>3+</sup>	ML/M.L	10.72
	ML <sub>2</sub> /ML.L	9.42
Zn <sup>2+</sup>	ML/M.L	7.15
	ML <sub>2</sub> /M.L <sup>2</sup>	12.4

## 1.1 Structures of IDA Complexes in Solid State

In the following, we will discuss the solid-state structure of some typical IDA complexes, which have coordinated additional Lewis-basic guests.

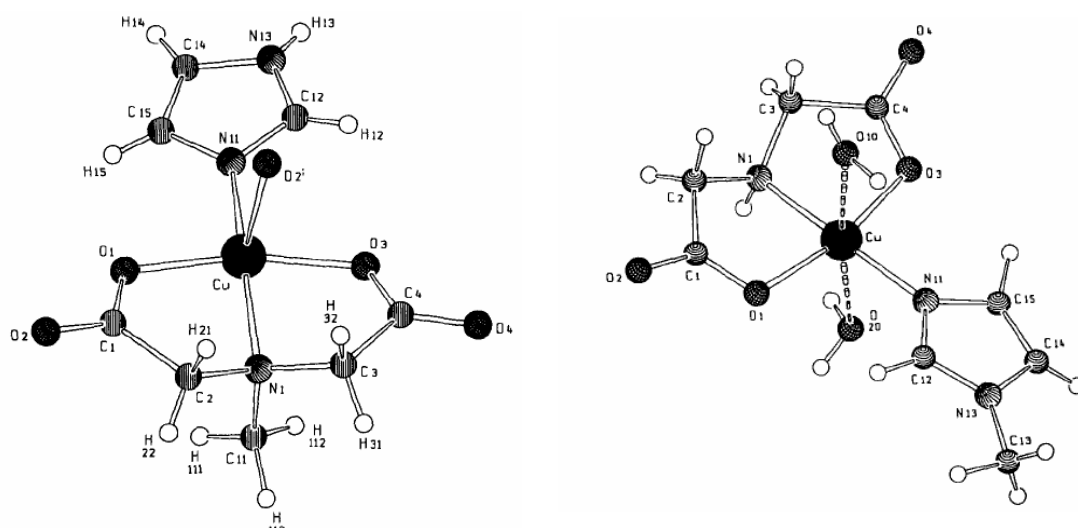
### 1.1.1 Cu(II) Complexes

A large number of Cu(II)-IDA complexes have been reported and structurally characterised. Cu(II) complexes of IDA ([Cu(IDA)(H<sub>2</sub>O)<sub>2</sub>]) form polymeric structures in the solid state.<sup>16,20</sup> The Cu(II) ion coordination geometry is a distorted octahedron.



**Figure 2.** A fragment of polymeric  $[\text{Cu}(\text{IDA})(\text{H}_2\text{O})_2]_n$ .

A large variety of complexes with IDA,<sup>23,24,25,26,27,28,29</sup> N-IDA<sup>30,31, 26</sup> or C-IDA<sup>25, 32</sup> derivatives as primary chelating agent and imidazoles<sup>30,23,24,25,26</sup> as an additional ligand have been studied. The investigation of their structures in the solid state gave several interesting correlations: In compounds prepared from equimolar amounts of Cu(II)/IDA/N-heterocyclic donor, the Cu(II) exhibits a distorted pyramidal coordination (type 4+1) or, in some cases, an octahedral coordination geometry (type 4+2 or 4+1+1) is shown.<sup>26</sup> The IDA or IDA derivative acts as a terdentate ligand with *mer*-chelation. In contrast, all known mixed-ligand complexes having a 1:1:2 Cu(II)/IDA/N-heterocyclic donor ratio show an elongated octahedral Cu(II) coordination with the IDA ligand as a *fac*-terdentate chelate.

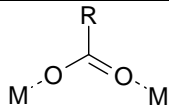
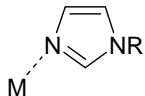
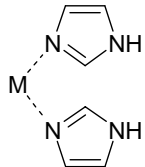


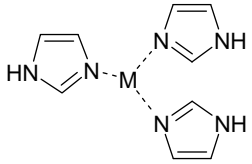
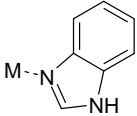
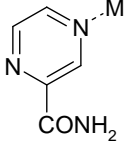
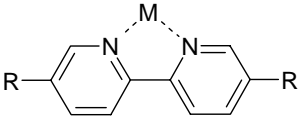
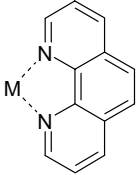
**Figure 3.** Structure of compound  $[\text{Cu}(\text{MIDA})(\text{ImH})]$  and  $[\text{Cu}(\text{IDA})[\text{MeImH}](\text{H}_2\text{O})_2]$ <sup>26</sup> in the solid state.

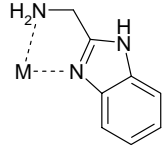
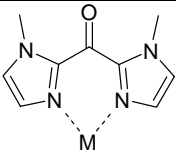
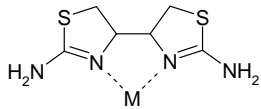
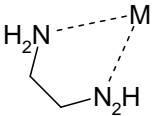
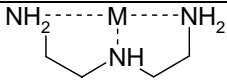
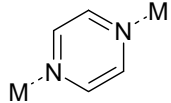
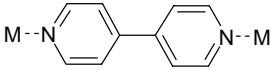
### **1.1.2 Other Transition Metal IDA Complexes with additional Ligand in the Solid State**

The large number of solid-state structures known of transition metal complexes that bear an additional typically weaker bound ligand prohibits their discussion in detail. Therefore, table 2 summarises all structures found in the Cambridge structural database where an IDA transition metal complex coordinates an additional complex ligand. Noticeable is the ability of IDA complexes to bind additional N-heterocyclic ligands, in particular imidazole and pyridine. The summarised information may guide the design of functionalised IDA complexes as chemosensors, for self-assembly or other purposes.

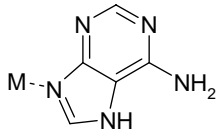
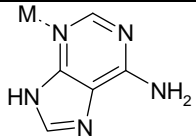
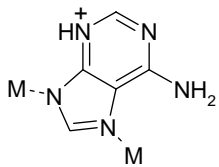
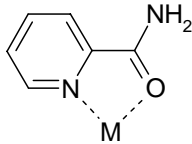
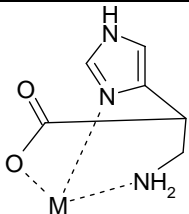
**Table 2.** References of X-ray structure analyses selected from the Cambridge structural database of transition metal IDA complexes coordinating an additional complex ligand (M = transition metal – IDA complex)

Additional Ligand	Metal Ions							
	Cu(II)	Ni(II)	Zn(II)	Fe(III)	Co(III)	Cr(III)	Mn(II)	Ru(II)
	R=Me <sup>33</sup>			R=Me <sup>34</sup> R=Ph <sup>35</sup> R=CH <sub>2</sub> OH <sup>36</sup> R=Ph-OH, CH <sub>2</sub> -CH=CH <sub>2</sub> <sup>37</sup>	R=Me <sup>33</sup>		R=Me <sup>38</sup>	R=Me <sup>39</sup> R=Ph <sup>40</sup>
	R=H <sup>25,26,32,41</sup> R=Me							
	See ref. <sup>41, 42</sup>							

		See ref. <sup>43</sup>						
	See ref. <sup>20</sup>							
	See ref. <sup>44</sup>							
	R=H <sup>28,29,32,45</sup> R=Me <sup>46</sup>	R=H <sup>47</sup>						
	See ref. <sup>32,46</sup>				See ref. <sup>48</sup>			

	See ref. <sup>49</sup>							
	See ref. <sup>50</sup>							
						See ref. <sup>51</sup>		
					See ref. <sup>52</sup>			
					See ref. <sup>53</sup>	See ref. <sup>54</sup>		
	See ref. <sup>55</sup>							
					See ref. <sup>56</sup>			



	See ref. <sup>57</sup>		See ref. <sup>56</sup>					
	See ref. <sup>57,58</sup>							
	See ref. <sup>59</sup>							
	See ref. <sup>60</sup>							
					See ref. <sup>61</sup>	See ref. <sup>62</sup>		

## 1.2 Recognition Processes in Solution

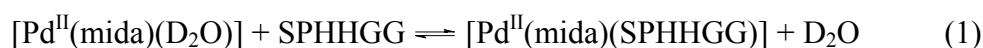
### 1.2.1 Peptide and Protein Binding by IDA Transition Metal Complexes

The affinity of IDA complexes to histidine residues is well documented in the solid state and in solution. Its main application is protein purification using metal ion affinity chromatography (IMAC) (see chapter 1.3.1). Some examples for peptide and protein binding in homogeneous solution are known.

#### 1.2.1.1 Coordination of two Hexapeptides to Cu(II) and Pd(II) Models of Metal Chelation site on IMAC resins

To improve protein purification methods based on immobilised metal ion affinity chromatography (IMAC) (see chapter 1.3.1) a deeper understanding of the interaction between protein and metal complex is required. A polyhistidine tail ( $\text{His}_{n=2 \text{ to } 6}$ ) is introduced by standard methods of molecular biology on the protein side. This creates affinity to an IMAC column.<sup>63,64,65</sup> By varying the amino acid sequence in the fused tail to SPHHGG, milder elution conditions of tagged proteins were achieved.<sup>66,67</sup>

The coordination of proteins or the affinity tag region to immobilised Cu(II)-IMAC binding sites is difficult to study by direct physical methods. Therefore, *Shepherd* investigated which amino acids or side-chain donors atoms of SPHHGG and HHHHHH peptide sequences coordinate to the metal ion.<sup>68</sup> The diamagnetic, square-planar  $[\text{Pd}^{\text{II}}(\text{mida})]$  chelate ( $\text{mida}^{2-}$  = methyliminodiacetate) was used as a soluble model for an IMAC binding site to approximate the distorted tetragonal Cu(II)-IDA coordination geometry. The investigation of the binding motif by  $^1\text{H}$ -NMR measurements assumed equilibrium (1).



EPR spectra and pH dependence of UV/Vis spectra of  $[\text{Cu}(\text{mida})(\text{SPHHGG})]$  and  $[\text{Cu}(\text{mida})(\text{HHHHHH})]$  provided additional details. From the data, a binding model with a three-point contact of the protein-affinity tags to the Cu(II)-IMAC column at pH 7 was derived.

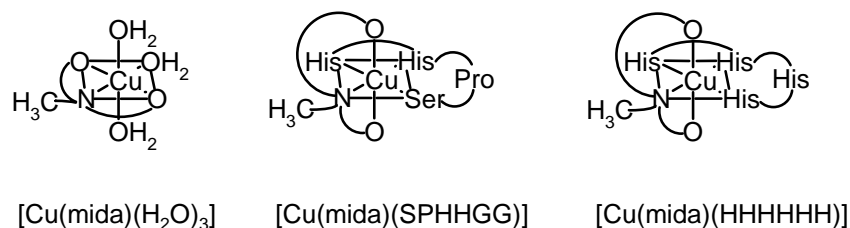


**Figure 4.** Geometry of investigated Cu(II) complexes.

#### 1.2.1.2 Recognition of Flexible Peptides by IDA Complexes in Water

Since 2000, the group of *Mallik* reported IDA metal complexes capable of binding strongly to histidine patterns of flexible peptides in water.<sup>69</sup> To achieve strong and selective binding the geometry of the IDA complex and the target histidine pattern need to be complementary.

To demonstrate their concept *Mallik* designed and synthesised water-soluble peptides with three histidine moieties at particular distances apart (12–16 Å). This distance corresponds to the inter-histidine distances (His1, His7, and His12 or 14) on the surface of the protein carbonic anhydrase. Figure 5 shows the structures of the peptides.

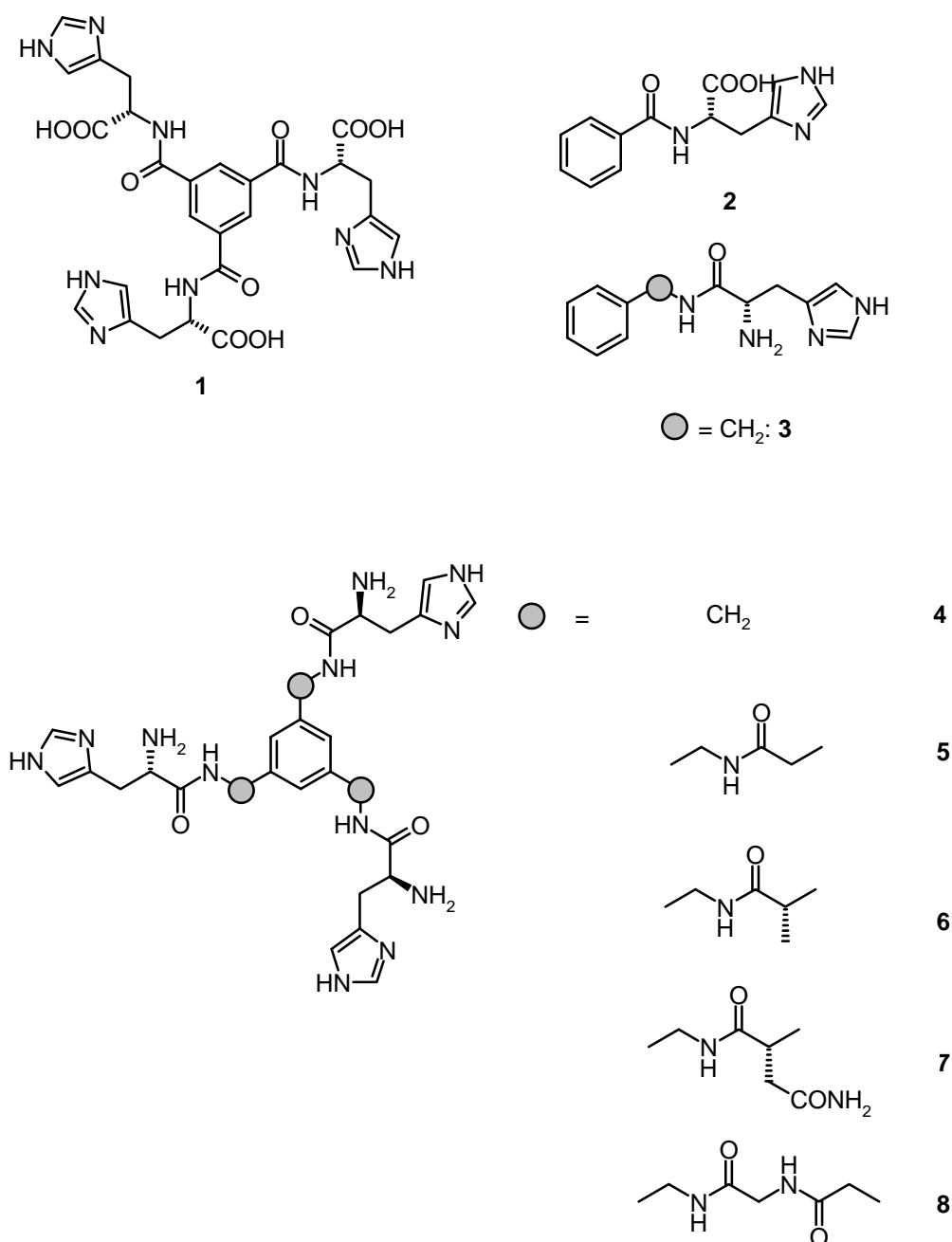


**Figure 5.** Structures of the histidine-containing peptides used in the binding studies.

From molecular modeling, the distance between the imidazole groups of the histidines was estimated to increase by approximately 4 Å when the peptide length increased by a glycine unit. The peptide **8** was designed to probe the role of flexibility in the recognition process (the inter-histidine distance for **8** was estimated to vary from ~ 18 to ~ 23 Å). Peptide **6** bears a hydrophobic methyl group, while **7** has a hydrophilic amide moiety in the side chain to study the effect of hydrophobicity on the recognition process. The monohistidine peptides **3** and **2** served as the controls for recognition studies.

They designed five Cu(II) complexes (figure 6) as binding sites for these studies with distances between the Cu(II) ions estimated to be  $\sim 12$  Å for **10**,  $\sim 16$  Å for **11**, and  $\sim 14$ – $18$  Å for **12** and **13**. The complex **9** with one Cu(II) ion serves as a control.

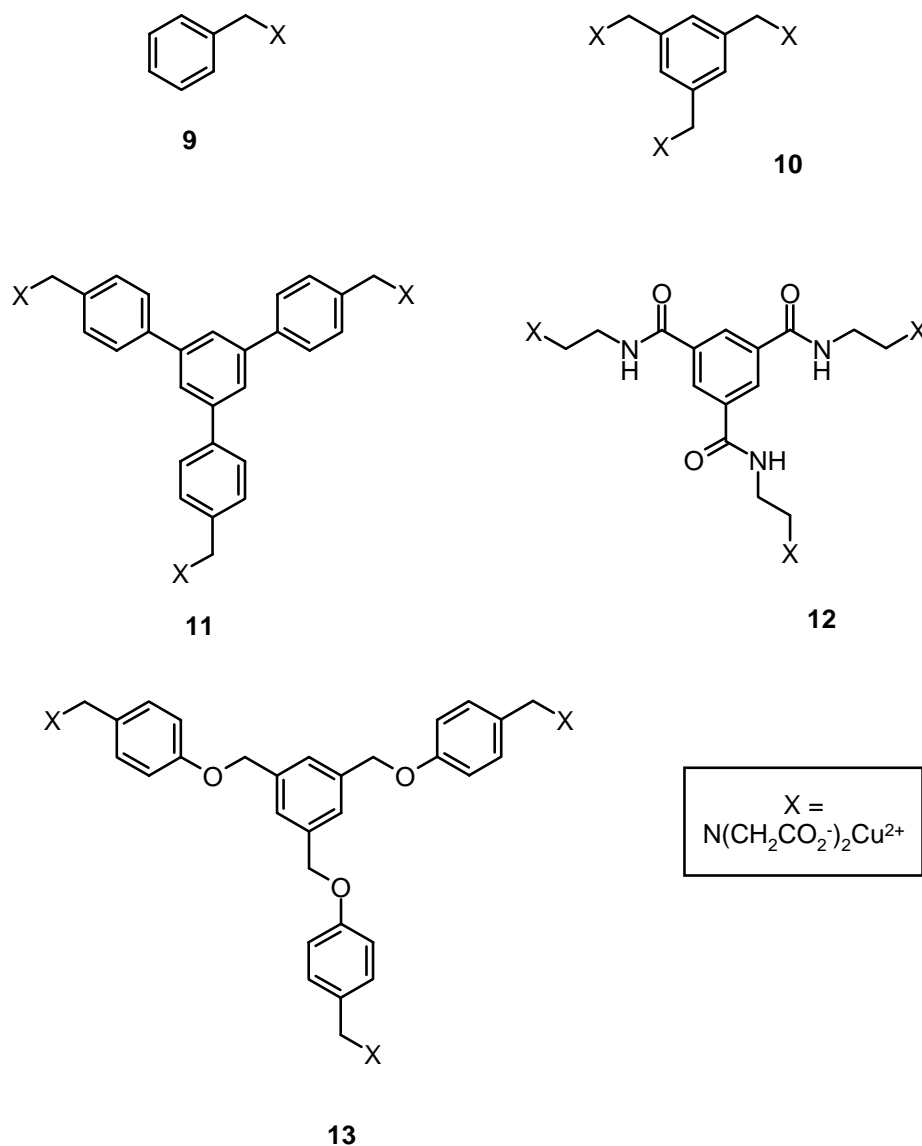


**Figure 6.** Structures of the metal complexes used in the recognition studies.

Using isothermal titration microcalorimetry (ITC) the binding constant ( $K_{st}$ ), reaction stoichiometry ( $n$ ), and enthalpy change ( $\Delta H$ ) of the recognition process was determined. A solution of metal complex ( $0.1 - 0.5$  mM) in the ITC cell was titrated with a peptide ( $0.80 - 5.0$  mM) both dissolved in 25 mM HEPES buffer at pH 7.0 and 25 °C.

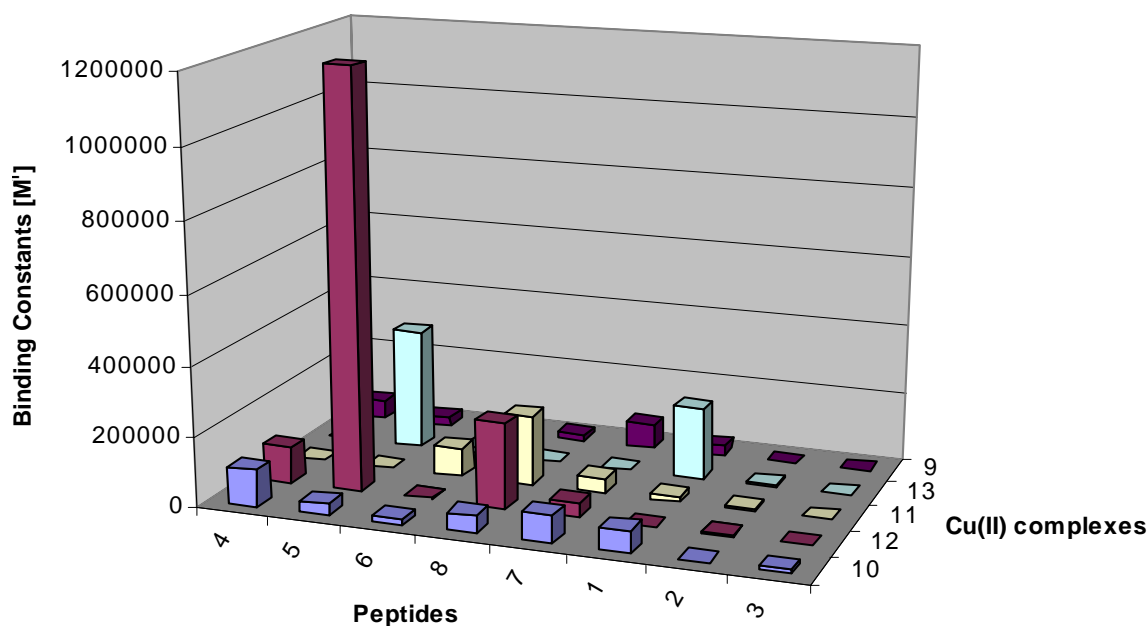


**Figure 7.** Binding constants of the model peptides with the metal complexes.

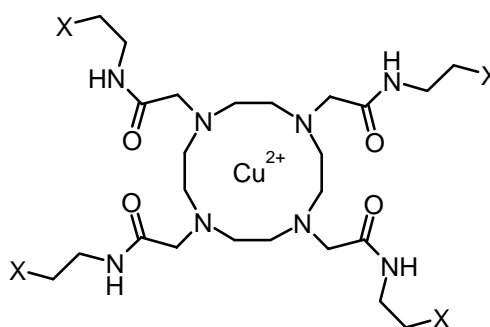
With the distance-matched peptide **5**, complex **12** showed a stronger binding affinity ( $K_{st} = 1.19 \cdot 10^6 \text{ M}^{-1}$ ) than with a shorter peptide (**4**,  $K_{st} = 104,400 \pm 22,800 \text{ M}^{-1}$ ) or a longer peptide (**8**,  $K_{st} = 243,600 \pm 24,500 \text{ M}^{-1}$ ). A hydrophobic side chain on peptide **6** had a devastating effect on the affinity for the metal complexes, due to unfavorable entropy changes. Introduction of a hydrophilic side chain on peptide **7** also led to large entropy losses and consequently decreased the affinity for the metal complexes. For all of the systems tested, the metal-ion-free ligands showed no measurable interaction by ITC under the same experimental conditions.

### 1.2.1.3 Protein Surface Recognition by a Designed Metal Complex

Extending the results from small peptide model compounds *Mallik et al.* were able to selectively bind to peptides and proteins by recognising unique patterns of surface-exposed histidines.<sup>70</sup>

The target protein was carbonic anhydrase (CA, bovine erythrocyte). CA displays six histidines on the surface (1, 7, 12, 14, 61, and 93). The distances separating the histidines 1, 7, 14 (or 12) are  $13 \pm 2 \text{ Å}$ ,  $16 \pm 2 \text{ Å}$ , and  $17 \pm 2 \text{ Å}$  respectively. Three other proteins were used as controls (chicken egg albumin, horse skeletal muscle myoglobin, and chicken egg lysozyme). Chicken egg albumin (CEA) has the same number of solvent-exposed histidines as CA (22, 23, 329, 332, 363, 371), but the pattern is different. Myoglobin (Mb)

has seven histidines on the surface (36, 48, 81, 97, 113, 116, 119), but with different distribution. Lysozyme has only one histidine (15) exposed on the surface. All of these proteins (target and controls) are known to interact with transition metal ions and complexes through the surface-exposed histidines.<sup>71</sup> In addition to the already mentioned complexes **9** – **13**, interactions with cyclen **14** were also tested by ITC.



**14**

**Figure 8.** Structure of **14**.

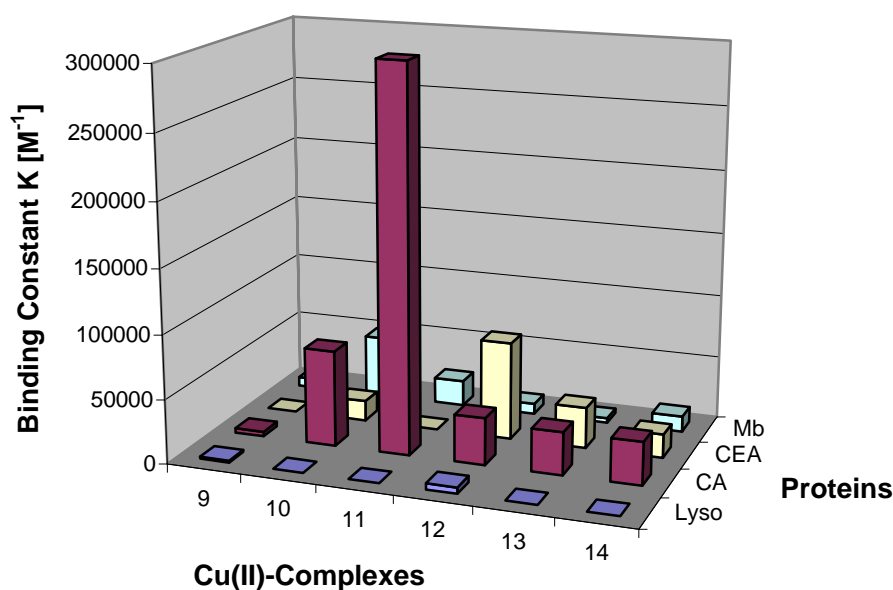


**Figure 9.** Binding constants of the metal complexes with the proteins HEPES buffer, 25 mM, pH = 7.0, 25 °C).

Comparison of the binding constants indicated that complex **11** is very selective for CA compared to CEA (300:1); with myoglobin, the selectivity is moderate (20:1). For myoglobin, two of the cupric ions of **11** may simultaneously bind to two histidine residues on the protein surface (His 113 and 116 or 119). This leads to a lower selectivity of **11** in distinguishing CA from myoglobin. To demonstrate selective binding of **11** to the target

protein, a mixture of CA and complex **9** ( $[CA] = 100\ \mu\text{M}$ ;  $[9] = 100\ \mu\text{M}$ ) was titrated with **11** ( $[11] = 0\text{--}500\ \mu\text{M}$ ). No change in the binding constant was observed for **11**. On the other hand, when a mixture of CA and **11** ( $[CA] = 100\ \mu\text{M}$ ;  $[11] = 100\ \mu\text{M}$ ) was titrated with **9** ( $[9] = 0\text{--}1\ \text{mM}$ ), no binding was detected. A mixture of the tested proteins ( $100\ \mu\text{M}$  each) was titrated with complex **11** to obtain an unchanged affinity of **11** towards CA ( $280000\ \text{M}^{-1}$ ). If CA was omitted from the protein mixture, only very weak binding ( $K < 1000\ \text{M}^{-1}$ ) was detected.

#### 1.2.1.4 Conjugation of poor Inhibitors with Surface Binding Groups

To convert a poor inhibitor of carbonic anhydrase into a good inhibitor, surface-histidine coordination was used to increase its affinity.<sup>72</sup>

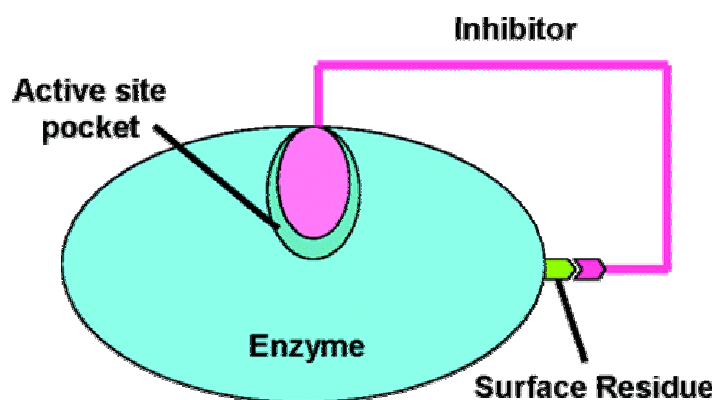


**Figure 10.** Surface-assisted enhancement in the binding of an inhibitor. The inhibitor binds at the active site pocket and to a surface-exposed His residue of the enzyme.

Benzene sulfonamide, a rather weak inhibitor for carbonic anhydrase ( $K_d = 120\ \mu\text{M}$ ), was converted to a very good inhibitor for the enzyme ( $K_d = 130\ \text{nM}$ ) as a result of this conjugation. For proof-of-concept five Cu(II)-complexes (figure 11) were designed and synthesised.



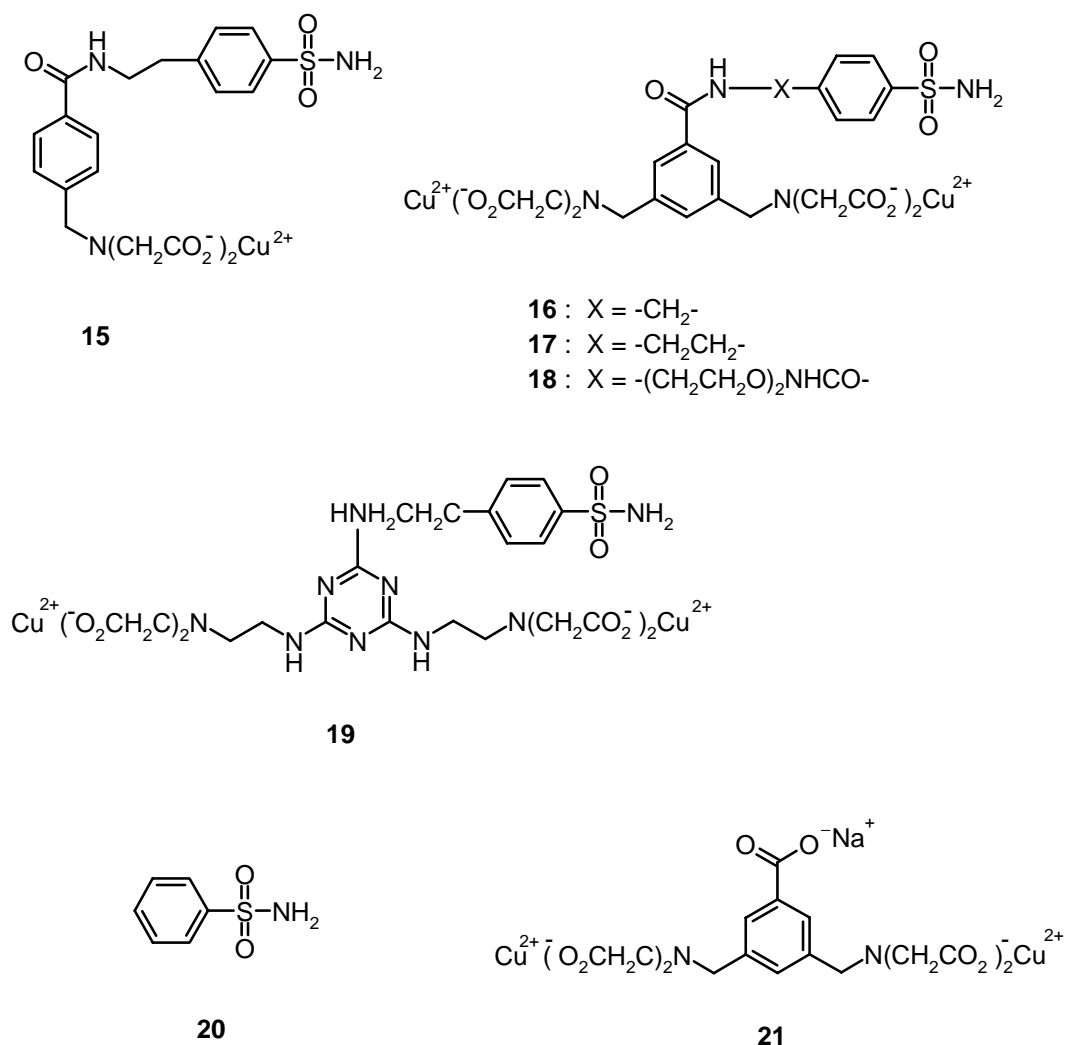


**Figure 11.** Structures of tested compounds.

The length of the spacer separating the benzene sulfonamide group from IDA was varied in these complexes. Benzene sulfonamide **20** and the di-Cu(II) complex **21** (lacking the benzene sulfonamide moiety) were used as controls for these studies. The binding constants of the complexes with carbonic anhydrase (bovine erythrocyte) were determined with isothermal titration calorimetry (25 mM HEPES buffer, pH = 7.0).

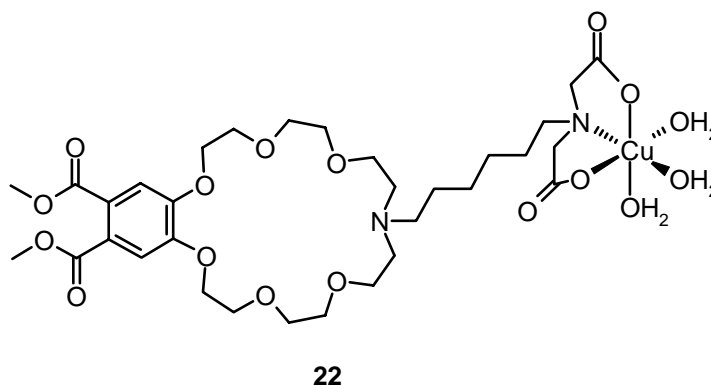
**Table 3.** Binding parameters of the complexes with carbonic anhydrase

Compound	Binding constant [L·mol <sup>-1</sup> ]	Enthalpy [kcal·mol <sup>-1</sup> ]
Complex <b>15</b>	$(4.6 \pm 0.07) \cdot 10^6$	$-26.4 \pm 0.8$
Complex <b>16</b>	$(1.9 \pm 0.03) \cdot 10^5$	$-51.7 \pm 5.8$
Complex <b>17</b>	$(7.5 \pm 0.1) \cdot 10^6$	$-36.9 \pm 4.2$
Complex <b>18</b>	$(5.4 \pm 0.02) \cdot 10^5$	$-30.3 \pm 2.6$
Complex <b>19</b>	$(4.3 \pm 0.03) \cdot 10^5$	$-45.5 \pm 2.2$
Control <b>20</b>	$(9.0 \pm 0.1) \cdot 10^3$	$-31.2 \pm 1.6$
Control <b>21</b>	$(22.8 \pm 1.3) \cdot 10^3$	$-129.0 \pm 3.2$

Affinities of the conjugates were considerably higher compared to the controls. Complex **17** showed the highest affinity for the enzyme, three orders of magnitude higher compared to the controls. The similar binding constants for complex **15** (one Cu(II) ion) and **17** (two Cu(II) ions) may indicate that one cupric ion binds to one histidine on the surface of the protein.

#### 1.2.1.5 Combination of Cu(II)-IDA and Crown Ether Binding Site

To amplify crown ether – ammonium ion binding in water *König et al.* prepared a peptide binding luminescent crown ether, which contains a pendant Cu(II)-IDA complex.<sup>73</sup>

**Figure 12.** The luminescent benzo-crown ether **22**.

No response of the emission properties is observed for **22** if treated with KSCN or *n*BuNH<sub>3</sub>Cl in buffered aqueous solution (50 mM HEPES, pH 7.5, 1 c = 10<sup>-5</sup> mol/L, up to 1000 equiv. ammonium ion), even with large excess of the salts. The aqueous solvent

competes with the crown ether for the cation binding and the ammonium-crown ether interaction is intercepted. The situation changes if the dipeptide His-Lys-OMe is added to a solution of **22**. Coordination of the *N*-terminal His to the Cu(II)-IDA complex of **22** makes the crown ether-ammonium ion binding intramolecularly and much more favorable.

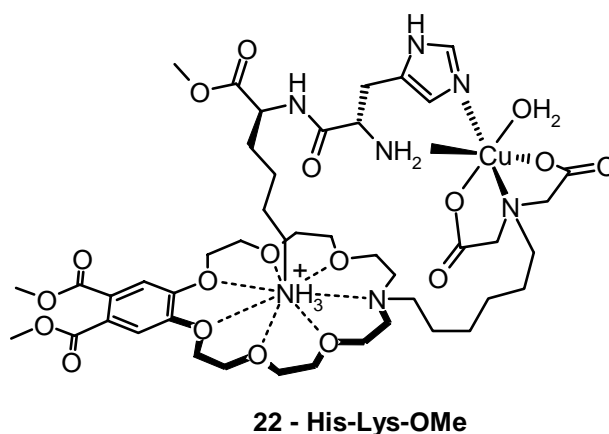


**Figure 13.** Proposed mode of binding of **22** and His-Lys-OMe.

Titration of **22** with His-Lys-OMe in HEPES buffer (50 mM, pH 7.5) resulted in a 1:1 complex as shown by a Job's plot analysis. With a binding constant of  $\log K = 4.22 \pm 0.05$  compound **22** binds the ammonium group of His-Lys-OMe with high affinity in buffered water. The emission intensity change of **22** in the presence of His-Lys-OMe can even be observed with the naked eye (see figure 14). No emission response is detected under the same conditions with the *N*-terminal acylated dipeptide Ac-His-Lys-OMe, which proves the importance of an *N*-terminal His for the overall binding process.

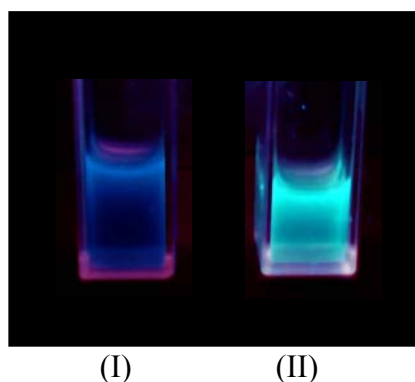


**Figure 14.** Emission intensity changes of solutions of **22** in buffered water in the presence of His-Lys-OMe (II) and without (I).

The use of His-OMe resulted in a 2:1 stoichiometry for the His-OMe–**22** aggregate. After binding of one His-OMe to Cu(II)-IDA one coordination site remains, which can accommodate the imidazole moiety of a second His-OMe while its ammonium group is

bound by the crown ether, leading to an increased emission intensity. The overall binding constant of His-OMe to **22** was determined to be  $\log K = 3.8 \pm 0.1$ . The binding motif allows the selective detection of N-terminal His groups, which is illustrated by the binding of tripeptide His-Gly-Gly. This peptide binds to **22** with the same 2:1 stoichiometry as observed for histidine and an overall affinity of  $\log K = 3.71 \pm 0.05$ . In an additional binding experiment it could be shown that the designed receptor **22** can selective detect the amino acid His among 20 natural  $\alpha$ -amino acids.

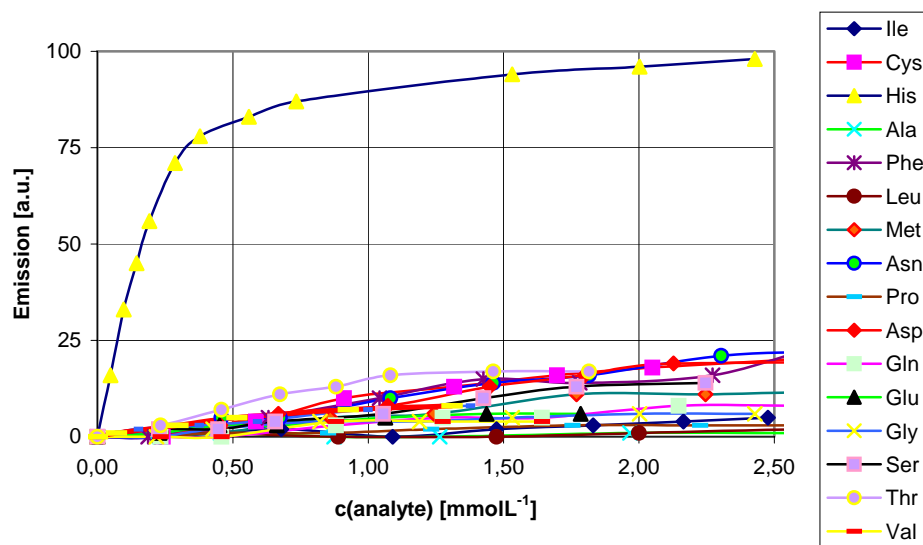


**Figure 15.** Response of the emission intensity of **22** to the presence of 20 natural  $\alpha$ -amino acids in aqueous buffered solution (50 mM HEPES, pH 7.5). (Tyr is not soluble in HEPES buffer, and the indole emission of Trp interferes with the emission of **22**).

### 1.2.2 Carbohydrate Recognition in Water

Several attempts to recognise carbohydrates selectively by means of synthetic receptors based on hydrogen bonding, charged interactions, or boronic acids have been made.<sup>74,75</sup> These suitable forces for sugar binding in apolar organic media become far less attractive in aqueous media.<sup>76</sup> Using metal coordination *Striegler et al.*<sup>77</sup> built up ternary ligand Cu(II) complexes for sugar binding in aqueous solutions. In order to find a suitable metal complex for selective binding of various carbohydrates (glucose **24**, galactose **25**, mannose **26**, or maltose **27**) they investigated several bi- and tridentate Cu(II) complexes (figure 16).

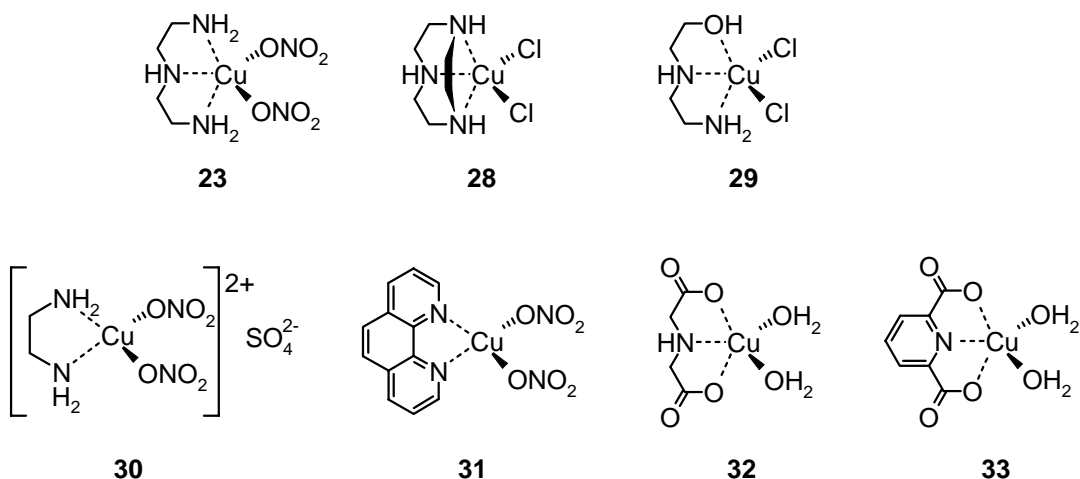


**Figure 16.** Structures of the Cu(II) complexes **23**, **28-33**.

The Cu(II) complexes from tridentate N- and N,O-ligands [(diethylenetriamine)copper(II)] dinitrate [CuDIEN]-(NO<sub>3</sub>)<sub>2</sub> **23**, [(triazacyclononane)copper(II)] dichloride [Cu(TACN)]Cl<sub>2</sub> **28**, and N-[(2-hydroxyethyl)ethylenediamine]copper(II) dichloride CuHEN **29**, coordinate hexoses **24-27** in identical stoichiometries. In contrast, decomposition of [(ethylenediamine)copper(II)]sulfate **30**, [(phenanthroline)-copper(II)] dinitrate **31**, copper(II)iminodiacetic acid **32**, and copper(II)pyridinedicarboxylic acid **33** occurs in alkaline solution (pH > 10.4), which prevents the observation of complex formation with the investigated sugars. Since strong binding of carbohydrates requires highly alkaline pHs, only Cu(II) complexes which are stable under these conditions are useful. Complex [Cu(styDIEN)](HCOO)<sub>2</sub> **34**, a potential binding site for molecular imprinted devices was also examined.

*Cis*-diol fragments are expected to lead to higher binding affinities than *trans*-diol motifs.<sup>78</sup> The binding constants of the 1:1 complexes of **23**, **29**, and **34** with **24-27** (scheme 2) were determined according to the method of *Rose and Drago*.<sup>79</sup>

**Scheme 2.** Complex formation of  $[\text{Cu}(\text{styDIEN})](\text{HCOO})_2$  **34** with **24-27** at pH = 12.40

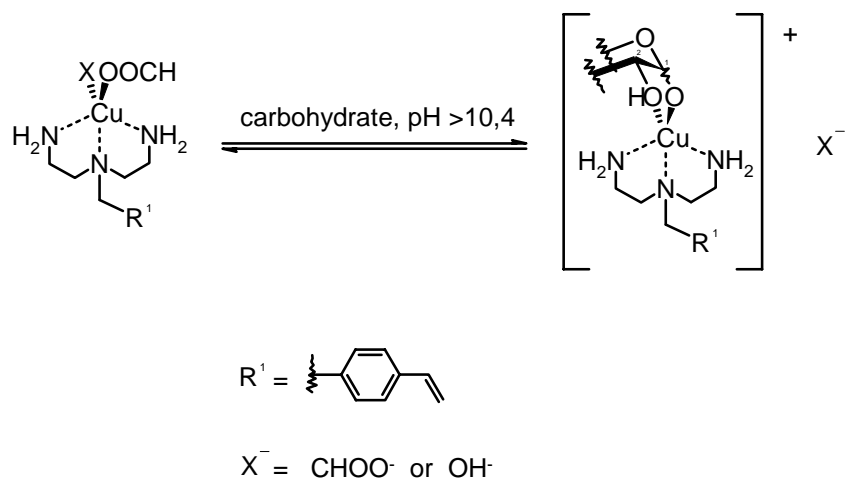


**Table 4.** Apparent binding constants ( $\text{p}K_{11}$ ) for ternary complexes formed from **23**, **29**, and **34** with **24-27**

	<b>23</b>	<b>29</b>	<b>34</b>
Compd.	$\text{p}K_{11}$	$\text{p}K_{11}$	$\text{p}K_{11}$
<b>24</b>	$3.73 \pm 0.12$	$3.37 \pm 0.31$	$3.61 \pm 0.17$
<b>25</b>	$3.70 \pm 0.09$	$3.41 \pm 0.43$	$3.64 \pm 0.12$
<b>26</b>	$3.68 \pm 0.12$	$3.05 \pm 0.41$	$3.38 \pm 0.19$
<b>27</b>	$3.75 \pm 0.12$	$3.41 \pm 0.26$	$3.62 \pm 0.09$

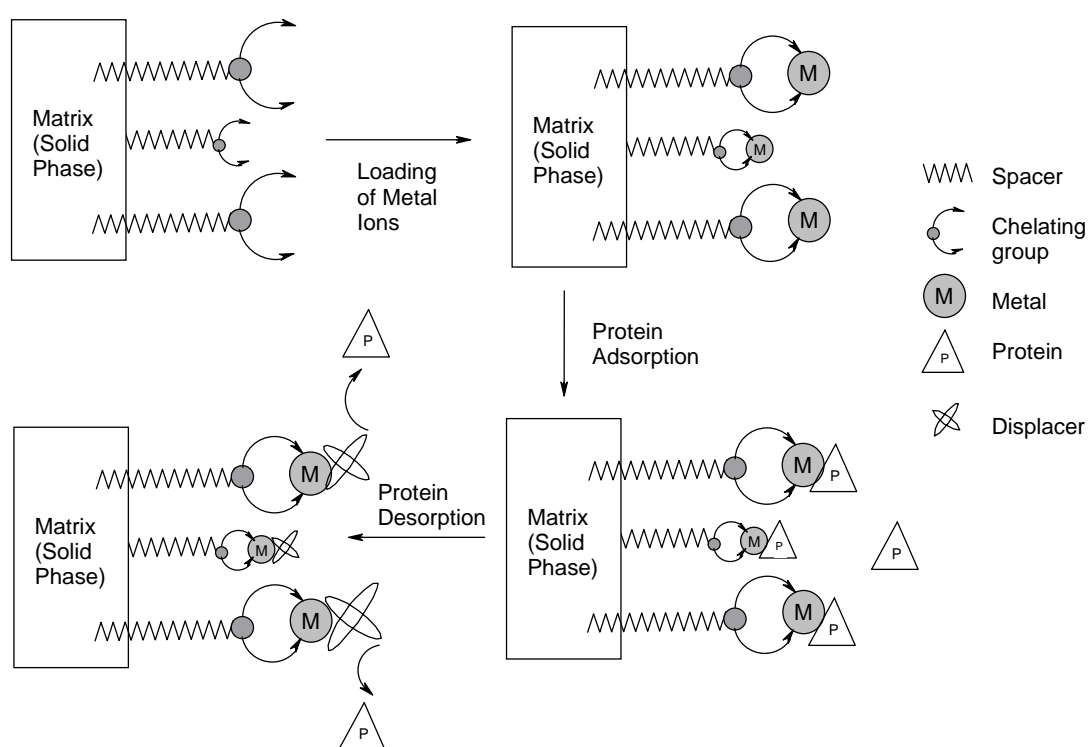
The ternary complexes formed from **24**, **25**, and **27** with **23**, **29**, or **34** show similar apparent binding constants, while those formed with **26** are a little lower. *Striegler et al.* attributed this to an rearrangement of the ligand–Cu(II)–mannose complex when complex formation with a *cis*-1,2-diol occurs at C<sup>2</sup> and C<sup>3</sup> instead of the preferred chelation by the hydroxyl groups at C<sup>1</sup> and C<sup>2</sup>.

## 1.3 Recognition Processes on Solid Surfaces

### 1.3.1 Immobilised metal ion affinity chromatography (IMAC)

Immobilised metal ion affinity chromatography (IMAC) is a widely used technique. It is a separation and purification method based on interfacial interactions between biopolymers in solution and metal ions immobilised on a solid support. The cross-linked polymer is hydrophilic. Introduced in 1975 by *Porath* and coworkers this purification method is presently one of the most popular methods for purification of recombinant proteins.<sup>80</sup>

**Scheme 3.** Schematic principle of the IMAC technique<sup>81</sup>

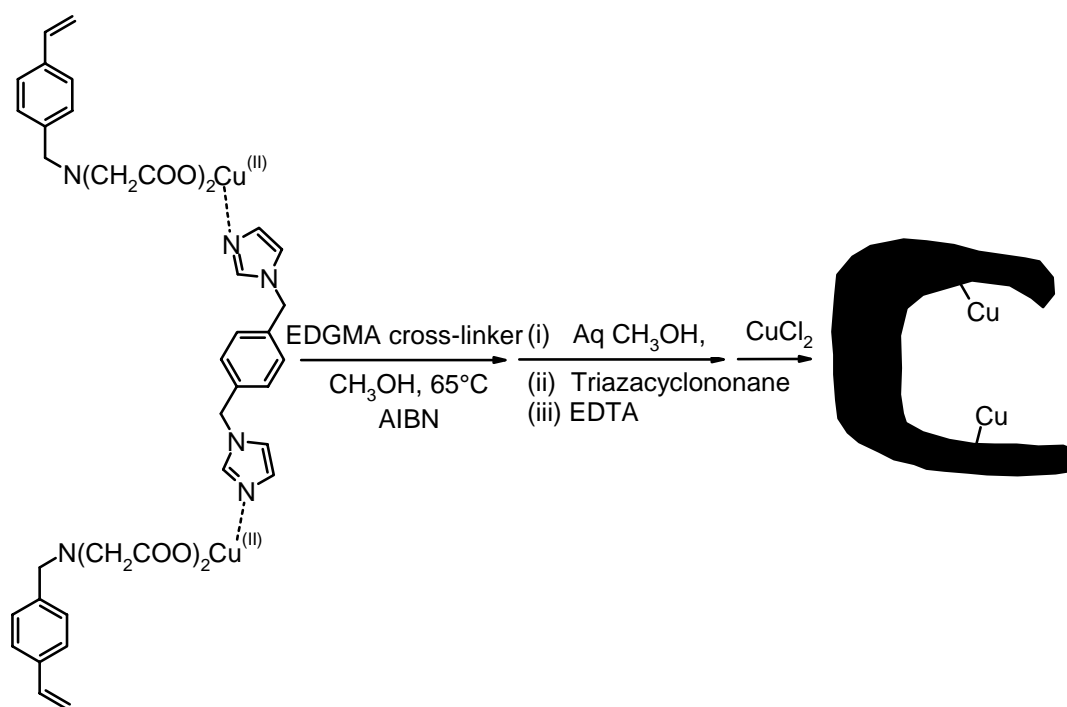


This interesting method of reversible coordination of His-tagged proteins to IDA metal complexes typically of Ni(II) or Cu(II) led to a huge number of review articles over the last decades.<sup>82</sup> Due to this comprehensive coverage of the topic and its specific application, we will not discuss the IMAC technique in detail in this review and refer the interested reader to the cited literature.

### 1.3.2 Molecular Imprinting

As demonstrated in *chapter 1.3.1* the design of synthetic molecules capable of recognising chemical entities in a specific and predictable manner is of great fundamental and practical importance. The principal paradigm of the molecular design of such materials involves the preorganisation of binding sites of the host system (receptor) around complementary binding sites of the guest molecule (substrate).<sup>83</sup> *Wulff* and coworkers developed an approach to substrate-selective polymers.<sup>84</sup> This technique of template polymerisation, also known as molecular imprinting, has been used to prepare polymeric materials for applications in molecular recognition and chromatographic separations. Template polymerisation produces cross-linked polymers containing functional groups strategically arranged in the polymer matrix. *Arnold et al.* report a variation of this template polymerisation technique to synthesise rigid macroporous polymers containing (Cu(II)-IDA) complexes.<sup>85,86</sup>

**Scheme 4.** Polymerisation recipe and workup of templated chelating polymers



For initial studies of template polymerisation using metal ion complexes a set of model templates was developed. Each of these templates **34-40** bears imidazole functionalities with slightly different arrangements. Compounds **41** and **42** are structural analogs of compounds **35** and **36** that contain no imidazole ligands for coordination of the metal ions.



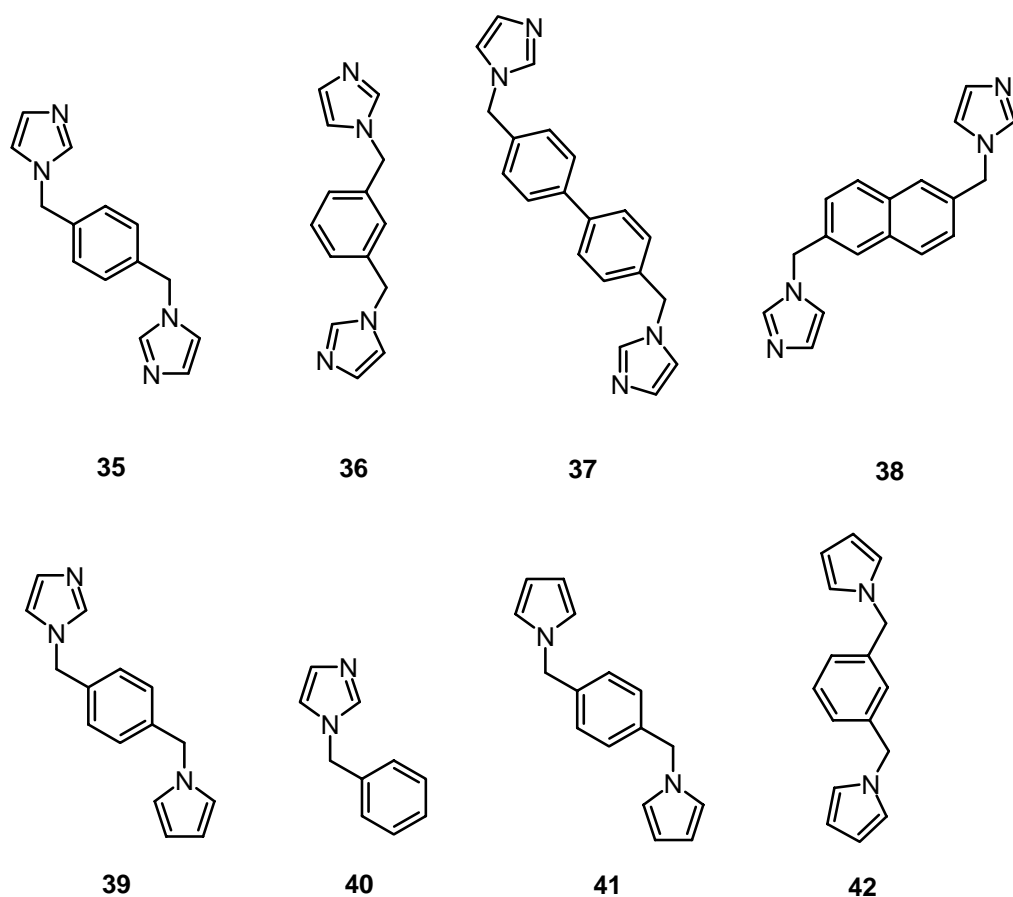


**Figure 17.** Set of imidazole templates **35-39** and structurally related pyrroles **41** and **42**.

In order to incorporate Cu(II) into the polymer at positions corresponding to the imidazole ligands of the templates, individual template-monomer assemblies were polymerised in the presence of a large excess of cross-linker. A control polymer with a random distribution of copper ions (P-1) was also prepared using the monofunctional ligand 1-benzylimidazole (**40**).

**Table 5.** Polymerisation and characterisation of metal-complexing polymers

polymer code	template used (mmol/g)	Cu(II) in polymer (mmol/g)	recovery of	
			Cu(II) (mmol/g)	template (mmol/g)
P-1	<b>40</b> (0.51)	0.52	0.48	0.49
P-2	<b>35</b> (0.26)	0.52	0.47	0.26
P-3	<b>36</b> (0.27)	0.53	0.49	0.26
P-4	<b>37</b> (0.25)	0.54	0.50	0.23

To determine some of the factors that influence the ability of the templated polymers to discriminate template from nontemplate molecules, individual and competitive binding was studied. Experiments with the nontemplated polymer (P-1) were used to distinguish non-specific metal ion binding from specific coordination.

**Table 6.** Substrate binding by templated and nontemplated polymers under saturation rebinding conditions

<b>entry</b>	<b>polymer</b>	<b>substrate</b>	<b>substrate bound (mmol/g)</b>
1	P-1	<b>35</b>	0.46
2	P-1	<b>36</b>	0.44
3	P-1	<b>37</b>	0.45
4	P-1	<b>38</b>	0.44
5	P-2	<b>35</b>	0.33
6	P-2	<b>36</b>	0.22
7	P-2	<b>37</b>	0.19
8	P-2	<b>38</b>	0.18
9	P-3	<b>35</b>	0.17
10	P-3	<b>36</b>	0.24
11	P-4	<b>37</b>	0.20
12	P-4	<b>38</b>	0.24

**Table 7.** Selectivity of templated and nontemplated polymers during competitive rebinding of bis(imidazole) substrates

entry	polymer	substrates	relative selectivity during rebinding
1	P-1	<b>35 + 36</b>	$\alpha_{35/36} = 1.02$
2	P-2	<b>35 + 36</b>	$\alpha_{35/36} = 1.17$
3	P-2	<b>35 + 37</b>	$\alpha_{35/37} = 1.35$
4	P-2	<b>35 + 38</b>	$\alpha_{35/38} = 1.32$
5	P-3	<b>35 + 36</b>	$\alpha_{36/35} = 1.15$
6	P-4	<b>35 + 37</b>	$\alpha_{37/35} = 1.22$

As shown in table 6, this random polymer binds nearly equal amounts of the four different bis(imidazole) substrates **35-38**. P-1 also exhibits no selectivity in a competitive binding experiment. In contrast, polymers prepared in the presence of a bis(imidazole) template show preferences for their own templates in both saturation and competitive rebinding experiments. The larger the structural differences between the substrates, the more pronounced are the selectivities. In the competitive rebinding experiments, P-2 shows a small but measurable selectivity for its own template over the close structural analog **36**, which differs only in the orientation of the imidazole groups. (**35** and **36** are in fact so similar that it is impossible to separate them by RP-HPLC). The separation factor increases to above 1.3 when the polymer is used to distinguish template **35** from substrates **37** and **38**, which have imidazole groups with larger distances.

Molecular imprinted polymers can also be used as selective adsorbents. However, chromatographic separation with these polymers showed the need to optimise the imprinting process. The relatively high degree of crosslinking needed to capture a specific arrangement of functional monomers in the solid polymer prevents the diffusion of substrates in the particles, which leads to band spreading and poor peak resolution. Access of very large substrates to binding sites can thus be severely impeded.

One approach to overcome these problems is to graft the monomer-template assemblies and a crosslinker onto a reactive support with the desired physico-mechanical properties.<sup>87,88</sup> *Arnold* and his group has investigated poly(trimethylpropane trimethacrylate) (TRIM, **45**) as a reactive surface for template polymerisation.<sup>89</sup>

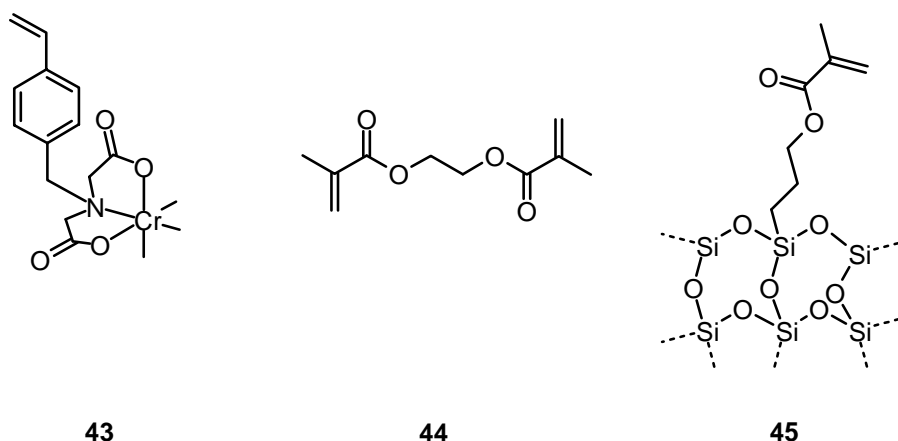


**Figure 18.** Monomers used for molecular imprinting.

During the polymerisation, it is necessary that the monomer-template assembly is held together by strong metal-to-ligand interactions. Unfortunately, very strong interactions with the template can interfere with the material's subsequent chromatographic performance. Tightly bound substrates experience very long retention times and excessive band spreading. Replacing the metal ion used during imprinting (Cu(II)) by others better suited for the chromatographic separation [i.e. Zn(II)] yields adsorbents capable of separating closely related bis-imidazole substrates. This “bait-and-switch” approach can significantly enhance the performance of molecular imprinted materials.

Chromatographic separation experiments with bis-imidazoles (**35-37**, **40**, **41**) showed the expected results. Retention of the imidazole-containing compounds on materials loaded with Cu(II) was so strong that no peaks were observed during isocratic elution. Substrate retention times were greatly reduced when the Cu(II) ions were replaced with Zn(II).

**Table 8.** Capacity factors ( $k'$ ) and chromatographic separation factors ( $\alpha_{i,j}$ ) for imidazole and substrates **37-40** on polymer-coated silica (LiChrosphere 1000) prepared using **37-40** as templates

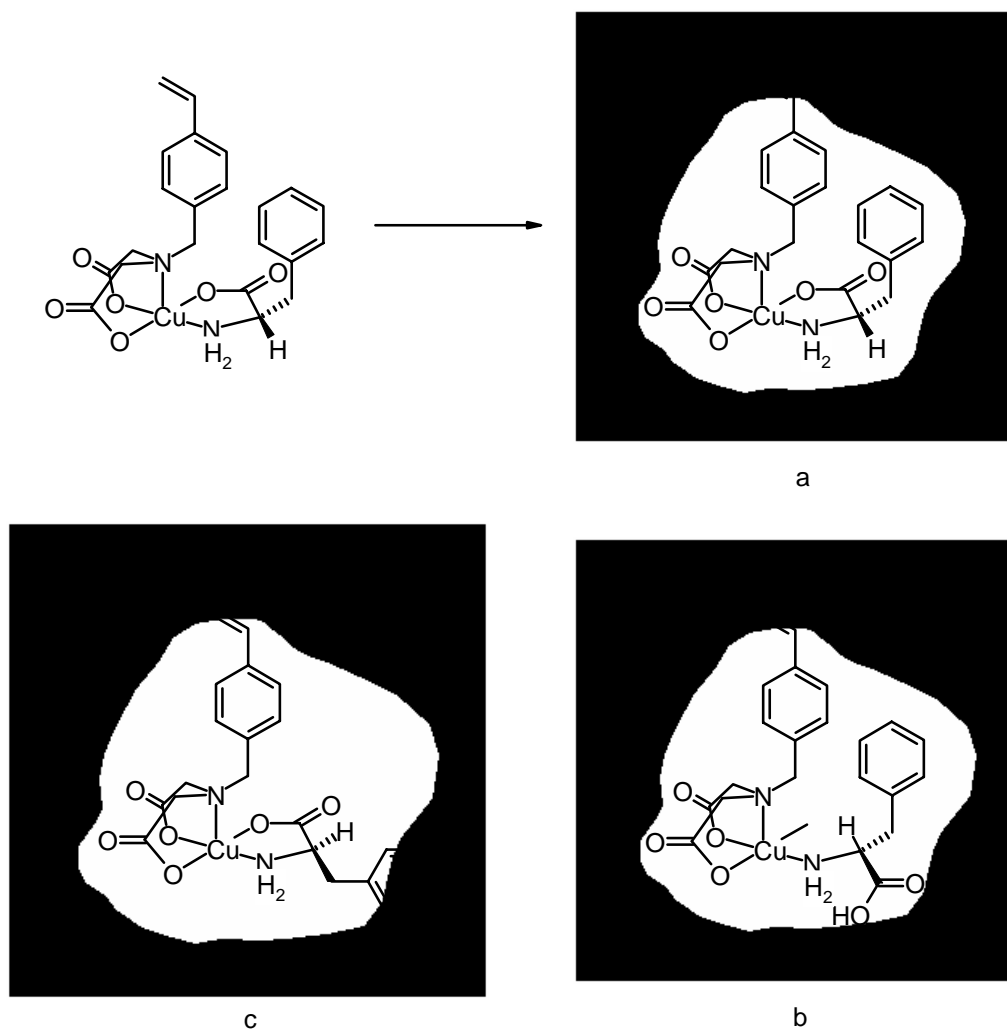
Substrate	Material prepared using:							
	<b>37</b>		<b>38</b>		<b>39</b>		<b>40</b>	
	$k'_i$	$(\alpha_{37,i})$	$k'_i$	$(\alpha_{38,i})$	$k'_i$	$(\alpha_{39,i})$	$k'_i$	$(\alpha_{40,i})$
<b>Imidazole</b>	0.75	1.16	0.69	8.1	1.5	5.8	1.7	6.6
<b>37</b>	0.87	-	0.69	8.1	1.7	5.1	1.8	6.3
<b>38</b>	2.9	0.30	5.6	-	6.6	1.4	7.7	1.5
<b>39</b>	2.6	0.33	3.5	1.6	8.7	-	6.3	1.8
<b>40</b>	2.7	0.32	1.5	3.9	2.9	3.0	11.3	-

Elution volumes ( $V_e$ ) were measured on 50 x 4.6 mm I.D. columns, 0.5 ml/min 100% methanol, 65 °C, with a sample size of 10  $\mu$ l of 0.4 mM solution. The mobile phase contained zinc acetate in the following concentrations: experiments on **37**-templated material, 50 mM; **38**-templated material, 50 mM; **39**-templated material, 40 mM; **40**-templated material, 30 mM.  $k' = (V_e - V_o)/V_o$ ,  $\alpha_{i,j} = (V_e - V_o)_i / (V_e - V_o)_j$

The material, which was prepared with the monodentate coordinating template **37**, retains the three bis-imidazole substrates **38**, **39**, and **40** to very similar extents. The binding sites in this “random” material have no basis to discriminate among the compounds. When the polymer-coated silica was prepared using bis-imidazole **38**, **39**, or **40**, as the template, the template was always the most strongly retained analyte.

In 1997, the same group reported an approach to preparing stereoselective ligand-exchange supports using molecular imprinting.<sup>90</sup> Several aliphatic and aromatic amino acids were investigated in order to evaluate the role of the side group in stereodifferentiation. Comparison with an achiral monomer based on iminodiacetate showed that the enantioselectivity of the adsorbent arises from the chirality of recognition sites created during polymerisation.

**Scheme 5.** Source of enantioselectivity in imprinted ligand-exchange materials. Molecular imprinting with L-Phe gives a cavity that is selective for L-Phe. (a) The L-isomer can simultaneously chelate to a metal ion and fit into the shape-selective cavity. (c) Rebinding of the D-isomer is hindered because chelation of the metal ion by the D-isomer is sterically unfavorable. (b) Alternately, if the molecule fits into the cavity, it cannot chelate Cu(II). This idealised picture of the origin of enantioselectivity is probably only true for a small fraction of the binding sites.



### 1.3.3 Metal Chelating Lipids

As the specific targeting of proteins to interfaces is important for applications in biomedicine and to study protein interactions in biological membranes *Arnold et al.* prepared chelating amphiphiles.<sup>91</sup> For targeting proteins to monolayer and bilayer assemblies, they synthesised a lipid with an IDA moiety in the head group (**46**). When loaded with Cu(II), small quantities of this IDA-lipid in monolayers and liposomes of distearoyl phosphatidylcholine (DSPC) effectively bind a small histidine-rich protein,

myoglobin. Horse heart myoglobin contains 11 histidines, of which at least four can coordinate to Cu(II)-IDA.<sup>92</sup>

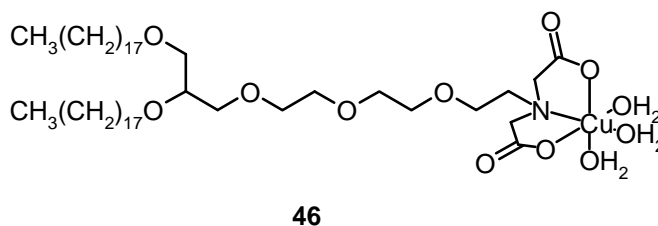


**Figure 19.** Cu(II)-IDA-lipid **46**.

The binding studies focus on myoglobin interacting with monolayers and vesicles of DSPC and IDA-lipid **46** containing Cu(II) or Ca(II). Because imidazole is not a good ligand for Ca(II) ( $K_a = 1.2 \text{ M}^{-1}$ ),<sup>93</sup> this divalent ion provides a noncoordinating surface for comparison. Monolayer surface pressure-area ( $\pi$ -A) isotherms, measurements of protein binding to liposomes, and ESR analyses of Cu(II)-containing liposomes in the presence of unmodified and diethyl pyrocarbonate (DEPC)-modified protein were used to examine the lipid – protein interactions. The results indicated that myoglobin is binding to these artificial membrane assemblies. The binding is significantly enhanced by coordination of surface histidines to Cu(II) ions immobilised at the membrane surface ( $K_a > 10^6 \text{ M}^{-1}$ ). One year later in 1995, the same group synthesised a new IDA-lipid unit.<sup>94</sup> In addition to the targeting function, it is also desirable to have the capability to directly probe molecular redistribution or assembly that accompanies protein binding. Thus the new IDA-lipid **47** (PSIDA) incorporated a fluorescent pyrene label in the lipid tail.

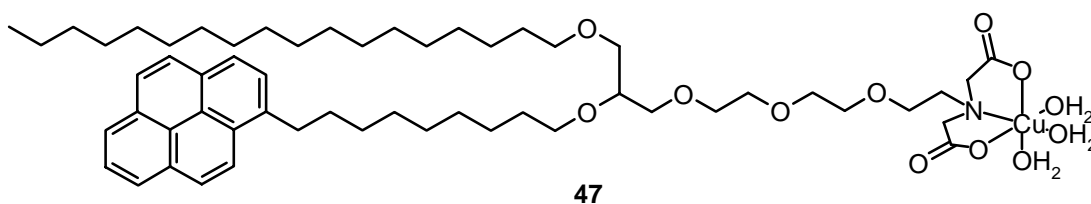


**Figure 20.** Fluorescent IDA-lipid **47**.

These emitting probes of the lipid membrane are sensitive to protein binding and recognition of lipid components. In the course of studying ligand-induced reorganisation of the fluorescent lipid **47** in membrane assemblies, *Arnold* and his group observed that metal ion binding can strongly affect the ratio of the excimer to monomer emission intensities. The pyrene-labeled IDA lipid also serves as a membrane “receptor mimic” in that binding of external ligands can induce its reorganisation in the membrane and change its

fluorescence properties.<sup>95,96</sup> Using these properties of the modified lipid, they show that a small globular protein, the soluble domain of cytochrome *b*<sub>5</sub>, can be targeted with high affinity to PSIDA-containing lipid monolayers via metal coordination to a six-histidine peptide appended to the protein's C-terminus (6-His cyt *b*<sub>5</sub>). The poly(histidine) fusion peptide and metal-chelating IDA lipid comprise an effective and versatile system for targeting proteins to lipid assemblies.

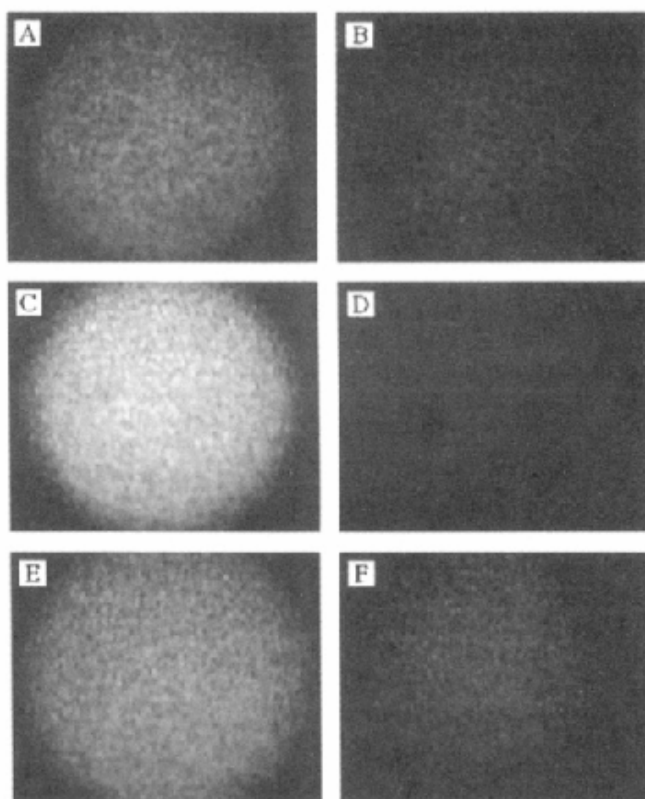


**Figure 21.** Fluorescence micrographs of fluorescein labeled 6-His cyt *b*<sub>5</sub> in the presence of metal-chelating lipid monolayers spread on a buffered subphase (20 mM MOPS, 100 mM NaCl, pH 7.5) at  $\pi = 25\text{mN/m}$ . (A) 10% PSIDA-Ni(II), (B) 10% PSIDA, no metal, (C) 30% PSIDA-Ni(II), (D) 30% PSIDA, no metal, (E) 100% PSIDA-Ni(II), and (F) 100% PSIDA, no metal.

In 1997 *Arnold et al.*<sup>97</sup> reported the use of such metal-chelating lipids in the application of 2D protein crystallisation. A 2D protein crystallisation requires the immobilisation and orientation of a protein at the monolayer surface in high concentration, without loss of mobility.<sup>98</sup> This mobility is supplied largely by the lipid monolayer. Crystallisation is generally performed using fluid-phase monolayers. For targeting proteins to the interface, various classes of interactions have been employed. In most cases, specific ligands have been used to promote crystallisation. In each instance, a unique lipid containing the appropriate affinity ligand was required. Using the concept of targeting proteins through



coordination of amino acid side chains to lipid-bound metal ions the same metal-containing lipid can be used to bind to a large variety of peptides. For this purpose lipid **48** was specifically designed for 2D crystallisation.

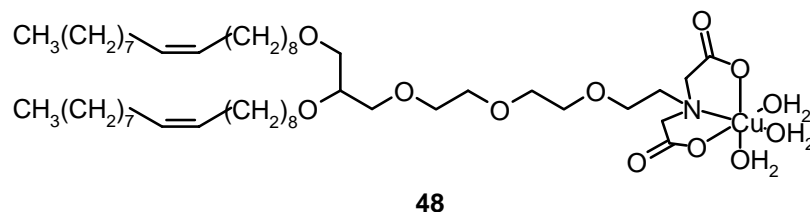


**Figure 22.** Metal chelating lipid **48**.

Unsaturated oleyl tails are utilized to provide the required monolayer fluidity. The utility of this lipid for 2D protein crystallisation is demonstrated using the tetrameric protein streptavidin. Fluorescence microscopy is used to confirm and further characterise the streptavidin crystallisation process.

## 2. Nitrilotriacetato (NTA) Complexes

### 2.1 Structures

First published in the same year as the IDA ligand, nitrilotriacetic acid (NTA) has been widely used as a chelate for more than 60 metal ions.<sup>99</sup> Most common are NTA complexes of Al(III),<sup>100</sup> Cu(II),<sup>101</sup> Cd(II),<sup>102</sup> Ni(II),<sup>103</sup> Zn(II),<sup>104</sup> Cr(II and III),<sup>105</sup> Fe(II and III)<sup>106</sup> and Co(II and III).<sup>107</sup> Table 9 summarises the metal ion binding affinity for some typical NTA complexes.

**Table 9.** Overview of binding constants of different metals towards NTA<sup>22</sup> measured at 20 °C (\* = 25 °C)

Ion	Equilibrium	log K
Fe <sup>2+</sup>	ML/M.L	8.33*
	ML <sub>2</sub> /M.L <sup>2</sup>	12.8*
Co <sup>2+</sup>	ML/M.L	10.38
	ML <sub>2</sub> /M.L <sup>2</sup>	14.33
Ni <sup>2+</sup>	ML/M.L	11.5
	ML <sub>2</sub> /M.L <sup>2</sup>	16.32
Cu <sup>2+</sup>	ML/M.L	12.94
	ML <sub>2</sub> /M.L <sup>2</sup>	17.42
Fe <sup>3+</sup>	ML/M.L	15.9
	ML <sub>2</sub> /M.L <sup>2</sup>	24.3*
Cd <sup>2+</sup>	ML/M.L	9.78
	ML <sub>2</sub> /M.L <sup>2</sup>	14.39
Zn <sup>2+</sup>	ML/M.L	10.66
	ML <sub>2</sub> /M.L <sup>2</sup>	14.24
Al <sup>3+</sup>	ML/M.L	11.4

### 2.1.1 Cu(II) complexes

The higher stability of the NTA complexes in comparison to the corresponding IDA analogues is due to the additional coordinating ligand site. Carboxylate donor groups and the central nitrogen atom provide the tetradentate chelation. The chelation of a Cu(II) ion leads to the formation of three five-membered rings.<sup>108</sup>

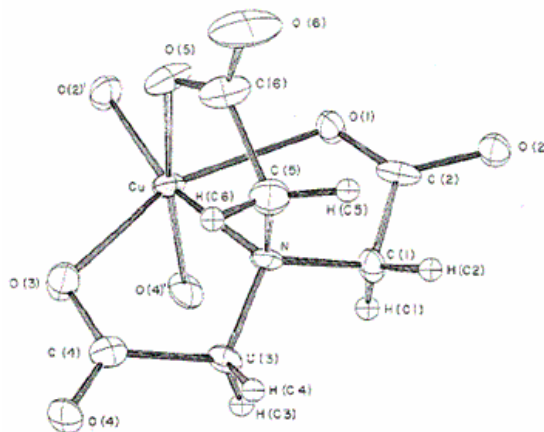


**Figure 23.** Structure of the Cu-NTA chelate in the solid state.<sup>108</sup>

The two remaining coordination sites on the copper ion can bind to Lewis-basic donor atoms.<sup>109</sup> Figure 24 shows two Cu(II)-NTA complexes and a trans-1,2-bis(4-pyridyl)ethylene (bpe) as bridging ligand.

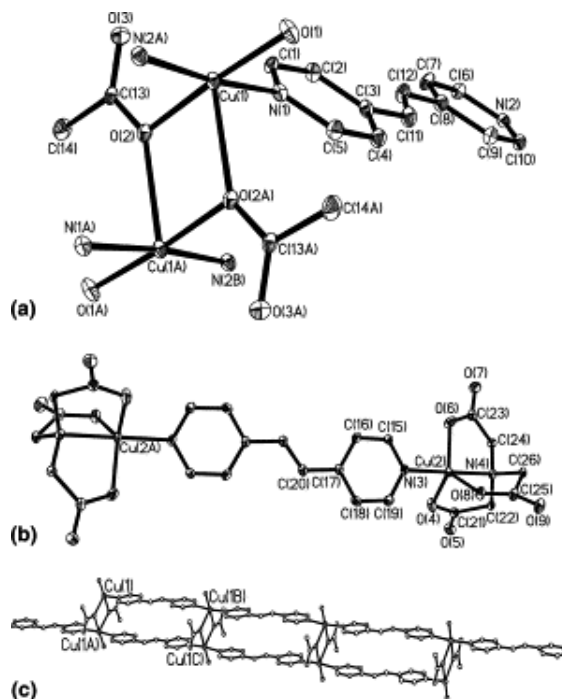


**Figure 24.** X-ray structure of  $[\text{Cu}_2(\text{nta})_2(\text{bpe})]^{2-}$  (b).

### 2.1.2 Ni(II) complexes

Ni(II)-NTA complexes were used to coordinate nucleobases as additional Lewis basic ligands.<sup>110</sup> The crystal structures of co-crystals of Ni(II)-NTA and adenine or cytosine demonstrate the potential of NTA complexes to form aggregates with such biologically interesting ligands. However, the X-ray structure reveals that hydrogen bonds and not a reversible coordination stabilise the aggregate of nucleobase and metal complex.

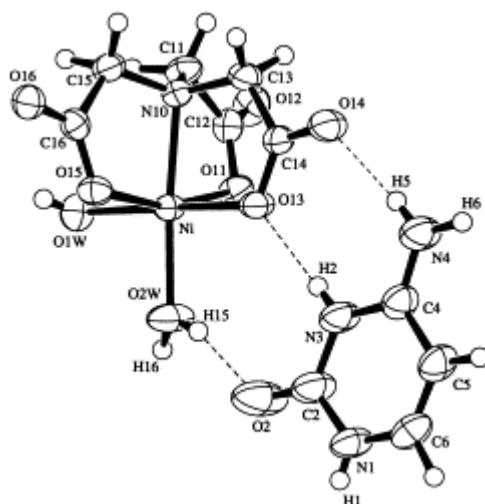


**Figure 25.** Molecular structure of  $[\text{Ni}(\text{nta})(\text{H}_2\text{O})_2] \cdot (\text{cytosinium}) \cdot 2 \text{H}_2\text{O}$  in the crystal.

### 2.1.3 Zn(II) complexes

The structure of the  $\text{Na}[\text{Zn}(\text{NTA})(\text{H}_2\text{O})]$  is isomorphous with the  $\text{Na}[\text{Cu}(\text{NTA})(\text{H}_2\text{O})]$  discussed above.<sup>111</sup> The structure consists of an intricate network of ligand-bridged coordination complexes. Two coordination sites, which remain vacant after NTA coordination of the Zn(II) ion are occupied by non-chelating O atoms from other  $[\text{Zn}(\text{NTA})]^-$  ions.

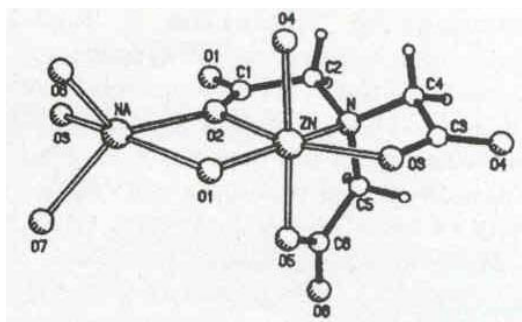


**Figure 26.** Structure of the  $\text{Na}[\text{Zn}(\text{NTA})(\text{H}_2\text{O})]$  complex in the crystal.

### 2.1.4 Cr(III) complexes

Chelating Cr(III) metal ions by NTA leads to different species in solution, depending on the pH.<sup>112</sup> Solutions of pH 5.5 result in the formation of  $\text{Cs}_2[\text{Cr}(\text{nta})_2(\mu\text{-OH})_2]\cdot 4\text{H}_2\text{O}$ , while solutions at pH 1 give  $[\text{Cr}(\text{nta})(\text{H}_2\text{O})_2]$  and at pH 5-6  $[\text{Cr}(\text{nta})(\text{H}_2\text{O})(\text{OH})]^-$  is obtained. A similar complex is formed when acetate is added (figure 27).<sup>113</sup>

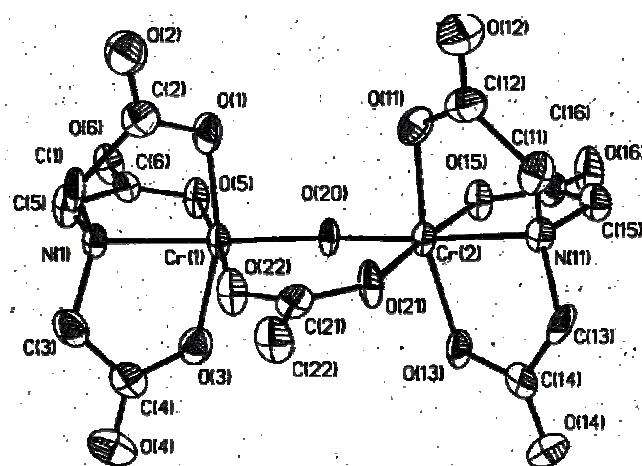


**Figure 27.** Molecular structure of the dimeric unit in  $\text{K}_2[\text{Cr}(\text{nta})(\text{OH})(\text{acetato-O,O})\text{Cr}(\text{nta})]\cdot 4\text{H}_2\text{O}$  in the solid state.<sup>113</sup>

The best investigated ligand for Cr(III)-NTA is imidazole.<sup>114</sup> The crystal structure of figure 28 shows two imidazole residues coordinating to the Cr(III) ion.

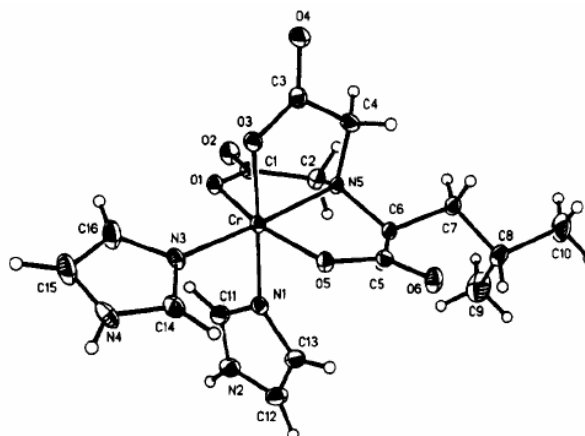


**Figure 28.** Crystal structure of Cr(III)-NTA coordinating additional imidazole groups.

### 2.1.5 Fe(III) complexes

A more oxophilic metal complex is obtained with Fe(III) ions as chelated metal ion with NTA. The octahedral coordination geometry of the complexes is similar to structures obtained with other metal ions.<sup>115</sup>

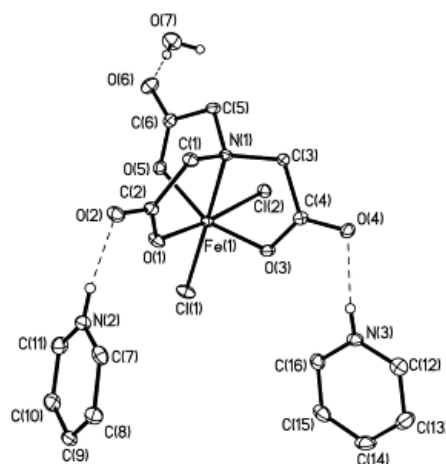


**Figure 29.** Structure of  $[\text{Fe}(\text{nta})\text{Cl}_2][\text{pyH}]_2$  in the solid state.<sup>116</sup>

The oxophilic character of these Fe(III)-NTA complexes is illustrated by their ability to bind to  $\beta$ -keto-carboxylates. The antibiotic ciprofloxacin coordinates to the iron center by its carboxy and keto oxygen atoms.

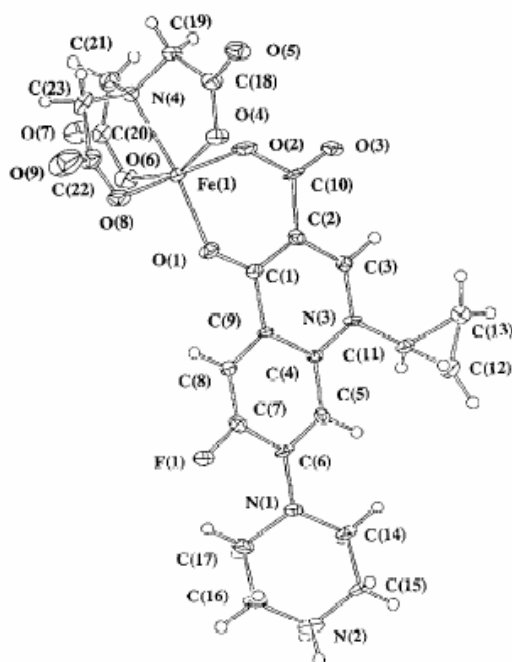


**Figure 30.** Structure of  $[\text{Fe}(\text{cip})(\text{nta})]$  (cip = ciprofloxacin) in the solid state.<sup>117</sup>

### 2.1.6 Co(III) complexes

NTA metal complexes with Co(III) ions have been investigated in detail. Crystal structures with NTA acting as a tridentate ligand,<sup>118</sup> tetradentate NTA ligand,<sup>119</sup> oxo-bridged Co(III)-NTA complexes,<sup>120</sup> complexed carbonate ions (see figure 31)<sup>121</sup> and complexed amino acids (see figure 32)<sup>122</sup> have been reported.

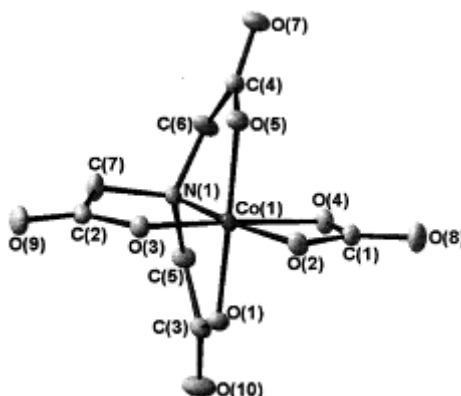


**Figure 31.** Structure of the  $[\text{Co}(\text{nta})(\text{CO}_3)]^{2-}$  anion in the solid state.

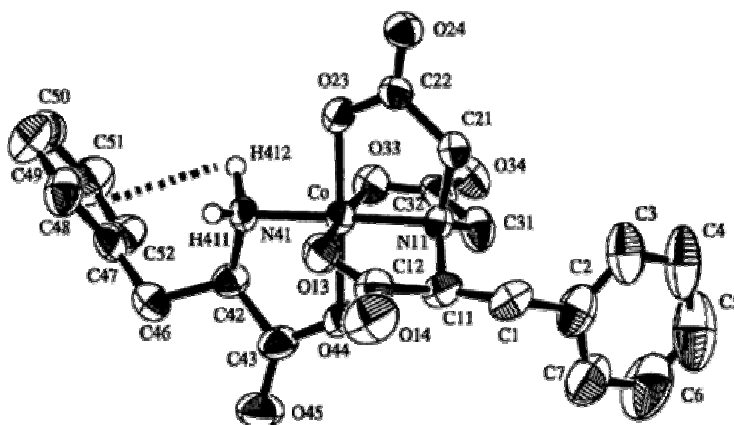


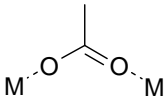
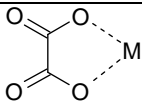
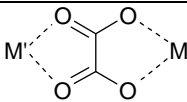
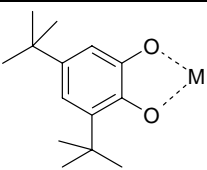
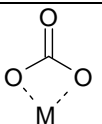
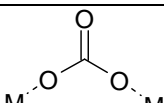
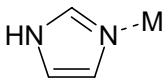
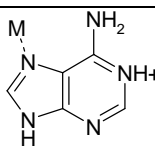
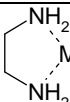
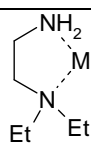
**Figure 32.** Structure of *trans*(N)- $[\text{Co}(\text{bcmpa})((R)\text{-phe})]^-$  anion in the solid state.

Overall, the reported crystal structure analyses of NTA complexes with Cu(II), Cr(III), Zn(II), Co(III) or Fe(II) ions, which coordinate additional ligands, show similar coordination geometries for the metal ion and the NTA ligand.

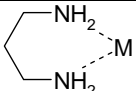
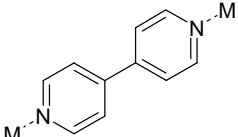
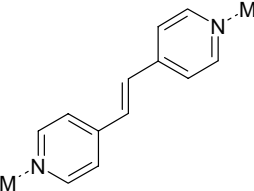
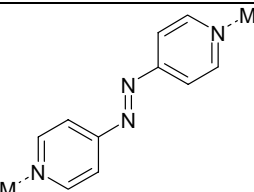
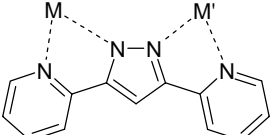
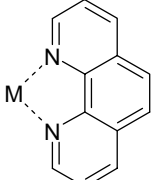
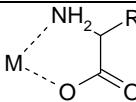
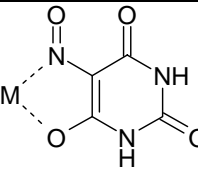
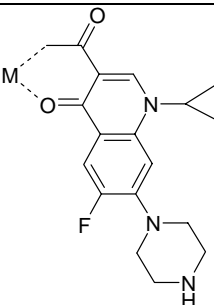
### 2.1.7 NTA complexes in solid state (tabulated)

Table 10 summarises all X-ray structures registered at the Cambridge Crystallographic Database according to the selection criteria previously mentioned.

**Table 10.** References of X-ray structure analyses selected from the Cambridge structural database of transition metal NTA complexes coordinating an additional complex ligand (M = transition metal – NTA complex)

Additional Ligand	Metal Ions				
	Cu(II)	Ni(II)	Co(III)	Fe(III)	Cr(III)
					See ref.
				See ref.	
			See ref. <sup>123</sup>		
				See ref. <sup>124</sup>	
			See ref.		
				See ref. <sup>125</sup>	
					See ref.
		See ref.			
			See ref. <sup>126</sup>		
			See ref.		



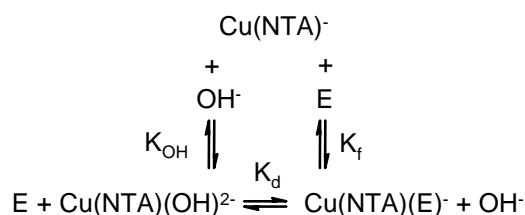
			See ref. <sup>127</sup>		
	See ref. <sup>128</sup>				
	See ref.				
	See ref. <sup>129</sup>				
					See ref. <sup>130</sup>
				See ref. <sup>131</sup>	
			R=Gly, Leu, Phe, Trp		
			See ref. <sup>132</sup>		
				See ref.	

## 2.2 Recognition Processes in Solution

### 2.2.1 Interactions of Acids, Amino Acids and their Esters with Divalent Metal NTA Complexes

*Angelici et al.* studied the interactions of complexes of divalent metal ions and quadridentate ligands with amino acids and their esters.<sup>133</sup> Divalent ions used for these experiments are manganese, cobalt, nickel, copper, zinc and lead. Binding constants of amino acids to these metal complexes were determined using potentiometric measurements. Titration data of stoichiometric mixtures of  $[\text{Cu}(\text{NTA})]^-$  and Gly or EtVal were fitted to the equilibrium shown in scheme 6, which involves the formation of a Cu(II) hydroxo species. The titration data show that hydroxo complex formation occurs only by the displacement of the acid or ester (E).

**Scheme 6.** Binding equilibrium between ester (E), hydroxo anion and  $[\text{Cu}(\text{NTA})]^-$



$K_d = [\text{MZO}H^{2-}][\text{E}]/[\text{MZE}^-][\text{OH}^-] = K_{\text{OH}}/K_f$ , where  $K_f$  is the formation constant of the acid or ester with  $[\text{Cu}(\text{NTA})]^-$ .<sup>134</sup> Similar experiments were carried out with the other metal ions; table 11 summarises the resulting data.

**Table 11.** Aggregate formation constants of  $[\text{M}(\text{NTA})]^-$  with glycine and ethyl valinate at 25 °C

$\text{M}^{2+}$	Log $K_{f\text{EtVal}}$	Log $K_{f\text{Gly}}$
Mn	$2.39 \pm 0.02$	$2.24 \pm 0.005$
Co	$1.88 \pm 0.014$	$3.65 \pm 0.014$
Ni	$2.03 \pm 0.011$	$4.95 \pm 0.011$
Cu	$2.88 \pm 0.002$	$5.46 \pm 0.008$
Zn	$1.58 \pm 0.08$	$3.64 \pm 0.007$
Pb	$1.55 \pm 0.10$	$1.93 \pm 0.009$

The assumption was made that only a mono ester complex is formed with a 1:1 ratio of  $[M(NTA)]^-$  and the ester. This is supported for copper ions by the observation that only a mono amine complex is observed with  $[Cu(NTA)]^-$  even in the presence of a 50-fold excess of ammonia. Measurements with other metal ions did not indicate the formation of bis-ester complexes under the experimental conditions. The authors do not report species distribution plots, therefore the pH at which complete aggregate formation occurs in solution remains unclear.

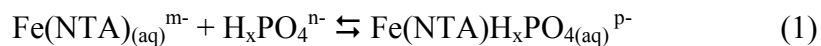
**Table 12.** Aggregate formation constants of  $[Cu(NTA)]^-$  with amino acids and their esters at 25 °C (log standard deviation <0.01)

Acid	pK <sub>a</sub>	Log K <sub>f</sub>	Ester	pK <sub>a</sub>	Log K <sub>f</sub>
Gly	2.35		Me	7.62	3.06
	9.78	5.44	Et	7.68	3.15
			n-Bu	7.78	3.33
Ala	2.34				
	9.87	5.42	Et	7.91	3.10
Phe	1.83				
	9.13	4.99	Et	7.12	2.77
Leu	2.36				
	9.60	5.35	Et	7.64	2.79
Val	2.32				
	9.62	5.10	Et	7.75	2.88
β-Ala	3.55				
	10.35	4.56	Et	9.13	3.65
His	1.85	4.16 (monodentate)			3.98
	6.04		Me	7.23	
	9.12	5.73 (bidentate)			4.90

The coordination of His and MeHis to  $[Cu(NTA)]^-$  leads to more complex equilibria, as these ligands are potentially tridentate. Cu(II)-His systems contain mixtures of species in which His is coordinated either as anion or in its zwitterionic form.<sup>135</sup>

Blakney *et al.* measured the binding constants of Gly to Cd(II)- and Zn(II)-NTA using NMR techniques.<sup>136</sup> The results confirm previously reported data from potentiometric

titrations. In 2003 *Crumbly et al.* reported ternary complexes of Fe(NTA) with phosphate and acetohydroxamic acid.<sup>137</sup> The investigated overall reaction is shown in equation 1, where  $\text{Fe(NTA)}_{(\text{aq})}^{m-}$  and  $\text{H}_x\text{PO}_4^{n-}$  represent the various hydrolyzed and protonated forms of the reactants, depending on pH.



The kinetics of the complex formation was followed using UV-spectroscopy and the same reaction was carried out with acetohydroxamic acid replacing phosphate.

### **2.2.2 Hexahistidine-Tag-Mediated Fluorescent Labeling with (Ni(II): Nitrilotriacetic Acid)<sub>n</sub> – Fluorochrome Conjugates<sup>138</sup>**

Structural and mechanistic characterisation of proteins by fluorescence resonance energy transfer (FRET) requires the ability to incorporate fluorescent probes at specific, defined sites. Proteins lacking these specific sites need to be modified. One strategy involves use of the “hexahistidine tag”<sup>139</sup> – i.e., the amino acid sequence His<sub>6</sub> – to target site-specific fluorescent labeling. The hexahistidine tag is known to interact tightly with transition-metal complexes, including Ni(II):nitrilotriacetic acid (Ni(II):NTA). The hexahistidine tag can be introduced at protein termini or internal sites by using standard molecular-biology procedures. These tags should interact tightly with (Ni(II):NTA)<sub>n</sub>-fluorochrome conjugates (figure 33).

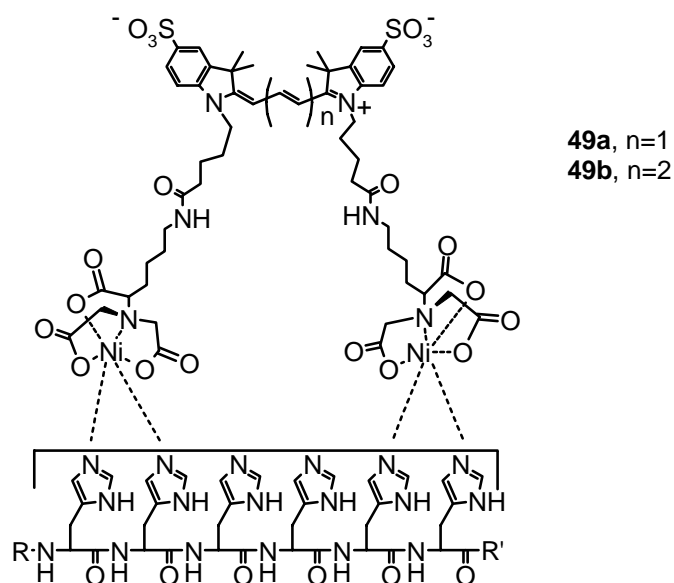
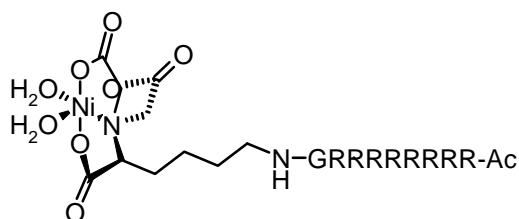


**Figure 33.** Schematic representation of the mode of interaction of **49a** or **49b** with the hexahistidine tag.

To test these hypotheses *Kapanidis et al.* synthesised derivatives of the widely used cyanine fluorochromes Cy3 and Cy5. Fluorescence anisotropy experiments established that **49a** and **49b** exhibit high affinity for the hexahistidine tag ( $K_D = 1.0 \mu\text{M}$  for **49a**;  $K_D = 0.4 \mu\text{M}$  for **49b**). Thus, titration of **49a** and **49b** with an otherwise identical protein lacking a hexahistidine tag results in little or no increase in fluorescence anisotropy. FRET experiments confirm that **49a** and **49b** exhibit high affinity and high specificity for the hexahistidine tag ( $K_D = 0.9 \mu\text{M}$  for **49a**;  $K_D = 0.3 \mu\text{M}$  for **49b**; specificity >95%).

### 2.2.3 Arginine Carrier Peptide Bearing Ni(II) NTA

The ability to bind very tightly to poly-His-tag proteins via NTA complexes stimulated *Futaki et al.* to combine this function with a carrier peptide, which is able to invade living cells.<sup>140</sup> Octaarginine was used as such a peptide and was linked to a NTA based chelator.



**50**

**Figure 34.** Arginine carrier peptide (R8-NTA-Ni(II), **50**) with binding site for His-tagged proteins.

Covalent cross-linking between the cargo proteins and the carrier peptide is necessary for the cellular introduction. The histidine-tagged enhanced green fluorescent protein (H6-EGFP) forms a noncovalent complex with the carrier peptide. The interactions ( $K_D = 4.2 \cdot 10^{-7}$  M) are strong enough that the protein penetrates into cells. Internalisation of the H6-EGFP was monitored by laser confocal microscopy after 3 h incubation of the protein with HeLa cells at 37 °C. Significant internalisation of H6-EGFP was observed when the cells were treated with H6-EGFP (10  $\mu$ M) in the presence of R8-NTA-Ni(II) (50  $\mu$ M).

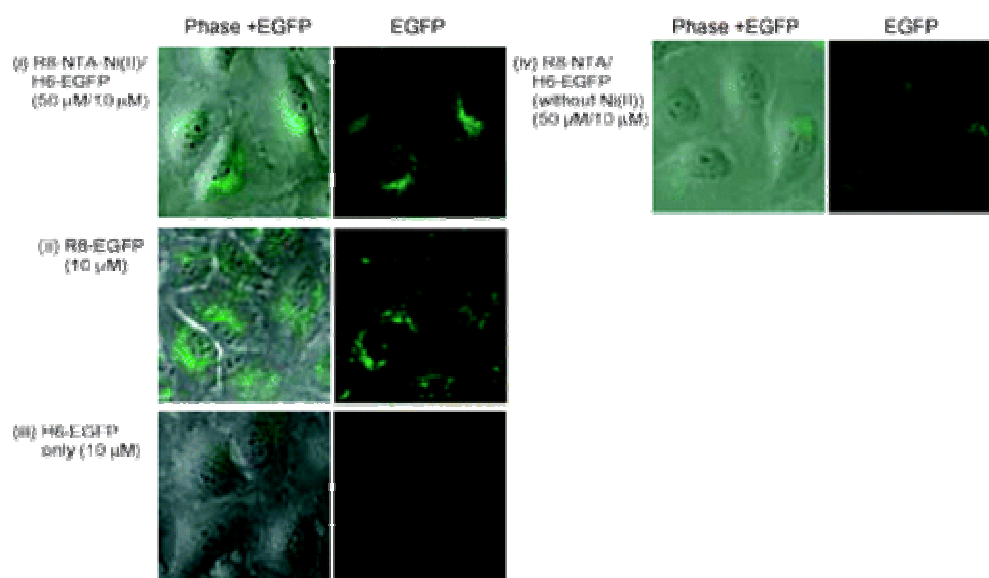


**Figure 35.** Confocal microscopic observation of the HeLa cells treated with R8-NTA-Ni(II)/H6-EGFP for 3 h.

## 2.3 Recognition on Surfaces

### 2.3.1 Immobilised Metal Ion Affinity Chromatography (IMAC)

Immobilised metal ion affinity chromatography (IMAC) on resins coupled with chelating agents is widely used to purify proteins containing exposed histidine and cysteine side chains. Recent reviews cover applications of the technique and studies thoroughly (see references cited at the 1.3.1. IDA IMAC chapter), so that we exclude this application from this overview.

### 2.3.2 Immobilisation of Ni(II)-NTA on Microtiter Plates

*Paborsky et al.* describe the application of a NTA derivative, *N,N*-bis[carboxymethyl]lysine (BCML), which can be coupled by simple amide chemistry to carboxyl groups on commercially available microtiter plates coated with maleic anhydride.<sup>141</sup>

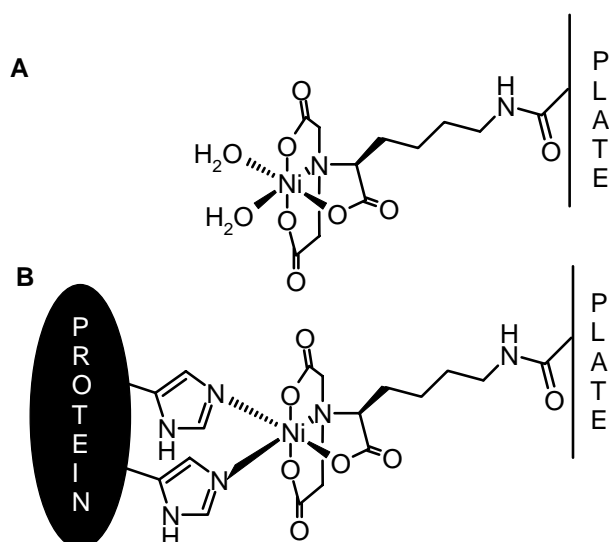


**Figure 36.** Immobilisation of proteins on microtiter plates derivatised with *N,N*-bis[carboxymethyl]lysine (BCML). Two adjacent histidine residues in a protein containing a 6His tag bind in bidentate fashion (B) to a BCML-derived plate (A).

The NTA modified plate was charged with Ni(II) ions and used to capture either recombinant IL8 or recombinant sTF, both engineered to contain 6His tags. The amount of each protein captured by the Ni(II)-NTA plate was measured by sandwich ELISA. To determine the specificity of the Ni(II)-NTA plate for proteins containing 6His tags, the capture of IL8-6His was compared with native IL8 (lacking a 6His tag) and the capture of 6His-sTF was compared with FLAG-sTF. The IL8-6His was bound by the Ni(II)-NTA plate in a dose-dependent manner, reaching saturation at approximately 5 nM. In contrast, the native IL8 did not bind the plate, indicating that the binding was specifically through the six histidine residues. Results comparing 6His-sTF and sTF lacking the 6His tag were similar.

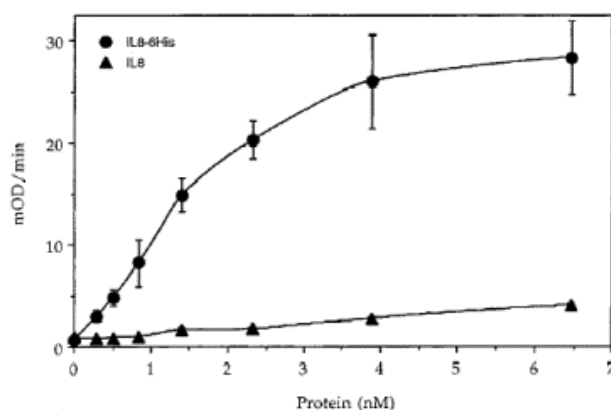


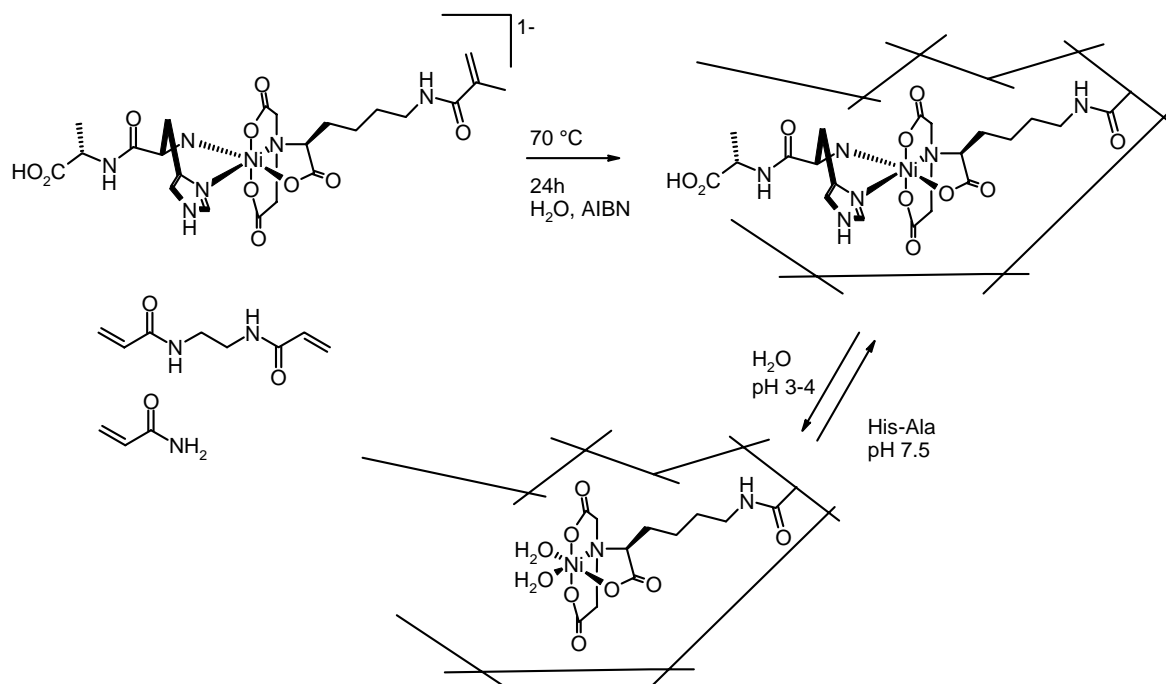
**Figure 37.** Specificity of Ni(II)-NTA plate for 6His-containing proteins. Purified IL8-6His (dots) or native IL8 (triangle) was added to the Ni(II)-NTA ELISA plate and binding was detected.

### 2.3.3 Molecular Imprinting of Ni(II)-NTA Complexes

The preparation of molecular imprinted polymers (MIPs) selective for amino acids and small peptides has been limited to traditional imprinting formulations, such as polyacrylates. Methacrylic acid is the functional monomer in organic solvents. *Hart et al.* developed a polymerisable acrylamide functionalised NTA ligand.<sup>142</sup> By incorporating a Ni(II) – NTA complex into the polymer they provided a “handle” to bind peptides containing N-terminal His residues in water. The ligand occupies four positions in the octahedral coordination sphere of Ni<sup>II</sup> leaving the remaining two for selective binding of His. The polymerisable methacrylamide – NTA – Ni(II) mixed complex was prepared by combining aqueous solutions of NTA monomer with NiSO<sub>4</sub>. The pre-polymerisation template complex was then formed by addition of the *N*-terminal histidine peptide His-Ala. Copolymerisation of this complex (5 mol%) with *N,N'*-ethylenebisacrylamide as cross-linking monomer (82 mol%) and acrylamide (13 mol%) provided a pale blue monolith.



**Scheme 7.** Schematic representation of the peptide imprinting process



The polymer-bound NTA – Ni(II) complex in the absence of peptide is pale green. Upon binding an N-terminal histidine peptide, the color changes to pale blue. This change lends itself to a colorimetric assay of binding of peptides to these materials. Binding isotherms were obtained for the template peptide (His-Ala) as well as three other peptide sequences.

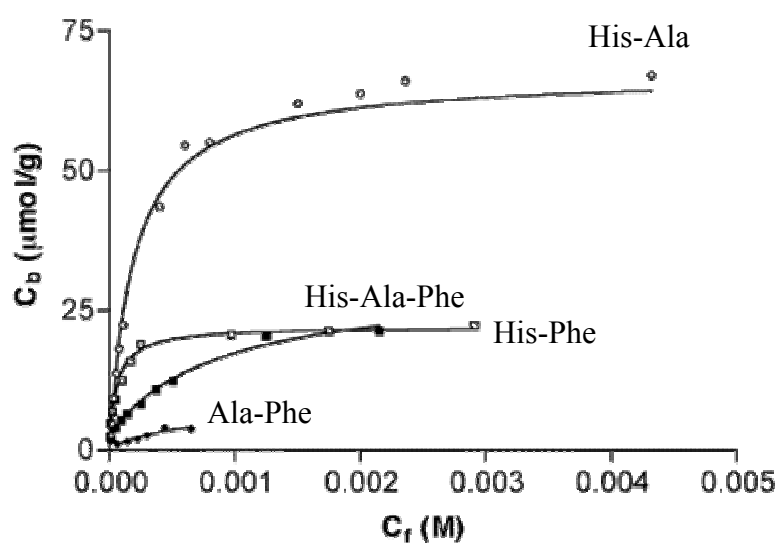


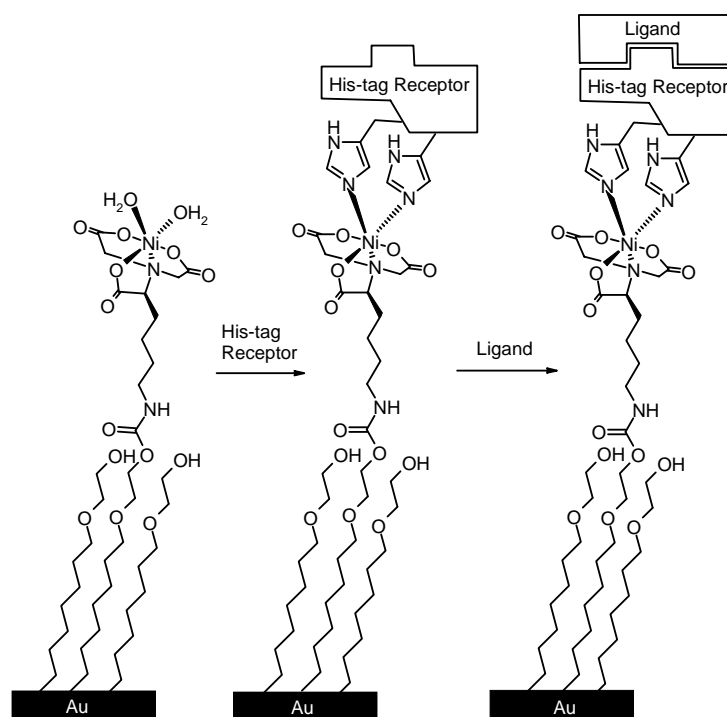
**Figure 38.** Binding isotherms for the rebinding peptides in aqueous solution to a polymer prepared using His-Ala as the template peptide.

It is clear from the binding data that the (His-Ala)-imprinted polymer has a significantly higher capacity for the template peptide over other sequences examined. Non-histidine containing peptides have almost no affinity for the polymer.

### 2.3.4 Immobilisation on Gold Surfaces<sup>143</sup>

Surface plasmon resonance (SPR) is a useful technique for measuring the kinetics of association and dissociation of ligands from proteins in aqueous solution.<sup>144</sup> Varieties of techniques have been used to immobilise proteins on silver or gold films for studies using SPR.<sup>144,145</sup> Whitesides *et al.* developed procedures to modify the surface of gold films by formation of self-assembled monolayers (SAMs) of alkanethiolates.<sup>146</sup> They describe the generation of a SAM functionalised with the Ni(II)-NTA group. Using this way to immobilise proteins wearing a stretch of His-tags, a surface was created, that would specifically immobilise a protein of interest while resisting non-specific binding of other proteins. Therefore, the requirement for non-specific, covalent modification of the protein was avoided.

**Scheme 8.** Procedure for immobilising proteins on surfaces to test for the ability of immobilised proteins to interact with ligands in solution



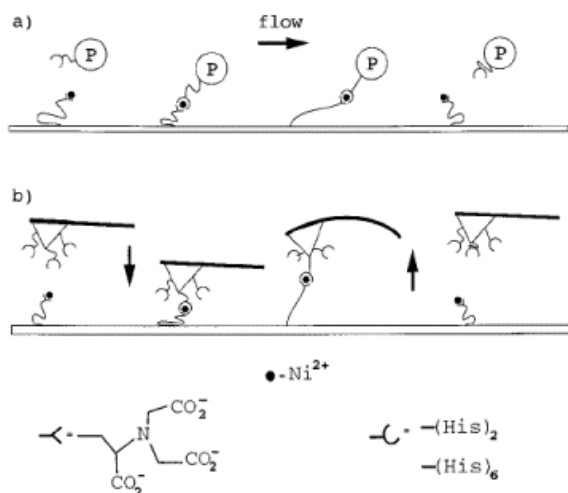
After the His-tag receptor is bound to the modified gold-surface, interactions between the receptor and a ligand in solution could be studied by SPR. A similar approach was used by

*Hoggett et al.* to measure the interaction between *E. Coli* core form of bacterial RNA and immobilised His-tagged form of  $\sigma^{70}$  factor.<sup>147</sup> *Vogel* and co-workers demonstrated the reversible binding of an anti-lysozyme F<sub>ab</sub> fragment modified with a C-terminal hexahistidine extension on similar gold-surfaces.<sup>148</sup> The apparent dissociation constants were determined using SPR and IR-spectroscopy and showed that the immobilisation did not affect the secondary structure of the protein.

Using gold particles as a label for bound Ni(II)-NTA to a His-tag attached to a protein, *Powell et al.* report the construction of Ni(II)-NTA groups fixed on a gold particle.<sup>149</sup> For detection using electron microscopy, it provides a high-resolution site-specific label. With metal enhancement (e.g., silver), the signal was detectable in the light microscope or by the naked eye.

The Ni(II)-NTA His-Tag approach has been used in several examples to create strong intermolecular interactions. However, how strong is the coordination bond between a histidine tag and Ni(II)-NTA? This question asked *Samorì et al.* in 2000.<sup>150</sup> To give an answer they simulated the process involved in the Ni(II)-NTA protein separation techniques by reproducing the approach, binding, stretching and unbinding under external forces between individual His tags and individual Ni(II)-NTA chelating groups in a single-molecule experiment with the scanning force microscope (SFM, see scheme 9).

**Scheme 9.** Sketch of the approach, binding, stretching, and unbinding of a) a His-tagged protein (p) under the flow inside an affinity chromatography column or on a biosensor surface and b) a His-tagged peptide covalently bound to an SFM tip in an approach and retraction cycle.



A n-His-tagged peptide ( $n = 2$  or  $6$ ), HCys-(Gly)<sub>6</sub>-(His)<sub>n</sub>-OH, was covalently attached on its Cys end to a gold-coated SFM tip. The tip was brought into proximity to a substrate

having exposed Ni(II)-NTA groups covalently bound through carboxymethylated dextran linkers, which were attached to a gold surface bearing an alkane C<sub>18</sub> chain. Whenever the *n* x His-tag of the peptide formed a chelate with a Ni(II)-NTA group, a molecular bridge was established between the tip and the substrate. The tip was subsequently retracted at a constant pulling velocity until the bridge broke. The probability of binding events increased from 28 % for 2 x His-tag to 42 % for a 6 x His-tag. Most of the unbinding traces exhibited a single rupture: the distribution of the forces was very broad and peaked at about 500 pN for the 6 x His-tag and about 300 pN for the 2 x His-tag.

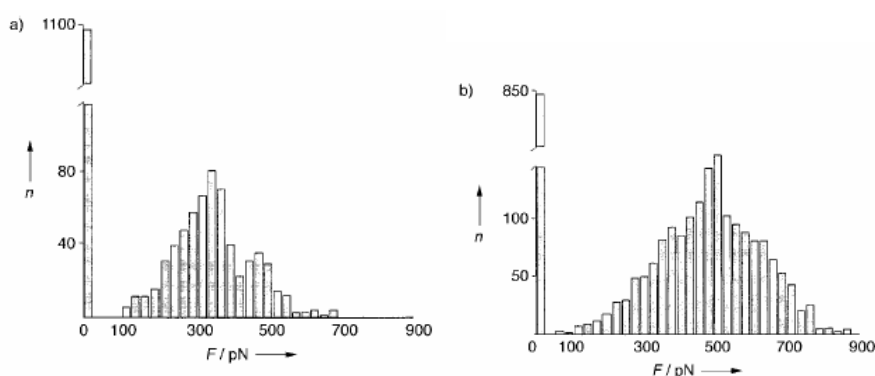
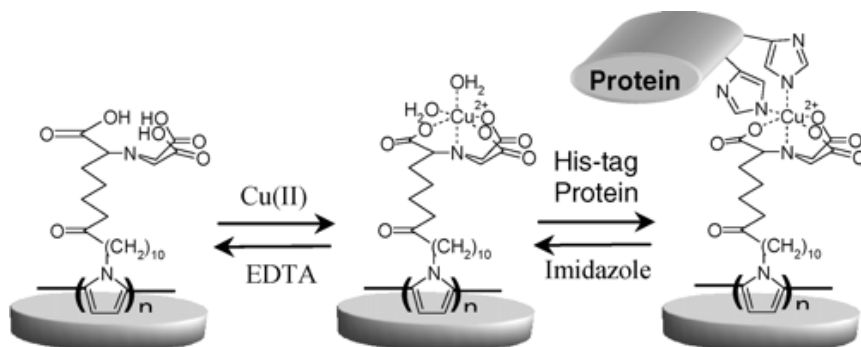


**Figure 39.** Histogram of the distribution (*n*, number of events) of all the unbinding forces (*F*) recorded with the Ni(II)-NTA-functionalised substrate and a) the 2xHis-tag and b) the 6xHis-tag.

### 2.3.5 Electropolymerisation of NTA-Complexes

The electrosynthesis of polymers is one of the known methods that allow the reproducible and precise functionalisation of conductive microsurfaces of complex geometry by organic molecules. *Gondran et al.* successfully synthesised and electro polymerised a NTA derivative bound to a poly(pyrrole) film.<sup>151</sup> The ability of this polymer to bind Cu(II) was investigated using cyclic voltametry.

**Scheme 10.** Schematic representation of the reversible immobilisation of His-tagged biomolecules to an electrogenerated poly(pyrrole)-NTA film



To examine the potential affinity of the metal-poly film for histidine tagged proteins, two platinum electrodes containing the chelating polymer with coordinated Cu(II) ions were soaked in 0.1 M phosphate buffer, one in the presence of His-tagged glucose oxidase (his-GOX, 0.1 mg/mL) and the other in the presence of regular glucose oxidase (GOX, 0.1 mg/mL). In the presence of oxygen, this enzyme catalyzes the oxidation of glucose with the concomitant production of  $H_2O_2$ . Its activity can be monitored via the electrochemical oxidation of  $H_2O_2$ . Using this technique, the electrode coated with his-GOX resulted in markedly higher maximum current density ( $j_{max}$ , determined at glucose saturating conditions) than the electrode incubated with GOX.

### 2.3.6 Metal Chelating Lipids

To link lipid technology to the concept of fusion proteins, *Tampé et al.* synthesised lipid molecules, which contain NTA as a metal chelator head-group able to bind electron donor groups such as imidazole or histidine.<sup>152</sup> The synthesis was carried out with two different amphipatic molecules, a phospholipid (DPPE, **51**), and a dioctadecylamine (DODA, **52**).

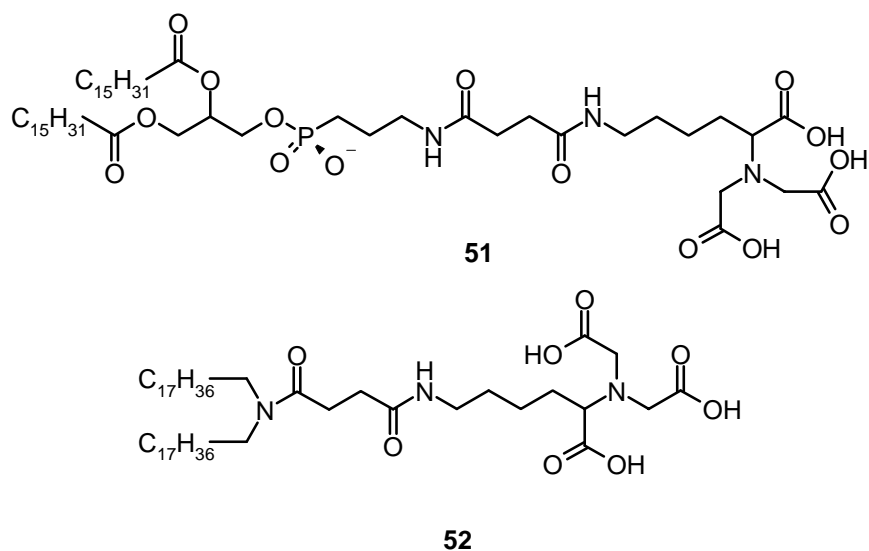
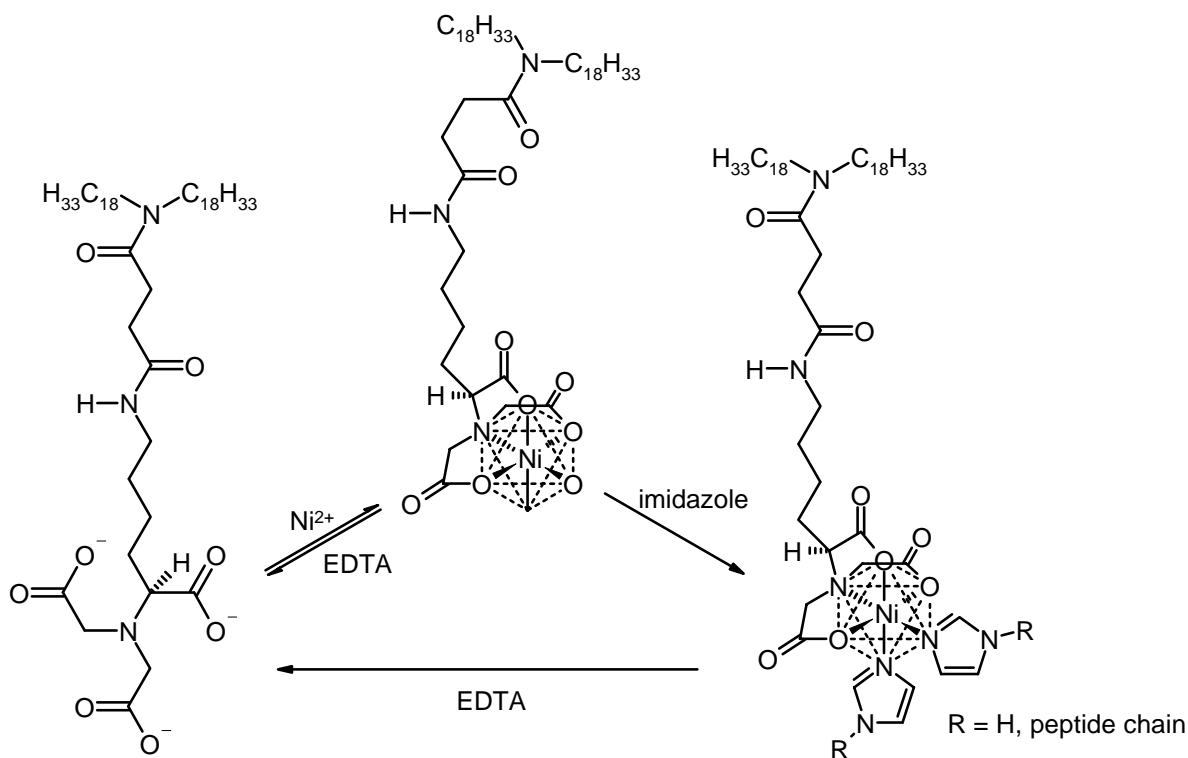


**Figure 40.** Two NTA-lipids.

The lipids were characterised chemically and physically by FTIR spectroscopy, mass spectroscopy, and film balance experiments. Both, NTA-lipids, NTA-DPPE and NTA-DODA spread at the air/water interface. The addition of Ni(II) resulted in complexed Ni(II)-NTA-DODA, which spreads at the air/water interface. Added imidazole interacts specifically with the metal-complexes on the lipid surface.

**Scheme 11.** Schematic illustration of complex formation and imidazole binding to Ni(II)-NTA-DODA at the lipid surface



Addition of EDTA, which has a higher binding affinity for the Ni(II) ions than NTA, reverses the binding event. Therefore, the immobilisation of any bound ligand can be disrupted under mild conditions. In 1995, the same group was able to immobilise fluorescence-labeled histidine-tagged biomolecules.<sup>153</sup> The two-dimensional organisation is visualised by epifluorescence microscopy and film balance-studies.

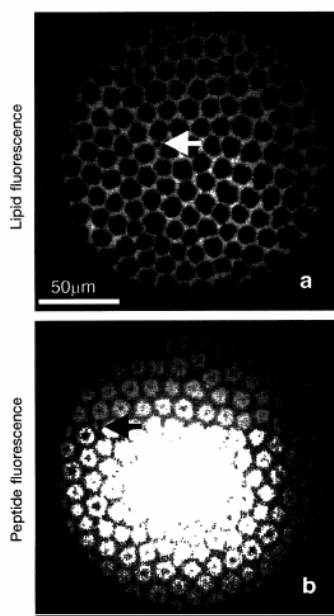


**Figure 41.** Lateral organisation and pattern formation of histidine-tagged peptides (6 nmol) at a Ni(II)-NTA-DOPA/DMPC (1:1) monolayer (10 nmol).

Similar lipid surfaces have been used to grow two-dimensional crystals and to determine structures of various His-tagged proteins.<sup>154</sup> This method of surface modifications using lipid bound metal complexes inspired *Nolan et al.* to modify microspheres by the formation of self-assembled bilayer membranes where the metal chelators have lateral mobility. Interactions on this surface were studied by flow cytometry.

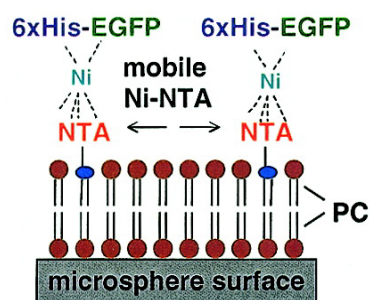
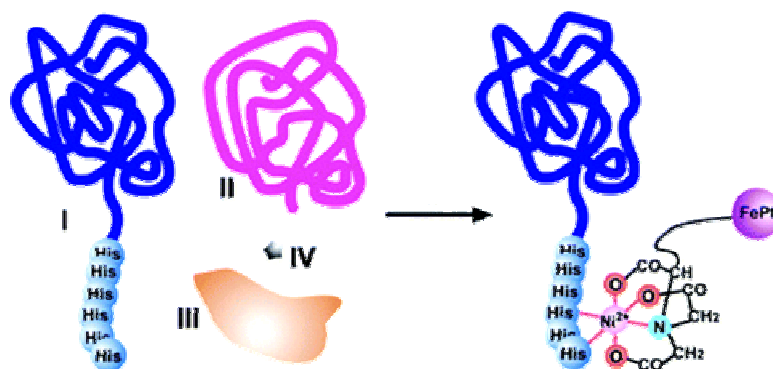


**Figure 42.** Self-assembled bilayers consisting of Ni(II)-NTA-DOGS (Ni(II)-1,2-dioleoyl-sn-glycero-3-[(N(5-amino-1-carboxypentyl)iminodiacetic acid)succinyl]) and egg phosphatidylcholine (PC) on the surface of silica microspheres that confer lateral mobility to the captured His-tagged protein.

### 2.3.7 NTA-Modified Magnetic Nanoparticles

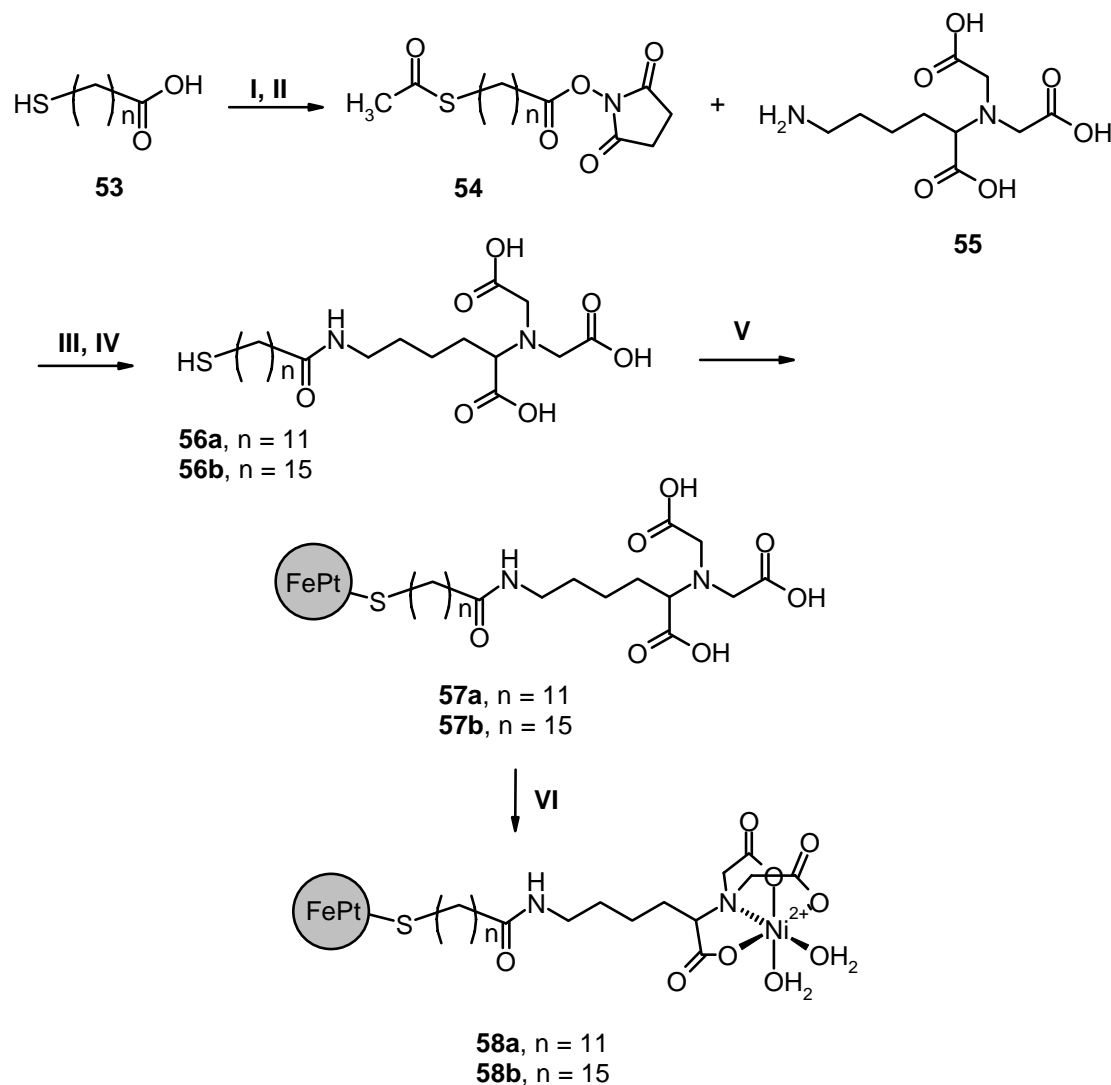
Trying to develop a simpler and more versatile platform for protein purification than IMAC, *Xu et al.* invented surface-modified magnetic nanoparticles as the binder, carrier and anchor for histidine-tagged proteins.<sup>155</sup> Using NTA to attach to FePt magnetic nanoparticles covalently, they developed a simple procedure to obtain pure proteins directly from the mixture of lysed cells within 10 min.

**Scheme 12.** The surface-modified magnetic nanoparticles selectively bind to histidine-tagged proteins in a cell lysate) I: 6His tagged protein; II: other proteins; III: cell debris; IV: colloid contaminants)





**Scheme 13.** Synthesis of NTA-modified magnetic nanoparticles ((I)  $\text{AcOCl}$ ,  $\text{Zn}$ , 85-90 %; (II)  $\text{NHS}$ ,  $\text{DCC}$ ; (III)  $\text{NaHCO}_3$ , 40-46 %; (IV)  $\text{H}_2\text{NNH}_2$ ,  $\text{AcOH}$ , 88-90 %; (V)  $\text{FePt}$  (3-4 nm); and (VI)  $\text{NiCl}_2 \cdot 6\text{H}_2\text{O}$  and buffer)



The procedure to use particles, such as **58**, for protein separation consists of three simple steps: (1) adding **58** into the suspension of the lysed cells and shaking for 5 min, (2) using a small magnet to attract the nanoparticles to the wall of the vial and washing them with deionised water to remove the residual protein solution, and (3) using concentrated imidazole solution to wash the nanoparticles to yield pure proteins. After releasing the proteins, washing with EDTA, buffer, and  $\text{NiCl}_2 \cdot 6\text{H}_2\text{O}$  solution, **58** can be recovered and reused.

### 2.3.8 Immobilisation on Quartz Surfaces

*Vogel et al.* reversibly immobilised His-tagged proteins on quartz in an oriented manner while their function is preserved.<sup>156</sup> The chelator NTA is covalently bound to the hydrophilic quartz surface and subsequently loaded with the divalent metal cation (e.g. Ni(II)). Additional electron-donating groups such as histidine residues subsequently fill the free coordination sites of the chelator-metal complex. The binding of the protein to the NTA is highly specific with reasonable affinities and in addition is fully reversible upon addition of a competitive ligand, reprotonation of the histidine residue, or removal of the metal ion via EDTA complexation (figure 43). Binding and removal from the surface of the modified quartz is visualised using green fluorescent protein in real-time measurements.

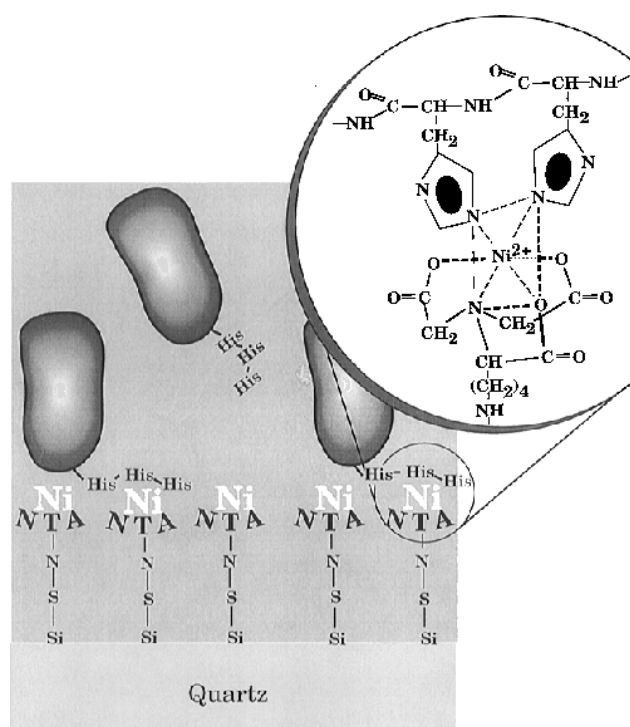


**Figure 43.** Schematic representation of the binding of a His-tagged protein to the quartz surface.

### 3. Bis(2-pyridylmethyl)-amine (BPA, DPA, BISPMA, DIPICA, BISPICAM)<sup>157</sup> Complexes

#### 3.1 Structures of BPA Complexes

In bis(2-pyridylmethyl)-amine (BPA) ligands the carboxylic acid functionalities of IDA are replaced by pyridines. First reported in 1964 by *Kabzinska*, this ligand and derivatives of it are used for complexation of over 50 different metal ions.<sup>158</sup> Most emphasis was put on the investigation of coordination compounds with Cu(II),<sup>159</sup> Zn(II)<sup>160</sup> and Fe(III) ions.<sup>161</sup>

**Table 13.** Selected binding constants of some important types of BPA complexes<sup>22</sup>

<b>Ion</b>	<b>Equilibrium</b>	<b>log K</b>
Co <sup>2+</sup>	ML/M.L	7.74
	ML <sub>2</sub> /M.L <sup>2</sup>	13.05
Ni <sup>2+</sup>	ML/M.L	8.7
	ML <sub>2</sub> /M.L <sup>2</sup>	16.60
Cu <sup>2+</sup>	ML/M.L	14.4
	ML <sub>2</sub> /M.L <sup>2</sup>	19.0
Zn <sup>2+</sup>	ML/M.L	7.57
	ML <sub>2</sub> /M.L <sup>2</sup>	11.93
Cd <sup>2+</sup>	ML/M.L	6.44
	ML <sub>2</sub> /M.L <sup>2</sup>	11.74

##### 3.1.1 Cu(II) Complexes

The Cu(II)-BPA complex [Cu(bpa)Cl<sub>2</sub>] was structurally examined by *Choi et al.*<sup>162</sup> In this compound the Cu(II) ion is coordinated by three nitrogen atoms of the BPA ligand and two chlorine anions in a distorted square-pyramidal environment. The basal plane is defined by the N(1), N(2), N(3) and Cl(2) atoms.

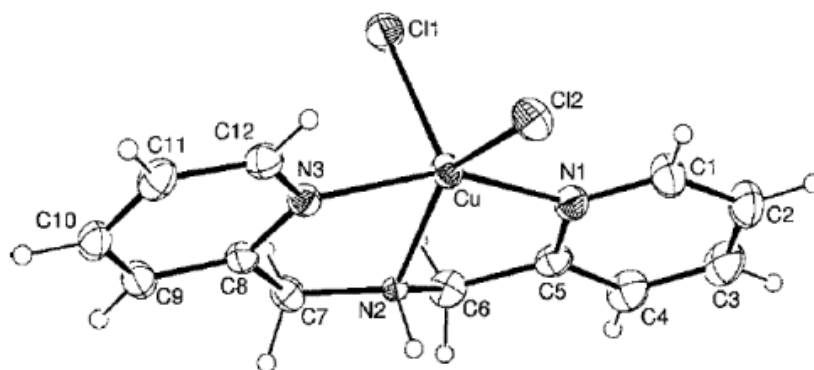


**Figure 44.** An ORTEP view of  $[\text{Cu}(\text{bpa})\text{Cl}_2]$  in the crystal with the atomic numbering scheme (30% probability ellipsoids shown).

Beside complexes with a 1:1 stoichiometry, Cu(II)-BPA coordination compounds with 2:1 stoichiometry are known, which have no vacant coordination sites and are therefore not discussed here.<sup>163</sup> The 1:1 complex can be used to bind additional electron donating groups. *Murakami et al.* reported X-ray structures, which show picolinate (figure 45) and  $\alpha$ -amino acids, like L-Phe (figure 46), coordinated to the Cu(II)-BPA complex.<sup>164</sup>

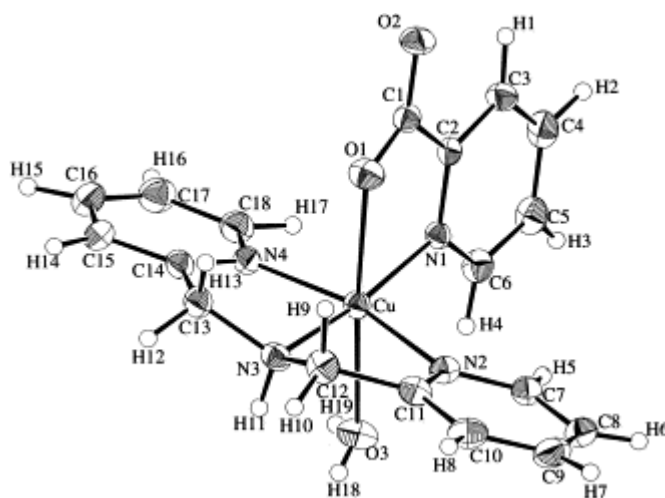


**Figure 45.** ORTEP drawing of  $[\text{Cu}(\text{bpa})(\text{pic})]\text{PF}_6 \cdot \text{H}_2\text{O}$ .

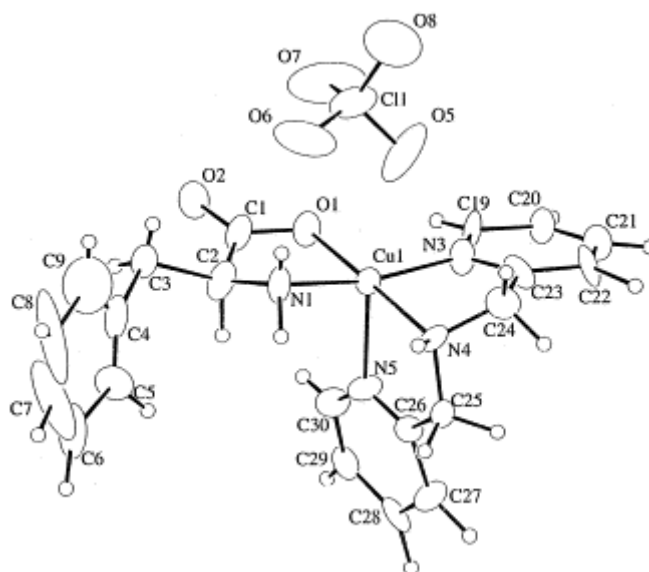


**Figure 46.** Structure of  $[\text{Cu}(\text{bpa})(\text{L-Phe})]\text{ClO}_4$  in the solid state.

A better understanding of the redox reactions between the metal center and the pterin cofactor in phenylalanine hydroxylase led *Yamauchi* and coworkers to examine the binding of pterin-6-carboxylate (ptc, as a cofactor model) to  $[\text{Cu}(\text{bpa})(\text{ptc})]\cdot\text{H}_2\text{O}\cdot\text{CH}_3\text{OH}$ .<sup>165</sup> The studies showed the Cu(II) binding modes of oxidised and reduced pterins. The redox activity of the examined  $[\text{Cu}(\text{bpa})]^{2+}$  - tetrahydropterin systems was influenced by the complex structure.

### 3.1.2 Zn(II) Complexes

The structure of  $[\text{Zn}(\text{bpa})(\text{H}_2\text{O})_2](\text{ClO}_4)_2$  shows a distorted octahedral coordinated Zn(II).<sup>166</sup> This geometry results from the three nitrogen donor groups of the chelating ligand BPA and the additional two water molecules.

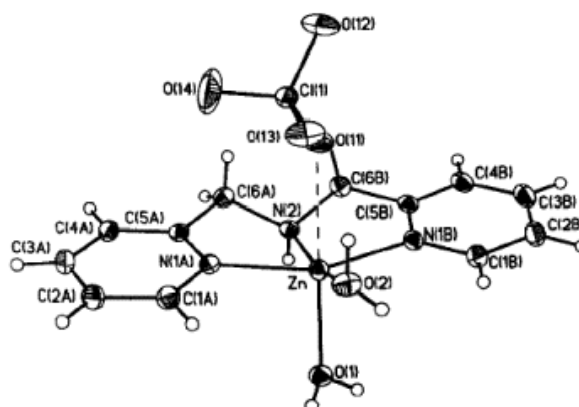


**Figure 47.** ORTEP drawing of the crystal structure of  $[\text{Zn}(\text{bpa})(\text{H}_2\text{O})_2]^{2+}$ .

In contrast to this structure *Wirbser et al.* reported a pentacoordinated Zn(II) structure.  $[\text{Zn}(\text{bpa})\text{Cl}_2]$  shows a trigonal bipyramidal coordination geometry in the solid state.<sup>167</sup>

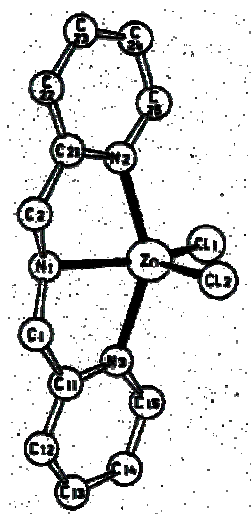


**Figure 48.** Structures of  $[\text{Zn}(\text{bpa})\text{Cl}_2]$  in the crystal.

As the BPA ligand uses only three coordination sites of an octahedral coordinating Zn(II) ion,  $[\text{Zn}(\text{bpa})_2]^{2+}$  complexes with a 2:1 ligand to metal ion stoichiometry are known.<sup>168</sup> One of the ions which can additionally bind to  $[\text{Zn}(\text{bpa})]^{2+}$  complexes are phosphates. In a more complicated structure *Vahrenkamp et al.* reported the first crystal structure of a phosphate - Zn(II)-BPA complex.<sup>169</sup>

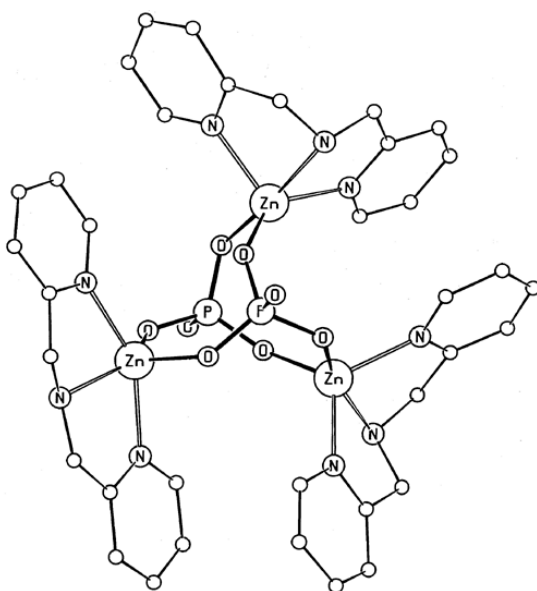


**Figure 49.** Structure of the complex  $(\text{BPA}\cdot\text{Zn})_3(\text{TolOPO}_3)_2]\text{HPO}_4$  (tolyl groups omitted for clarity) in the solid state.

The ability of  $[\text{Zn}(\text{bpa})]^{2+}$  to bind phosphate is discussed in the chapter of recognition processes in solution (*Chapter 5.2.2*) in detail.

### 3.1.3 Fe(III) Complexes

Crystal structures of  $[\text{Fe}(\text{bpa})\text{Cl}_3]$  (figure 50)<sup>170</sup> and  $[\text{Fe}(\text{bpa})_2(\text{BF}_4)_2]$ <sup>171</sup> show similar structures with the metal ion in an octahedral coordination.

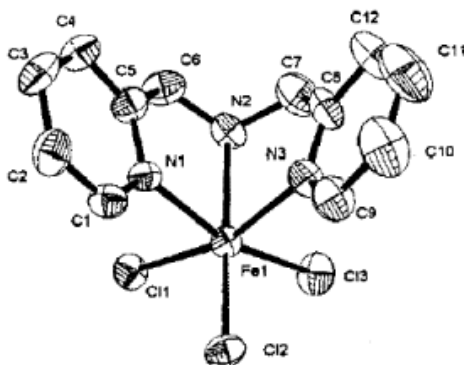


**Figure 50.** ORTEP view of  $[\text{Fe}(\text{bpa})\text{Cl}_3]$  in the solid state.

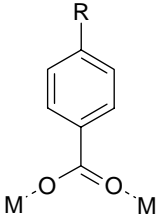
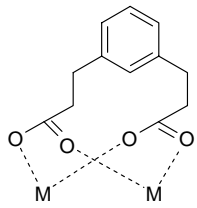
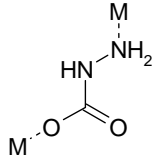
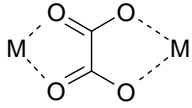
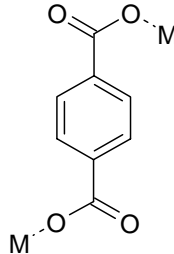
### 3.1.4 BPA Complexes in Solid State (tabulated)

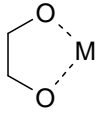
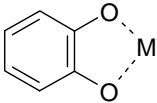
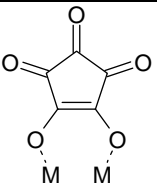
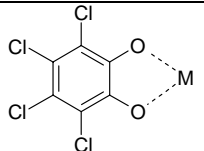
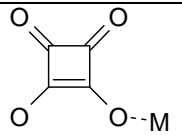
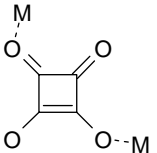
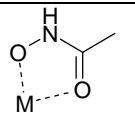
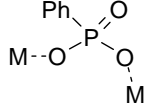
Table 14 summarises all X-ray structures registered in the Cambridge Crystallographic Database according to the selection criteria previously mentioned.

**Table 14.** References of X-ray structure analyses selected from the Cambridge structural database of transition metal BPA complexes coordinating an additional complex ligand (M = transition metal – BPA complex)

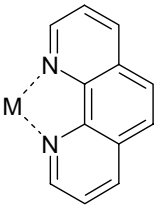
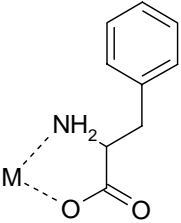
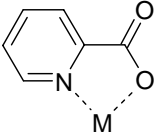
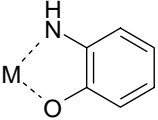
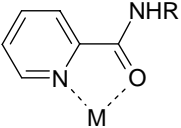
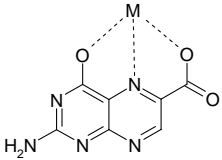
Additional Ligand	Metal Ions							
	Zn(II)	Cu(II)	Fe(III)	Ni(II)	Co(III)	Mn(II)	Cr(III)	Re(II)
	R=Me <sup>172,173</sup>	R=Me <sup>172,174,175</sup> R = Et	R=Me <sup>161,172</sup> R=Et <sup>172,176</sup> R=Hex <sup>177</sup> R=(CH <sub>2</sub> ) <sub>3</sub> -Ph <sup>178</sup> R=CH <sub>2</sub> -Cl <sup>179</sup> R=Ph <sup>180</sup>	R=Me <sup>173,175</sup> R=Et	R=Me <sup>181</sup>	R=Me <sup>182</sup> R=Et <sup>183</sup> R=Ph <sup>182,184</sup>	R=Me <sup>185</sup>	
			See ref. <sup>186</sup>					
	See ref. <sup>172,,187</sup>		See ref. <sup>172,187</sup>					



			R=Ph <sup>188</sup>		R=H <sup>189</sup>			
			See ref. <sup>190</sup>					
					See ref. <sup>181</sup>			
		See ref. <sup>191</sup>						
		See ref. <sup>192</sup>						

								See ref. <sup>193</sup>
								See ref. <sup>193</sup>
		See ref. <sup>194</sup>						
			See ref. <sup>195</sup>					
						See ref. <sup>196</sup>		
		See ref. <sup>197</sup>						
						See ref. <sup>198</sup>		
					See ref. <sup>199</sup>			

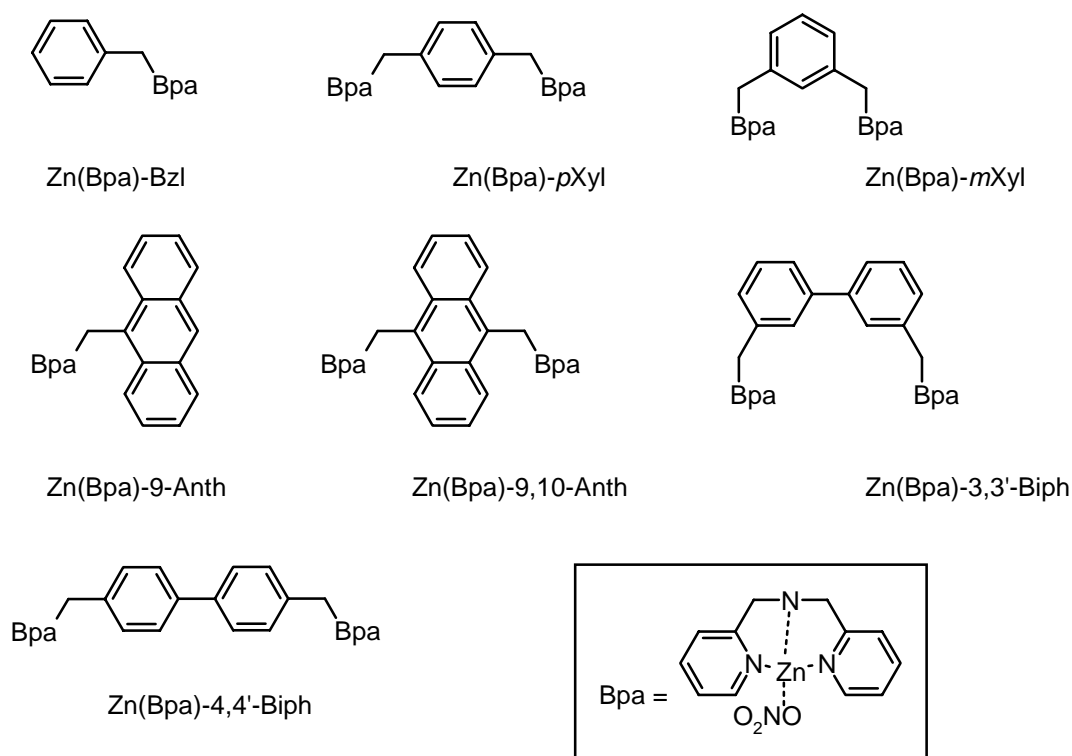
					See ref. <sup>200</sup>			
	R=Ph <sup>201</sup>	R=pNPh	R=Ph	R=Ph				
	R=Ph <sup>202</sup> R=p-Tol	R=Ph <sup>203</sup>						
	See ref. <sup>204</sup>	See ref. <sup>205</sup>						
		See ref. <sup>205</sup>	See ref. <sup>206</sup>					
		See ref. <sup>207</sup>						
		See ref. <sup>207</sup>	See ref. <sup>180</sup>					

		See ref. <sup>159,164</sup>						
		See ref. <sup>164</sup>						
		See ref. <sup>164</sup>						
								See ref. <sup>208</sup>
		See ref. <sup>209</sup>	See ref. <sup>210</sup>	See ref. <sup>211</sup>				
		See ref. <sup>165</sup>						

## 3.2 Recognition Processes in Solution

### 3.2.1 Surface Recognition of $\alpha$ -helical peptides in aqueous solution

*Hamachi et al.* used the  $[\text{Zn}(\text{bpa})]^{2+}$ -based coordination chemistry for the design of artificial receptors in aqueous solution.<sup>212,213</sup> A Zn(II) bispicolylamine complex is employed as a binding site for histidine residues because of its good affinity in aqueous solution. Five dinuclear Zn(II)-BPA complexes including meta- or para-xylene, 9,10-dimethylantracene and 3,3'- or 4,4'-dimethylbiphenyl as a linker were prepared. Two mononuclear Zn(II) complexes based on benzyl-BPA or 9-anthrylmethyl-BPA were used for comparison. The target molecules for binding are four helical model peptides with one or two His located on one side of the  $\alpha$ -helix (shown in figure 51).



	1	5	10	15	
peptide (H-16)	Ac-AEAAA	KEAAA	KEAAA	HA-NH <sub>2</sub>	i
peptide (H-12,16)	Ac-AEAAA	KEAAK	HAAA	HA-NH <sub>2</sub>	i,i+4
peptide (H-9,16)	Ac-AEAAA	KEA	HAK	EEAAHA-NH <sub>2</sub>	i,i+7
peptide (H-5,16)	Ac-AEAA	HKE	AAAKE	EEAAHA-NH <sub>2</sub>	i,i+11

**Figure 51.** Molecular structures of  $[\text{Zn}(\text{bpa})]^{2+}$ -based receptors and their target peptide sequences.

For the rapid screening of the affinity of these Zn(II)-BPA based receptors to the four peptides, the receptor-induced conformational change of the peptides was examined by circular dichroism spectroscopy.

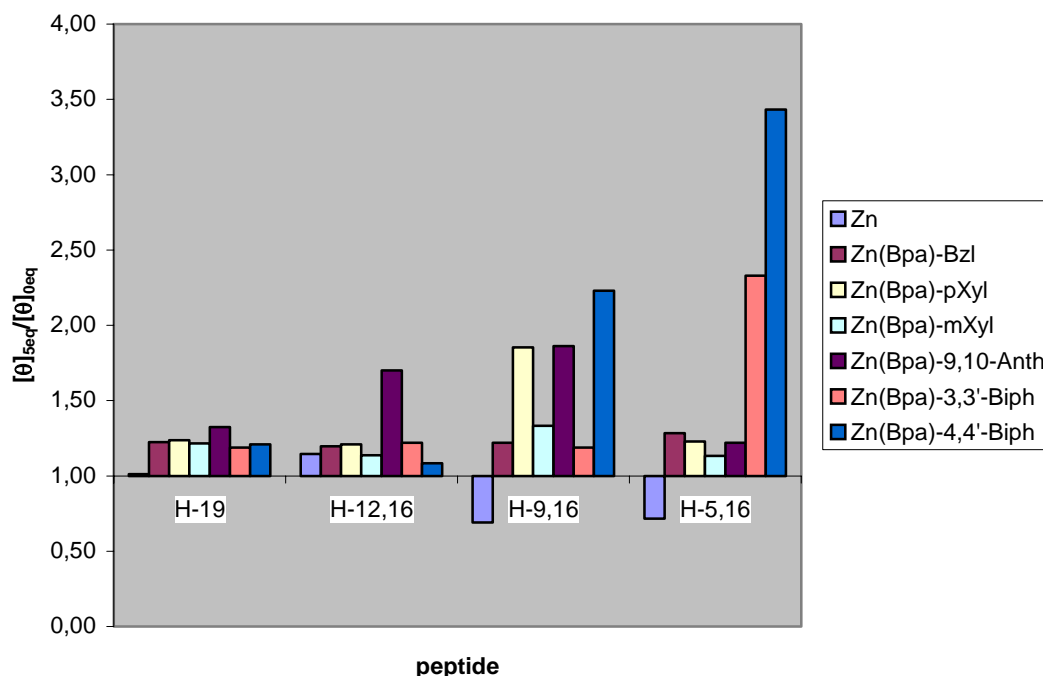


**Figure 52.** Changes of  $\theta$  values at 222 nm upon addition of 5 equiv. of  $[\text{Zn}(\text{bpa})]^{2+}$ -based receptors to the corresponding peptides. [Peptide] = 50  $\mu\text{M}$  in 10 mM borate buffer (pH 8.0) at 10°C.

It is apparent that helicity significantly increases upon receptor addition for peptides having two His residues, but not for the mono-His peptide. The helical conformation of H-12,16 peptide, is selectively stabilised by Zn(BPA)-9,10-anthracene. For the H-9,16 peptide, Zn(BPA)-pXyl, Zn(BPA)-9,10-Anth, and Zn(BPA)-4,4'-Biph show similar effects. In the case of H-5,16 peptide, Zn(BPA)-4,4'-Biph selectively induces a helical conformation. Neither Zn(II)-cations nor a Zn(BPA)-Bzl mononuclear receptor effectively induces a conformational change of the peptides.

The Job's plot based on CD measurements shows its maximum at 0.5 of the molar fraction of the receptor (inset of figure 53). Consistently, ESI-TOF mass spectroscopy, under identical conditions, displayed a 1:1 complex between the receptor and the peptide as a major species.

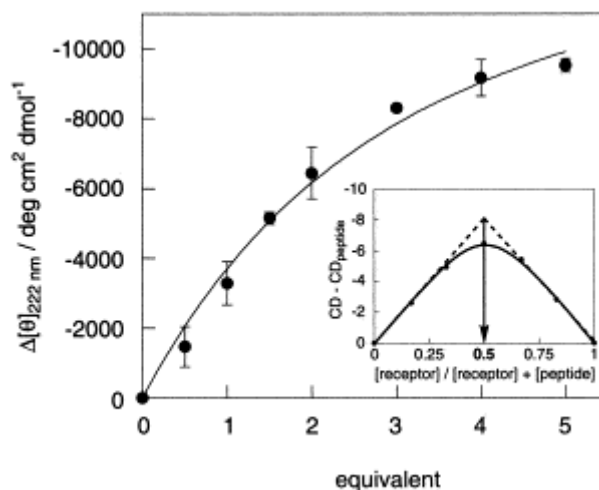


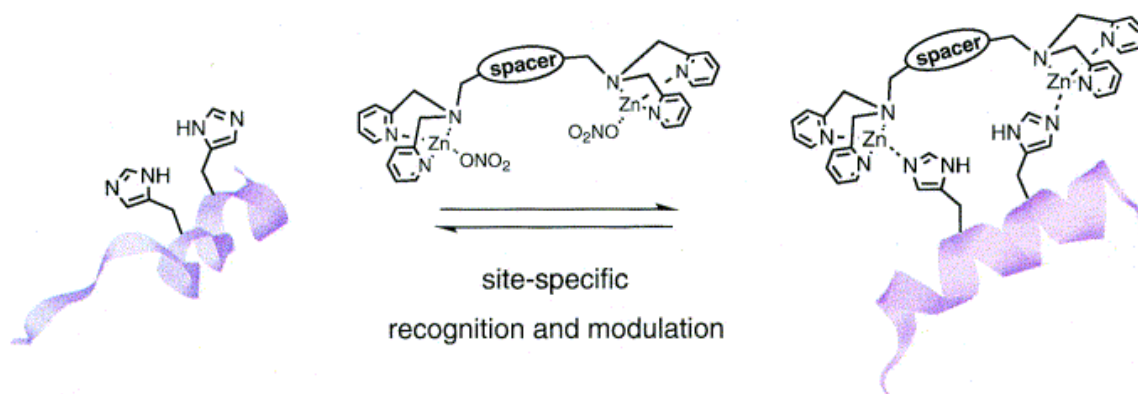
**Figure 53.** CD titration curve of H-12,16 peptide with Zn(BPA)-9,10-Anth. The error limits were derived from three titration experiments. Inset: Job's plot of this combination (the total concentration is 100  $\mu$ M).

Thus, the binding stoichiometry was determined to be 1:1 ratio and the CD titration curve, which obeys a typical saturation behavior (figure 53), plotted at 222 nm gave a binding constant ( $K_{ass}$ ) of  $10^{3.9}$   $M^{-1}$ . Similar titration curves and Job's plots were obtained for other combinations and the affinity constants are summarised in table 15. All receptor - peptide combinations selected by screening have an affinity in the range of  $10^{4.0}$  to  $10^{5.0}$  L/mol.

**Table 15.** Binding constants of the Zn (BPA) molecules with various peptides

Peptide	Receptor	$K_{ass}$ ( $M^{-1}$ )
H-12,16	Zn(BPA)-9,10-Anth	$(8.5 \pm 2.7) \cdot 10^3$
H-9,16	Zn(BPA)-9,10-Anth	$(1.3 \pm 0.7) \cdot 10^4$
H-9,16	Zn(BPA)-pXyl	$(2.5 \pm 0.7) \cdot 10^4$
H-9,16	Zn(BPA)-4,4'-Biph	$(2.5 \pm 0.4) \cdot 10^4$
H-5,16	Zn(BPA)-4,4'-Biph	$(3.9 \pm 0.6) \cdot 10^4$

**Scheme 14.** Schematic representation of side chain selective peptide recognition by a  $[\text{Zn}(\text{bpa})]^{2+}$ -based receptor



### 3.2.2 Artificial receptors for phosphorylated peptides

*Hamachi* and his group have used  $[\text{Zn}(\text{bpa})]^{2+}$  based receptors to selectively bind phosphorylated peptides and ATP.<sup>213, 214,215</sup> Anthracene derivatives having two Zn(II)-BPA moieties selectively coordinate phosphorylated amino acids and signal the binding by a change in emission. When phosphorylated tyrosine (p-Tyr) was added to the aqueous solution of the dinuclear compound **59**, *Hamachi et al.* observed a significant increase of emission of the anthracene chromophore (figure 55).

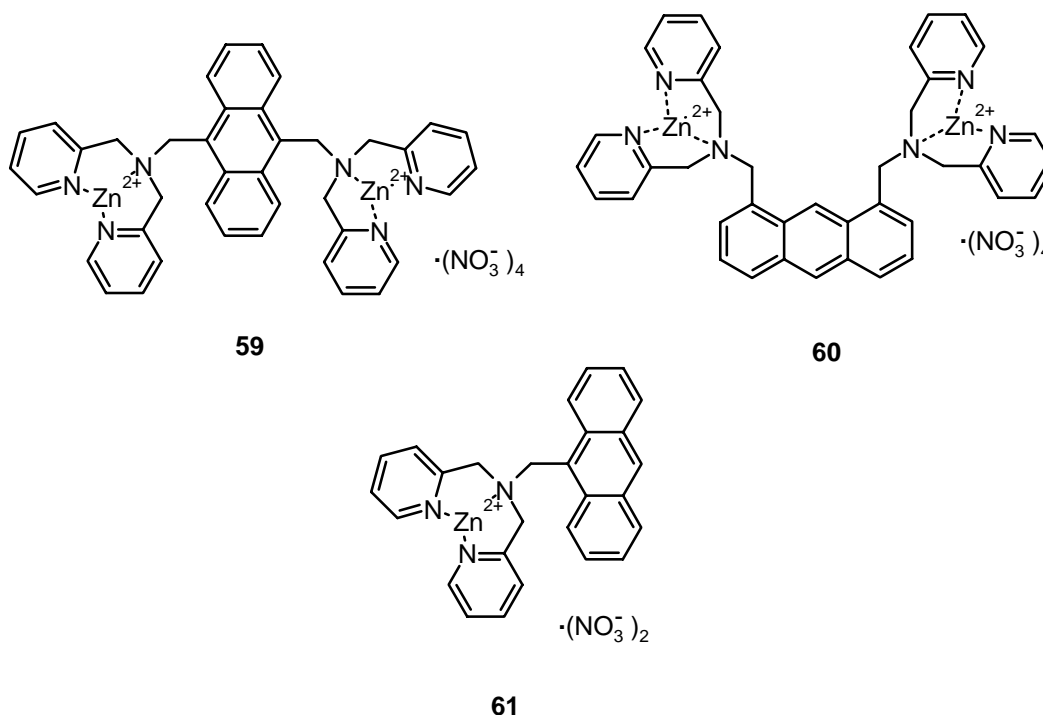


**Figure 54.** Emitting mono- and dinuclear Zn(II) complexes.



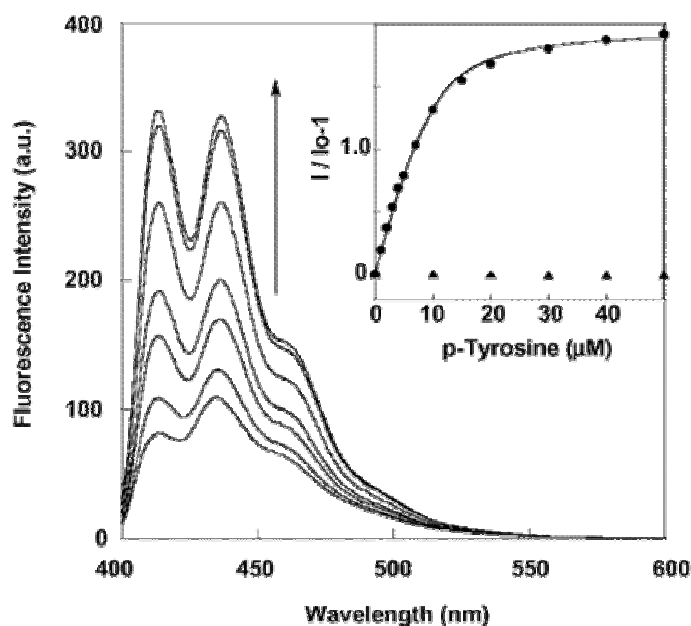


**Figure 55.** Emission changes of compound **59** (10  $\mu$ M) upon addition of p-Tyr: [p-Tyr] = 0, 1.0, 3.0, 5.0, 10, 30, 50  $\mu$ M from the lowest to the top trace. The spectra were measured in 10 mM HEPES buffer (pH 7.2) at 20°C,  $\lambda_{\text{ex}}$  = 380 nm.

These receptors strongly bind and fluorometrically sense phosphorylated species such as phosphate and p-Tyr in the range of  $10^{-6}$ - $10^{-5}$  M in a neutral aqueous solution. No fluorescent response is induced by other anions, such as sulfate, nitrate, acetate, and chloride. Job's plot analyses of the binding of these receptor and p-Tyr reveal a 1:1 stoichiometry (inset of figure 56).

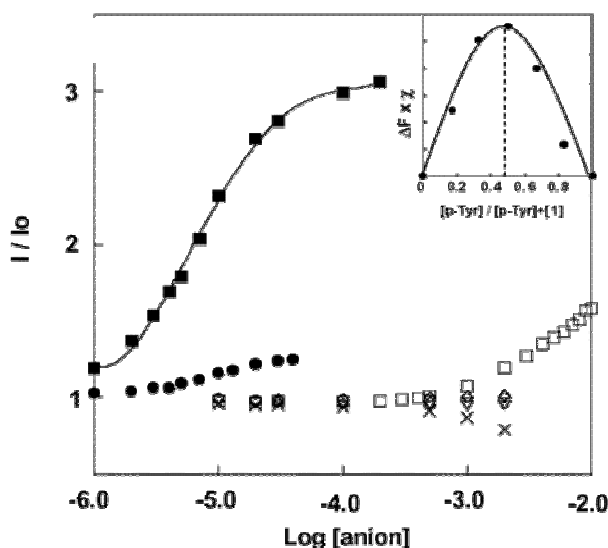


**Figure 56.** Relative emission response of compound **59** to the anion concentration (log[anion]): phosphate (●), p-Tyr (■), chloride (○), acetate (◇), sulfate (Δ), nitrate (▽), carbonate (□), azide (x).  $\lambda_{\text{ex}}$  = 380 nm. Inset: Job's plot of compound **59** (= 1) and p-Tyr.

NMR studies suggested that two Zn (BPA) sites equally contribute to the phosphate ion binding. Cocystal structures of the complex with phenyl phosphate support this expected coordination geometry.<sup>202</sup>

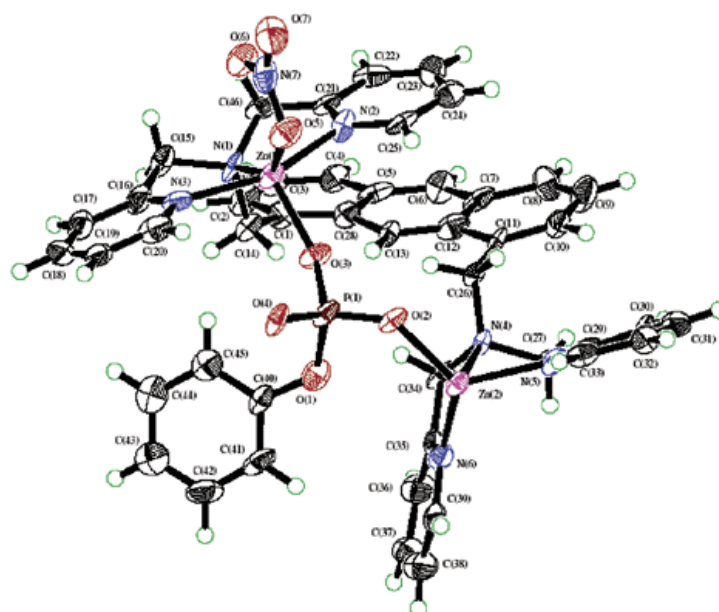


**Figure 57.** ORTEP drawing of the complex of **59** with phenyl phosphate.

Based on these results, *Hamachi* subsequently examined the sensing ability of these receptors towards phosphorylated peptides in aqueous solution. Three kinds of phosphorylated peptides (peptide-a, -b, -c) and a non-phosphorylated peptide (peptide-d, scheme 15) for comparison were used to investigate receptor binding.

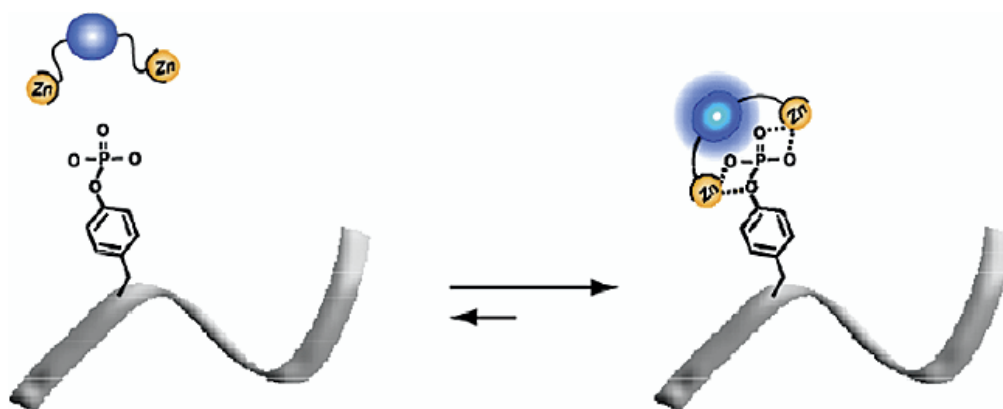
**Scheme 15.** (Top) Amino acid sequences of the phosphorylated peptides and (bottom) schematic depiction of the interaction of receptor **59**, **60** with a phosphorylated peptide

Peptide a: Glu-Glu-Glu-Ile-pTyr-Glu-Glu-Phe-Asp

Peptide b: Arg-Arg-Phe-Gly-pSer-Ile-Arg-Arg-Phe

Peptide c: Lys-Ser-Gly-pTyr-Leu-Ser-Ser-Glu

Peptide d: Glu-Glu-Glu-Ile-Tyr-Glu-Glu-Phe-Asp



The fluorescence intensity of **59** significantly increases by addition of less than 1  $\mu\text{M}$  of peptide-a. The binding is remarkably strong with the affinity of  $10^7 \text{ M}^{-1}$ . A photograph of the fluorescence change of the receptor **59** upon addition of peptide-a is shown in figure 58.

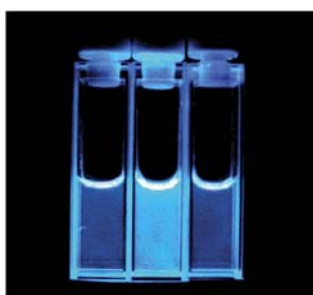
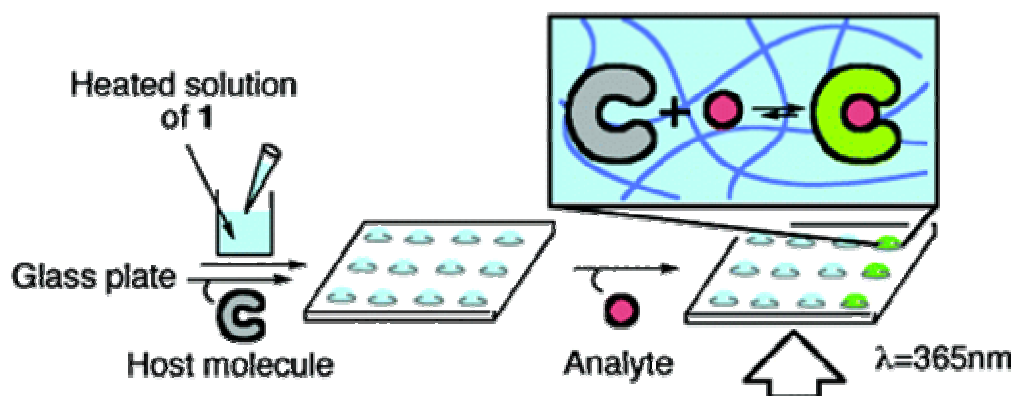


**Figure 58.** Increased emission of the receptor **59** in the presence of phosphorylated peptide-a (middle); the solution of **59** only (left); **59** in the presence of non-phosphorylated peptide-d (right).

Apparently, the blue fluorescence is greatly intensified by the phosphorylated peptide-a, whereas the non-phosphorylated peptide-d does not induce a fluorescence change. Such visualisations stimulated the same group to immobilise the artificial receptors **59** and **61** in

a gel matrix without loss of their binding capability displayed in solution.<sup>216</sup> The binding constant in the gel is 3-fold smaller compared to homogeneous solution. Therefore, the previously observed discrimination between phosphorylated and non-phosphorylated peptides is still valid. For rapid sensing, the hydrogel was miniaturised and arranged into an array on a glass support.

**Scheme 16.** Preparation scheme of a semi – wet sensor array (**1** is the monomer of the hydrogel)



This chip was used for receptor screening as shown in figure 59. Variations of receptors, pH, metal salts, and presence of phosphorylated peptide could be screened on one chip.

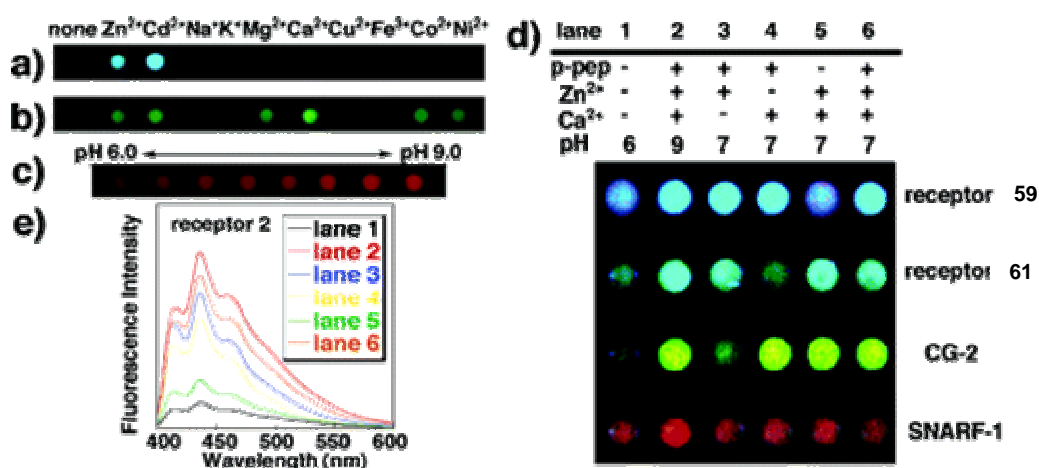
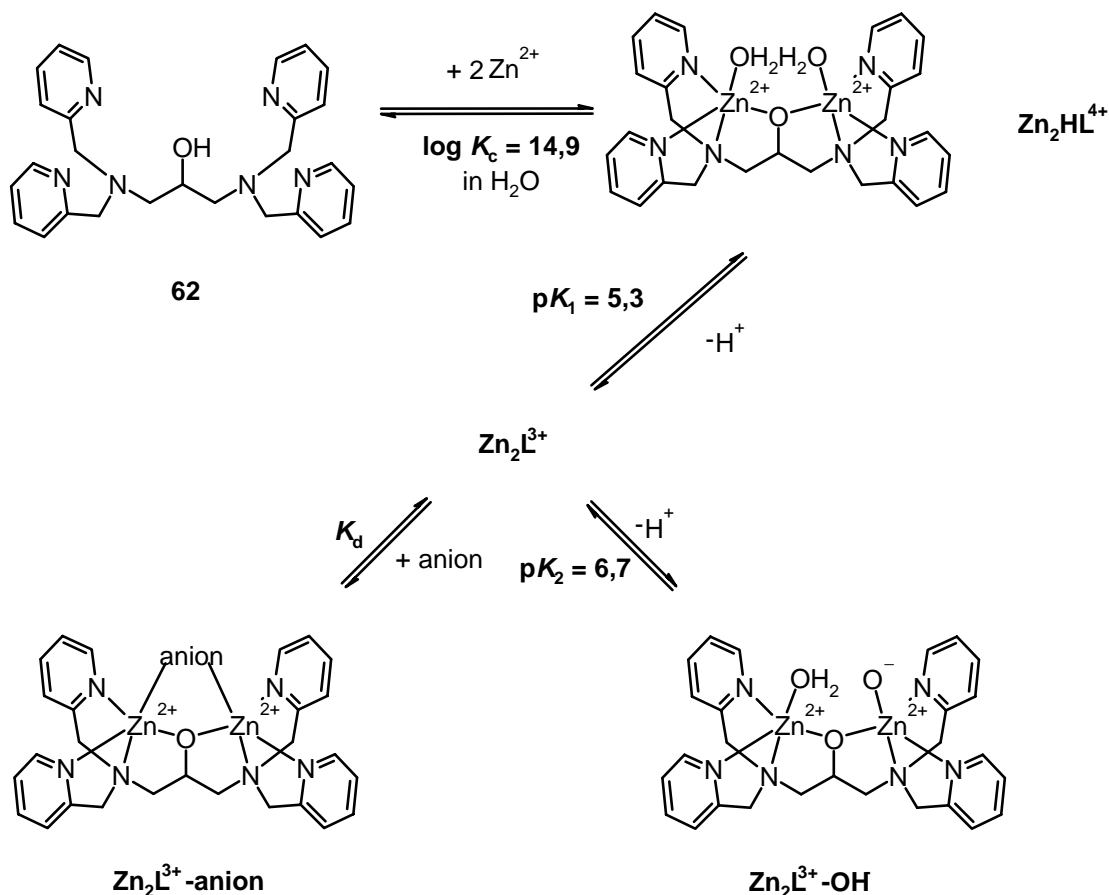


**Figure 59.** Images of sensing patterns of a semi-wet chemosensor chip containing (a) **59** (80  $\mu\text{M}$ ), (b) CG-2 (Ca(II) probe) (50  $\mu\text{M}$ ) in the presence of various metal cations, or (c) SNARF-1 (pH probe) (100  $\mu\text{M}$ ) at various pHs. (d) An image of an integrated molecular recognition hydrogel chip for mixed solution assay.

The receptor **59** based detection system for phosphorylated peptides was also used to detect the presence of phosphorylated peptides in SDS-Page gel electrophoresis.<sup>217</sup> Other groups synthesised modified BPA-ligands to bind to phosphates.<sup>218, 219, 220</sup> Here, two  $[\text{Zn}(\text{bpa})]^{2+}$  binding units and additional hydroxy coordination was used for anion binding.

**Scheme 17.** Structure of BPA-ligand used for complexation experiments



The solution binding processes were investigated by potentiometric titration. The species distribution plot shows the  $\text{Zn}_2\text{L}^{3+}$  phenylphosphate aggregate as the only species between pH 5 and 8. This compound is present in the solid state as found by X-ray structure analysis.

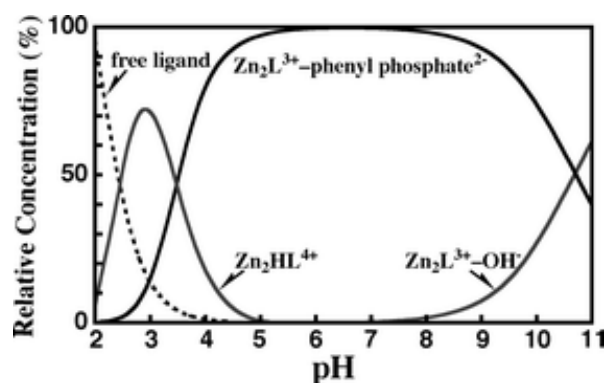


**Figure 60.** Species distribution diagram of **62** ( $1 \text{ mmol dm}^{-3}$ ) in the presence of Zn(II) ion ( $2 \text{ mmol dm}^{-3}$ ) and phenyl phosphate $^{2-}$  ( $1 \text{ mmol dm}^{-3}$ ) as a function of pH in aqueous solution at  $25^\circ\text{C}$  with  $I = 0.10$ . Free ligand is a total of metal-free ligand species ( $\text{HL}\cdot\text{nH}^+$ ).

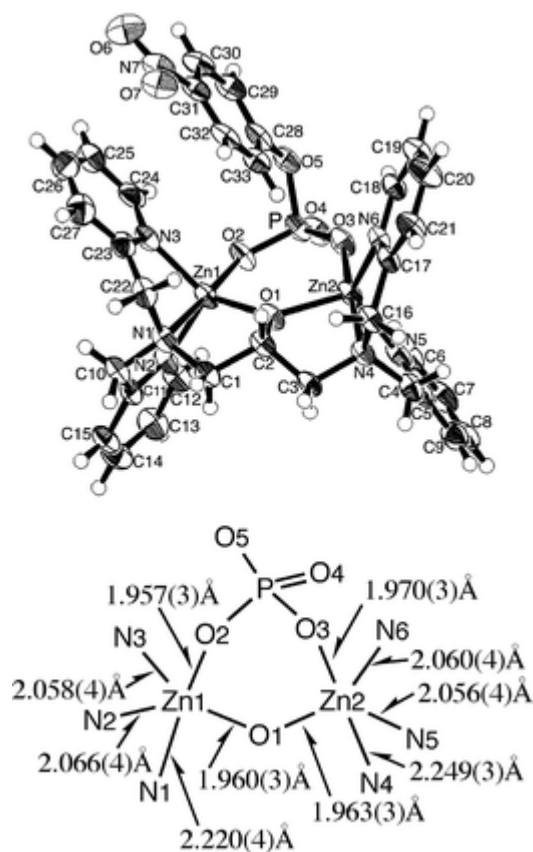
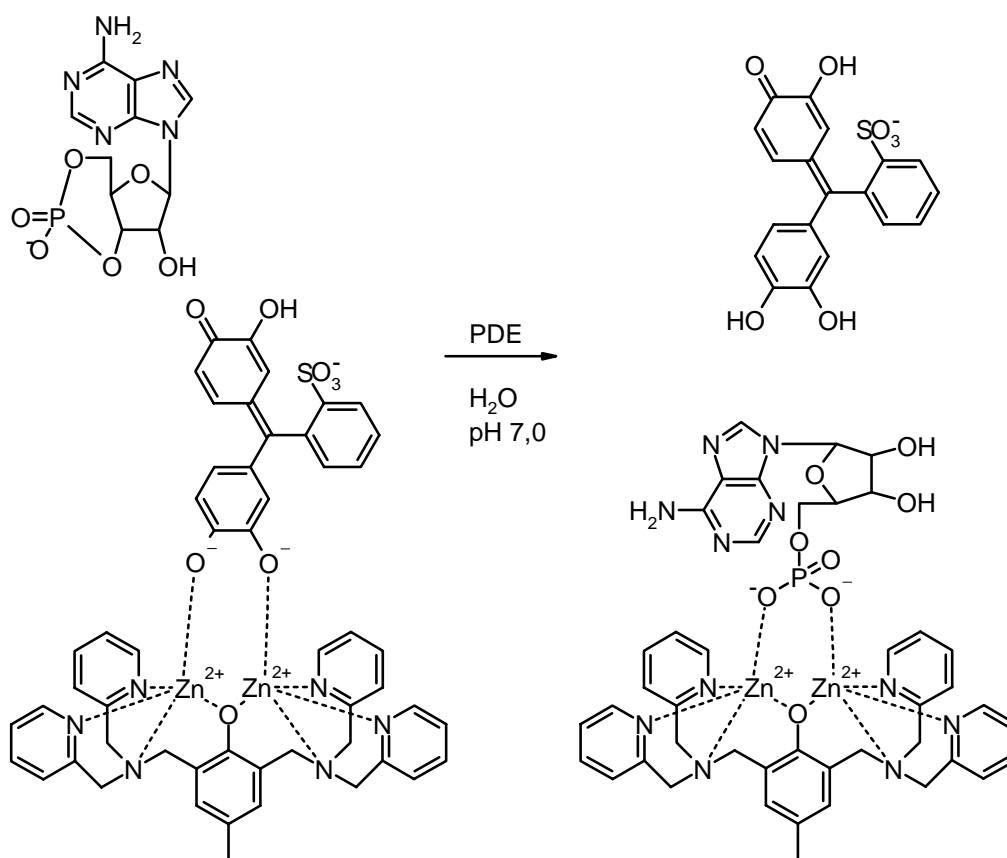


**Figure 61.** Crystal structure of p-nitrophenyl phosphate $^{2-}$ -bound di-Zn(II) complex.

*Kim et al.* designed a receptor for AMP binding based on BPA ligands.<sup>219</sup> Using a 4-methyl-phenyl group as linker to bridge the BPA ligands they created a binuclear complex with similar structure as the compound from *Koike*.

**Scheme 18.** Schematic representation of the AMP chemosensor



Sensing AMP is achieved by displacement of pyrocatechol violet. The AMP binding is monitored by the amount of free pyrocatechol violet in solution. The binding was investigated spectrophotometrically and by isothermal titration calorimetry.

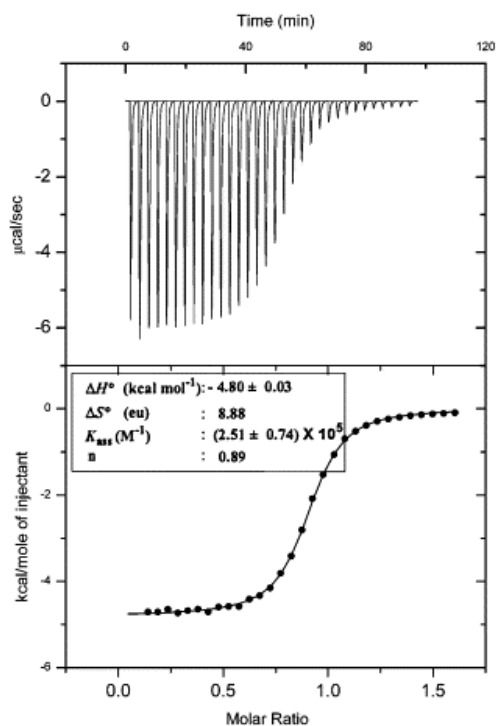
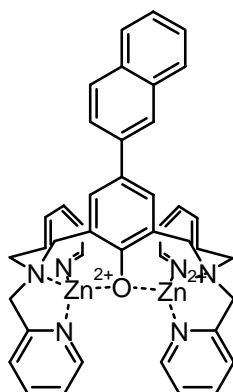


**Figure 62.** The ITC plot for the titration of  $[\text{Zn}_2(\text{H-bpmp})]^{3+}$  (0.5 mM) with AMP (5 mM) in aqueous HEPES buffer pH 7.0 at 30 °C.

Using a similar approach *Smith et al.* reported a indicator displacement system for fluorescent detection of phosphate oxyanions under physiological conditions.<sup>221</sup> *Hong* and coworkers reported a fluorescent PPI (pyrophosphate,  $\text{P}_2\text{O}_7^{4-}$ ) sensor based on a naphthalene-BPA system, which shows high sensitivity and selectivity over a wide pH range for PPI ions relative to other anions, including ATP and ADP. The presence of PPI is signaled by changes in the emission intensity of the luminescent receptor.



**63**

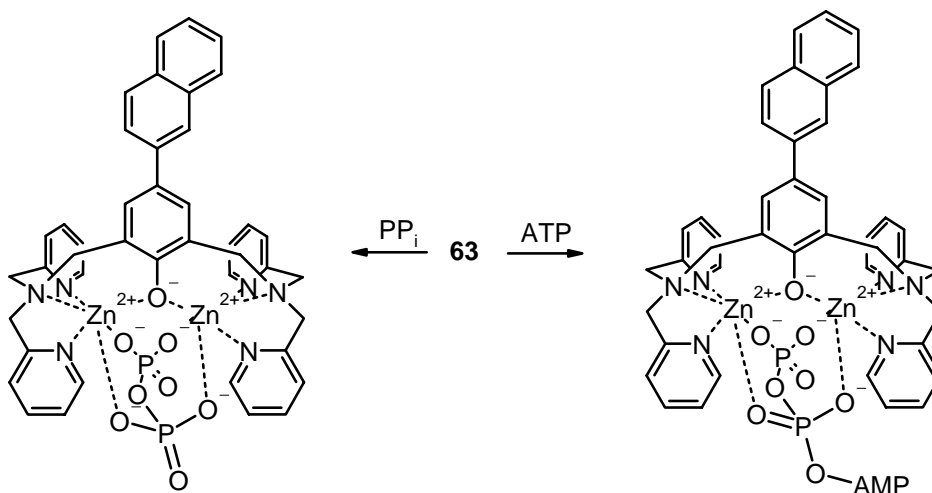
**Figure 63.** Structure of *Hongs* PP1 sensor **63**.



Upon addition of PPi, a six-fold increase of the emission intensity is noted. Added ATP leads to a twofold increase of emission intensity.

The binding mode for PPi-**63** is illustrated in scheme 19, which is based on previous work involving a structurally similar sensor and its X-ray crystal structure.

**Scheme 19.** Proposed mechanism for the complexation of sensor **63** with PPi and ATP



The observed selectivity for PPi over ATP can be understood from the structure of the guest and the charge density of four O-P oxygen atoms of the guest involved in the complexation. The total anionic charge density of the four O-P oxygen atoms involved in the complexation of ATP with **63** is smaller than that of the four O-P oxygen atoms of PPi. Therefore, the binding affinity of ATP is reduced drastically, and observed fluorescence changes are smaller relative to PPi binding.

### 3.3 Recognition Processes on Solid Surfaces

#### 3.3.1 Sensors for Phosphatidylserine-containing Membranes

Using the sensor metal complex **59** from *Hamachi*, the group of *Smith* showed its use to detect the presence of anionic phospholipids, particularly phosphatidylserine (PS), on the surface of vesicles and cells.<sup>222</sup> However, the excitation wavelength is in the UV range and therefore not compatible with the lasers in most flow cytometers. This prompted Smith and co-workers to design a second generation of sensors.<sup>223</sup>

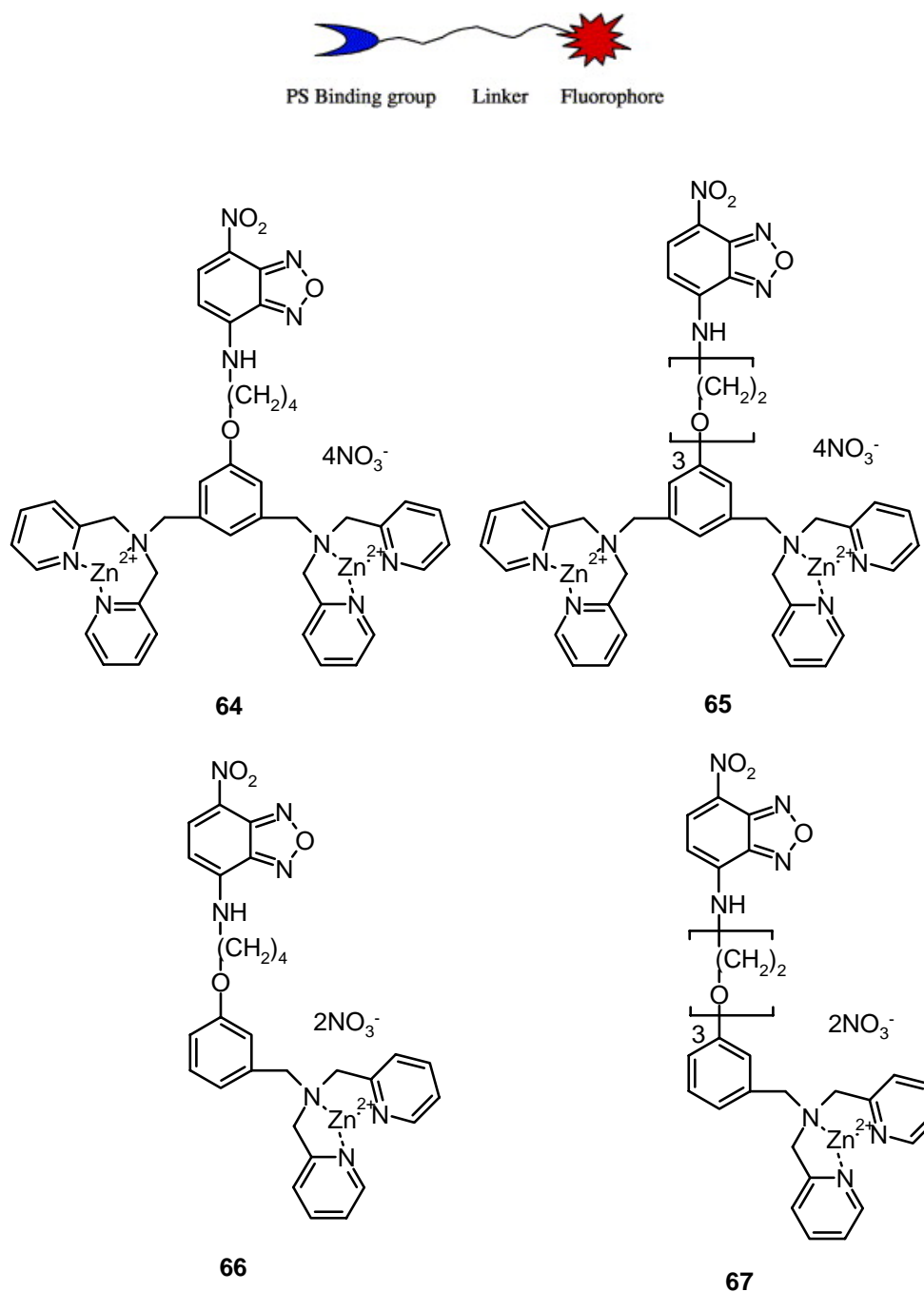
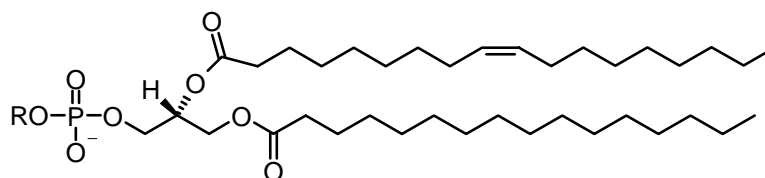


**Figure 64.** Coordination complexes **64-67** as potential PS sensors.

The titration experiments involved addition of unilamellar vesicles composed of 1:1 POPC:POPS, 1:1 POPC:POPA, 1:1 POPC:POPG, or 100 % POPC to a 1  $\mu$ M solution of **64** or **65**.



68

Formula for R	Phospholipid
-H	POPA
$-\text{CH}_2\text{CH}_2\text{N}(\text{CH}_3)_3^+$	POPC
$-\text{CH}_2\text{CH}(\text{NH}_3^+)\text{COO}^-$	POPS
$-\text{CH}_2\text{CH}(\text{OH})\text{CH}_2\text{OH}$	POPG

**Figure 65.** Head group structure of common phospholipids.

The resulting isotherms fit to a 1:1 binding model, which allowed calculation of apparent phospholipid binding constants. As the sensors were not expected to bind the zwitterionic POPC head group, this titration was performed as a control to determine specificity of the sensors for anionic PS.

**Table 16.** Sensor/phospholipid binding constants ( $K_a$ )

Sensor	$K_a \times 10^4 \text{ (M}^{-1}\text{)}^a$			
	100 % POPC	1:1 POPC:POPS	1:1 POPC:POPG	1:1 POPC:POPA
<b>64</b>	<1	23.3±1.7	14.2±3.8	11±6.0
<b>65</b>	<1	5.3±2.0	2.0±0.5	2.0±0.3
<b>66</b>	<1 <sup>b</sup>	11.5±5.5	-	-
<b>67</b>	<1 <sup>b</sup>	7.7±3.3	-	-

<sup>a</sup> Values are average of at least three independent measurements.

<sup>b</sup> Values are average of two independent measurements.

The effect of only one Zn(II)-BPA unit in the sensor structure was evaluated using control compounds **66** and **67**. Vesicles composed of 100 % POPC or 1:1 POPC:POPS were added to a 1  $\mu\text{M}$  solution of **66** or **67**. The emission of butyl-linked sensor **66** with 1:1 POPC:POPS is about two times that observed with 100% POPC vesicles, whereas the

intensity ratio with TEO-linked sensor **67** is about five. Thus, it is clear that the hydrophilic TEO-linker is more useful for detecting PS-containing membranes over PC-only membranes. The emission of sensor **65** with two  $[\text{Zn}(\text{bpa})]^{2+}$  units is significantly higher than that obtained with **67**, indicating that the second  $[\text{Zn}(\text{bpa})]^{2+}$  unit increases the interactions that produce a stronger response to PS-containing membranes.

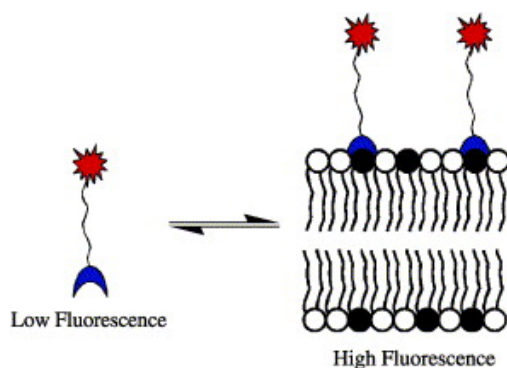
The PS sensitivity of sensor **65** was investigated in additional titration experiments with POPC vesicles enriched with various amounts POPS. A solution of **65** (1  $\mu\text{M}$ ) was titrated with vesicles composed of POPC and 0-50 % POPS. Sensor **65** can readily detect the presence of bilayer membranes containing 5 % PS.

**Table 17.** Sensor **65**/phospholipid binding constants ( $K_a$ ) for vesicles with varying PS content

	<b>95:5 POPC:POPS</b>	<b>90:10 POPC:POPS</b>	<b>80:20 POPC:POPS</b>	<b>50:50 POPC:POPS</b>
$K_a \times 10^4 (\text{M}^{-1})^a$	1.0 $\pm$ 0.3	2.2 $\pm$ 0.5	5.7 $\pm$ 0.5	5.3 $\pm$ 2.0

<sup>a</sup> Values are average of at least three independent measurements.

**Scheme 20.** Sensing of PS-containing membranes. PS is represented with filled head group, PC is unfilled head group



Until now, no surface-immobilised BPA complexes and their use in molecular recognition have been reported.

## 4. Tris(2-pyridylmethyl)-amine (TPA, TMPA) Complexes

### 4.1 Structures of TPA Complexes

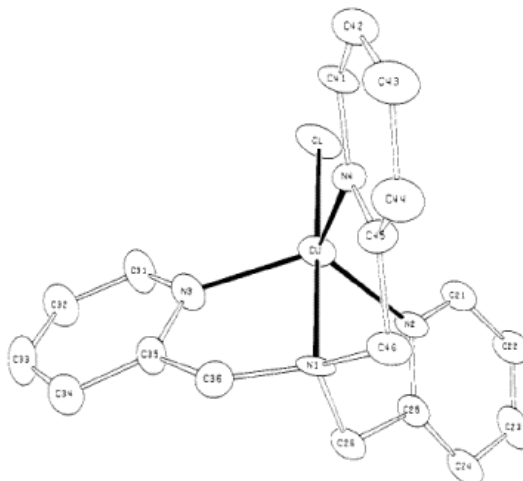
Substitution of the carboxylic acid functionalities of NTA by pyridine leads to the TPA ligand. Da Mota first reported the ligand in 1969 and a large number of derivatives have been used for complexation of metal ions.<sup>224</sup> Beside Ni(II)<sup>225</sup> and Co(III)<sup>226</sup> complexes, most reports cover investigations of Cu(II),<sup>227</sup> Zn(II)<sup>228</sup> and Fe(III) ion complexation.<sup>229</sup>

**Table 18.** Overview of typical binding constants of different metal ions to the TPA ligand<sup>22</sup>

Ion	Equilibrium	log K
Co <sup>2+</sup>	ML/M.L	11.4
Ni <sup>2+</sup>	ML/M.L	14.5
Cu <sup>2+</sup>	ML/M.L	16.2
Zn <sup>2+</sup>	ML/M.L	11.0
Fe <sup>2+</sup>	ML/M.L	8.7

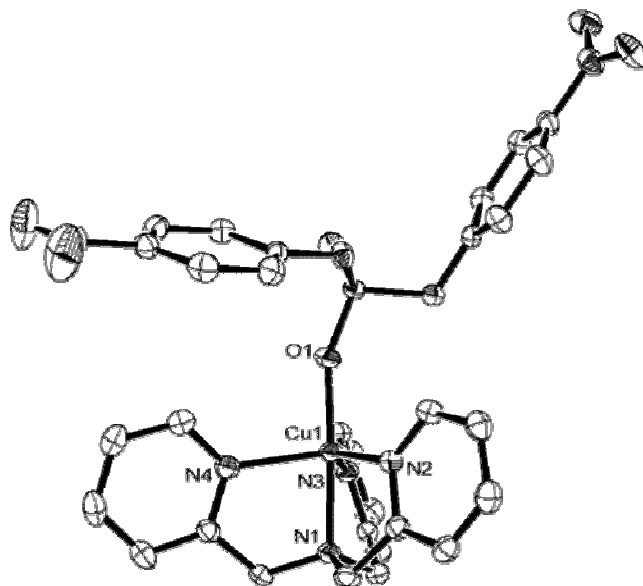
#### 4.1.1 Cu(II) Complexes

The structure of the Cu(II) complex of TPA was reported by *Karlin et al.*<sup>230</sup> Indicated by the similar Cu(II)-N bond lengths and bond angles the copper ion is found in a trigonal bipyramidal coordination geometry.



**Figure 66.** ORTEP drawing of  $[\text{Cu}(\text{tpa})(\text{Cl})]^+$ .

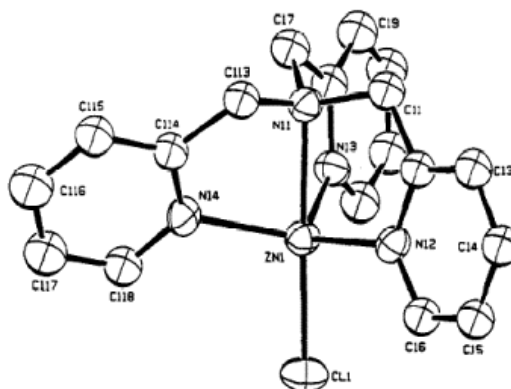
These copper complexes have the ability to bind additional phosphate ions, which is illustrated by a structure of the 1:1 complex of  $[\text{Cu}(\text{tpa})]^{2+}$  and BNPP (= bis(p-nitrophenyl) phosphate).<sup>231</sup>



**Figure 67.** ORTEP diagram (50% probability ellipsoids) of the cationic portion of  $[\text{Cu}(\text{tpa})(\text{BNPP})]\text{ClO}_4$ . Hydrogen atoms are omitted for clarity.

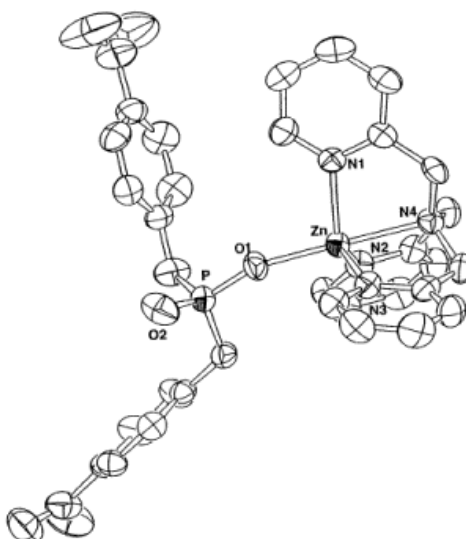
### 4.1.2 Zn(II) Complexes

The crystal structure of  $[\text{Zn}(\text{tpa})\text{Cl}]\text{ClO}_4$  shows the ligand maintaining a helical twist in which the dihedral angle between the plane of each pyridine ring and the axis of the M-N(11) bond is between  $12$  and  $22^\circ$ .<sup>232</sup>



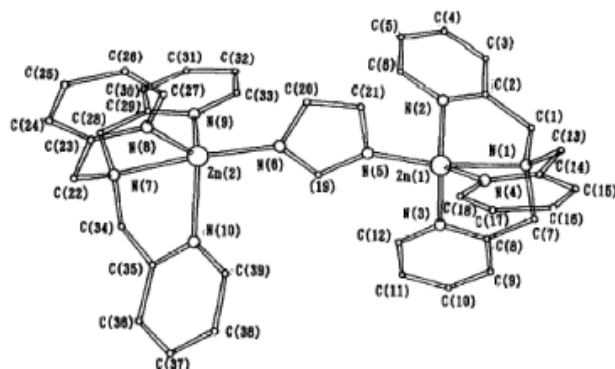
**Figure 68.** ORTEP diagram (30% probability ellipsoids) of the cationic portion of  $[\text{Zn}(\text{tpa})\text{Cl}]\text{ClO}_4$ .

Thus, the overall shape of the cationic portion of the molecule resembles a propeller. The complex is potentially chiral. In the crystal, the compounds are found as racemate with their mirror images. Similar to the Cu(II) complex the analogous Zn(II) complex binds to BNPP.<sup>233</sup>



**Figure 69.** An ORTEP drawing (40% probability drawing) of the cationic portion of  $[\text{Zn}(\text{tpa})(\text{BNPP})]\text{ClO}_4$ .

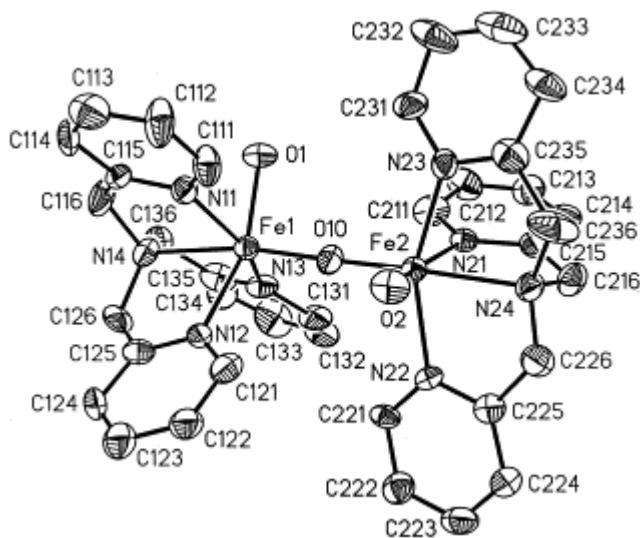
Adams *et al.* also reported a 2:1 complex of  $[\text{Zn}(\text{tpa})]^{2+}$  and BNPP.<sup>234</sup> The ability of this metal complex to bind imidazole is demonstrated by the structure of the 2:1 complexation of  $[\text{Zn}(\text{tpa})]^{2+}$  and deprotonated imidazole.<sup>235</sup> Each of the two zinc atoms is pentacoordinated by four nitrogen atoms from TPA and one nitrogen atom from bridging imidazolate ligand in an approximately trigonal bipyramidal structure. The distance between the two zinc atoms in the Zn-Im-Zn moiety is 6.078 Å.



**Figure 70.** Cationic structure of  $[(\text{tpa})\text{Zn}(\text{im})\text{Zn}(\text{tpa})]^{3+}$ .

#### 4.1.3 Fe(III) Complexes

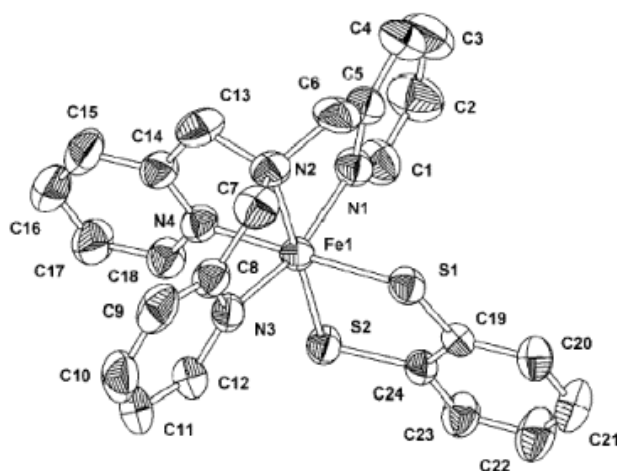
Fe(III) complexes of TPA were found to crystallise as an oxo-bridged dimer.<sup>236</sup>



**Figure 71.** ORTEP diagram of the dinuclear cation in  $[\{\text{Fe}(\text{tpa})(\text{H}_2\text{O})\}_2\text{O}]^{2+}$  ( $\text{ClO}_4$ )<sub>4</sub>·3H<sub>2</sub>O·0.25CH<sub>3</sub>CH<sub>2</sub>OH.

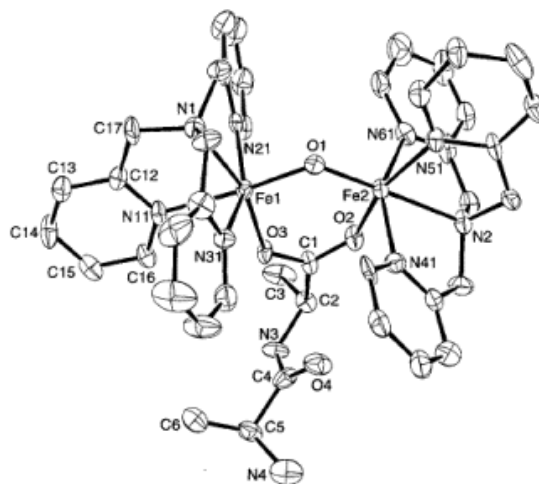


An interesting substrate which can bind to these Fe(III)-TPA complexes is dithiolate 1,2-benzenethiol (= H<sub>2</sub>dtc) (figure 72).<sup>237</sup>



**Figure 72.** Ellipsoid plot of the cation in [Fe(tpa)(dtc)]ClO<sub>4</sub>·0.25 MeOH.

Next to complexes with diphenylphosphates,<sup>238</sup> and acetates,<sup>239</sup> structures with natural amino acids and dipeptides were investigated (figure 73).<sup>240</sup>

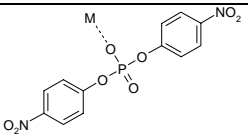
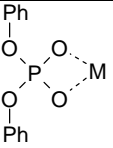
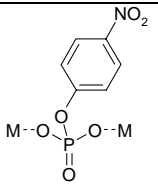


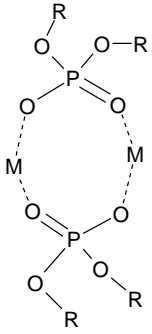
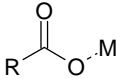
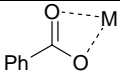
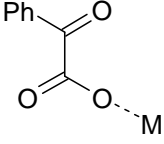
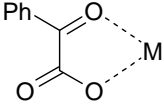
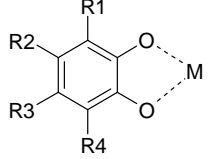
**Figure 73.** ORTEP drawing of the complex cation in [Fe<sub>2</sub>(μ-O)(μ-L-alanyl-L-alanine)(tpa)<sub>2</sub>](ClO<sub>4</sub>)<sub>4</sub>·2CH<sub>3</sub>CN·C<sub>4</sub>H<sub>9</sub>OH.

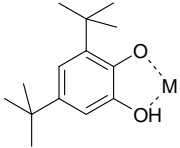
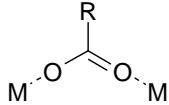
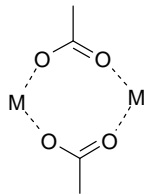
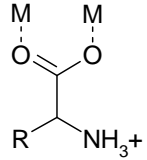
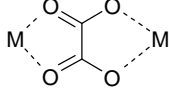
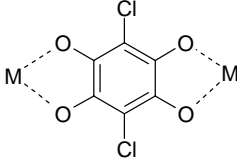
#### 4.1.4 TPA Complexes in Solid State (tabulated)

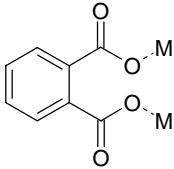
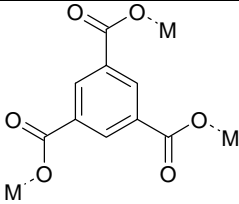
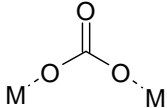
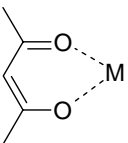
Table 19 summarises all X-ray structures registered at the Cambridge Crystallographic Database according to the selection criteria previously mentioned.

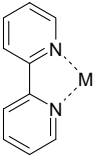
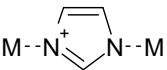
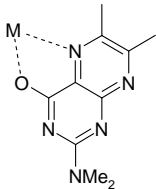
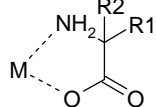
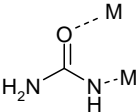
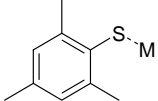
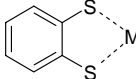
**Table 19.** References of X-ray structure analyses selected from the Cambridge structural database of transition metal TPA complexes coordinating an additional complex ligand (M = transition metal – TPA complex)

Additional Ligand	Metal Ions							
	Zn(II)	Cu(II)	Fe(III)	Ni(II)	Co(III)	Mn(II)	Cr(III)	Ru(II)
	See ref. <sup>233</sup>	See ref. <sup>231</sup>						
			See ref. <sup>238</sup>					
	See ref. <sup>234</sup>	See ref. <sup>241</sup>						

	R=Bzl <sup>242</sup>			R=Ph				
	R=Ph		R= <sup>t</sup> Butyl <sup>243</sup>					
			See ref. <sup>244</sup>					
		See ref. <sup>227</sup>	See ref. <sup>245,246</sup>					
			See ref. <sup>247,245</sup>					
			R1-R4=H <sup>248</sup> R1-R4=Cl, Br <sup>195,237,249</sup> R1,R3=H R2, R4= <sup>t</sup> Butyl <sup>250</sup>					

			See ref. <sup>251</sup>					
			R=Me, Ph <sup>238,252</sup> R=CH=CH-COOH <sup>253</sup>			R=Me <sup>254</sup>	R=Me <sup>255</sup>	R=Et <sup>256</sup>
			See ref. <sup>239</sup>					
			Val, Pro, Ala-Ala					
				See ref. <sup>225</sup>				
						See ref. <sup>257</sup>		

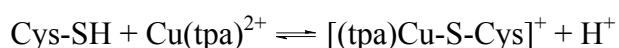
			See ref. <sup>253</sup>					
		See ref. <sup>258</sup>						
		See ref. <sup>259</sup>	See ref. <sup>253</sup>	See ref. <sup>260</sup>			See ref. <sup>261</sup>	
	See ref. <sup>262</sup>	See ref. <sup>262</sup>						
			See ref. <sup>263</sup>					
	See ref. <sup>198</sup>			See ref. <sup>198</sup>	See ref. <sup>198</sup>			

								See ref. <sup>264</sup>
	See ref. <sup>235</sup>							
								See ref. <sup>265</sup>
					R1=H, Me R2=H, Me <sup>226</sup>			
			See ref. <sup>229</sup>					
			See ref. <sup>229</sup>					
			See ref. <sup>237</sup>					

## 4.2 Recognition Processes in Solution

### 4.2.1 Recognition of Cysteines

*Holwerda* and co-workers examined the complexation of  $[\text{Cu}(\text{tpa})]^{2+}$  with cysteine.<sup>266</sup> An intense, symmetric absorption band with  $\lambda_{\text{max}}$  at 396 nm was observed upon mixing cysteine with  $[\text{Cu}(\text{tpa})]^{2+}$  throughout the pH range 4.0 - 6.0. Stopped-flow studies at 396 nm indicated that complexation was complete within the mixing time (3 ms), even at low cysteine concentrations. Excellent linear  $(A_e - A_o)^{-1}$  vs.  $[\text{Cys}]^{-1}$  correlations were found within the pH range 3.99-5.80, indicating the exclusive formation of a 1:1 cysteine- $[\text{Cu}(\text{tpa})]^{2+}$  adduct. The formation constant ( $K_f$ ) was calculated to be  $K_f = (1.21 \pm 0.06) \cdot 10^2 \text{ M}^{-1}$ . The pH dependence of  $K_f$  is consistent with the formation of a thiolate sulfur-Cu(II) bond:



### 4.2.2 Phosphate Recognition in Solution

As known from X-ray structures  $[\text{Zn}(\text{tpa})]^{2+}$  has the ability to bind to phosphates.<sup>233,234</sup> In 2003 *Mareque Rivas et al.* reported  $^{31}\text{P}\{^1\text{H}\}$  NMR titration experiments of dibenzyl phosphate (= dbp) with  $[\text{Zn}(\text{tpa})]^{2+}$  in  $\text{D}_2\text{O}$  at pD 7.4. The addition of increasing amounts of the Zn(II) complex to solutions of DBP caused a progressive upfield shift of the  $^{31}\text{P}$  signal relative to free DBP. During these studies, other ligands with additional amino groups were used.

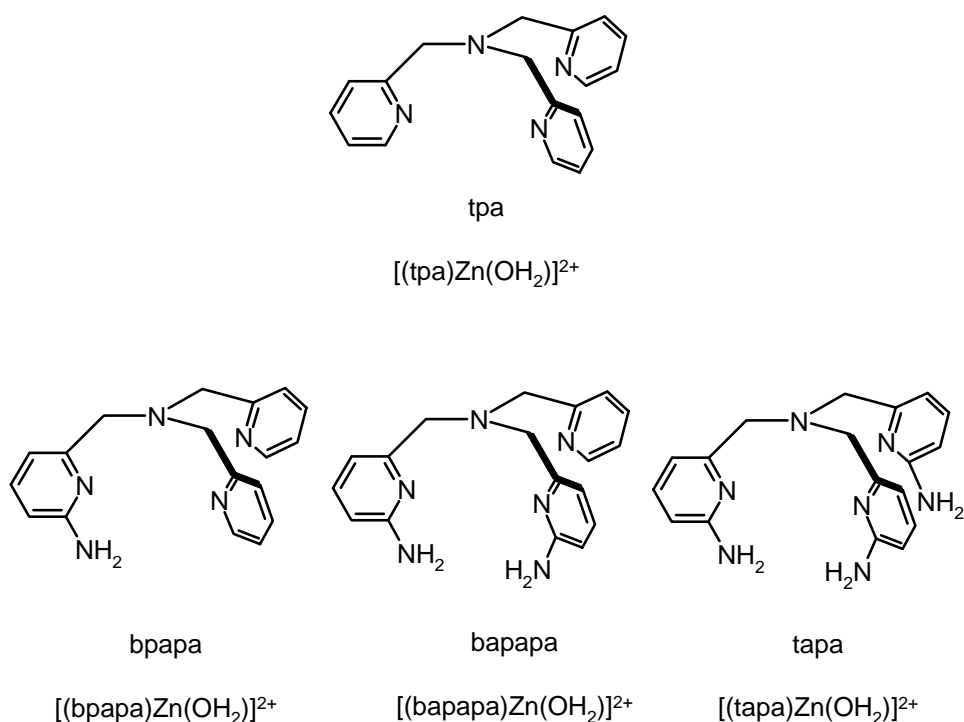


**Figure 74.** TPA ligands with additional amino groups.<sup>267</sup>

The additional electron donating amino groups do not participate in metal complexation, but form hydrogen bonds to the coordinated phosphate ion as confirmed by the X-ray structure of  $[\text{Zn}(\text{bpapa})]^{2+}$  (bpapa is a tpa with one additional amino groups; see figure 74).

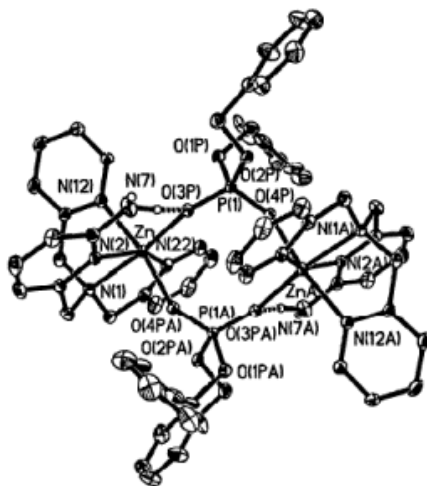
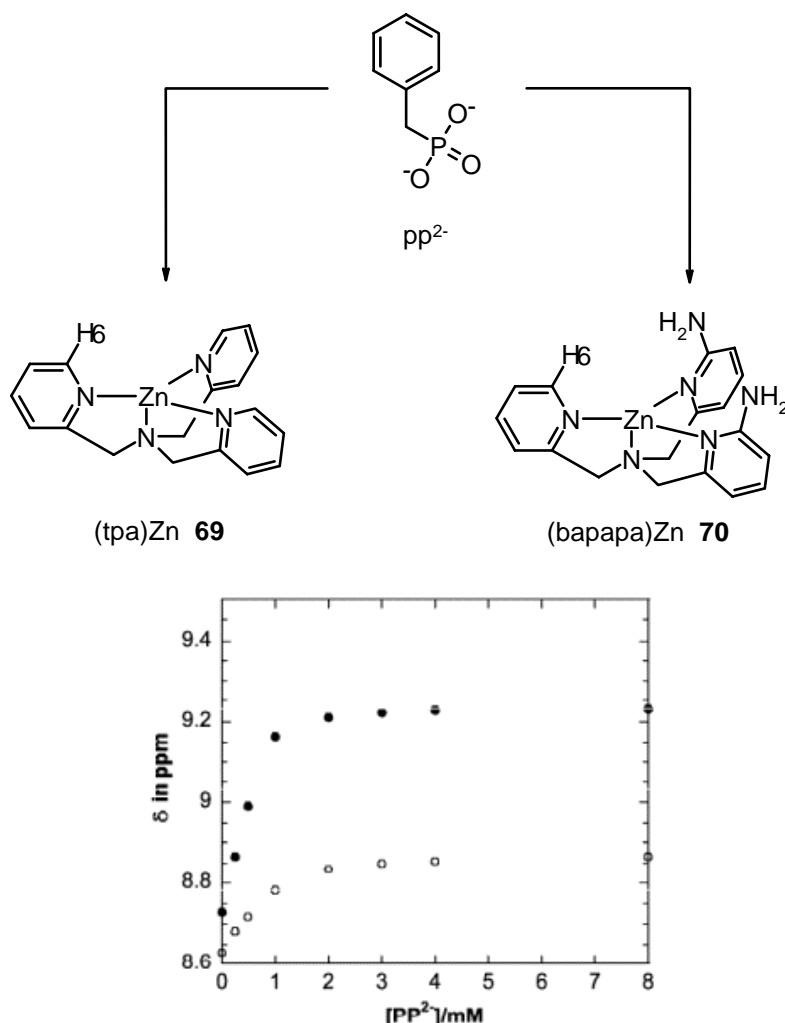


**Figure 75.** A thermal ellipsoid plot of  $[(\text{bpapa})\text{Zn}(\mu\text{-}\eta^2\text{-DBP})_2\text{Zn}(\text{bpapa})]^{2+}$ .

Supported by this additional interaction, the binding of the phosphate ion to the BPAPA-complex is stronger than the binding to the TPA-complex. This effect was also observed during binding studies of phenylphosphate ( $\text{PP}^{2-}$ ) to the metal complexes **69** and **70**.<sup>268</sup>

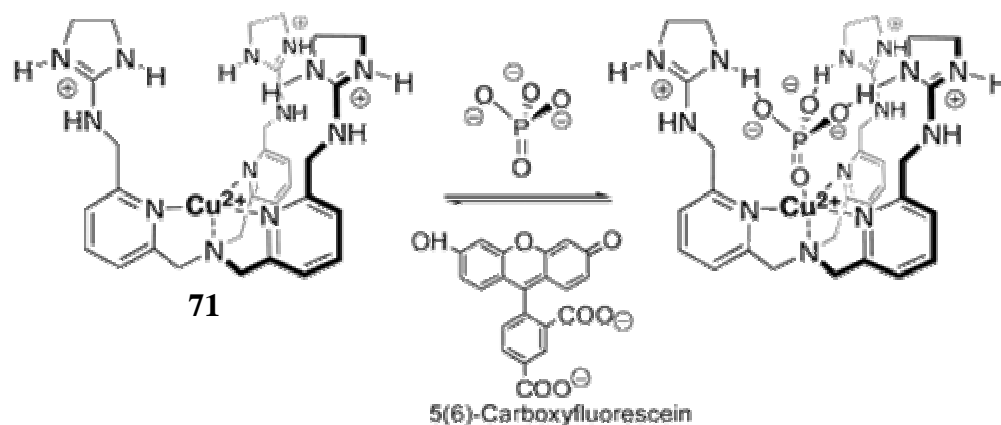


**Scheme 21.** Changes of the proton chemical shift of H6 of **69** (1mM in D<sub>2</sub>O) (o) and **70** (1mM in D<sub>2</sub>O) (●) upon addition of increasing amounts of PP at pH 7 ± 0.1 (50 mM HEPES)



A similar system was used to bind phosphate ions, supported by additional interactions to guanidinium moieties.<sup>269</sup> The chemosensor developed in this study takes advantage of an indicator-displacement assay comprised of metallo-host **71** and 5(6)-carboxyfluorescein.

**Scheme 22.** Assembly for phosphate ion detection using an indicator-displacement assay



Upon addition of aliquots of **71** to a solution of 5(6)-carboxyfluorescein, binding proceeds in a 1:1 stoichiometry with a color change from yellow to light orange. Added aliquots of a phosphate solution reverts the light orange color of the host-dye complex into the yellow color of free dye in solution. This indicates that the phosphate ion displaces the dye from the host cavity.

### 4.3 Recognition Processes on Solid Surfaces

Until now, no applications are reported using immobilised TPA-complexes for binding of guest molecules on supporting surfaces.

## References:

---

- <sup>1</sup> (a) Rogers, C.W.; Wolf, M.O. *Coord. Chem. Rev.* **2002**, 341. (b) Pin; F.; Bernardo, M.A.; Garcia-Espana, E. *Eur. J. Inorg. Chem.* **2000**, 10, 2143.
- <sup>2</sup> (a) Armstrong, R.N. *Biochem.* **2000**, 39, 13625. (b) Costamagna, J.; Ferraudi, G.; Matsuhira, B.; Campos-Vallette, M.; Canales, J.; Villagram, M.; Vargas, J.; Aguirre, M.J. *Coord. Chem. Rev.* **2000**, 196, 125. (c) Holm, R.H.; Kennepohl, P.; Solomon, E. *Chem. Rev.* **1996**, 96, 2239.
- <sup>3</sup> (a) Ward, M.D. *Ann. Rep. Prog. Chem. Section A: Inorg. Chem.* **2002**, 90, 55. (b) Borovik, A.S. *Comm. Inorg. Chem.* **2002**, 23, 45. (c) Amendola, V.; Fabrizzi, L.; Pallavicini, P. *Coord. Chem. Rev.* **2001**, 216, 435.
- <sup>4</sup> (a) Schmuck, C.; Geiger, L. *Chem. Commun.* **2004**, 15, 1698. (b) Schmuck, C.; Geiger, L. *J. Am. Chem. Soc.* **2004**, 126, 8898. (c) Nowick, J.S.; Chung, D.M.; Maitra, K.; Maitra, S.; Stigers, K.D.; Sun, Y. *J. Am. Chem. Soc.* **2000**, 122, 7654. (d) Nowick, J.S.; Smith, E.M.; Ziller, J.W.; Shaka, A.J. *Tetrahedron* **2002**, 58, 727. (e) Tsai, J.H.; Waldman, A.S.; Nowick, J.S. *Bioorg. Med. Chem.* **1999**, 7, 29.
- <sup>5</sup> Ait-Haddou, H.; Wiskur, S. L.; Lynch, V. M.; Anslyn, E. V. *J. Am. Chem. Soc.* **2001**, 123, 11296.
- <sup>6</sup> Wright, A. T.; Anslyn, E. V. *Org. Lett.* **2004**, 6, 1341.
- <sup>7</sup> (a) Smith, J.A.; Collins, J.G.; Patterson, B.T.; Keene, F.R. *Dalton Trans.* **2004**, 9, 1277. (b) Rice, C.R.; Baylies, C.J.; Harding, L.P.; Jeffery, J.C.; Paul, R.L.; Ward, M.D. *J. Chem. Soc., Dalton Trans.* **2001**, 20, 3039. (c) Goshe, A.J.; Crowley, J.D.; Bosnich, B. *Hel. Chim. Acta* **2001**, 84, 2971. (d) Jurek, P.E.; Martell, A.E. *Inorg. Chem.* **1999**, 38, 6003.
- <sup>8</sup> Baldini, L.; Wilson, A.J.; Hong, J.; Hamilton, A.D. *J. Am. Chem. Soc.* **2004**, 126, 5656.
- <sup>9</sup> Kral, V.; Rusin, O.; Schmidtchen, F.P. *Org. Lett.* **2001**, 3, 873.
- <sup>10</sup> (a) Bonar-Law, R.P.; Mackay, L.G.; Walter, C.J.; Marvaud, V.; Sanders, J.K.M. *Pure and Appl. Chem.* **1994**, 66, 803. (b) Nakash, M.; Sanders, J.K.M. *J. Org. Chem.* **2000**, 65, 7266.
- <sup>11</sup> (a) Hayashi, T.; Aya, T.; Nonoguchi, M.; Mizutani, T.; Hisaeda, Y.; Kitagawa, S.; Ogoshi, H. *Tetrahedron* **2002**, 58, 2803. (b) Wang, C.Z.; Zhu, Z.A.; Li, Y.; Yun, T.C.; Wen, X.; Fang, M.M.; Chan, W.L.; Chan, A.S.C. *New J. Chem.* **2001**, 276, 9093. Binding in water: (c) Imai, H.; Munakata, H.; Uemori, Y.; Sakura, N. *Inorg. Chem.* **2004**, 43, 1211. (d) Mizutani, T.; Wada, K.; Kitagawa S. *J. Am. Chem. Soc.* **1999**, 121, 11425.
- <sup>12</sup> (a) Malinowski, V. Tumir, L.; Piantanida, I.; Zinic, M.; Schneider, H.J. *Europ. J. Org. Chem.* **2002**, 22, 3785. (b) Munakata, H.; Kanzaki, T.; Nakagawa, S.; Imai, H.; Uemori, Y. *Chem. Pharm. Bull.* **2001**, 49, 1573.
- <sup>13</sup> Wada, K.; Mizutani, T.; Kitagawa, S. *J. Org. Chem.* **2003**, 68, 5123.
- <sup>14</sup> (a) Prodi, A.; Chiorboli, C.; Scandola, F.; Iengo, E.; Alessio, E.; Dobrawa, R.; Wuerthner, F. *J. Am. Chem. Soc.* **2005**, 127, 1454. (b) You, C.; Wuerthner, F. *Org. Lett.*

- 
- 2004**, 6, 2401. (c) Wuerthner, F.; Vollmer, M.S.; Effenberger, F.; Emele, P.; Meyer, D.U.; Port, H.; Wolf, H.C. *J. Am. Chem. Soc.* **1995**, 117, 8090.
- <sup>15</sup>Heintz, W. Justus Liebigs Ann. Chem. **1862**, 122, 257.
- <sup>16</sup>Podder, A.; Dattagupta, J.K.; Saha, N.N.; Saenger, N. *Acta Crystallogr.* **1979**, B35, 53.
- <sup>17</sup>Kramanenco, F.G.; Polynova, T.N.; Porsai-Koshits, M.A.; Chalvi, V.P.; Kumivanova, G.N.; Martynenko, L.I. *Zh. Strukt. Khim.* **1973**, 14, 744.
- <sup>18</sup>(a) Wu, Y.R.; Long, L.S.; Huang, R.B.; Zheng, L.S.; Ng, S.W. *Acta Cryst.* **2003**, E59, m390. (b) Mammano, N.J.; Templeton, D.H.; Zalkin, A. *Acta Cryst.* **1977**, B33, 1251. (c) Burshtein, I.F.; Poznyak, A.L. *Kristallografiya* **2000**, 45, 465. (d) Valach, F.; Hoang, N.N.; Lukes, I. *Chemical Papers* **1996**, 50, 115. (e) Morel, A.C.; Choquesillo-Lazarte, D.; Alarcon-Payer, C.; González-Pérez, J.M.; Castiñeiras, A.; Niclós-Gutiérrez, J. *Inorg. Chem. Comm.* **2003**, 6, 1354.
- <sup>19</sup>(a) Walters, M.A.; Vapnyar, V.; Bolour, A.; Incarvito, C.; Rheingold, A.L. *Polyhedron* **2003**, 22, 941. (b) Napoli, A. *J. Inorg. Nuc. Chem.* **1972**, 34, 1347.
- <sup>20</sup>Román-Alpiste, M.J.; Martín-Ramos, J.D.; Castiñeiras-Campos, A.; Bugella-Altamirano, E.; Sicilia-Zafra, A.G.; González-Pérez, J.M.; Niclós-Gutiérrez, J. *Polyhedron* **1999**, 18, 3341.
- <sup>21</sup>(a) Schmitt, W.; Jordan, P.A.; Henderson, R.K.; Moore, G.R.; Anson, C.E.; Powell, A.K. *Coord. Chem. Rev.* **2002**, 228, 115. (b) Klyén, M.; Lakatos, A.; Latajka, R.; Labádi, I.; Salifoglou, A.; Raptopoulou, C.P.; Kozlowaki, H.; Kiss, T. *J. Chem. Soc., Dalton Trans.* **2002**, 18, 3578. (c) Hong, L.; Duan-Jun, X.; Kai-Liang, Y. *Acta Cryst.* **2003**, E59, m671. (d) Mootz, D.; Wunderlich, H. *Acta Cryst.* **1980**, B36, 445.
- <sup>22</sup>Martell, A.E.; Smith, P.M. *Critical Stability Constants*; Plenum Press: New York, 1975; Vol.2.
- <sup>23</sup>Dung, N.H.; Viossat, B.; Busnot, A.; Pérez, J.M.; Niclós-Gutiérrez, J.; Gardette, F. *Inorg. Chim. Acta* **1990**, 174, 145.
- <sup>24</sup>Castiñeiras-Campos, A.; Busnot, A.; Abarca, M. E.; Sicilia-Zafra, A.G.; González-Pérez, J.M.; Niclós-Gutiérrez, J. *Inorg. Chim. Acta*, **1994**, 215, 73.
- <sup>25</sup>Castiñeiras-Campos, A.; Tercero, J.M.; Matilla, A.; González, J.M.; Sicilia, A.G.; Niclós, J. *J. Coord. Chem.* **1995**, 35, 61.
- <sup>26</sup>Castiñeiras-Campos, A.; Sicilia-Zafra, A.G.; González-Pérez, J.M.; Niclós-Gutiérrez, J.; China, E.; Mederos, A. *Inorg. Chim. Acta* **1996**, 241, 39.
- <sup>27</sup>Dung, N.H.; Viossat, B.; Busnot, A.; Sicilia-Zafra, A.G.; González-Pérez, J.M.; Niclós-Gutiérrez, J. *Inorg. Chim. Acta* **1990**, 169, 9.
- <sup>28</sup>Nardin, G.; Randaccio, L.; Bonomo, R.P.; Rizzareli, E. *J. Chem. Soc., Dalton Trans.* **1980**, 3, 369.
- <sup>29</sup>Castiñeiras, A.; Abarca, M.E.; De la Cueva, I.; González, J.M.; Niclós, J. *J. Coord. Chem.* **1993**, 30, 273.

- 
- <sup>30</sup>González Pérez, J.M.; Dung, N.H.; Niclós-Gutiérrez, J.; Viossat, B.; Busnot, A.; Vincente-Gelabert, M.L. *Inorg. Chim. Acta* **1989**, *166*, 155.
- <sup>31</sup>Niclós-Gutiérrez, J.; Abarca-García, E.; Viossat, B.; Dung, N.H.; Busnot, A.; Hemidy, J.F. *Acta Crystallogr.* **1993**, *C 49*, 19.
- <sup>32</sup>Rojas-González, P.X.; Choquesillo-Lazarte, D.; González-Pérez, J.M.; Ruíz-García, S.A.; Carballo, R.; Castiñeiras, A.; Niclós-Gutiérrez, J. *Polyhedron* **2003**, *22*, 1027.
- <sup>33</sup>Lisheng Cai; Wenge Xie; Mahmoud, H.; Ying Han; Wink, D.J.; Sichu Li; O'Connor, C.J. *Inorg. Chim. Acta* **1997**, *263*, 231.
- <sup>34</sup>(a) Furutachi, H.; Murayama, M.; Shiohara, A.; Yamazaki, S.; Fujinami, S.; Uehara, A.; Suzuki, M.; Ogo, S.; Watanabe, Y.; Maeda, Y. *Chem. Commun.* **2003**, 1900. (b) Murch, B.P.; Bradley, F.C.; Que Junior, L. *J. Am. Chem. Soc.* **1986**, *108*, 5027.
- <sup>35</sup>Kawata, S.; Nakamura, M.; Yamashita, Y.; Asai, K.; Kikuchi, K.; Ikemoto, I.; Katada, M.; Sano, H. *Chem. Lett.* **1992**, 135.
- <sup>36</sup>Tanase, T.; Inoue, C.; Ota, E.; Yano, S.; Takahashi, M.; Takeda, M. (2000) *Inorg. Chim. Acta* **2000**, *297*, 18.
- <sup>37</sup>Kato, M.; Yamada, Y.; Inagaki, T.; Mori, W.; Sakai, K.; Tsubomura, T.; Sato, M.; Yano, S. *Inorg. Chem.* **1995**, *34*, 2645.
- <sup>38</sup>Gorun, S.M.; Stibrany, R.T.; Lillo, A. (1998) *Inorg. Chem.* **1998**, *37*, 836.
- <sup>39</sup>(a) Tanase, T.; Yamada, Y.; Tanaka, K.; Miyazu, T.; Kato, M.; Lee, K.; Sugihara, Y.; Mori, W.; Ichimura, A.; Kinoshita, I.; Yamamoto, Y.; Haga, M.; Sasaki, Y.; Yano, S. *Inorg. Chem.* **1996**, *35*, 6230. (b) Tanase, T.; Kato, M.; Yamada, Y.; Tanaka, K.; Lee, K.; Sugihara, Y.; Ichimura, A.; Kinoshita, I.; Haga, M.; Sasaki, Y.; Yamamoto, Y.; Nagano, T.; Yano, S. *Chem. Lett.* **1994**, 1853.
- <sup>40</sup>Mikata, Y.; Takeshita, N.; Miyazu, T.; Miyata, Y.; Tanase, T.; Kinoshita, I.; Ichimura, A.; Mori, W.; Takamizawa, S.; Yano, S. *J. Chem. Soc., Dalton Trans.* **1998**, 1969.
- <sup>41</sup>(a) Wang Bo-Yi; Wang Ming; Zheng Pei-Ju; Liu Zhi-Jun; Chen Dong; Qu Yun; Tang Wen-Xia *Jiegou Huaxue (Chin.) (Chinese J. Struct. Chem.)* **1989**, *8*, 283. (b) Chen Dong; Liu Zhijun; Tang Wenxia; Dai Anbang; Liu Wangxi; Wang Boyi; Wang Ming; Zheng Peiju *Acta Crystallogr., Sect. C: Cryst. Struct. Commun.* **1990**, *46*, 1426. (c) Shkol'nikova, L.M.; Poznyak, A.L.; Sotman, S.S. *Zh. Neorg. Khim. (Russ.) (Russ. J. Inorg. Chem.)* **1995**, *40*, 776. (d) Burshtein, I.F.; Poznyak, A.L.; Stopolyanskaya, L.V. *Zh. Neorg. Khim. (Russ.) (Russ. J. Inorg. Chem.)* **1999**, *44*, 1251.
- <sup>42</sup>Polyakova, I.N.; Poznyak, A.L.; Sergienko, V.S. *Zh. Neorg. Khim. (Russ.) (Russ. J. Inorg. Chem.)* **2001**, *46*, 633.
- <sup>43</sup>Polyakova, I.N.; Poznyak, A.L.; Sergienko, V.S. *Kristallografiya (Russ.) (Crystallogr. Rep.)* **2000**, *45*, 833.
- <sup>44</sup>Brandi-Blanco, M.P.; Gonzalez-Perez, J.M.; Choquesillo-Lazarte, D.; Carballo, R.; Castiñeiras, A.; Niclos-Gutierrez, J. *Inorg. Chem. Commun.* **2003**, *6*, 270.
- <sup>45</sup>Marsh, R.E.; Bernal, I. *Acta Crystallogr., Sect. B: Struct. Sci.* **1995**, *51*, 300.

- 
- <sup>46</sup>Craven, E.; Cungen Zhang; Janiak, C.; Rheinwald, G.; Lang, H. Z. *Anorg. Allg. Chem.* **2003**, 629, 2282.
- <sup>47</sup>Bugella-Altamirano, E.; Gonzalez-Perez, J.M.; Choquesillo-Lazarte, D.; Carballo, R.; Castineiras, A.; Niclos-Gutierrez, J. *Inorg. Chem. Commun.* **2002**, 5, 727.
- <sup>48</sup>Sadikov, G.G.; Poznyak, A.L.; Antsyshkina, A.S.; Sergienko, V.S. *Kristallografiya (Russ.) (Crystallogr. Rep.)* **2001**, 46, 40.
- <sup>49</sup>de La Cueva, I.S.; Sicilia, A.G.; Gonzalez, J.M.; Bugella, E.; Castineiras, A.; Niclos-Gutierrez, J. *React. Funct. Polym.* **1998**, 36, 211.
- <sup>50</sup>Burns, C.J.; Field, L.D.; Hambley, T.W.; Lin, T.; Ridley, D.D.; Turner, P.; Wilkinson, M.P. *ARKIVOC* **2001**, 2, 157.
- <sup>51</sup>Bing-Xin Liu; Duan-Jun Xu *Acta Crystallogr., Sect. C: Cryst. Struct. Commun.* **2004**, 60, m137.
- <sup>52</sup>(a) Burshtein, I.F.; Poznyak, A.L.; Stopolyanskaya, L.V. *Zh. Neorg. Khim. (Russ.) (Russ. J. Inorg. Chem.)* **1998**, 43, 1632. (b) Gladkikh, O.P.; Polynova, T.N.; Poznyak, A.L.; Porai-Koshits, M.A. (1993) *Koord. Khim. (Russ.) (Coord. Chem.)* **1993**, 19, 133.
- <sup>53</sup>(a) Burshtein, I.F.; Poznyak, A.L.; Stopolyanskaya, L.V. *Koord. Khim. (Russ.) (Coord. Chem.)* **1997**, 23, 912. (b) Obodovskaya, A.E.; Shkol'nikova, L.M.; Poznyak, A.L. *Zh. Neorg. Khim. (Russ.) (Russ. J. Inorg. Chem.)* **1992**, 37, 594.
- <sup>54</sup>Subramaniam, V.; Kyu-Wang Lee; Hoggard, P.E. *Inorg. Chim. Acta* **1994**, 216, 155.
- <sup>55</sup>(a) Xu Duanjun; Cheng Chaorong; Xu Yuanzhi; Zhou Kangjing (1987) *Jiegou Huaxue (Chin.) (Chinese J. Struct. Chem.)* **1987**, 6, 39. (b) Xu Yuanzhi; Cheng Chaorong; Xu Duanjun; Chen Deyu *Huaxue Wuli Xuebao (Chin.) (Chin. J. Chem. Phys.)* **1989**, 2, 450. (c) Suarez-Varela, J.; Colacio, E.; Romerosa, A.; Avila-Roson, J.C.; Hidalgo, M.A.; Romero, J. *Inorg. Chim. Acta* **1994**, 217, 39.
- <sup>56</sup>Xu Duanjun; Cheng Caorong; Xu Yuanzhi; Hu Shengzhi *Jiegou Huaxue (Chin.) (Chinese J. Struct. Chem.)* **1989**, 8, 81.
- <sup>57</sup>Bugella-Altamirano, E.; Choquesillo-Lazarte, D.; Gonzalez-Perez, J.M.; Sanchez-Moreno, M.J.; Marin-Sanchez, R.; Martin-Ramos, J.D.; Covelo, B.; Carballo, R.; Castineiras, A.; Niclos-Gutierrez, J. *Inorg. Chim. Acta* **2002**, 339, 160.
- <sup>58</sup>Sanchez-Moreno, M.J.; Choquesillo-Lazarte, D.; Gonzalez-Perez, J.M.; Carballo, R.; Castineiras, A.; Niclos-Gutierrez, J. *Inorg. Chem. Commun.* **2002**, 5, 800.
- <sup>59</sup>Rojas-Gonzalez, P.X.; Castineiras, A.; Gonzalez-Perez, J.M.; Choquesillo-Lazarte, D.; Niclos-Gutierrez, J. *Inorg. Chem.* **2002**, 41, 6190.
- <sup>60</sup>Bugella-Altamirano, E.; Gonzalez-Peres, J.M.; Choquesillo-Lazarte, D.; Niclos-Gutierrez, J.; Castineiras-Campos, A. *Z. Anorg. Allg. Chem.* **2000**, 626, 930.
- <sup>61</sup>Yasui, T.; Ama, T.; Yonemura, T.; Kawaguchi, H. *Kochi Daigaku Rigakubu Kiyo Kagaku* **1999**, 20, 17.
- <sup>62</sup>Sato, M.; Kosaka, M.; Watabe, M. (1985) *Bull. Chem. Soc. Jpn.* **1985**, 58, 874.

- 
- <sup>63</sup>Hochuli, E.; Bannwarth, W.; Dobeli, H.; Gentz, R.; Suder, D. *Bio/Technology* **1988**, *6*, 1321.
- <sup>64</sup>Genz, R.; Certa, U.; Takacs, B.; Matile, H.; Dobelji, H.; Pink, P.; Mackay, M.; Bone, N.; Scaife, J.G. *EMBO J.* **1988**, *7*, 225.
- <sup>65</sup>(a) Skerra, A.I.; Pfitzinger, I.; Plunkthun, A. *Bio/Technology* **1991**, *9*, 273. (b) Lilius, G.; Persson, M.; Bulow, L.; Mosbach, K. *Eur. J. Biochem.* **1991**, *198*, 499.
- <sup>66</sup>Goud, G.N.; Patwardhan, A.V.; Beckmann, E.J.; Atai, M.M.; Koepsel, R.R. *Int. J. biol. Chromatogr.* **1997**, *3*, 123.
- <sup>67</sup>Patwardhan, A.V.; Goud, G.N.; Koepsel, R.R.; Atai, M.M. *J. Chromatogr.* **1997**, 787, 91.
- <sup>68</sup>Chen, Y.; Pasquinelli, R.; Atai, M.; Koepsel, R.R.; Kortes, R.A.; Shepherd, R.E. *Inorg. Chem.* **2000**, *39*, 1180.
- <sup>69</sup>(a) Sun, S.; Fazal, M.A.; Roy, B.C.; Mallik, S. *Org. Lett.* **2000**, *2*, 911. (b) Sun, S.; Fazal, M.A.; Roy, B.C.; Chandra, B.; Mallik, S. *Inorg. Chem.* **2002**, *41*, 1584.
- <sup>70</sup>(a) Roy, B.C.; Fazal, M.A.; Sun, S.; Mallik, S. *J. Chem. Soc., Chem. Commun.* **2000**, 547. (b) Fazal, M.A.; Roy, B.C.; Sun, S.; Mallik, S.; Rodgers, K.R. *J. Am. Chem. Soc.* **2001**, *123*, 6283.
- <sup>71</sup>Sadler, P.J.; Viles, J.H. *Inorg. Chem.* **1996**, *35*, 4490.
- <sup>72</sup>(a) Bildhan, C.R.; Hegge, R.; Rosendahl, T.; Jia, X.; Lareau, R.; Mallik, S.; Srivastava, D.K. *Chem. Commun.* **2003**, *18*, 2328. (b) Banerjee, A.L.; Swanson, M.; Roy, B.C.; Jia, X.; Halder, M.K.; Mallik, S.; Srivastava, D.K. *J. Am. Chem. Soc.* **2004**, *126*, 10875. (c) Roy, B.C.; Banerjee, A.L.; Swanson, M.; Jia, X.; Halder, M.K.; Mallik, S.; Srivastava, D.K. *J. Am. Chem. Soc.* **2004**, *126*, 13206.
- <sup>73</sup>Kruppa, M.; Mandl C.; Miltschitzky, S.; König, B. *J. Am. Chem. Soc.* **2005**, *127*, **3362**.
- <sup>74</sup>Davis, A. P.; Wareham, R. S. *Angew. Chem. Int. Ed.* **1999**, *38*, 2979.
- <sup>75</sup>James, T. D.; Samankumara Sandanayake, K. R. A.; Shinkai, S. *Angew. Chem. Int. Ed.* **1996**, *35*, 1910.
- <sup>76</sup>Nagai, Y.; Kobayashi, K.; Toi, H.; Aoyama, Y. *Bull. Chem. Soc. Jpn.* **1993**, *66*, 2965.
- <sup>77</sup>Striegler, S.; Tewes, E. *Eur. J. Inorg. Chem.* **2002**, *2*, 487.
- <sup>78</sup>Angyal, S. J. *Adv. Carbohydr. Chem. Biochem.* **1991**, *49*, 19.
- <sup>79</sup>Connors, K. A. Binding constants – *The Measurement of Molecular Complex Stability*, John Wiley & Sons, New York, 1987.
- <sup>80</sup>Porath, J.; Carlsson, J.; Belfrage, G. *Nature* **1975**, *258*, 598.
- <sup>81</sup>Ueda, E.K.M.; Gout, P.W.; Morganti, L. *J. Chromat. A* **2003**, 988, 1.
- <sup>82</sup>(a) Suen, S.-Y.; Liu, Y.C.; Chang, C-S. *J. Chromat. B* **2003**, 797, 305. (b) Shepherd, R. E. *Coord. Chem. Rev.* **2003**, *247*, 147. (c) Gaberc-Porekar, V.; Menart, V. *J. Biochem.*

---

*Biophys. Methods* **2001**, 49, 335. (d) Chaga, G. S. *J. Biochem. Biophys. Methods* **2001**, 49, 313. (e) Arnold F.H. *Bio/Technol.* **1991**, 9, 151. (f) Porath, J. *Trends in Anal. Chem.* **1988**, 7, 254.

<sup>83</sup>Rebek, J., Jr. *Acc. Chem. Res.* **1990**, 23, 399.

<sup>84</sup>For a review, see: Wulff, G. In *Biomimetic Polymers*; Gebelein, C.G., Ed.; Plenum Press: New York, 1990; p 1.

<sup>85</sup>Dhal, P.K.; Arnold, F.H. *J. Am. Chem. Soc.* **1991**, 113, 7417.

<sup>86</sup>Dhal, P.K.; Arnold, F.H. *Macromolecules* **1992**, 25, 7051.

<sup>87</sup>Arnold, F.H.; Plunkett, S.; Dhal, P.K.; Vidyasankar, S. *Poly. Preprints* **1995**, 36, 97.

<sup>88</sup>Plunkett, S.D.; Arnold, F.H. *J. Chromat. A* **1995**, 708, 19.

<sup>89</sup>Dhal, P.K.; Vidyasankar, S.; Arnold, F.H. *Chem. Mater.* **1993**, 7, 154.

<sup>90</sup>Vidyasankar, S.; Ru, M.; Arnold, F.H. *J. Chromat. A* **1997**, 775, 51.

<sup>91</sup>Shnek, D.R.; Pack, D.W.; Sasaki, D.Y.; Arnold, F.H. *Langmuir* **1994**, 10, 2382.

<sup>92</sup>Wuenschell, G.E.; Wen, E.; Todd, R.; Schnek, D.R.; Arnold, F.H. *J. Chromatogr.* **1991**, 543, 345.

<sup>93</sup>Schubert, J. *J. Am. Chem. Soc.* **1954**, 76, 3442.

<sup>94</sup>Ng, K. Pack, D.W.; Sasaki, D.Y.; Arnold, F.H. *Langmuir* **1995**, 11, 4048.

<sup>95</sup>Sasaki, D.Y.; Shnek, D.R.; Pack, D.W.; Arnold, F.H. *Angew. Chem. Int. Ed. Engl.* **1995**, 34, 905.

<sup>96</sup>Pack, D.W.; Arnold, F.H. *Chemistry and Physics of Lipids* **1997**, 86, 135.

<sup>97</sup>Pack, D.W.; Chen, G.; Maloney, K.M.; Chen, C.; Arnold, F.H. *J. Am. Chem. Soc.* **1997**, 119, 2479.

<sup>98</sup>Kornberg, R.D.; Darst, S.A. *Curr. Opin. Struct. Biol.* **1991**, 1, 642.

<sup>99</sup>Rajabalee, F.J.M. *J. Inorg. Nucl. Chem.* **1974**, 36, 557.

<sup>100</sup>(a) Valle, G.; Bombi, G.G.; Corain, B.; Favarato, M.; Zatta, P. *J. Chem. Soc., Dalton Trans.* **1989**, 8, 1513. (b) Tewari, B.B. *J. Chromat. A* **1995**, 718, 454.

<sup>101</sup>(a) Shepherd, R.E.; Hodgson, G.M.; Margerium, D.W. *Inorg. Chem.* **1971**, 10, 989. (b) Dung, N.H.; Viossat, B.; Busnot, A.; González Pérez, J.M.; González García, S.; Niclós Gutiérrez, J. *Inorg. Chem.* **1988**, 27, 1227. (c) Fábán, I. *Inorg. Chem.* **1993**, 32, 1184. (d) Saxena, V.K.; Srivastava, M.N. *J. Inorg. Biochem.* **1990**, 38, 37.

<sup>102</sup>(a) Laham, S.; Rajabalee, F.J.M. *Bioinorg. Chem.* **1973**, 2, 243. (b) Almeida Paz, F.A.; Klinowski, J. *J. Phys. Org. Chem.* **2003**, 16, 772. (c) Rabenstein, D.L.; Blakney, G. *Inorg. Chem.* **1973**, 12, 128.

<sup>103</sup>(a) Jackons, N.E.; Margerum, D.W. *Inorg. Chem.* **1967**, 6, 2038. (b) Erickson, L.E.; Ho, F. F.-L.; Reilley, C.N. *Inorg. Chem.* **1970**, 9, 1148.



- 
- <sup>104</sup>(a) Budkuley, J.S.; Naik, G.K. *Thermochimica Acta* **1998**, 320, 115. (b) Sharma, G.; Tandon, J.P. *J. Inorg. Nucl. Chem.* **1970**, 32, 1273.
- <sup>105</sup>(a) Sharma, C.L.; Jain, P.K.; De, T.K. *J. Inorg. Nucl. Chem.* **1980**, 42, 1681. (b) Visser, H.G.; Leipoldt, J.G.; Purcell, W.; Mostert, D. *Polyhedron* **1994**, 13, 1051. (c) Bhattacharyya, S.K.; Banerjee, R. *Polyhedron* **1997**, 16, 3371.
- <sup>106</sup>(a) Gustafson, R.L.; Martell, A.E. *J. Phys. Chem.* **1963**, 67, 576. (b) Cox, D.D.; Que, L. *J. Am. Chem. Soc.* **1988**, 110, 8085.
- <sup>107</sup>(a) Mentasti, E. *J. Chem. Soc., Dalton Trans.* 1982, 4, 721. (b) Chattopadhyay, S.P.; Banerjee, D. *Polyhedron* 1994, 13, 1981. (c) Visser, H.G.; Purcell, W.; Basson, S.S. *Trans. Met. Chem.* **2002**, 27, 461. (d) Visser, H.G.; Purcell, W.; Basson, S.S. *Trans. Met. Chem.* **2001**, 26, 175. (e) Smith, B.B.; Sawyer, D.T. *Inorg. Chem.* **1968**, 7, 922. (f) Meloon, D.R.; Harris, G.M. *Inorg. Chem.* **1977**, 16, 434.
- <sup>108</sup>Whitlow, S.H. *Inorg. Chim.* **1973**, 12, 2286.
- <sup>109</sup>(a) Baolong, L.; Bazong, L.; Jianping, L.; Yong Z. *Inorg. Chem. Commun.* **2003**, 6, 725. (b) Baolong, L.; Bazong, L.; Xia, Z.; Yong Z. *Inorg. Chem. Commun.* **2003**, 6, 1304. (c) Huawa, Y.; Juen S.; Liaorong, C.; Baosheng, L. *Polyhedron* **1996**, 15, 3891.
- <sup>110</sup>Abdus Salam, Md.; Aoki, K. *Inorg. Chim. Acta* **2000**, 311, 15.
- <sup>111</sup>Oliver, J.D.; Barnett, B.L.; Strickland, L.C. *Acta Cryst.* **1984**, B40, 377.
- <sup>112</sup>(a) Visser, H.G.; Purcell, W.; Basson, S.S. *Polyhedron* **1999**, 18, 2795. (b) Koine, N.; Bianchini, R.J.; Legg, J.I. *Inorg. Chem.* **1986**, 25, 2835.
- <sup>113</sup>Green, C.A.; Koine, N.; Legg, J.I.; Willett, R.D. *Inorg. Chim. Acta* **1990**, 176, 87-93.
- <sup>114</sup>(a) Bocarsly J.R.; Barton, J.K. *Inorg. Chem.* **1989**, 28, 4189. (b) Bocarsly J.R.; Chiang, M.Y.; Bryant L.; Barton, J.K. *Inorg. Chem.* **1990**, 29, 4898. (c) Bocarsly J.R.; Barton, J.K. *Inorg. Chem.* **1992**, 31, 2827.
- <sup>115</sup>(a) Malfant, I.; Morgenstern-Badarau, I.; Philoche-Levisalles, M.; Lloret, F. *J. Chem. Soc., Chem. Commun.* **1990**, 19, 1338. (c) Heath, S.L.; Powell, A.K.; Utting, H.L.; Helliwell, M. *J. Chem. Soc.; Dalton Trans.* **1992**, 2, 305.
- <sup>116</sup>Walters, M.A.; Vapnyar V.; Bolour, A.; Incarvito, C.; Rheingold, A.L. *Polyhedron* **2003**, 22, 941.
- <sup>117</sup>Wallis, S.C.; Gahan, L.R.; Charles, B.G.; Hambley, T.W. *Polyhedron* **1995**, 14, 2835.
- <sup>118</sup>Polyakova, I.N.; Poznyak, A.L.; Egorova, O.A. *Russ. J. Coord. Chem.* **2001**, 27, 852.
- <sup>119</sup>Battaglia, L.P.; Corradi Bonamartini, A.; Vidoni Tani, M.E. *Acta Cryst., Sec. B* **1975**, B31, 1160.
- <sup>120</sup>Visser, H.G.; Purcell, W.; Basson, S.S.; Claassen Q. *Polyhedron* **1997**, 16, 2851.
- <sup>121</sup>Visser, H.G.; Purcell, W.; Basson, S.S. *Polyhedron* **2001**, 20, 185.
- <sup>122</sup>(a) Kumita, H.; Jitsukawa, K.; Masuda, H.; Einaga, H. *Inorg. Chim. Acta* **1998**, 283, 160. (b) Kumita, H.; Kato, T.; Jitsukawa, K.; Einaga, H.; Masuda, H. *Inorg. Chem.* **2001**,

- 
- 40, 3936. (c) Jitsukawa, K.; Morioka, T.; Masuda, H. Ogoshi, H.; Einaga, H. *Inorg. Chim. Acta* **1994**, 216, 249. (d) Kumita, H.; Morioka, T.; Ozawa, T.; Jitsukawa, K.; Einaga, H.; Masuda, H. *Bull. Chem. Soc. Jpn.* **2001**, 74, 1035. (e) Gladkikh, O.P.; Polynova, T.N.; Porai-Koshits, M.A.; Poznyak, A.L. *Koord. Khim. (Russ.) (Coord. Chem.)* **1992**, 18, 1156.
- <sup>123</sup>Yamada, Y.; Tanabe, M.; Miyashita, Y.; Okamoto, K. *Polyhedron* **2003**, 22, 1455.
- <sup>124</sup>(a) White, L.S.; Nilsson, P.V.; Pignolet, L.H.; Que Junior, L. *J. Am. Chem. Soc.* **1984**, 106, 8312. (b) Que Junior, L.; Kolanczyk, R.C.; White, L.S. *J. Am. Chem. Soc.* **1987**, 109, 5373.
- <sup>125</sup>Fujita, T.; Ohba, S.; Nishida, Y.; Goto, A.; Tokii, T. *Acta Crystallogr., Sect. C: Cryst. Struct. Commun.* **1994**, 50, 544.
- <sup>126</sup>Gladkikh, O.P.; Polynova, T.N.; Porai-Koshits, M.A.; Poznyak, A.L. *Koord. Khim. (Russ.) (Coord. Chem.)* **1992**, 18, 1131.
- <sup>127</sup>Swaminathan, K.; Sinha, U.C.; Chatterjee, C.; Phulambrikar, A.; Padmanabhan, V.M.; Bohra, R. *Acta Crystallogr., Sect. C: Cryst. Struct. Commun.* **1989**, 45, 566.
- <sup>128</sup>Quanming Wang; Xintao Wu; Wenjian Zhang; Tianlu Sheng; Ping Lin; Jianmin Li *Inorg. Chem.* **1991**, 38, 2223.
- <sup>129</sup>(a) Bao-Long Li; Yan Xu; Qi Liu; Hua-Qin Wang; Zheng Xu *Chin. J. Chem.* **2002**, 20, 187. (b) Baolong Li; Yan Xu; Yi Dong; Jietong Chen; Zheng Xu *J. Chem. Cryst.* **2001**, 31, 357.
- <sup>130</sup>Ni-iya, K.; Fuyuhiko, A.; Yago, T.; Nasu, S.; Kuzushita, K.; Morimoto, S.; Kaizaki, S. *Bull. Chem. Soc. Jpn.* **2001**, 74, 1891.
- <sup>131</sup>Yaoyu Feng; Say-Leong Ong; Jiangyong Hu; Wun-Jern Ng *Acta Crystallogr., Sect. C: Cryst. Struct. Commun.* **2002**, 58, m34.
- <sup>132</sup>Almazan, F.; Garcia-Espana, E.; Mollar, M.; Lloret, F.; Julve, M.; Faus, J.; Solans, X.; Alins, N. *J. Chem. Soc., Dalton Trans.* **1990**, 2565.
- <sup>133</sup>Hopgood, D.; Angelici, R.J. *J. Am. Chem. Soc.* **1968**, 90, 2508.
- <sup>134</sup>(a) Newlin, D.E.; Pellack, M.A.; Nakon, R. *J. Am. Chem. Soc.* **1977**, 99, 1078. (b) Dembowski, J.S.; Kurtz, D.C.; Nakon, R. *Inorg. Chim. Acta* **1988**, 152, 209.
- <sup>135</sup>Perrin, D.D.; Sharma, V.S. *J. Chem. Soc. A* **1967**, 724.
- <sup>136</sup>Rabenstein, D.L.; Blakney, G. *Inorg. Chem.* **1973**, 12, 128.
- <sup>137</sup>Gabricevic, M.; Crumbliss, A.L. *Inorg. Chem.* **2003**, 42, 4098.
- <sup>138</sup>Kapanidis, A.N.; Ebright, Y.W.; Ebright, R.H. *J. Am. Chem. Soc.* **2001**, 123, 12123.
- <sup>139</sup>(a) Hochuli, E.; Bannwarth W.; Dobeli, H.; Gentz, R.; Stuber, D. *BioTechnol.* **1988**, 6, 1321. (b) Crowe, J.; Dobeli, H.; Gentz, R.; Hochuli, E.; Stuber, D.; Henco, K. *Methods Mol. Biol.* **1994**, 31, 371.

- 
- <sup>140</sup>Futaki, S.; Niwa, M.; Nakase, I.; Tadokoro, A.; Zhang, Y.; Nagaoka, M.; Wakako, N.; Sugiura, Y. *Bioconjugate Chem.* **2004**, *15*, 475.
- <sup>141</sup>Paborsky, L.R.; Dunn, K. E.; Gibbs, C.S.; Dougherty, J.P. *Anal. Biochem.* **1996**, *234*, 60.
- <sup>142</sup>(a) Hart, B.R.; Shea, K.J. *J. Am. Chem. Soc.* **2001**, *123*, 2072. (b) Hart, B.R.; Shea, K.J. *Macromol.* **2002**, *35*, 6192.
- <sup>143</sup>Abad, J.M.; Mertens, S.F.L.; Pita, M.; Fernandez, V.M.; Schiffrin, D.J. *J. Am. Chem. Soc.* **2005**, *127*, 5689.
- <sup>144</sup>(a) Liedberg, B.; Nylander, C.; Lundström, I. *Sens. Actuators* **1983**, *4*, 299. (b) Daniels, P.B.; Deacon, J.K.; Eddowes, M.J.; Pedley, D.G. *Sens. Actuators* **1988**, *16*, 11. (c) Löfas, S.; Johnsson, B. *Chem. Commun.* **1990**, 1526. (d) Nieba, L.; Nieba-Axmann, S.E.; Persson, A.; Hämäläinen, M.; Edebratt, F.; Hansson, A.; Lidholm, J.; Magnusson, K.; Karlsson, A.F.; Plückthun, A. *Anal. Biochem.* **1997**, *252*, 217.
- <sup>145</sup>Flanagan, M.T.; Pantell, R.H. *Electron. Lett.* **1984**, *20*, 968.
- <sup>146</sup>Sigal, G.B.; Bamdad, C.; Barberis, A.; Strominger, J.; Whitesides, G.M. *Anal. Chem.* **1996**, *68*, 490.
- <sup>147</sup>Ferguson, A.L.; Hughes, A.D.; Tufail, U.; Baumann, C.G.; Scott, D.J.; Hoggett, J.G. *FEBS Letters* **2000**, *481*, 281.
- <sup>148</sup>Kröger, D.; Liley, M.; Schiweck, W.; Skerra, A.; Vogel, H. *Biosens. Bioelectron.* **1999**, *14*, 155.
- <sup>149</sup>Hainfeld, J.F.; Liu, W.; Halsey, C.M.R.; Freimuth, P.; Powell, R.D. *J. Struct. Biol.* **1999**, *127*, 185.
- <sup>150</sup>Conti, M.; Falini, G.; Samorì, B. *Angew. Chem. Int. Ed.* **2000**, *39*, 215.
- <sup>151</sup>Haddour, N.; Cosnier, S.; Gondran, C. *J. Am. Chem. Soc.* **2005**, *127*, 5752.
- <sup>152</sup>(a) Schmitt, L.; Dietrich, C.; Tampé, R. *J. Am. Chem. Soc.* **1994**, *116*, 8485. (b) Gritsch, S.; Neumaier, K.; Schmitt, L.; Tampé, R. *Biosens. Bioelectron.* **1995**, *10*, 805. (c) Schmitt, L.; Bohanon, T.M.; Denzinger, S.; Ringsdorf, H.; Tampé, R. *Angew. Chem.* **1996**, *108*, 344.
- <sup>153</sup>Dietrich, C.; Schmitt, L.; Tampé, R. *Proc. Natl. Acad. Sci. USA* **1995**, *92*, 9014.
- <sup>154</sup>(a) Kubalek, E.W.; Le Grice, S.F.J.; Brown, P.O. *J. Struct. Biol.* **1994**, *113*, 117. (b) Dietrich, C.; Boscheinen, O.; Scharf, K.D.; Schmitt, L.; Tampé, R. *Biochemistry* **1996**, *35*, 1100. (c) Vénien-Bryan, C.; Balvoine, F.; Toussaint, B.; Mioskowski, C.; Hewat, E.A.; Helme, B.; Vignais, P.M. *J. Mol. Biol.* **1997**, *274*, 687. (d) Bischler, N.; Balvoine, F.; Milkereit, P.; Tschochner, H.; Mioskowski, C.; Schultz, P. *Biophys. J.* **1998**, *74*, 1522. (e) Celia, H.; Wilson-Kubalek, E.; Milligan, R.A.; Teyton, L. *Proc. Natl. Acad. Sci. USA* **1999**, *96*, 5634. (f) Kienberger, F.; Moser, R.; Schindler, H.; Blaas, D.; Hinterdorfer, P. *Single Mol.* **2001**, *2*, 99. (g) Courty, S.; Lebeau, L.; Martel, L.; Lenné, P.F.; Balvoine, F.; Dischert, W.; Konovalov, O.; Mioskowski, C.; Legrand, J.F.; Vénien-Bryan, C. *Langmuir* **2002**, *18*, 9502.

- 
- <sup>155</sup>Xu, C.; Xu, K.; Gu, H.; Zhong, X.; Guo, Z.; Zheng, R.; Zhang, X.; Xu, B. *J. Am. Chem. Soc.* **2004**, *126*, 3392.
- <sup>156</sup>Schmid, E.L.; Keller, T.A.; Dienes, Z.; Vogel, H. *Anal. Chem.* **1997**, *69*, 1979.
- <sup>157</sup>As there are many different abbreviations of this ligand in literature only bpa will be used in the following chapters.
- <sup>158</sup>(a) Kabzinska, B. *Ann. Pharm. Fr.* **1964**, *22*, 685. (b) Romary, J.K.; Barger, J.D.; Bunds, J.E. *Inorg. Chem.* **1969**, *7*, 1142.
- <sup>159</sup>(a) Rarig, R.S.; Zubieta, J. *J. Sol. Stat. Chem.* **2002**, *167*, 370. (b) Wahnnon, D.; Hynes, R.C.; Chin, J. *J. Chem. Soc., Chem. Commun.* **1994**, *12*, 1441. (c) Hartman, J.R.; Vachet, R.W.; Pearson, W.; Wheat, J.W.; Callahan, J.H. *Inorg. Chim. Acta* **2003**, *343*, 119. (d) Niklas, N.; Heinemann, F.W.; Hampel, F.; Clark, T.; Alsfasser, R. *Inorg. Chem.* **2004**, *43*, 4663. (e) Huang, G.S.; Su, C.C.; Wang, S.L.; Liao, F.L.; Lin, K.J. *J. Coord. Chem.* **2000**, *49*, 211. (f) Murali, M.; Palaniandavar, M. *Trans. Met. Chem.* **1996**, *21*, 142. (g) Nakon, R.; Rechani, P.R.; Angelici, R.J. *J. Am. Chem. Soc.* **1974**, *96*, 2117.
- <sup>160</sup>(a) Yahiro, M.; Kaneiwa, H.; Onaka, K.; Komiyama, M. *J. Chem. Soc., Dalton Trans.* **2004**, *4*, 605. (b) Brand, U.; burth, R.; Vahrenkamp, H. *Inorg. Chem.* **1996**, *35*, 1083.
- <sup>161</sup>(a) Goto, M.; Koga, N.; Ohse, Y.; Kudoh, Y.; Kukihara, M.; Okuno, Y.; Kurisaki, H. *Inorg. Chem.* **2004**, *43*, 5120. (b) Rodriguez, M.C.; Lambert, F.; Morgenstern-Badarau, I. *Inorg. Chem.* **1997**, *36*, 3525. (c) Leising, R.A. Kim, J.; Pérez, M.A.; Que, L. *J. Am. Chem. Soc.* **1993**, *115*, 9524. (d) Fernandes, C.; Wardell, J.L.; Horn, A.; Skakle, J.M.S.; Drago, V. *Polyhedron* **2004**, *23*, 1419. (e) Hazell, A.; McKenzie, C.J.; Nielsen, L.P. *Polyhedron* **2000**, *19*, 1333. (f) Viswanathan, R.; Palaniadavar, M.; Balasubramanian, T.; Muthiah, P.T.; *J. Chem. Soc., Dalton Trans.* **1996**, *12*, 2519. (g) Thomas, K.R.J.; Velusamy, M.; Palaniandavar, M. *Acta Crystal., Section C* **1998**, *C54*, 741. (h) O'Brien, R.J.; Richardson, J.F.; Buchanan, R.M. *Acta Crystal., Section C* **1991**, *C47*, 2307. (i) Trukhan, V.M.; Gritsenko, O.N.; Nordlander, E.; Shteinman, A.A. *J. Inorg. Biochem.* **2000**, *79*, 41.
- <sup>162</sup>Choi, K.Y.; Ryu, H.; Sung, N.D.; Suh, M. *J. Chem. Cryst.* **2003**, *33*, 947.
- <sup>163</sup>(a) Palaniandavar, M.; Butcher, R.J.; Addison, A.W. *Inorg. Chem.* **1996**, *35*, 467. (b) Huang, G.S.; Lai, J.K.; Ueng, C.H.; Su, C.C. *Trans. Met. Chem.* **2000**, *25*, 84.
- <sup>164</sup>(a) Muratami, T.; Hatakeyama, S.; Igarashi, S.; Yukawa, Y. *Inorg. Chim. Acta* **2000**, *310*, 96. (b) Muratami, T.; Orihashi, Z.; Kikuchi, Y.; Igarashi, S.; Yukawa, Y. *Inorg. Chim. Acta* **2000**, *303*, 148.
- <sup>165</sup>Funahashi, Y.; Kato, C.; Yamauchi, O. *Bull. Chem. Soc. Jpn.* **1999**, *72*, 415.
- <sup>166</sup>Gultneh, Y.; Khan, A.R.; Blaise, D.; Chaudhry, S.; Ahvazi, B.; Marvey, B.B.; Butcher, R.J. *J. Inorg. Biochem.* **1999**, *75*, 7.
- <sup>167</sup>Wirbser, J. Vahrenkamp, H. *Zeit. Naturfor.* **1992**, *47*, 962.
- <sup>168</sup>Glerup, J.; Goodson, P.A.; Hodgson, D.J.; Michelsen, K.; Nielsen, K.M.; Weihe, H. *Inorg. Chem.* **1992**, *31*, 4611.
- <sup>169</sup>Groß, F.; Müller-Hartmann, A.; Vahrenkamp, H. *Eur. J. Inorg. Chem.* **2000**, *12*, 2363.

- 
- <sup>170</sup>Mandon, D.; Nopper, A.; Litrol, T.; Goetz, S. *Inorg. Chem.* **2001**, *40*, 4803.
- <sup>171</sup>Butcher, R.J.; Addison, A.W. *Inorg. Chim. Acta* **1989**, *158*, 211.
- <sup>172</sup>(a) Toftlund, H.; Murray, K.S.; Zwack, P.R.; Taylor, L.F.; Anderson, O.P. *Chem. Commun.* **1986**, 191. (b) Nishino, S.; Hosomi, H.; Ohba, S.; Matsushima, H.; Tokii, T.; Nishida, Y. *J. Chem. Soc., Dalton Trans.* **1999**, 1509. (c) Ghiladi, M.; Jensen, K.B.; Jianzhong Jiang; McKenzie, C.J.; Morup, S.; Sotofte, I.; Ulstrup, J. *J. Chem. Soc., Dalton Trans.* **1999**, 2675. (d) Ito, S.; Okuno, T.; Matsushima, H.; Tokii, T.; Nishida, Y. *J. Chem. Soc., Dalton Trans.* **1996**, 4037. (e) Jensen, K.B.; McKenzie, C.J.; Simonsen, O.; Toftlund, H.; Hazell, A. *Inorg. Chim. Acta* **1997**, **257**, 163. (f) Zhong-Ming Wang; Hong-gen Wang; Xue-Bing Leng; Yun-Ti Chen *J. Mol. Struct.* **2001**, 597, 199. (g) Seong-Ju Kang; Nam Hwi Hur; H.G.Jang *Bull. Korean Chem. Soc.* **1998**, *19*, 654. (h) Borovik, A.S.; Que Junior, L.; Papaefthymiou, V.; Munck, E.; Taylor, L.F.; Anderson, O.P. *J. Am. Chem. Soc.* **1988**, *110*, 1986. (i) Borovik, A.S.; Papaefthymiou, V.; Taylor, L.F.; Anderson, O.P.; Que Junior, L. *J. Am. Chem. Soc.* **1989**, *111*, 6183. (j) Ghiladi, M.; McKenzie, C.J.; Meier, A.; Powell, A.K.; Ulstrup, J.; Wocadlo, S. *J. Chem. Soc., Dalton Trans.* **1997**, 4011. (k) Holman, T.R.; Andersen, K.A.; Anderson, O.P.; Hendrich, M.P.; Juarez-Garcia, C.; Munck, E.; Que Junior, L. *Angew. Chem., Int. Ed.* **1990**, *29*, 921.
- <sup>173</sup>(a) Adams, H.; Bradshaw, D.; Fenton, D.E. (2002) *J. Chem. Soc., Dalton Trans.* **2002**, 925. (b) Adams, H.; Bradshaw, D.; Fenton, D.E. *Inorg. Chim. Acta* **2002**, *332*, 195.
- <sup>174</sup>Nishida, Y.; Shimo, H.; Maehara, H.; Kida, S. *J. Chem. Soc., Dalton Trans.* **1985**, 1945.
- <sup>175</sup>(a) Yamaguchi, K.; Akagi, F.; Fujinami, S.; Suzuki, M.; Shionoya, M.; Suzuki, S. *Chem. Commun.* **2001**, 375. (b) Yamaguchi, K.; Koshino, S.; Akagi, F.; Suzuki, M.; Uehara, A.; Suzuki, S. *J. Am. Chem. Soc.* **1997**, *119*, 5752.
- <sup>176</sup>Holman, T.R.; Juarez-Garcia, C.; Hendrich, M.P.; Que Junior, L.; Munck, E. *J. Am. Chem. Soc.* **1990**, *112*, 7611.
- <sup>177</sup>Maeda, Y.; Tanigawa, Y.; Matsumoto, N.; Oshio, H.; Suzuki, M.; Takashima, Y. *Bull. Chem. Soc. Jpn.* **1994**, *67*, 125.
- <sup>178</sup>Manago, T.; Hayami, S.; Oshio, H.; Osaki, S.; Hasuyama, H.; Herber, R.H. Maeda, Y. *J. Chem. Soc., Dalton Trans.* **1999**, 1001.
- <sup>179</sup>Trukhan, V.M.; Pierpont, C.G.; Jensen, K.B.; Nordlander, E.; Shteinman, A.A. *Chem. Commun.* **1999**, 1193.
- <sup>180</sup>(a) Menage, S.; Fujii, H.; Hendrich, M.P.; Que Junior L. *Angew. Chem., Int. Ed.* **1994**, *33*, 1660. (b) Costas, M.; Cady, C.W.; Kryatov, S.V.; Ray, M.; Ryan, M.J.; Rybak-Akimova, E.V.; Que Junior, L. *Inorg. Chem.* **2003**, **42**, 7519. (c) Dick, S.; Weiss, A.; Wagner, U.; Wagner, F.; Grosse, G. *Z. Naturforsch., B: Chem. Sci.* **1997**, *52*, 372. (d) Hayashi, Y.; Suzuki, M.; Uehara, A.; Mizutani, Y.; Kitagawa, T. *Chem. Lett.* **1992**, 91. (e) Hayashi, Y.; Kayantani, T.; Sugimoto, H.; Suzuki, M.; Inomata, K.; Uehara, A.; Mizutani, Y.; Kitagawa, T.; Maeda, Y. *J. Am. Chem. Soc.* **1995**, *117*, 11220.
- <sup>181</sup>(a) Ghiladi, M.; Gomez, J.T.; Hazell, A.; Kofod, P.; Lumtscher, J.; McKenzie, C.J. *Dalton Trans.* **2003**, 1320. (b) Kayatani, T.; Hayashi, Y.; Suzuki, M. Uehara, A. *Bull. Chem. Soc. Jpn.* **1994**, *67*, 2980.

- <sup>182</sup>(a) Romero, I.; Dubois, L.; Collomb, M.-N.; Deronzier, A.; Latour, J.-M.; Pecaut, J. *Inorg. Chem.* **2002**, *41*, 1795. (b) Diril, H.; Hsiu-Rong Chang; Xiaohua Zhang; Larsen, S.K.; Potenza, J.A.; Pierpont, C.G.; Schugar, H.J.; Isied, S.S.; Hendrickson, D.N. *J. Am. Chem. Soc.* **1987**, *109*, 6207. (c) Diril, H.; Hsiu-Rong Chang; Nilges, M.J.; Xiaohua Zhang; Potenza, J.A.; Schugar, H.J.; Isied, S.S.; Hendrickson, D.N. *J. Am. Chem. Soc.* **1989**, *111*, 5102. (d) Dubois, L.; Dao-Feng Xiang; Xian-Shi Tan; Pecaut, J.; Jones, P.; Baudron, S.; Le Pape, L.; Latour, J.-M.; Baffert, C.; Chardon-Noblat, S.; Collomb, M.-N.; Deronzier, A. *Inorg. Chem.* **2003**, *42*, 750. (e) Mok, H.J.; Davis, J.A.; Pal, S.; Mandal, S.K.; Armstrong, W.H. *Inorg. Chim. Acta* **1997**, *263*, 385. (f) Blanchard, S.; Blain, G.; Riviere, E.; Nierlich, M.; Blondin, G. *Chem.-Eur. J.* **2003**, *9*, 4260. (g) Blanchard, S.; Blondin, G.; Riviere, E.; Nierlich, M.; Girerd, J.-J. *Inorg. Chem.* **2003**, *42*, 4568. (h) Karsten, P.; Neves, A.; Bortoluzzi, A.J.; Strahle, J.; Maichle-Mossmer, C. *Inorg. Chem. Commun.* **2002**, *5*, 434. (i) Pal, S.; Chan, M.K.; Armstrong, W.H. *J. Am. Chem. Soc.* **1992**, *114*, 6398. (j) Chan, M.K.; Armstrong, W.H. *J. Am. Chem. Soc.* **1989**, *111*, 9121. (k) Suzuki, M.; Sugisawa, T.; Senda, H.; Oshio, H.; Uehara, A. *Chem. Lett.* **1989**, 1091. (l) Pal, S.; Gohdes, J.W.; Wilisch, W.C.A.; Armstrong, W.H. *Inorg. Chem.* **1992**, *31*, 713. (m) Pal, S.; Armstrong, W.H. *Inorg. Chem.* **1992**, *31*, 5417. (n) Mandal, S.K.; Armstrong, W.H. (1995) *Inorg. Chim. Acta* **1995**, 229, 261.
- <sup>183</sup>Holman, T.R.; Zhingang Wang; Hendrich, M.P.; Que Junior, L. *Inorg. Chem.* **1995**, *34*, 134.
- <sup>184</sup>Suzuki, M.; Mikuriya, M.; Murata, S.; Uehara, A.; Oshio, H. *Bull. Chem. Soc. Jpn.* **1987**, *60*, 4305.
- <sup>185</sup>Toftlund, H.; Simonsen, O.; Pedersen, E. *Acta Chem. Scand.* **1990**, *44*, 676.
- <sup>186</sup>Dongwhan Lee; Lippard, S.J. *Inorg. Chim. Acta* **2002**, *341*, 1.
- <sup>187</sup>(a) Borovik, A.S.; Que Junior L. *J. Am. Chem. Soc.* **1988**, *110*, 2345. (b) Borovik, A.S.; Hendrich, M.P.; Holman, T.R.; Munck, E.; Papaefthymiou, V.; Que Junior, L. *J. Am. Chem. Soc.* **1990**, *112*, 6031. (c) Lanznaster, M.; Neves, A.; Bortoluzzi, A.J.; Szpoganicz, B.; Schwingel, E. (2002) *Inorg. Chem.* **2002**, *41*, 5641.
- <sup>188</sup>Maeda, Y.; Ishida, A.; Ohba, M.; Sugihara, S.; Hayami, S. (2002) *Bull. Chem. Soc. Jpn.* **2002**, *75*, 2441.
- <sup>189</sup>Suzuki, M.; Ueda, I.; Kanatomi, H.; Murase, I. *Chem. Lett.* **1983**, 185.
- <sup>190</sup>(a) Bernard, E.; Moneta, W.; Laugier, J.; Chardon-Noblat, S.; Deronzier, A.; Tuchagues, J.-P.; Latour, J.-M. (1994) *Angew. Chem., Int. Ed.* **1994**, *33*, 887. (b) Lambert, E.; Chabut, B.; Chardon-Noblat, S.; Deronzier, A.; Chottard, G.; Bousseksou, A.; Tuchagues, J.-P.; Laugier, J.; Bardet, M.; Latour, J.-M. *J. Am. Chem. Soc.* **1997**, *119*, 9424.
- <sup>191</sup>(a) Foxon, S.P.; Walter, O.; Koch, R.; Rupp, H.; Muller, P.; Schindler S. *Eur. J. Inorg. Chem.* **2004**, 344. (b) Calatayud, M.L.; Castro, I.; Sletten, J.; Lloret, F.; Julve, M. *Inorg. Chim. Acta* **2000**, *300*, 846. (c) Castro, I.; Faus, J.; Julve, M.; Mollar, M.; Monge, A.; Gutierrez-Puebla, E. *Inorg. Chim. Acta* **1989**, *161*, 97.
- <sup>192</sup>Cano, J.; De Munno, G.; Sanz, J.L.; Ruiz, R.; Lloret, F.; Faus, J.; Julve, M. *An. Quim.* **1997**, *93*, 174.

- 
- <sup>193</sup>Sugimoto, H.; Sasaki, Y. *Chem. Lett.* **1997**, 541.
- <sup>194</sup>Castro, I.; Sletten, J.; Faus, J.; Julve, M.; Journaux, Y.; Lloret, F.; Alvarez, S. *Inorg. Chem.* **1992**, **31**, 1889.
- <sup>195</sup>Merkel, M.; Schnieders, D.; Baldeau, S.M.; Krebs, B. *Eur. J. Inorg. Chem.* **2004**, 783.
- <sup>196</sup>Bang, E.; Michelsen, K.; Nielsen, K.M.; Pederson, E. *Acta Chem. Scand.* **1989**, **43**, 748.
- <sup>197</sup>Kani, Y.; Ohba, S.; Ito, S.; Nishida, Y. *Acta Crystallogr., Sect. C: Cryst. Struct. Commun.* **2000**, **56**, e195.
- <sup>198</sup>Makowska-Grzyska, M.M.; Szajna, E.; Shipley, C.; Arif, A.M.; Mitchell, M.H.; Halfen, J.A.; Berreau, L.M. *Inorg. Chem.* **2003**, **42**, 7472.
- <sup>199</sup>Jin Seog Seo, Nack-Do Sung, Hynes, R.C.; Jik Chin *Inorg. Chem.* **1996**, **35**, 7472.
- <sup>200</sup>Jin Seog Seo; Hynes, R.C.; Williams, D.; Jik Chin; Nack-Do Sung *J. Am. Chem. Soc.* **1998**, **120**, 9943.
- <sup>201</sup>(a) Jang, Ho G.; Hendrich, P.; Que Junior, L. *Inorg. Chem.* **1993**, **32**, 911. (b) Albedyhl, S.; Averbuch-Pouchot, M.T.; Belle, C.; Krebs, B.; Pierre, J.L.; Saint-Aman, E.; Torelli, S. *Eur. J. Inorg. Chem.* **2001**, 1457. (c) Belle, C.; Gautier-Luneau, I.; Karmazin, L.; Pierre, J.-L.; Albedyhl, S.; Krebs, B.; Bonin, M. *Eur. J. Inorg. Chem.* **2002**, 3087. (d) Schepers, K.; Bremer, B.; Krebs, B.; Henkel, G.; Althaus, E.; Mosel, B.; Muller-Warmuth, W. *Angew. Chem., Int. Ed.* **1990**, **29**, 531.
- <sup>202</sup>Ojida, A.; Mito-oka, Y.; Sada, K.; Hamachi, I. *J. Am. Chem. Soc.* **2004**, **126**, 2454.
- <sup>203</sup>Foxon, S.P.; Torres, G.R.; Walter, O.; Pedersen, J.Z.; Toftlund, H.; Huber, M.; Falk, K.; Haase, W.; Cano, J.; Lloret, F.; Julve, M.; Schindler, S. *Eur. J. Inorg. Chem.* **2004**, 335.
- <sup>204</sup>Lee, D.H.; Im, J.H.; Son, S.U.; Chung, Y.K.; Hong, J.I. *J. Am. Chem. Soc.* **2003**, **125**, 7752.
- <sup>205</sup>Castro, I.; Calatayud, M.L.; Sletten, J.; Lloret, F.; Cano, J.; Julve, M.; Seitz, G.; Mann, K. *Inorg. Chem.* **1999**, **38**, 4680.
- <sup>206</sup>Suzuki, M.; Fujinami, S.; Hibino, T.; Hori, H.; Maeda, Y.; Uehara, A.; Suzuki, M. *Inorg. Chim. Acta* **1998**, **283**, 124.
- <sup>207</sup>Chiou-Yuh Wu; Chan-Cheng Su *Polyhedron* **1997**, **16**, 383.
- <sup>208</sup>Sugimoto, H.; Sasaki, Y. *Chem. Lett.* **1998**, 197.
- <sup>209</sup>Rowland, J.M.; Olmstead, M.M.; Mascharak, P.K. *Inorg. Chim. Acta* **2002**, **332**, 37.
- <sup>210</sup>Chiou, Y.-M.; Que Junior, L. *Angew. Chem., Int. Ed.* **1994**, **33**, 1886.
- <sup>211</sup>Faus, J.; Julve, M.; Amigo, J.M.; Debaerdemaeker, T. *J. Chem. Soc., Dalton Trans.* **1989**, 1681.
- <sup>212</sup>Mito-oka, Y.; Tsukiji, S.; Hiraoka, T.; Kasagi, N.; Shinkai, S.; Hamachi, I. *Tet. Lett.* **2001**, **42**, 7059.

- 
- <sup>213</sup>Ojida, A.; Miyahara, Y.; Kohira, T.; Hamachi, I. *Biopolymers* **2004**, 76, 177.
- <sup>214</sup>(a) Ojida A.; Mito-oka, Y.; Inoue, M.; Hamachi, I. *J. Am. Chem. Soc.* **2002**, 124, 6256. (b) Ojida A.; Mito-oka, Y.; Inoue, M.; Hamachi, I. *J. Am. Chem. Soc.* **2003**, 125, 10184.
- <sup>215</sup>Ojida, A.; Park, S.; Mito-oka, Y.; Hamachi, I. *Tet. Lett.* **2002**, 43, 6193.
- <sup>216</sup>Yoshimura, I.; Miyahara, Y.; Kasagi, N.; Yamane, H.; Ojida, A.; Hamachi, I. *J. Am. Chem. Soc.* **2004**, 126, 12204.
- <sup>217</sup>Ojida, A.; Kohira, T.; Hamachi, I. *Chem. Lett.* **2004**, 33, 1024.
- <sup>218</sup>Kinoshita, E.; Takahashi, M.; Takeda, H.; Shiro, M.; Koike, T. *J. Chem. Soc., Dalton Trans.* **2004**, 8, 1189.
- <sup>219</sup>Han, M.S.; Kim, D.H. *Bioorg. Med. Chem. Lett.* **2003**, 13, 1079.
- <sup>220</sup>Lee, D.H.; Kim, S.Y.; Hong, J.I. *Angew. Chem.* **2004**, 116, 4881.
- <sup>221</sup>Hanshaw, R.G.; Hilkert, S.M.; Jiang, H.; Smith, B.D. *Tet. Lett.* **2004**, 45, 8721.
- <sup>222</sup>Koulov, A.V.; Stucker, K.A.; Lakshmi, C.; Smith, B.D. *Cell Death Differ.* **2003**, 10, 1357.
- <sup>223</sup>Laksmi, C.; Hanshaw, R.G.; Smith, B.D. *Tetrahedron* **2004**, 60, 11307.
- <sup>224</sup>da Mota, M.M.; Rodgers, J.; Nelson, S.M. *J. Chem. Soc. A* **1969**, 13, 2036.
- <sup>225</sup>(a) Xu, J.Y.; Bian, H.D.; Gu, W.; Yan, S.P.; Cheng, P.; Liao, D.Z.; Jiang, Z.H.; Shen, P.W. *J. Mol. Struct.* **2003**, 646, 237. (b) Yang, L.Y.; Peng, Y.; Bian, F.; Yan, S.P.; Liao, D.Z.; Cheng, P.; Jiang, Z.H. *J. Coord. Chem.* **2003**, 56, 961. (c) Szajna, E.; Dobrowolski, P.; Fuller, A.L.; Arif, A.M.; Berreau, L.M. *Inorg. Chem.* **2004**, 43, 3988. (d) Ito, M.; Kawano, H.; Takeuchi, T.; Takita, Y. *Chem. Lett.* **2000**, 29, 372.
- <sup>226</sup>(a) Failes, T.W. *Acta Cryst.* **2004**, E60, m781. (b) Failes, T.W. *Acta Cryst.* **2003**, E59, m616. (c) Otter, C.A.; Hartshirn, R.M. *J. Chem. Soc., Dalton Trans.* **2004**, 1, 150. (d) Mandel, J.B.; Maricondi, C.; Douglas, B.E. *Inorg. Chem.* **1988**, 27, 2990.
- <sup>227</sup>(a) Zheng, H.; Que, L. *Inorg. Chim. Acta* **1997**, 263, 301. (b) Neubrand, A.; Thaler, F.; Körner, M.; Zahl, A.; Hubbard, C.D.; van Eldik, R. *J. Chem. Soc., Dalton Trans.* **2002**, 6, 957. (c) Mukhopadhyay, U.; Bernal, I.; Massoud, S.S.; Mautner, F.A. *Inorg. Chim. Acta* **2004**, 357, 3673.
- <sup>228</sup>Madden, D.P.; Mota, M.M.; Nelson, S.M. *J. Chem. Soc. (A)* **1970**, 790.
- <sup>229</sup>(a) Zang, Y.; Que, L. *Inorg. Chem.* **1995**, 34, 1030. (b) Zheng, H.; Zang, Y.; Dong, Y.; Young, V.G.; Que, L. *J. Am. Chem. Soc.* **1999**, 121, 2226. (c) Corsi, D.M.; Murthy, N.N.; Young, V.G.; Karlin, K.D. *Inorg. Chem.* **1999**, 38, 848. (d) Kryatov, S.V.; Nazarenko, A.Y.; Robinson, P.D.; Rybak-Akimova, E.V. *Chem. Commun.* **2000**, 11, 921. (e) Mandon, D.; Machkour, A.; Goetz, S.; Welter, R. *Inorg. Chem.* **2002**, 41, 5364. (f) Viswanathan, R.; Palaniandavar, M.; Balasubramanian, T.; Muthiah, T.P. *Inorg. Chem.* **1998**, 37, 2943. (g) Kim, J.; Dong, Y.; Larka, E.; Que, L. *Inorg. Chem.* **1996**, 35, 2369.



- 
- <sup>230</sup>Karlin, K.D.; Hayes, J.C.; Juen, S.; Hutchinson, J.P.; Zubieta, J. *Inorg. Chem.* **1982**, *21*, 4108.
- <sup>231</sup>Zhu, L.; dos Santos, O.; Koo, C.W.; Rybstein, M.; Pape, L.; Canary, J.W. *Inorg. Chem.* **2003**, *42*, 7912.
- <sup>232</sup>Allen, C.S.; Chuang, C.L.; Cornebise, M.; Canary, J.W. *Inorg. Chim. Acta* **1995**, 239, 29.
- <sup>233</sup>Ito, M.; Fujita, K.; Chitose, F.; Takeuchi, T.; Yoshida, K.; Tacita, Y. *Chem. Lett.* **2002**, *6*, 594.
- <sup>234</sup>Adams, H.; Bailey, N.A.; Fenton, D.E.; He, Q.Y. *J. Chem. Soc., Dalton Trans.* **1995**, *4*, 697.
- <sup>235</sup>Mao, Z.W.; Hang, Q.W.; Tang, W.X.; Liu, S.X.; Wang, Z.M.; Huang, J.L. *Polyhedron* **1996**, *15*, 321.
- <sup>236</sup>Whittlesey, B.R.; Pang, Z.; Holwerda, R.A. *Inorg. Chim. Acta* **1999**, *284*, 124.
- <sup>237</sup>Merkel, M.; Pascaly, M.; Wieting, M.; Duda, M.; Rompel, A. *Z. Anorg. Allg. Chem.* **2003**, *629*, 2216.
- <sup>238</sup>Norman, R.E.; Yan, S.; Que, L.; Backes, G.; Ling, J.; Sanders-Loehr, J.; Zhang, J.H.; O'Connor, C. *J. Am. Chem. Soc.* **1990**, *112*, 1554.
- <sup>239</sup>Ménage, S.; Zang, Y.; Hendrich, M.P.; Que, L. *J. Am. Chem. Soc.* **1992**, *114*, 7786.
- <sup>240</sup>Umakoshi, K.; Tsuruma, Y.; Oh, C.E.; Takasawa, A.; Yasukawa, H.; Sasaki, Y. *Bull. Chem. Soc. Jpn.* **1999**, *72*, 433.
- <sup>241</sup>Adams, H.; Bailey, N.A.; Fenton, D.E.; Qing-Yu He *J. Chem. Soc., Dalton Trans.* **1997**, 1533.
- <sup>242</sup>Rivas, J.C.M.; de Rosales, R.T.M.; Parsons, S. *Dalton Trans.* **2003**, 4385.
- <sup>243</sup>Mandal, S.K.; Que Junior, L. (1997) *Inorg. Chem.* **1997**, *36*, 5424.
- <sup>244</sup>Yang Zang; Elgren, T.E.; Y. Dong; Que Junior, L. *J. Am. Chem. Soc.* **1993**, *115*, 811.
- <sup>245</sup>Chiou, Y.-M.; Que Junior, L. *J. Am. Chem. Soc.* **1995**, *117*, 3999.
- <sup>246</sup>Chiou, Y.-M.; Que Junior, L. *Inorg. Chem.* **1995**, *34*, 3270.
- <sup>247</sup>Chiou, Y.-M.; Que Junior, L. (1992) *J. Am. Chem. Soc.* **1992**, *114*, 7567.
- <sup>248</sup>Du-Hwan Jo; Chiou, Y.-M.; Que Junior, L. *Inorg. Chem.* **2001**, *40*, 3181.
- <sup>249</sup>Pascaly, M.; Duda, M.; Schweppe, F.; Zurlinden, K.; Muller, F.K.; Krebs, B. *J. Chem. Soc., Dalton Trans.* **2001**, 828.
- <sup>250</sup>Jang, Ho G.; Cox, D.D.; Que Junior, L. *J. Am. Chem. Soc.* **1991**, *113*, 9200.
- <sup>251</sup>Chiou, Y.-M.; Que Junior, L. *Inorg. Chem.* **1995**, *34*, 3577.

- 
- <sup>252</sup>(a) Shiping Yan; Cox, D.D.; Pearce, L.L.; Juarez-Garcia, C.; Que Junior, L.; Zhang, J.H.; O'Connor, C.J. *Inorg. Chem.* **1989**, 28, 2507. (b) Okuno, T.; Ito, S.; Ohba, S.; Nishida, Y. *J. Chem. Soc., Dalton Trans.* **1997**, 3547. (c) Norman, R.E.; Peterson, N.L.; Shih-Chi Chang *Acta Crystallogr., Sect. C: Cryst. Struct. Commun.* **1997**, 53, 452.
- <sup>253</sup>Norman, R.E.; Holz, R.C.; Menage, S.; O'Connor, C.J.; Zhang, J.H.; Que Junior, L. *Inorg. Chem.* **1990**, 29, 4629.
- <sup>254</sup>Oshio, H.; Ino, E.; Mogi, I.; Ito T. *Inorg. Chem.* **1993**, 32, 5697.
- <sup>255</sup>Gafford, B.G.; Marsh, R.E.; Schaefer, W.P.; Zhang, J.H.; O'Connor, C.J.; Holwerda, R.A. *Inorg. Chem.* **1990**, 29, 4652.
- <sup>256</sup>Koshi, C.; Umakoshi, K.; Sasaki, Y. *Chem. Lett.* **1997**, 1155.
- <sup>257</sup>Feng Xiang; Chun Ying Duan; Xiang Shi Tan; Yong Jiang Liu; Wen Xia Tang *Polyhedron* **1998**, 17, 2647.
- <sup>258</sup>Oshio, H.; Ichida, H. *J. Phys. Chem.* **1995**, 99, 3294.
- <sup>259</sup>Tyeklar, Z.; Paul, P.P.; Jacobson, R.R.; Farooq, A.; Karlin, K.D.; Zubieta, J. *J. Am. Chem. Soc.* **1989**, 111, 388.
- <sup>260</sup>Ito, M.; Takita, Y. *Chem. Lett.* **1996**, 929.
- <sup>261</sup>Dalley, N.K.; Xiaolan Kou; O'Connor, C.J.; Holwerda, R.A. *Inorg. Chem.* **1996**, 35, 2196.
- <sup>262</sup>(a) Murthy, N.N.; Karlin, K.D. *Chem. Commun.* **1993**, 1236. (b) Shiping Yan; Jianzhong Cui; Xin Liu; Peng Cheng; Daizheng Liao; Zonghui Jiang; Genglin Wang; Honggen Wang; Xinkan Yao *Sci. China, Ser. B* **1999**, 42, 535.
- <sup>263</sup>Yang Zang; Jinheung Kim; Yanhong Dong; Wilkinson, E.C.; Appelman, E.H.; Que Junior, L. *J. Am. Chem. Soc.* **1997**, 119, 4197. Makowska-Grzyska, M.M.; Szajna, E.; Shipley, C.; Arif, A.M.; Mitchell, M.H.; Halfen, J.A.; Berreau, L.M. *Inorg. Chem.* **2003**, 42, 7472.
- <sup>264</sup>Bjernemose, J.; Hazell, A.; McKenzie, C.J.; Mahon, M.F.; Nielsen, L.P.; Raithby, P.R.; Simonsen, O.; Toftlund, H.; Wolny, J.A. *Polyhedron* **2003**, 22, 875.
- <sup>265</sup>Kojima, T.; Sakamoto, T.; Matsuda, Y.; Ohkubo, K.; Fukuzumi, S. *Angew. Chem., Int. Ed.* **2003**, 42, 4951.
- <sup>266</sup>Baek, H.K.; Holwerda, R.A. *Inorg. Chem.* **1983**, 22, 3452.
- <sup>267</sup>Mareque Rivas, J.C.; Prabakaran, R.; de Rosales, R.T.M. *Chem. Commun.* **2004**, 1, 76.
- <sup>268</sup>Mareque Rivas, J.C.; de Rosales, R.T.M.; Parsons, S. *Chem. Commun.* **2004**, 5, 610.
- <sup>269</sup>(a) Tobey, S.L.; Anslyn, E.V. *Org. Lett.* **2003**, 5, 2029. (b) Tobey, S.L.; Jones, B.D.; Anslyn, E.V. *J. Am. Chem. Soc.* **2003**, 125, 4026. (c) Tobey, S.L.; Anslyn, E.V. *J. Am. Chem. Soc.* **2003**, 125, 14807.

## B. Main Part

### 1. Investigation of Metal Complex – Amino Acid Side Chain Interactions by Potentiometric Titration<sup>i</sup>

This chapter deals with the application of potentiometric titrations as a screening method for interactions of metal complexes with additional substrates related to side chains of amino acids.<sup>ii</sup> The resulting data was analysed by a computer program (HyperQuad2000) to determine every equilibrium constant involved in the titration experiment.<sup>iii</sup>

---

<sup>i</sup> Kruppa, M.; Frank, D.; Leffler-Schuster, H.; König, B. *Inorg Chem.* **2005**, *under revision*.

<sup>ii</sup> All potentiometric titrations were performed by H. Leffler-Schuster.

<sup>iii</sup> Data analysis was carried out by D. Frank as reported in his Zulassungsarbeit.

## 1.1 Introduction

In 1975 *Porath* published a new type of chromatography which was first called "metal chelate chromatography", but later termed "immobilised metal (ion) affinity chromatography" (IMAC).<sup>1</sup> The technique uses the different affinity of proteins to metal complexes immobilised on a chromatographic support.<sup>2</sup>

To find suitable metal complexes for this purification method it is necessary to know how strong metal ions are bound to a chelate (problem of metal leaching<sup>3</sup>). This information can be obtained using potentiometric titration of desired metal and chelate.<sup>4</sup> IDA and NTA complexes are well investigated in this respect.<sup>5,6</sup> But next to the binding between metal and immobilised chelate the interactions of substrate and metal complex are essential for the use in chelating purification methods. Weak binding will not generate a good separation. Very strong interactions will block all binding sites. Potentiometric titration can reveal equilibria between metal complexes and additional ligands.<sup>7</sup> The binding of amino acids towards different metal complexes was investigated,<sup>8</sup> but in most of the data the  $\alpha$ -amine and Carboxylate amino acid functional group are used to chelate the metal complex. Working with peptide or proteins, these binding processes are not relevant. C-terminal Carboxylate and N-terminal amine of one protein will not chelate a metal complex. The support of additional side chain functionalities is essential for a binding event. The histidine-tag strategy, in which several imidazole side chains and the N-terminal amino group reversibly coordinate to a metal complex, demonstrates this impressively. To understand which side chains of natural amino acids are suitable for metal coordination potentiometric titration may provide information.

We report here the use of potentiometric titration to screen interactions between several metal complexes (figure 76) and functional groups of amino acid side chains. In addition to the well investigated IMAC metal complexes **72-75** we focus our investigation on M(II) cyclen complexes **76-79**.

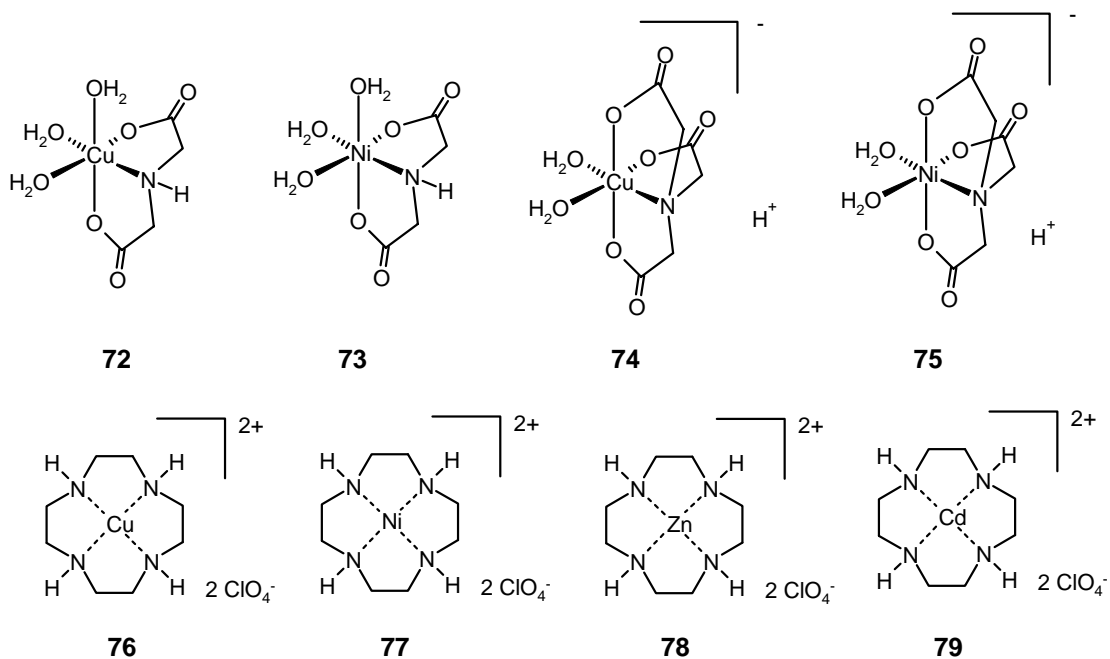


**Figure 76.** Structures of metal complexes **72-79** investigated in this study.

We represent typical amino acids side chain functional groups by butyl amine (Lsy), acetic acid (Glu, Asp), ethanol (Ser, Thr), ethane thiole (Cys), imidazole (His), N-ethylguanidine hydrochloride (Arg), phenol (Tyr) and disodium phenylphosphate (phosphorylated Tyr). The investigation of each metal complex – substrate combination consists of three experiments. In two initial potentiometric titrations, we examine the properties of substrate and metal complex separately. The obtained  $pK_s$  values for substrate and metal complex are then used to analyse the titration curve of a 1:1 mixture of substrate and metal complex.

## 1.2 Results and Discussion

First, the substances resembling the side chain functional groups of natural amino acids (with exception of amide and thioether) were titrated, to determine their  $pK_a$  values for our experimental conditions. Table 20 summarises the results and compares with literature reported values.

**Table 20.** Determination of  $pK_a$  values for the different functional group

Compound	Deprotonation reaction(s)	$pK_a$ (this work)	$pK_a$ (Lit.)
butylamine	$\text{But-NH}_3^+ / \text{But-NH}_2 + \text{H}^+$	11.3	10.6 <sup>6</sup>
di-Sodium-phenylphosphate <sup>a</sup>	$\text{RPO}_4\text{H}_2 / \text{RPO}_4\text{H}^- + \text{H}^+$	1.0	0.8 <sup>9</sup>
	$\text{RPO}_4\text{H}^- / \text{RPO}_4^{2-} + \text{H}^+$	6.2	6.2 <sup>10</sup>
acetic acid	$\text{HAc} / \text{Ac}^- + \text{H}^+$	4.7	4.7 <sup>6</sup>
ethanol	$\text{EtOH} / \text{EtO}^- + \text{H}^+$	<sup>b</sup>	15.9 <sup>6</sup>
ethanthiole	$\text{EtSH} / \text{EtS}^- + \text{H}^+$	13.2	10.1 – 11.3 <sup>11</sup>
imidazole <sup>a</sup>	$\text{ImH}_2^+ / \text{ImH} + \text{H}^+$	7.3	7.0 <sup>6</sup>
	$\text{ImH} / \text{Im}^- + \text{H}^+$	<sup>b</sup>	14.4 <sup>6</sup>
N-ethylguanidine-hydrogenchloride	$\text{RNH}_3^+ / \text{RNH}_2 + \text{H}^+$	<sup>b</sup>	13.4 <sup>12</sup>
phenol	$\text{PhOH} / \text{PhO}^- + \text{H}^+$	10.2	10.0 <sup>6</sup>

<sup>a</sup> 1 eq  $\text{HClO}_4$  for each protonation step was added

<sup>b</sup> Determination of  $pK_a$  value not possible using TEAOH

The potentiometric titration of the metal complexes **72-79** was used to determine the  $pK_a$  values of the deprotonation of coordinated water molecule(s). In cases of **74** and **75** an initial deprotonation of the third carbonic acid is taking place before the required NTA complex is formed.

**Table 21.** Potentiometric Titration of metal complexes investigated in this study

Metal complex	Deprotonation reaction(s)	pKa
Cu(II)-IDA ( <b>72</b> )	$[\text{Cu}(\text{ida})(\text{H}_2\text{O})_3] / [\text{Cu}(\text{ida})(\text{OH})(\text{H}_2\text{O})_2]^- + \text{H}^+$	9.0
Ni(II)-IDA ( <b>73</b> )	$[\text{Ni}(\text{ida})(\text{H}_2\text{O})_3] / [\text{Ni}(\text{ida})(\text{OH})(\text{H}_2\text{O})_2]^- + \text{H}^+$	9.8
Cu(II)-NTA ( <b>74</b> )	$[\text{Cu}(\text{ntaH})(\text{H}_2\text{O})_3] / [\text{Cu}(\text{nta})(\text{H}_2\text{O})_2]^- + \text{H}^+$	2.1
	$[\text{Cu}(\text{nta})(\text{H}_2\text{O})_2]^- / [\text{Cu}(\text{nta})(\text{OH})(\text{H}_2\text{O})]^{2-} + \text{H}^+$	9.9
	$[\text{Cu}(\text{nta})(\text{H}_2\text{O})(\text{OH})]^- / [\text{Cu}(\text{nta})(\text{OH})_2]^{3-} + \text{H}^+$	12.8
Ni(II)-NTA ( <b>75</b> )	$[\text{Ni}(\text{ntaH})(\text{H}_2\text{O})_3] / [\text{Ni}(\text{nta})(\text{H}_2\text{O})_2]^- + \text{H}^+$	2.1
	$[\text{Ni}(\text{nta})(\text{H}_2\text{O})_2]^- / [\text{Ni}(\text{nta})(\text{OH})(\text{H}_2\text{O})]^{2-} + \text{H}^+$	13.8
Cu(II)-Cyc ( <b>76</b> )	$[\text{Cu}(\text{cyc})(\text{H}_2\text{O})]^{2+} / [\text{Cu}(\text{cyc})(\text{OH})]^+ + \text{H}^+$	12.9
Ni(II)-Cyc ( <b>77</b> )	$[\text{Ni}(\text{cyc})(\text{H}_2\text{O})]^{2+} / [\text{Ni}(\text{cyc})(\text{OH})]^+ + \text{H}^+$	12.5
Zn(II)-Cyc ( <b>78</b> )	$[\text{Zn}(\text{cyc})(\text{H}_2\text{O})]^{2+} / [\text{Zn}(\text{cyc})(\text{OH})]^+ + \text{H}^+$	8.1
Cd(II)-Cyc ( <b>79</b> )	$[\text{Cd}(\text{cyc})(\text{H}_2\text{O})]^{2+} / [\text{Cd}(\text{cyc})(\text{OH})]^+ + \text{H}^+$	11.2

The potentiometric titrations to identify interactions between a functional group and a metal complex were carried out at a constant 1:1 substrate to metal complex ratio. Variation of the ratio was not expected to yield extra information, and was not attempted.

### M(II)-IDA Titration

As an already established system for poly-His-tag binder M(II)-IDA complexes were used to verify the screening method. Cu(II)- and Ni(II)-IDA complexes are known to have the highest affinity towards histidines.<sup>2</sup> Figure 77 shows the affinities of all tested substrates towards these metal complexes **72** and **73**. As expected, among all tested compounds only imidazole showed significant binding affinity to the metal complexes.

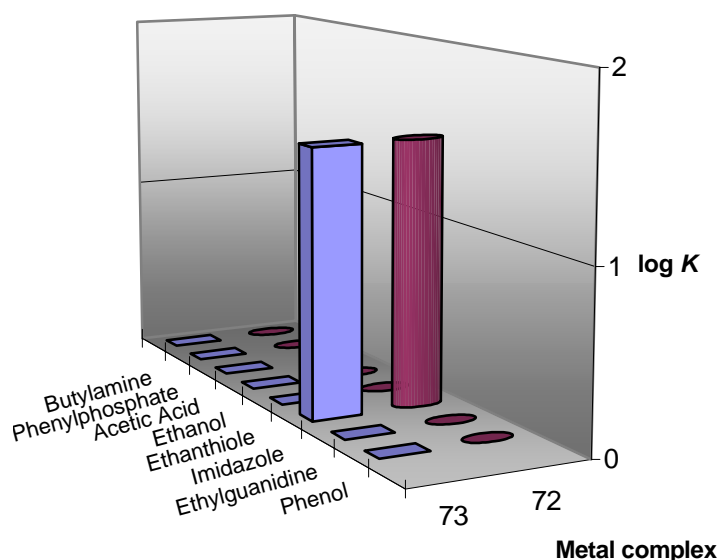
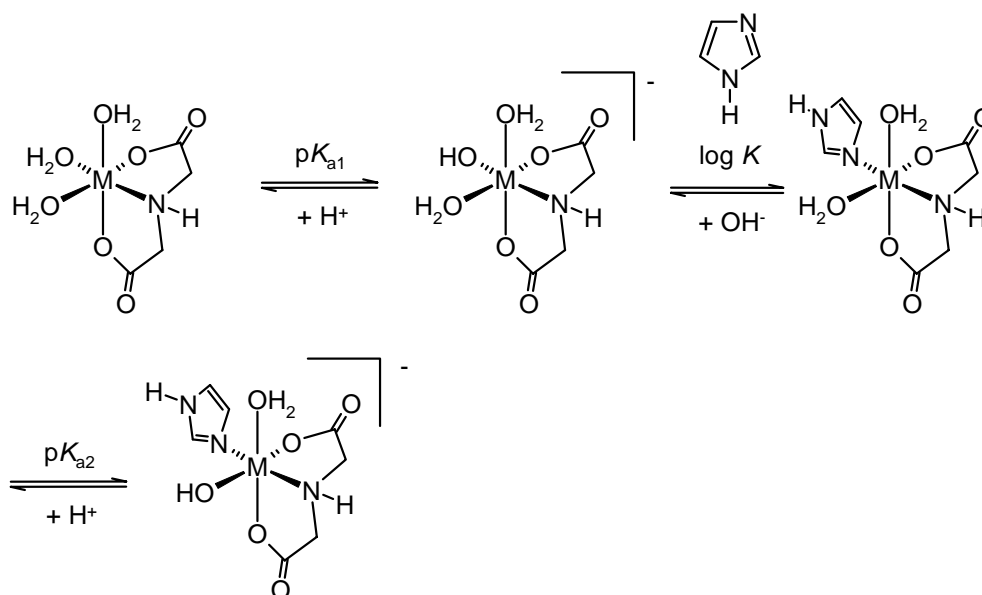


**Figure 77.** Potentiometric screening results for Cu(II)-IDA **72** and Ni(II)-IDA **73** complexes.

All other experiments showing no binding event were analysed by two independent equilibria already known from the separate titration experiments. The  $pK_a$  values fit very well to the data obtained and summarised in table 20 and table 21.

The equilibria shown in scheme 23 were used to analyse the potentiometric data. The initial deprotonation step ( $pK_{a1}$  values can be found in table 21) is followed by a 1:1 complexation of imidazole and  $M(II)$ -IDA<sup>13</sup> ( $pK_{a2}$  (**72**) = 13.0,  $pK_{a2}$  (**73**) = 12.9).

**Scheme 23.** Deprotonation and binding equilibria used to fit potentiometric titration data of imidazole in the presence of **72** or **73**





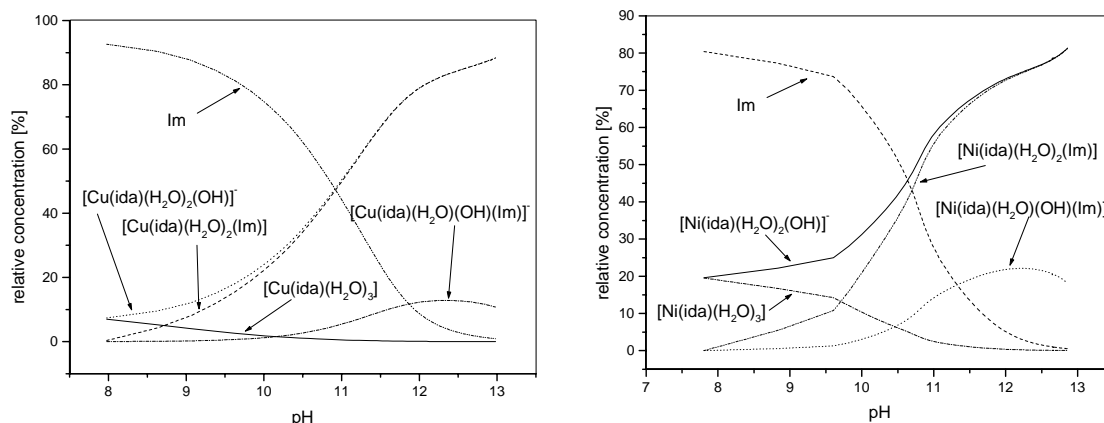


**Figure 78.** Species distribution plots of **72** (left) and **73** (right) in the presence of imidazole.

The species distribution plots of **72** and **73** are similar. The increase in deprotonated  $[\text{Cu}(\text{ida})(\text{H}_2\text{O})_2(\text{OH})]^-$  is more continuous with increasing basicity, while the Ni(II) complex is deprotonated very slowly until a pH of 9.5. Similar characteristics are observed for the aggregate formed between metal complex and imidazole. At the end of titration (pH 13) both imidazole-metal complex aggregates represent nearly 85 % of the complexes species.

### M(II)-NTA Titration

In the last decade NTA complexes were used more frequently than IDA complex for immobilisation of His-tagged proteins. Possessing an additional Carboxylate function for metal complexation, the binding between chelate and metal ion is tighter.<sup>14</sup>

In the same way as shown for IDA, the NTA complexes **74** and **75** were used in a potentiometric screening experiment. Figure 79 illustrates the affinities of all tested substrates to the metal complexes **74** and **75**. Among all tested compounds only imidazole showed affinity to the metal complexes.

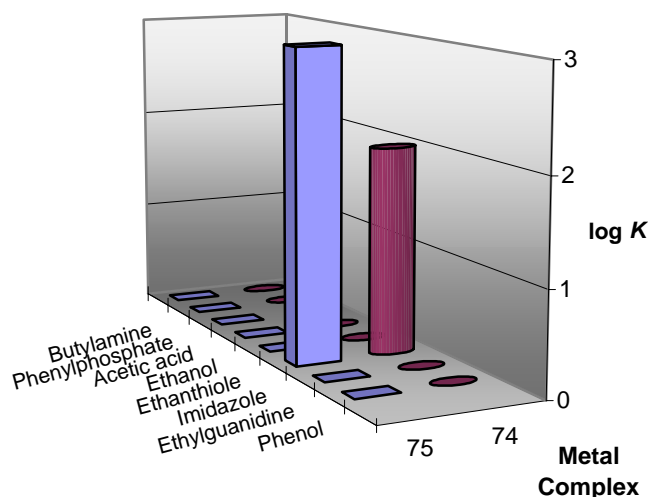


**Figure 79.** Potentiometric screening results for Cu(II)-NTA **74** and Ni(II)-NTA **75** complexes.

Similar to the titration of the M(II)-IDA complexes, data from titrations without binding process were analysed by two independent deprotonation equilibria of substrate and metal complex. The  $pK_a$  values derived fit very well to the previously obtained data in table 20 and table 21.

The first reaction taking place is a proton transfer and takes place after mixing imidazole with **74** or **75**. Imidazole is protonated and the NTA complex is formed (scheme 24). Starting the potentiometric titration, imidazole is deprotonated again. The equilibria used for analysis of the obtained data are shown in scheme 24.  $pK_{a1}$  values are listed in table 21. The deprotonation of the formed imidazole-M(II)-NTA complex is only observed for titration of **74** ( $pK_{a2} = 13.8$ ).

**Scheme 24.** Deprotonation and binding equilibria assumed to fit potentiometric titration data of imidazole in the presence of **74** or **75**

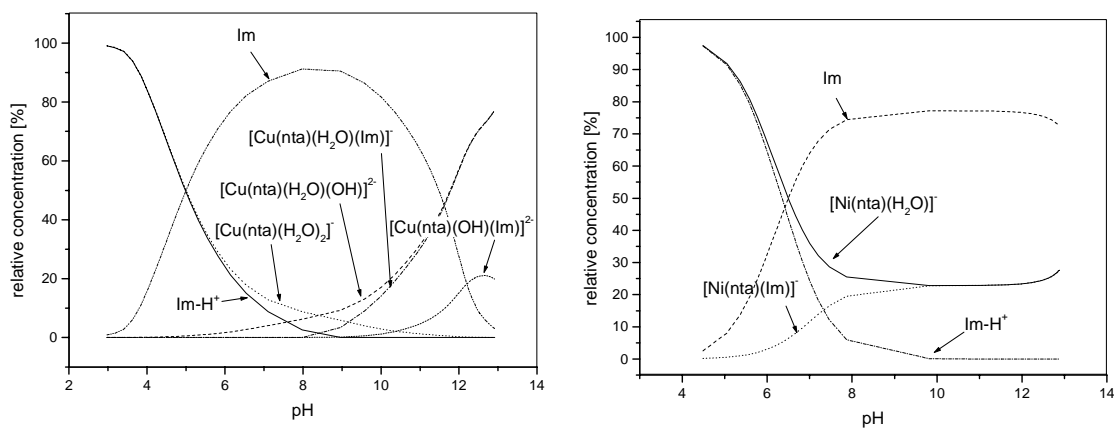
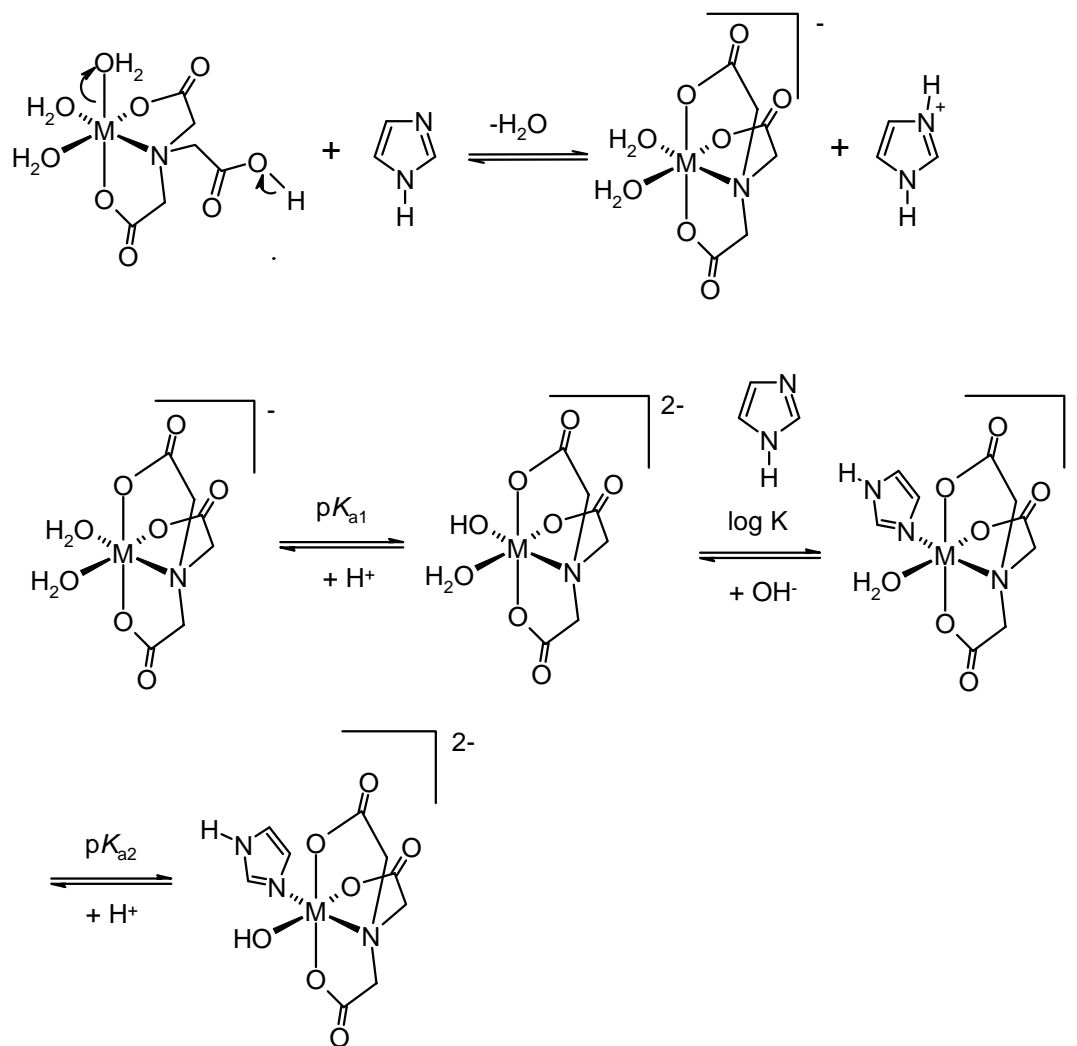


**Figure 80.** Species distribution plots of **74** (left) and **75** (right) in the presence of imidazole.

Comparing the binding between imidazole and **74** with the interactions between imidazole and **75** some differences are observed. The interactions of **75** and imidazole is stronger compared to the Cu(II) complex. While the binding to the Ni(II) complex starts around pH 6, the Cu(II) complex starts interacting with imidazole only after reaching pH 8.

### M(II) Cyclen Titration

The previous chapters demonstrated the ability of potentiometric screening to identify substrate-metal complex interactions. Cyclen complexes are known to show high affinities towards several functional groups, like phosphates or imides.<sup>15,16</sup> Potentiometric measurements were used to find unknown interactions between side chain functionalities of natural amino acids and these M(II)-cyclen complexes. Figure 81 shows the affinities of the examined substrates to the cyclen complexes **76-79**. In addition to the previously described interactions of phosphates and Zn(II)-cyclen **78** the measurement reveal, that imidazole is binding to Zn(II)-cyclen **78** and Cd(II)-cyclen **79**.

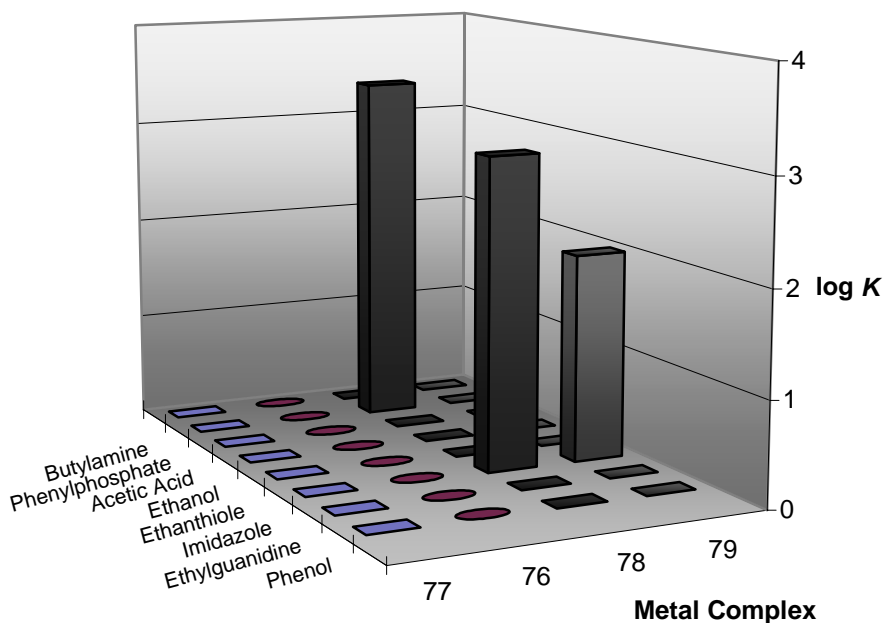


**Figure 81.** Potentiometric screening results for Cu(II)-cyclen **76**, Ni(II)-cyclen **77**, Zn(II)-cyclen **78**, and Cd(II)-cyclen **79** complexes.

All other titrations resulted just in the independent deprotonation of two compounds in solution. Scheme 25 illustrates the assumed equilibria for potentiometric data fitting of the titration of Zn(II)-cyclen in the presence of di-sodium phenylphosphate. Phenylphosphate and water coordinated to **78** show protonation equilibria with  $pK_a$  values of 6.0 and 8.4, resp.

**Scheme 25.** Equilibria assumed in the titration of **78** in the presence of phenylphosphate

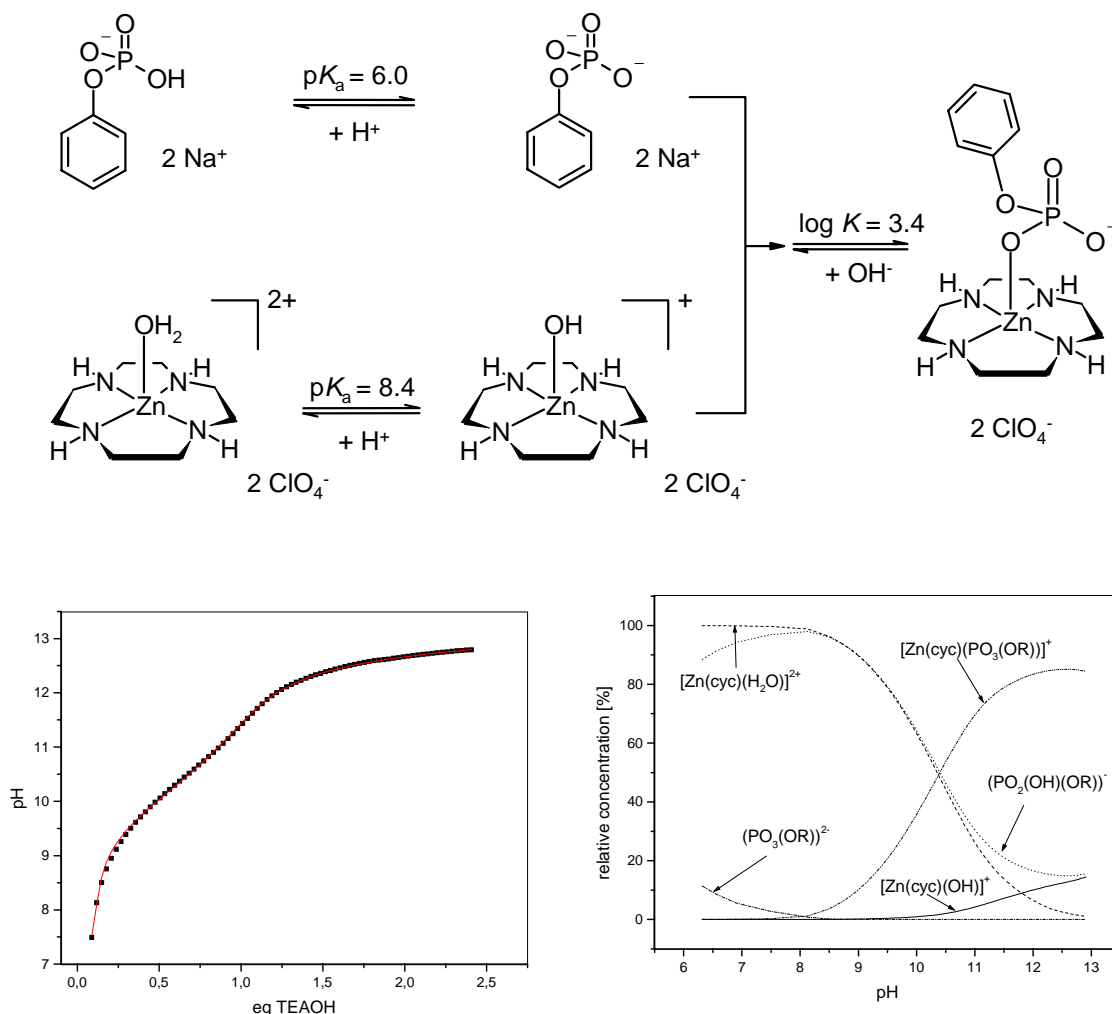


**Figure 82.** Potentiometric titration data (left) of a 1:1 mixture of **78** and phenylphosphate (black dots are experimental data; red line is the calculated fitting) and species distribution plot (right).

The distribution plot of the interaction between **78** and phenylphosphate shows that binding starts at around pH 9 and at pH 11 approx. 70 % of **78** is coordinated by phenylphosphate. Analysing the potentiometric titration of **78** and imidazole resulted in more complex equilibria. Initial one imidazole coordinates to one cyclen. At around pH 9.5 this imidazole is deprotonated, promoted by the Lewis acidic metal complex. The negatively charged imidazole now attracts a second Zn(II)-cyclen complex and forms a 2:1 Zn(II)-cyclen – imidazole aggregate.

**Scheme 26.** Deprotonation and binding equilibria of **78** and imidazole

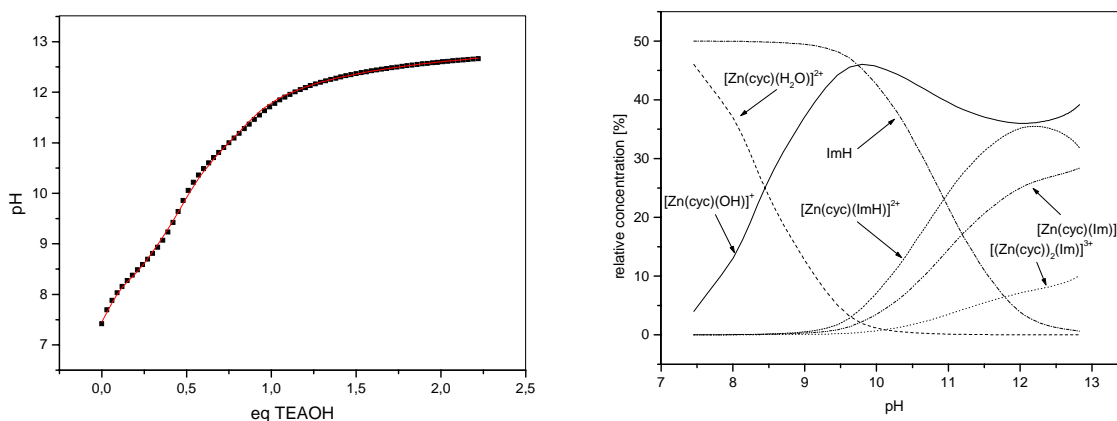
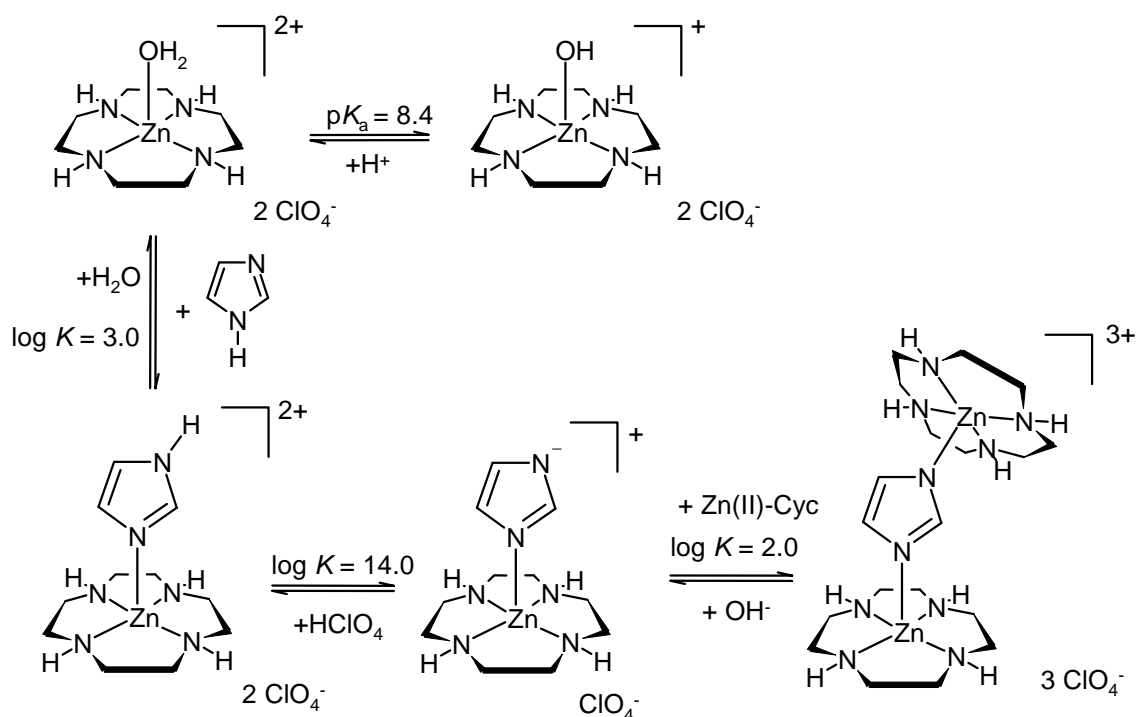


**Figure 83.** Potentiometric titration data (left) of a 1:1 mixture of **78** and imidazole (black dots are experimental data; red line is the calculated fitting) and species distribution plot (right).

The titration experiment of an equimolar mixture of **79** and imidazole resulted in very simple deprotonation-binding equilibrium and is shown in scheme 27.

**Scheme 27.** Deprotonation and binding equilibrium of **79** and imidazole

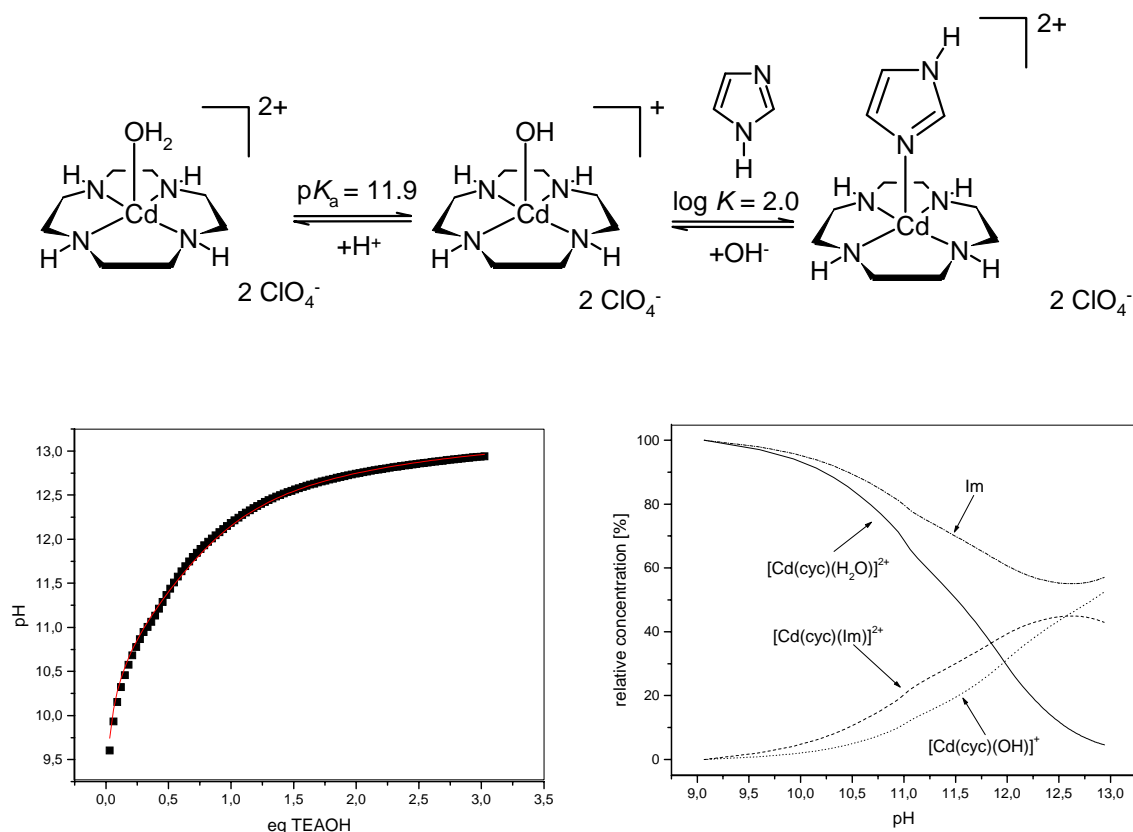


**Figure 84.** Potentiometric titration data (left) of a 1:1 mixture of **79** and imidazole (black dots are experimental data; red line is the calculated fitting) and species distribution plot (right).

### 1.3 Conclusion

Based on potentiometric titration data it was possible to prove substrate-metal-complex interactions in aqueous solution. In addition to already known interactions of M(II)-IDA/M(II)-NTA and imidazole binding of imidazole to M(II)-cyclen was discovered. Cd(II)-cyclen showed imidazole binding and Zn(II)-cyclen binds to imidazole and phosphate. The newly identified metal complex to amino acid side chain functional group interactions, and the excluded interactions, may help to develop and optimise new IMAC polymers for protein purification.

## References:

- <sup>1</sup> Porath, J.; Carlsson, J.; Belfrage, G. *Nature* **1975**, 258, 598.
- <sup>2</sup> For reviews about IMAC see: (a) Ueda, E.K.M.; Gout P.W.; Morganti, L. *J. Chromat. A* **2003**, 988, 1. (b) Shepherd, R.E. *Coord. Chem. Rev.* **2003**, 247, 147. (c) Suen, S.Y.; Liu, Y.C.; Chang, C.S. *J. Chromat. B* **2003**, 797, 305. (d) Chaga, G.S. *J. Biochem. Biophys. Methods* **2001**, 49, 313. (e) Gaberc-Porekar, V.; Menart, V. *J. Biochem. Biophys. Methods* **2001**, 49, 335.
- <sup>3</sup> Hamilton, S.; Odili, J.; Pacifico, M.D.; Wilson, G.D.; Kupsch, J.-M. *Hybridoma and Hybridomics* **2003**, 22, 347.
- <sup>4</sup> (a) Plush, S.E.; Lincoln, S.F.; Wainwright, K.P. *Dalton Trans.* **2004**, 1410. (b) Borges, F.; Lima, J.L.F.C.; Pinto, I.; Reis, S.; Siquet, C. *Hel.Chim. Acta* **2003**, 86, 3081. (c) Bazzicalupi, C.; Bencini, A.; Berni, E.; Bianchi, A.; Borsari, L.; Giorgi, C.; Valtancoli, B.; Lodeiro, C.; Lima, J.C.; Parola, A.J.; Pina, F. *Dalton Trans.* **2004**, 591.
- <sup>5</sup> (a) Magyar, J.S.; Godwin, H.A. *Anal. Biochem.* **2003**, 320, 39. (b) Kula, R.J.; Rabenstein, D.L. *Anal. Chem.* **1996**, 38, 1934. (c) Jiang, J.; Renshaw, J.C.; Sarsfield, M.J.; Livens, F.R.; Collison, D.; Charnock, J.M.; Eccles, H. *Inorg. Chem.* **2003**, 42, 1233. (d) Alderighi, L.; Gans, P.; Midollini, S.; Vacca, A. *Inorg. Chim. Acta* **2003**, 356, 8. (e) Torres, J.; Kremer, C.; Kremer, E.; Dominguez, S.; Mederos, A.; Arrita, J.M. *Inorg. Chim. Acta* **2003**, 355, 175. (f) Zachariou, M.; Traverso, I.; Spiccia, L.; Hearn, M.T.W. *J. Phys. Chem.* **1996**, 100, 12680. (g)
- <sup>6</sup> Martell, A.E.; Smith, P.M. *Critical. Stability Constants*; Plenum Press: New York, 1975; Vol.1-5.
- <sup>7</sup> Craven, E.; Zhang, C.; Janiak, C.; Rheinwald, G.; Lang, H. *Z. Anorg. Allg. Chem.* **2003**, 629, 2282.
- <sup>8</sup> (a) Dembowski, J.S.; Kurtz, D.C.; Nakon, R. *Inorg. Chim. Acta* **1988**, 152, 209. (b) Hopgood, D.; Angelici, R.J. *J. Am. Chem. Soc.* **1968**, 90, 2508. (c) Sharma, G.; Tandon, J.P. *Talanta* **1971**, 18, 1163.
- <sup>9</sup> Morton, Q.J. *Pharm. Pharmacd.* **1930**, 3, 483.
- <sup>10</sup> Gupta, S.C.; Islam, N.B.; Wahlen, D.L.; Yagi, H.; Jerina, D.M. *J. Org. Chem.* **1987**, 52, 3812.
- <sup>11</sup> (a) Sokolina, L.F.; Afanasèv, Y.M. *J. Appl. Chem. USSR* **1982**, 55, 2738. (b) Bernasconi, C.F.; Killion, R.B.; Fassberg, J.; Rappoport, Z. *J. Am. Chem. Soc.* **1989**, 111, 6862.
- <sup>12</sup> Davis, E. *J. Am. Chem. Soc.* **1933**, 55, 739.
- <sup>13</sup> The binding constants could only be determined as approx. values. The fitting of the titration curves was not influenced by variation of the logK values (+/- 0.5).
- <sup>14</sup> log K(Cu(II)-IDA) = 10.56; log K(Cu(II)-NTA) = 12.94; log K(Ni(II)-IDA) = 8.3; log K(Ni(II)-NTA) = 11.5.
- <sup>15</sup> (a) Reichenbach-Klinke, R.; Kruppa, M.; König, B. *J. Am. Chem. Soc.* **2002**, 124, 12999-13007. (b) Subat, M.; Borovik, A.S.; König, B. *J. Am. Chem. Soc.* **2004**, 126, 3185-3190. (c) Aoki, S.; Kimura, E. *Rev. Mol. Biotechnol.* **2002**, 90, 129-155.
- <sup>16</sup> Reichenbach-Klinke, R.; König, B. *J. Chem. Soc., Dalton Trans.* **2002**, 121.



## 1.4 Experimental Section

### 1.4.1 Instruments and general techniques

**Melting points (mp)** were determined with a Büchi SMP 20 and are uncorrected.

**IR-spectra** were recorded with a Bio-Rad FTS 2000 MX FT-IR and Bio-Rad FT-IR FTS 155.

**NMR:** Bruker Avance 600 ( $^1\text{H}$ : 600.1 MHz,  $^{13}\text{C}$ : 150.1 MHz,  $T = 300\text{ K}$ ), Bruker Avance 400 ( $^1\text{H}$ : 400.1 MHz,  $^{13}\text{C}$ : 100.6 MHz,  $T = 300\text{ K}$ ), Bruker Avance 300 ( $^1\text{H}$ : 300.1 MHz,  $^{13}\text{C}$ : 75.5 MHz,  $T = 300\text{ K}$ ). The chemical shifts are reported in  $\delta$  [ppm] relative external standards (solvent residual peak). The spectra were analysed by first order, the coupling constants are in Hertz [Hz]. Characterisation of the signals: s = singlet, d = doublet, t = triplet, q = quartet, m = multiplet, bs = broad singlet, dd = double doublet, dt = double triplet, ddd = double double doublet. Integration is determined as the relative number of atoms. Error of reported values: chemical shift: 0.01 ppm for  $^1\text{H}$ -NMR, 0.1 ppm for  $^{13}\text{C}$  - NMR; Coupling constants: 0.1 Hz. The used solvent is reported for each spectrum.

**MS-Spectra:** Varian CH-5 (EI), Finnigan MAT 95 (CI; FAB and FD), Finnigan MAT TSQ 7000 (ESI). Xenon serves as the ionisation gas for FAB.

**X-Ray:** Data collections were performed at  $173 (\pm 1)\text{ K}$  with graphite-monochromated Mo-K $\alpha$  radiation ( $\lambda = 0.71073\text{ \AA}$ ) on a STOE-IPDS diffractometer. The structures of the compounds were solved by direct methods SIR97 and refined by full-matrix least-squares on  $F^2$  using SHELXL-97.

**Optical rotation** was measured on a Perkin Elmer Polarimeter 241 with sodium lamp at 589 nm in a specified solvent.

**Elemental Analysis:** Microanalytical Laboratory of the University of Regensburg.

**Thin layer chromatography (TLC)** was performed on alumina plates coated with silica gel (Merck silica gel 60 F 254, layer thickness 0.2 mm). Visualisation was accomplished by UV-light ( $\lambda = 254\text{ nm}$ ) and ninhydrine in EtOH.

**Column chromatography** was performed on silica gel (70-230 mesh) from Merck.

**General Material.** TEAOH (Merck), TEAP (Fluka), mono sodium phthalate (Merck), perchloric acid (60%, Merck), Iminodiacetic acid (IDA) (Fluka),  $\text{Cu}_2(\text{CO}_3)(\text{OH})_2$  (Alfa Aesar),  $\text{NiCO}_3 \cdot 2\text{NiOH}(\text{OH})_2 \cdot 4\text{H}_2\text{O}$  (Alfa Aesar), nitrilotriacetic acid (Fluka), cyclen (Schering), copper(II) perchlorate hexahydrate (Alfa Aesar), nickel(II) perchlorate hexahydrate (Alfa Aesar), zinc(II) perchlorate hexahydrate (Alfa Aesar), cadmium(II) perchlorate hexahydrate (Alfa Aesar), ethanol (Merck), acetic acid (100%, Merck), phenol (Merck), imidazole (Fluka), butylamine (Fluka), N-ethylguanidine hydrochloride (Vocado), and di-sodium phenyl phosphate (Fluka) were bought and used without further purification.

**Potentiometric Titrations.** All titrations were performed under  $\text{N}_2$  atmosphere with a computer controlled pH-meter (pH 3000, WTW) and dosimat (Dosimat 665, Metrohm). For all titrations 0.1 M perchloric acid and 0.1 M tetraethylammonium hydroxide (TEAOH) in water containing tetraethylammonium perchlorate (TEAP) to maintain an ionic strength of  $I = 0.1$  were used. TEAOH solutions were calibrated with mono sodium phthalate. A titration of perchloric acid with TEAOH solution was used for calibration and to determine  $\log K_w$ . The Irving-factor ( $A_I$ ) was determined according to  $\text{pH}_{\text{measurement}} = \text{pH}_{\text{real}} + A_I$ . All measurements were performed at 25 °C. Data analysis was performed on a computer using Hyperquad2000 (Version 2.1, P. Gans).

## X-Ray Data

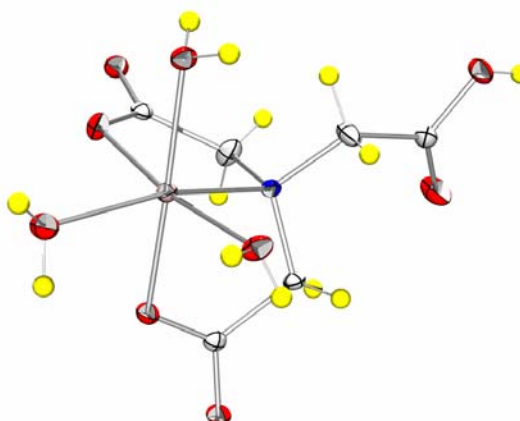
$[\text{Cu}(\text{ida})(\text{H}_2\text{O})_2]$  (**72**)

$\text{C}_4\text{CuH}_9\text{NO}_6$ ,  $M_r = 230.66$ , blue translucent prism, orthorhombic, Space group  $Pbc_a$ ,  $a = 10.2310(7)$  Å,  $b = 10.4043(7)$  Å,  $c = 13.6500(12)$  Å,  $\alpha = \beta = \gamma = 90$ ,  $Z = 8$ ,  $V = 1452.99(19)$  Å<sup>3</sup>,  $D_x = 2.109$  mg/m<sup>3</sup>,  $\mu = 2.999$  mm<sup>-1</sup>,  $F(000) = 936$ , Crystal size 0.60 x 0.20 x 0.20 mm,  $\theta$ -range for data collections 2.98 to 25.86 °, Index ranges  $-12 \leq h \leq 12$ ,  $-12 \leq k \leq 12$ ,  $-16 \leq l \leq 16$ , Reflections collected/unique 18368/1390 [ $R_{\text{int}} = 0.0287$ ], Data/restraints/parameters 1390/1/145, Goodness-of-fit on  $F^2$  1.096, Final  $R$  indices [ $I > 2\sigma(I)$ ]  $R_1 = 0.0165$ ,  $wR_2 = 0.0488$   $R$  indices (all data)  $R_1 = 0.0185$ ,  $wR_2 = 0.0498$ , largest diff. peak and hole 0.306 and -0.418 e. Å<sup>-3</sup>.



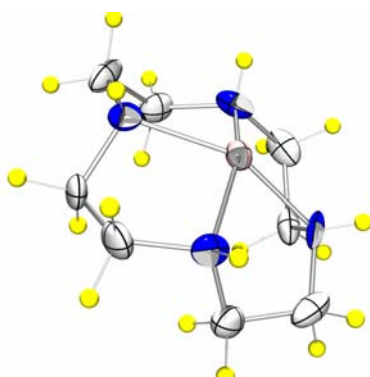
**H[Ni(NTA)(H<sub>2</sub>O)<sub>3</sub>] (75)**

C<sub>6</sub>H<sub>12</sub>NNiO<sub>9</sub>,  $M_r = 299.99$ , turquoise translucent stick, orthorhombic, Space group  $Pbc_a$ ,  $a = 6.5876(4) \text{ \AA}$ ,  $b = 12.3015(9) \text{ \AA}$ ,  $c = 27.8271(16) \text{ \AA}$ ,  $\alpha = \beta = \gamma = 90^\circ$ ,  $Z = 8$ ,  $V = 2255.0(3) \text{ \AA}^3$ ,  $D_x = 1.884 \text{ mg/m}^3$ ,  $\mu = 1.771 \text{ mm}^{-1}$ ,  $F(000) = 1328$ , Crystal size  $0.60 \times 0.30 \times 0.10 \text{ mm}$ ,  $\theta$ -range for data collections  $2.21$  to  $25.23^\circ$ , Index ranges  $-7 \leq h \leq 7$ ,  $-14 \leq k \leq 14$ ,  $-32 \leq l \leq 32$ , Reflections collected/unique 19824/2014 [ $R_{\text{int}} = 0.0411$ ], Data/restraints/parameters 2014/0/223, Goodness-of-fit on  $F^2$  1.063, Final  $R$  indices [ $I > 2\sigma(I)$ ]  $R_1 = 0.0204$ ,  $wR_2 = 0.0546$   $R$  indices (all data)  $R_1 = 0.0215$ ,  $wR_2 = 0.0552$ , largest diff. peak and hole  $0.368$  and  $-0.208 \text{ e. \AA}^{-3}$ .



**[Cu(cyc)](ClO<sub>4</sub>)<sub>2</sub> (76)**

C<sub>8</sub>Cl<sub>2</sub>CuH<sub>20</sub>N<sub>4</sub>O<sub>8</sub>,  $M_r = 433.0$ , blue stick, orthorhombic, Space group  $P2_1/n$ ,  $a = 8.9260(8) \text{ \AA}$ ,  $b = 15.0469(10) \text{ \AA}$ ,  $c = 11.9045(11) \text{ \AA}$ ,  $\alpha = \gamma = 90^\circ$ ,  $\beta = 92.904(11)^\circ$ ,  $Z = 4$ ,  $V = 1596.8(2) \text{ \AA}^3$ ,  $D_x = 1.808 \text{ mg/m}^3$ ,  $\mu = 1.748 \text{ mm}^{-1}$ ,  $F(000) = 892$ , Crystal size  $0.48 \times 0.06 \times 0.06 \text{ mm}$ ,  $\theta$ -range for data collections  $2.66$  to  $25.86^\circ$ , Index ranges  $-10 \leq h \leq 10$ ,  $-18 \leq k \leq 18$ ,  $-14 \leq l \leq 14$ , Reflections collected/unique 5937/5941 [ $R_{\text{int}} = 0.0000$ ], Data/restraints/parameters 5941/0/221, Goodness-of-fit on  $F^2$  0.851, Final  $R$  indices [ $I > 2\sigma(I)$ ]  $R_1 = 0.0407$ ,  $wR_2 = 0.0897$   $R$  indices (all data)  $R_1 = 0.0676$ ,  $wR_2 = 0.0955$ , Absolute structure parameter none, largest diff. peak and hole  $0.623$  and  $-0.337 \text{ e. \AA}^{-3}$ .



### 1.4.2 Synthesis

#### *[Cu(ida)(H<sub>2</sub>O)<sub>2</sub>] (72):*

Iminodiacetic acid (IDA) (2.40 g, 18.8 mmol) and Cu<sub>2</sub>(CO<sub>3</sub>)(OH)<sub>2</sub> (2.00 g, 9.0 mmol) were dissolved in water (150 mL). The solution was stirred at 60 °C for 2 h. The blue suspension formed was cooled to r.t. and filtered. Slowly evaporation of the solvent delivered **72** (8.0 mmol, 1.85 g, 89 %) as dark blue crystals.

mp > 200 °C. – IR (KBr) [cm<sup>-1</sup>]:  $\tilde{\nu}$  = 3453, 3273, 2932, 1574, 1396. – Elemental analysis calcd. (%) for C<sub>4</sub>CuH<sub>9</sub>NO<sub>6</sub> (230.66): C 20.82, H 3.93, N 6.07; found C 21.04, H 3.69, N 6.02.

#### *[Ni(ida)(H<sub>2</sub>O)<sub>3</sub>] (73):*

Iminodiacetic acid (IDA) (1.00 g, 7.5 mmol) and NiCO<sub>3</sub>·2NiOH(OH)<sub>2</sub>·4H<sub>2</sub>O (0.94 g, 2.5 mmol) were dissolved in water (150 mL). The solution was stirred at 60 °C for 2 h. The bluish-green suspension formed was cooled to r.t. and filtered. Slowly evaporation of the solvent delivered **73** (2.2 mmol, 0.62 g, 88 %) as turquoise crystals.

mp > 200 °C. – IR (KBr) [cm<sup>-1</sup>]:  $\tilde{\nu}$  = 3456, 3279, 2935, 1568, 1406. – MS (ESI, MeOH/H<sub>2</sub>O/MeCN/AcOH): m/z (%) = 207 (100) [Ni(ida) + NH<sub>4</sub><sup>+</sup>]. – Elemental analysis calcd. (%) for C<sub>4</sub>H<sub>9</sub>NiNO<sub>6</sub> (225.80): C 21.34, H 4.03, N 6.22; found C 21.12, H 3.88, N 6.10.

#### *H[Cu(nta)(H<sub>2</sub>O)<sub>3</sub>] (74):*

Nitrilotriacetic acid (NTA) (2.00 g, 10.5 mmol) and Cu<sub>2</sub>(OH)<sub>2</sub>CO<sub>3</sub> (1.16 g, 5.2 mmol) were dissolved in MeCN (40 mL). The mixture was refluxed for 3 h and was filtered

immediately. The resulting blue solution was evaporated and crystallisation yielded **74** (9.2 mmol, 2.81 g, 88%) as blue crystals.

mp > 200 °C. – IR (KBr) [cm<sup>-1</sup>]:  $\tilde{\nu}$  = 3333, 2943, 2651, 2593, 2362, 1593, 916, 763. – MS (ESI, MeOH/H<sub>2</sub>O/MeCN/AcOH): m/z (%) = 250 (100) [Cu(nta)<sup>-</sup>], 333 (76 %), [Cu(nta)<sup>-</sup> + 2 MeCN]. – Elemental analysis calcd. (%) for C<sub>6</sub>CuH<sub>12</sub>NO<sub>9</sub> (304.98): C 21.61, H 3.97, N 4.59; found C 21.65, H 3.50, N 4.20.

*H[Ni(nta)(H<sub>2</sub>O)<sub>3</sub>] (75):*

Nitrilotriacetic acid (NTA) (5.00 g, 26.2 mmol) and NiCO<sub>3</sub>·2 Ni(OH)<sub>2</sub>·4H<sub>2</sub>O (3.26 g, 8.6 mmol) were dissolved in MeCN (150 mL). After refluxing for 1 h the solution was concentrated under reduced pressure. The blue-green solid was crystallised in water. **75** (7.9 mmol, 2.37 g, 92 %) is a green crystalline solid.

mp > 200 °C. – IR (KBr) [cm<sup>-1</sup>]:  $\tilde{\nu}$  = 3502 cm<sup>-1</sup>, 3934, 2724, 988, 912. – MS (ESI, MeOH/H<sub>2</sub>O/MeCN/AcOH): m/z (%) = 246 (100) [Ni(nta)<sup>-</sup>]. – Elemental analysis calcd. (%) for C<sub>6</sub>H<sub>12</sub>NNiO<sub>9</sub> (299.99): C 24.00, H 4.03, N 4.67; found C 23.72, H 3.82, N 4.32.

*[Cu(cyc)](ClO<sub>4</sub>)<sub>2</sub> (76):*

Cyclen (0.70 g, 4.0 mmol) and copper(II) perchlorat-hexahydrate (1.50 g, 4.0 mmol) were separately dissolved in MeOH (15 mL) and the solutions combined. The resulting suspension is refluxed for 30 min. The precipitating needles were filtered off and the filtrate concentrated. The blue amorphous solid was crystallised in methanol. **76** (3.8 mmol, 1.65 g, 94 %) is a dark blue crystal.

mp > 200 °C. – IR (KBr) [cm<sup>-1</sup>]:  $\tilde{\nu}$  = 3285 cm<sup>-1</sup>, 2938, 2906, 1084, 625. – MS (ESI, MeCN): m/z (%) = 117 (24) [Cu(cyc)<sup>2+</sup>], 138 (100) [Cu(cyc)<sup>2+</sup> + MeCN], 158 (44) [Cu(cyc)<sup>2+</sup> + 2 MeCN], 334 (38) [Cu(cyc)<sup>2+</sup> + ClO<sub>4</sub><sup>-</sup>], 705 (< 5) [2 Cu(cyc)<sup>2+</sup> + 2 ClO<sub>4</sub><sup>-</sup> + Cl<sup>-</sup>], 769 (5) [2 Cu(cyc)<sup>2+</sup> + 3 ClO<sub>4</sub><sup>-</sup>]. – Elemental analysis calcd. (%) for C<sub>8</sub>Cl<sub>2</sub>CuH<sub>20</sub>N<sub>4</sub>O<sub>8</sub> (433.0): C 22.10, H 4.62, N 12.97; found C 22.17, H 4.62, N 12.97.

*[Ni(cyc)](ClO<sub>4</sub>)<sub>2</sub> (77):*

Cyclen (0.49 g, 2.9 mmol) and nickel(II) perchlorat-hexahydrate (1.04 g, 2.9 mmol) were separately dissolved in MeOH (15 mL) and the solutions combined. The resulting suspension was refluxed for 30 min. The mixture was evaporated to dryness and the amorphous solid was crystallised in methanol. **77** (2.6 mmol, 1.10 g, 90 %) is a yellow-brown solid.

mp > 200 °C. – IR (KBr) [ $\text{cm}^{-1}$ ]:  $\tilde{\nu}$  = 3429, 3259, 2939, 2888, 1089. – MS (ESI, MeOH/H<sub>2</sub>O/MeCN/AcOH): m/z (%) = 115 (12) [Ni(cyc)<sup>2+</sup>], 136 (58) [Ni(cyc)<sup>2+</sup> + MeCN], 156 (100) [Ni(cyc)<sup>2+</sup> + 2 MeCN], 177 (20) [Ni(cyc)<sup>2+</sup> + 3 MeCN], 299 (20) [Ni(cyc)<sup>2+</sup> - H<sup>+</sup>], 265 (10) [Ni(cyc)<sup>2+</sup> + Cl<sup>-</sup>], 289 (28) [Ni(cyc)<sup>2+</sup> + CH<sub>3</sub>COO<sup>-</sup>], 229 (15) [Ni(cyc)<sup>2+</sup> + ClO<sub>4</sub><sup>-</sup>]. – Elemental analysis calcd. (%) for C<sub>8</sub>Cl<sub>2</sub>H<sub>20</sub>N<sub>4</sub>NiO<sub>8</sub> (429.92): C 22.35, H 4.69, N 13.03; found C 21.89, H 4.53, N 12.71.

*[Zn(cyc)](ClO<sub>4</sub>)<sub>2</sub> (78):*

Cyclen (0.90 g, 5.4 mmol) and zinc(II) perchlorat-hexahydrate (2.00 g, 5.4 mmol) were separately dissolved in MeOH (15 mL) and the solutions combined. The resulting suspension was refluxed for 30 min. The mixture was evaporated to dryness and the amorphous solid was crystallised in methanol. **78** (2.6 mmol, 1.10 g, 90 %) is a colourless crystalline solid.

mp >200 °C. – IR (KBr) [ $\text{cm}^{-1}$ ]:  $\tilde{\nu}$  = 3429, 3178, 2918, 3259, 2953, 1090. – MS (ESI, MeOH/H<sub>2</sub>O/MeCN/AcOH): m/z (%) = 110 (8) [Zn(cyc)<sup>2+</sup>], 138 (100) [Zn(cyc)<sup>2+</sup> + MeCN], 295 (26) [Zn(cyc)<sup>2+</sup> + CH<sub>3</sub>COO<sup>-</sup>], 335 (58) [Zn(cyc)<sup>2+</sup> + ClO<sub>4</sub><sup>-</sup>], 773 (13) [2 Zn(cyc)<sup>2+</sup> + 3 ClO<sub>4</sub><sup>-</sup>]. – Elemental analysis calcd. (%) for C<sub>8</sub>Cl<sub>2</sub>H<sub>20</sub>N<sub>4</sub>O<sub>8</sub>Zn (436.61): C 22.01, H 4.62, N 12.83; found C 21.76, H 4.80, N 12.65.

*[Cd(cyc)](ClO<sub>4</sub>)<sub>2</sub> (79):*

Cyclen (1.64 g, 9.5 mmol) and cadmium(II) perchlorat-hexahydrate (4.00 g, 9.5 mmol) were separately dissolved in MeOH (15 mL) and the solutions combined. The resulting suspension was refluxed for 30 min. The mixture was evaporated to dryness and the amorphous solid was crystallised in methanol. **79** (3.8 mmol, 1.65 g, 94 %) is a colourless crystalline solid.

mp > 200 °C. – IR (KBr) [ $\text{cm}^{-1}$ ]:  $\tilde{\nu}$  = 3499, 3318, 29096, 2864, 1089, 626. – MS (ESI, MeCN): m/z (%) = 142 (12) [Cd(cyc)<sup>2+</sup>], 163 (100) [Cd(cyc)<sup>2+</sup> + MeCN], 183 (64) [Cd(cyc)<sup>2+</sup> + 2 MeCN], 385 (24) [Cd(cyc)<sup>2+</sup> + ClO<sub>4</sub><sup>-</sup>], 867 (36) [2 Cd(cyc)<sup>2+</sup> + 3 ClO<sub>4</sub><sup>-</sup>]. – Elemental analysis calcd. (%) for C<sub>8</sub>CdCl<sub>2</sub>H<sub>20</sub>N<sub>4</sub>O<sub>8</sub> (484.0): C 19.87, H 4.17, N 11.59; found C 19.34, H 4.27, N 11.30.

## 2. Molecular Recognition using Modular Receptor Synthesis

Most synthetic receptors already published in literature (see introduction) have one thing in common: Each receptor is designed for binding to a specific substrate. Therefore, each project starts by synthesising a desired receptor using the individual expertise of the different research groups.

However, if the final receptor is divided into single recognition segments, which can be linked via standardised reactions, a simple and modular access towards a wide variety of synthetic receptors can be achieved (figure 85).

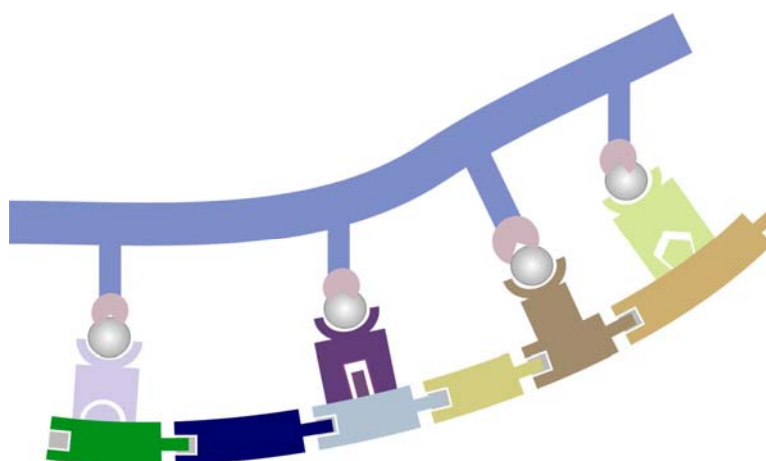


**Figure 85.** A substrate (blue) is bound by a synthetic receptor (multi colour) assembled by a building block approach.

One of the best established methods for covalent linking of molecules is the peptide coupling. The possibility of orthogonal protection of amines and acids, the simple activation of carbonic acids in coupling reactions and the stability of the amide bond are reasons for the wide use of this ligation method. Therefore, the linkage of building blocks for molecular recognition to extended synthetic receptors should be easily done using peptide coupling.

Building blocks of a receptor construction kit can be separated into different classes (figure 86).

### Terminal Recognition units **A**:

The receptor molecule is assembled by peptide coupling. For that reason every receptor backbone contains a N-terminal and a C-terminal ending which can be addressed by terminal recognition units **A** (chapter 2.1).

### Recognition units in the side chain of natural amino acids **B**:

To incorporate a recognition unit within the receptor structure, side chains of natural amino acids can be used. The recognition units **B** can be linked to lysines, aspartic acids or glutamic acids by peptide coupling. Tyrosines can be addressed by substitution reactions (chapter 2.2.1).

### Unnatural amino acids with binding sites **C**:

Possessing an amine and a carboxylate this building block can be connected like any other natural amino acid into a receptor molecule. The side chain of this unnatural amino acid **C** already contains a chelator, which is used for the desired recognition process. Therefore, no additional linkage of the binding site (which is necessary for building block **B**) is needed (chapter 2.2.2).

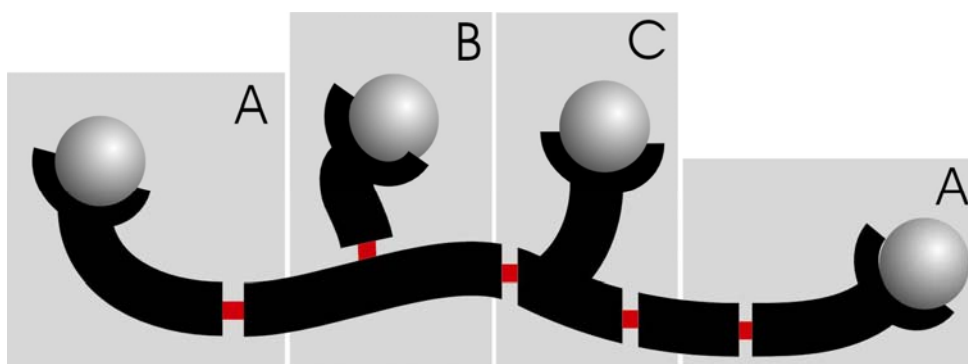


**Figure 86.** Terminal recognition units (**A**); building blocks with side chain functionality transferable into a recognition unit (**B**); receptor building blocks combining amino acid functionality and recognition unit (**C**) (red bars represent the amide bonds).

The following chapters describe the synthesis and use of different recognition building blocks. In many cases natural amino acids serve as the starting material.



## 2.1 Terminal Receptor Building Blocks

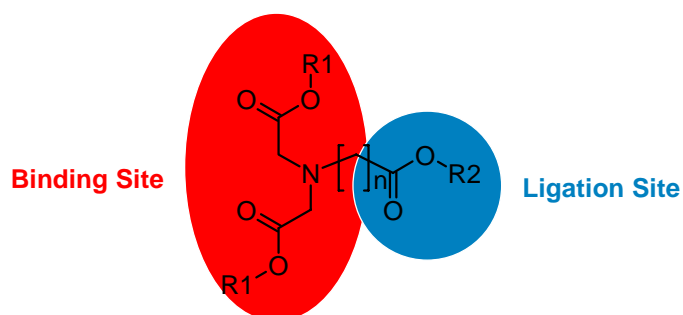
### 2.1.1 N-terminal Receptor Building Blocks

N-terminal building blocks are chelators functionalised with an additional carboxylic acid. Peptide coupling to the N-terminal end or a lysine side chain allows incorporating them into the synthetic receptor chain.

#### 2.1.1.1 IDA-Building Blocks

N-terminal IDA building blocks contain two carboxylates (red ellipse), which have to be protected orthogonally to the carboxyl group for ligation with the receptor (blue circle). Therefore, one main task was the choice of suitable protecting groups. An overview is given in table 22.

**Table 22.** Possible variations for carbonic acid protection



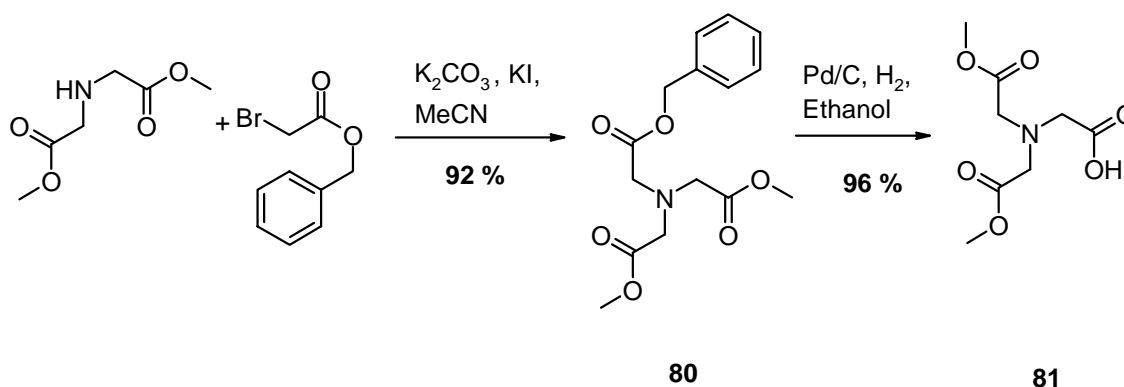
R1	R2	Cleavage of R2	Cleavage of R1
<i>Me, Et</i>	<i><sup>t</sup>Bu</i>	HCl/Ether or TFA/DCM	LiOH, Water/Acetone
<i>Me, Et</i>	<i>Bzl</i>	Pd/C, H <sub>2</sub>	LiOH, Water/Acetone
<i><sup>t</sup>Bu</i>	<i>Bzl</i>	Pd/C, H <sub>2</sub>	HCl/Ether or TFA/DCM
<i>Bzl</i>	<i><sup>t</sup>Bu</i>	HCl/Ether or TFA/DCM	Pd/C, H <sub>2</sub>

The deprotection of the recognition unit protecting groups will take place in a multifunctional complex receptor compound. Some of the final compounds will not allow

all reaction conditions. Therefore, harsh reaction conditions for deprotection must be avoided. R1 has to represent a protecting group, which is orthogonal to the total receptor synthesis. The cleavage of R2 generates zwitterionic compounds, which are difficult to purify. In addition, some of the starting compounds are not easily prepared or are very expensive.

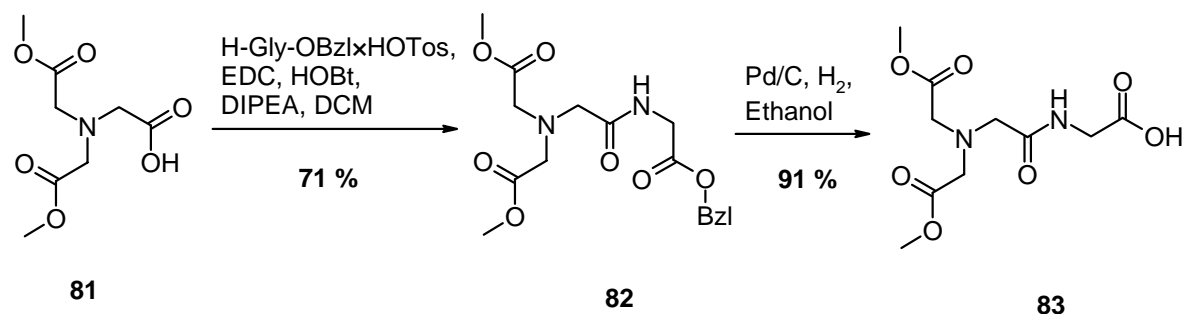
First a synthesis was chosen with methylester protected IDA-units. The carbonic acid for ligation towards the receptor molecule was benzyl protected. Via hydrogenolytic cleavage of the benzylester, a differentiation between the two types of carbonic acids was possible. As shown in scheme 28 **80** was obtained in good yields using an alkylation of dimethyl iminodiacetate hydrochloride. The following deprotection using Pd/C under 10 bar H<sub>2</sub>-atmosphere was nearly quantitatively.

**Scheme 28.** Synthesis of the N-terminal IDA-receptor **81**



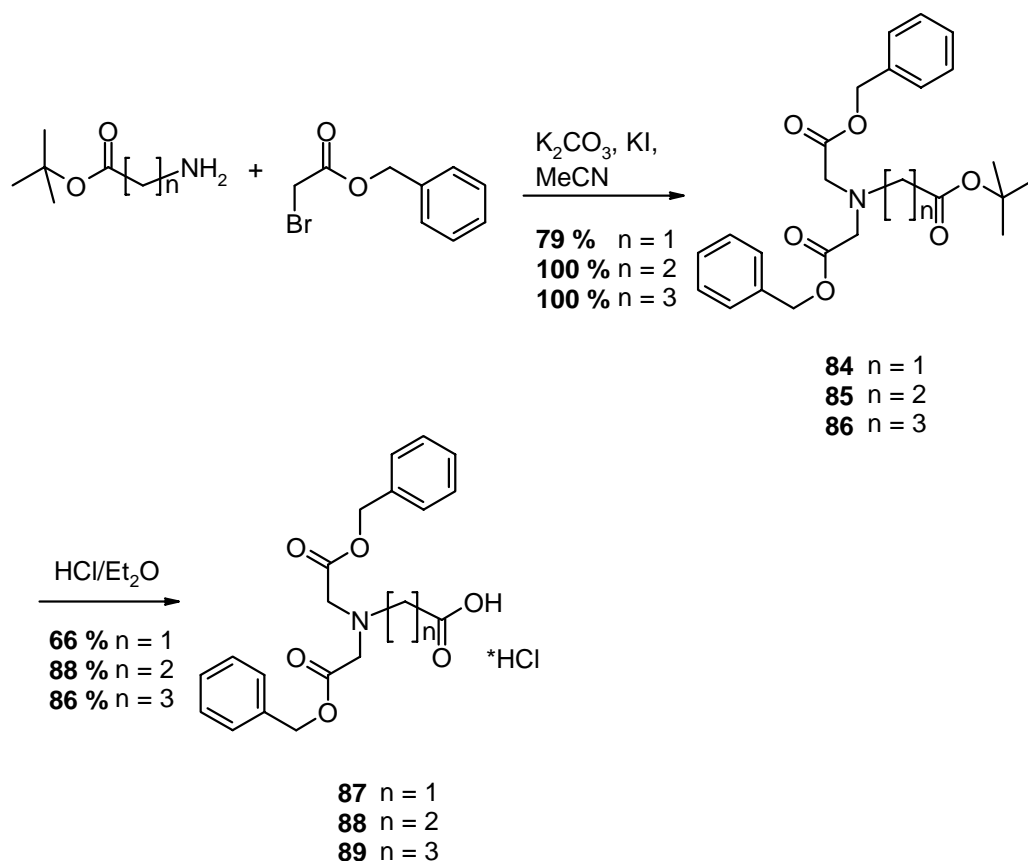
To develop optimal coupling conditions for such kind of terminal receptors, **81** was reacted with H-Gly-OBzl. Using EDC/HOBt to create the active ester of **81** it was possible to obtain **82** in good yields (scheme 29). The by one glycine unit extended building block **82** was hydrogenolytically deprotected. **83** can now be used for further coupling reactions in receptor synthesis.

**Scheme 29.** Extension of the terminal recognition unit **81** with one glycine unit



These methylester protected recognition unit cannot be used in receptors which are instable towards bases. Building blocks with benzylester protected binding sites are needed for such receptor synthesis. **84**, **85**, and **86** were obtained in good to very good yields via double alkylation of H-Gly-O<sup>t</sup>Bu, H-β-Ala-O<sup>t</sup>Bu or H-γ-Abu-O<sup>t</sup>Bu with benzylbromoacetate respectively. The following deprotection of the *tert*-butylesters yielded in the N-terminal IDA-units **87**, **88**, and **89** (scheme 30).

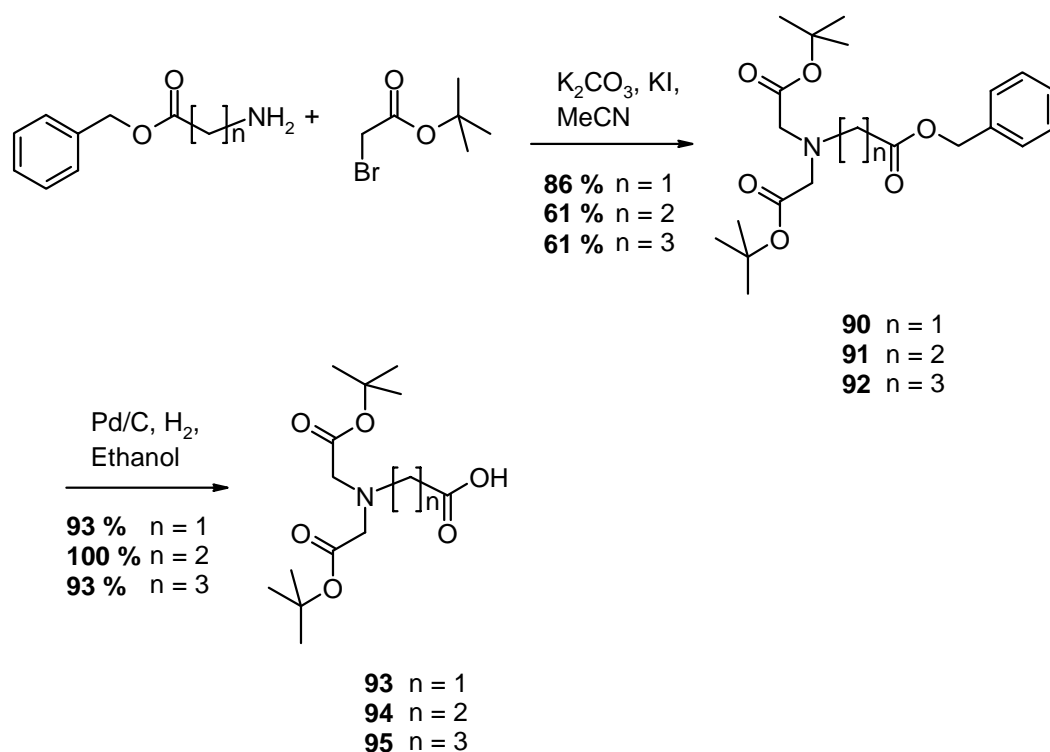
**Scheme 30.** Synthesis of N-terminal recognition units with benzylester protected IDA-chelators



The advantage of benzylester protecting groups is the easy work up without additional purification after hydrogenolytical cleavage.

If the final receptor molecule is unstable towards hydrogenolytical and basic reaction conditions, *tert*-butylesters can be used to protect the IDA binding site. The deprotection of the chelating unit is accomplished at strong acidic conditions. The benzylester-protected derivatives of glycine,  $\beta$ -alanine, and  $\gamma$ -aminobutyric acid were converted into the *tert*-butyl protected building blocks **90**, **91**, and **92** respectively using double alkylation of the primary amine (scheme 31). The benzylester could be cleaved nearly quantitatively to obtain the zwitterions **93**, **94**, and **95** respectively.

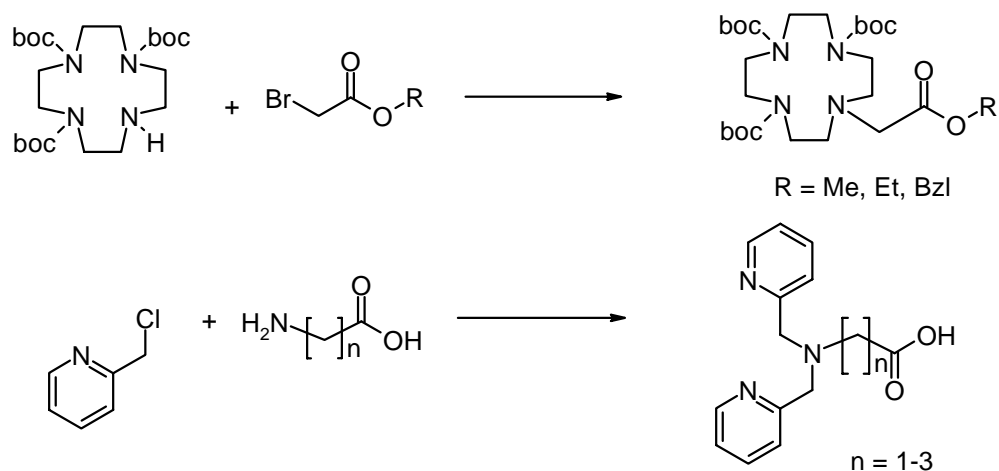
**Scheme 31.** N-terminal IDA-building blocks with *tert*-butylester protected binding site



### 2.1.1.2 BPA-, Cyclen-, and NTA-Building Blocks

BPA<sup>1</sup>- and cyclen-building blocks<sup>2</sup> with N-terminal ligation functionality could be obtained in similar reactions (scheme 32). Other research groups have already published these reactions.

**Scheme 32.** Literature known syntheses of N-terminal cyclen and BPA building blocks



NTA-recognition units with an additional acid are synthesised using the amino acids aspartic and glutamic acid.<sup>i</sup>

## 2.1.2 C-terminal Receptor Building Blocks

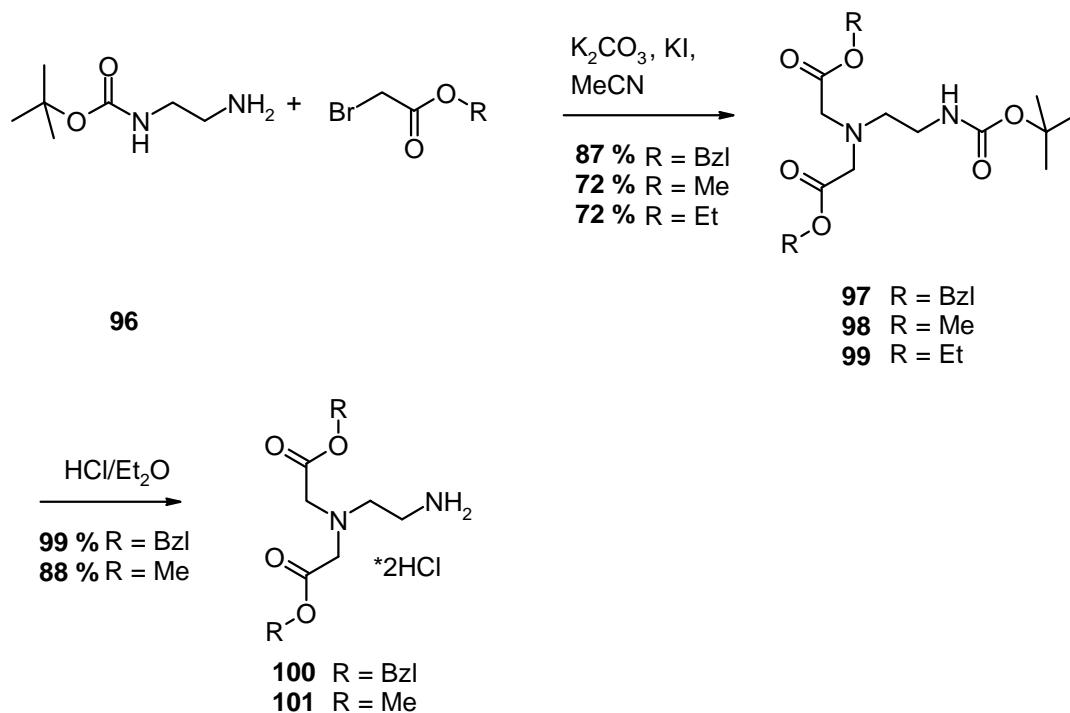
Receptor building blocks possessing an additional amine as ligation functionality are named C-terminal recognition units. They are used as recognition building blocks, which can be linked to the C-terminal end, an aspartic or a glutamic acid of a receptor molecule.

### 2.1.2.1 IDA-Building Blocks

Due to the easy access to mono Boc-protected ethylenediamine **96**,<sup>3</sup> this diamine was taken as a basis for the first receptor synthesis (scheme 33). Using a nucleophilic substitution reaction, this amine was converted into the IDA units **97**, **98**, and **99** with good yields.

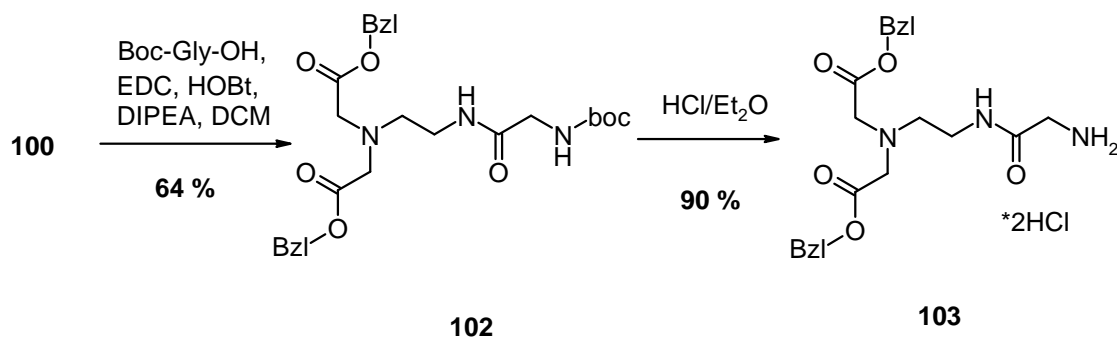
<sup>i</sup> Ritter, S. unpublished results.

**Scheme 33.** Synthesis of C-terminal building blocks **100** and **101**



The Boc-group was deprotected in HCl saturated ether with good yields to obtain the ammonium chlorides **100** and **101**. Peptide coupling with moderate yields resulted in **102**. One problem of this reaction is the possibility of an intramolecular lactam formation of the terminal amine. The cleavage of the Boc-group gave the extended N-terminal receptor **103** (scheme 34).

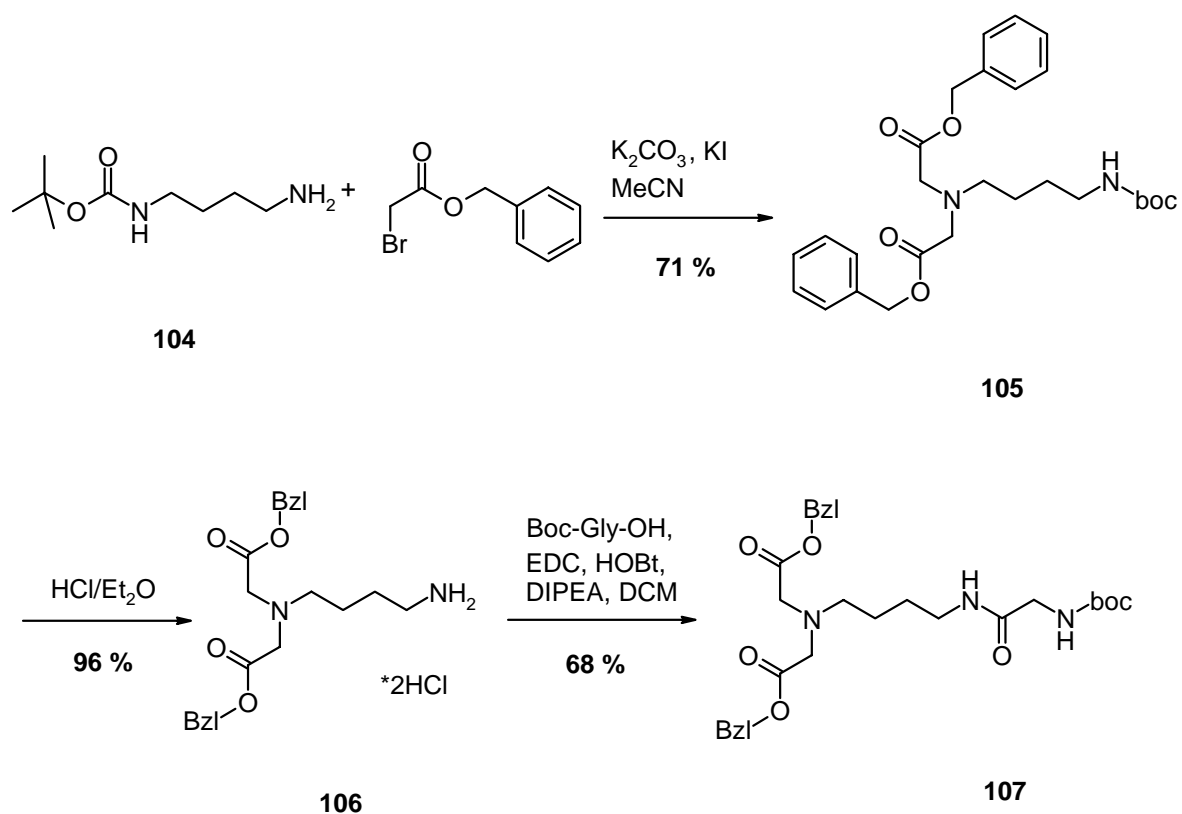
**Scheme 34.** Peptide coupling of the N-terminal IDA unit **100**



Mono-Boc-butylidiamine **104**<sup>4</sup> reacts analogously. The resulting **106** was used for peptide coupling with Boc-Gly-OH. A less favourable intramolecular lactamisation of the

recognition unit was expected due to the formation of an eight-membered ring. Unfortunately, the yield of the synthesis of **107** increased just a little compared to the synthesis of **102**(scheme 35).

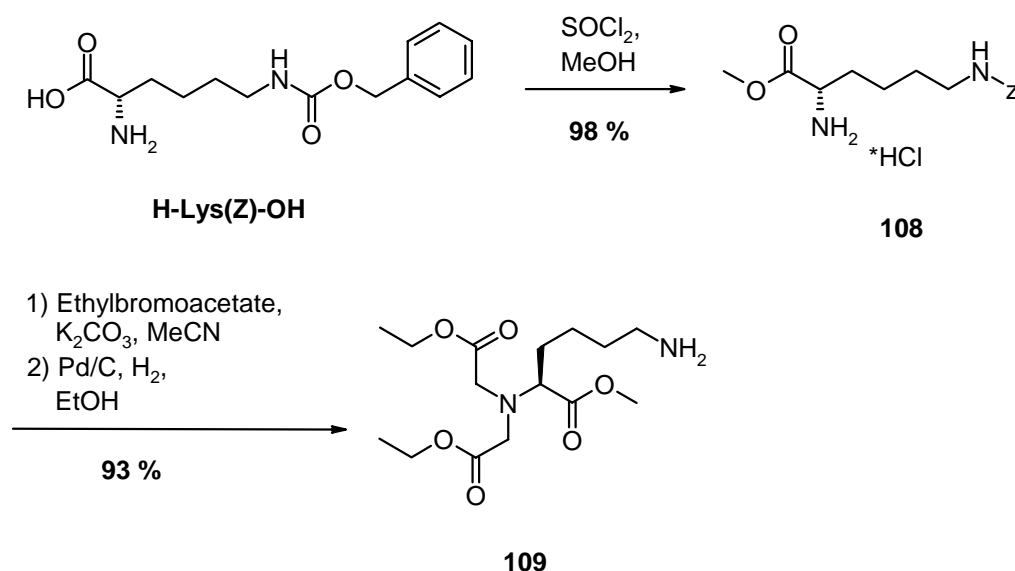
**Scheme 35.** Synthesis of the C-terminal IDA unit **107**



### 2.1.2.2 NTA-Building Blocks

C-terminal NTA-units are accessible using lysine.<sup>5</sup> On optimisation of this literature-known reaction, **109** was obtained in 91 % yield starting from H-Lys(Z)-OH (scheme 36).

**Scheme 36.** Optimised synthesis of C-terminal NTA receptor building block **109**

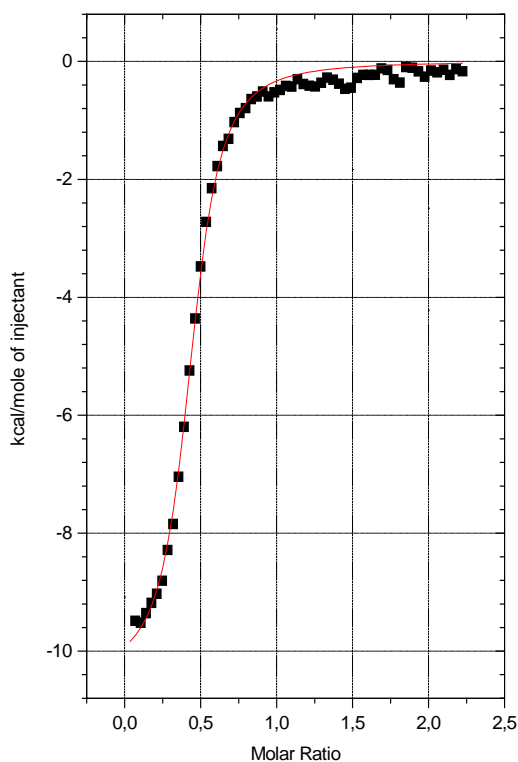
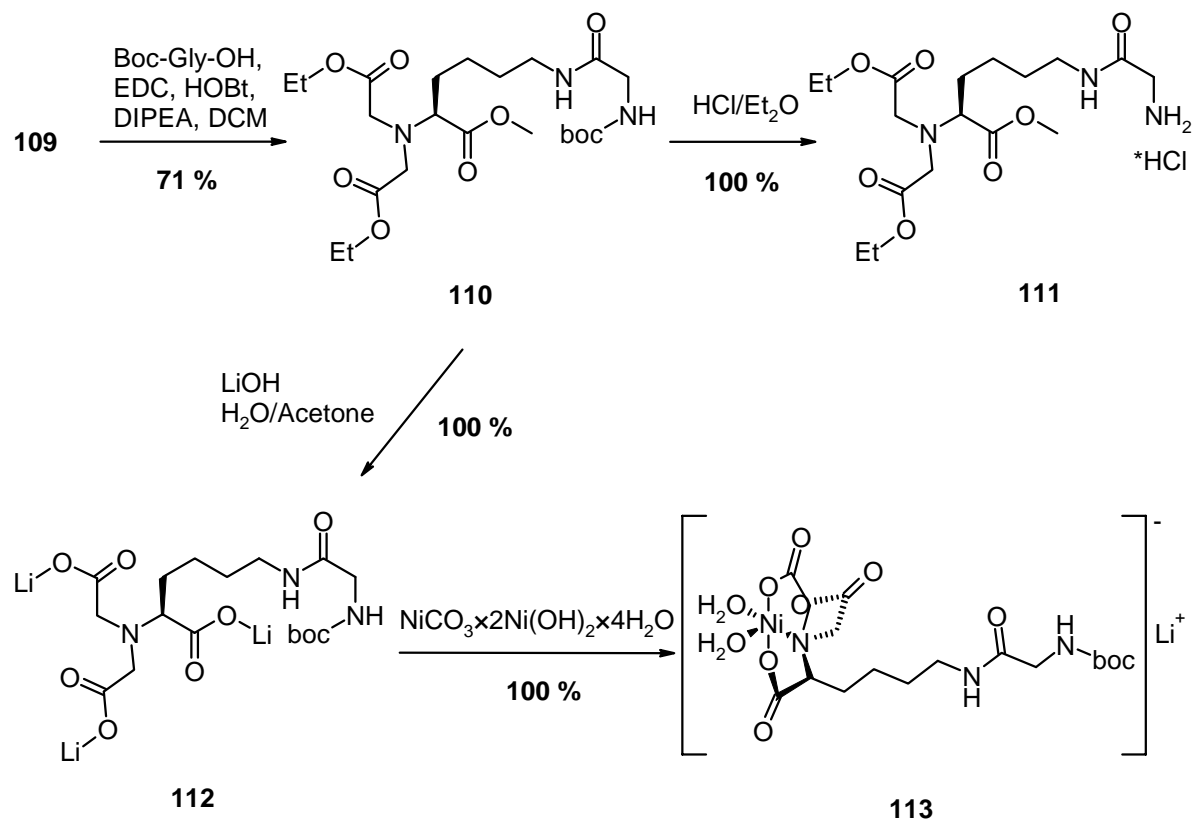


The intensive use of this receptor unit is discussed in chapter 3 in more detail. Necessary for the successful incorporation of **109** into receptor molecules is an efficient coupling method. In this case, the combination of EDC and HOBt once again gave the best results. The sequence of adding the reagents is important for the success of the coupling reaction. High yields were only obtained if the active ester was formed under ice cooling before the amine was added. The elongation of the receptor by one glycine unit gave **110** in 71 % yield. The Boc-deprotection yielded **111** quantitatively (scheme 37).

In addition to optimising the coupling reaction, it is also essential to adjust the deprotection and complexation reaction of the NTA-unit. For this reason, **110** was hydrolysed with LiOH in a mixture of acetone/water 3:1 over night at room temperature. The resulting lithium carboxylate **112** was used for complexation of Ni(II), which is quantitative. **113** was used for microcalorimetric titration of the pentapeptide H-His-Leu-Leu-Val-Phe-OMe in DMSO (figure 87) to prove the high affinity of this peptide based receptor to terminal histidine.



**Scheme 37.** Coupling and complexation of **109**



1:1 binding ratio

$N = 0.89$

$K = (5.02 \pm 0.33) \cdot 10^5 \text{ M}^{-1}$

$\Delta H = -(9.36 \pm 0.08) \text{ kcal} \cdot \text{mol}^{-1}$

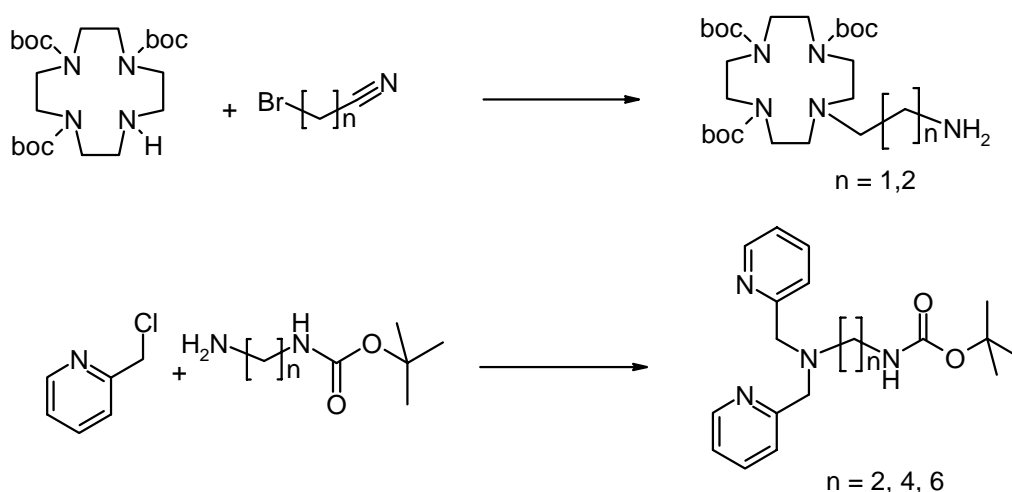
$\Delta S = -5.32 \text{ kcal} \cdot \text{mol}^{-1} \cdot \text{K}^{-1}$

**Figure 87.** Microcalorimetric titration of **113** ( $c = 0.1 \text{ mM}$ ) and H-His-Leu-Leu-Val-Phe-OMe ( $c = 1 \text{ mM}$ ) in DMSO.

### 2.1.2.3 BPA- and Cyclen-Building Blocks

C-terminal cyclen building blocks have been already published.<sup>6</sup> Analogue Boc-protected BPA-units are available using a double alkylation of mono-Boc-protected diamines and were published by *Nagano et al.* and *Kim et al.* (scheme 38).<sup>7</sup>

**Scheme 38.** Synthesis of cyclen and BPA receptor building blocks reported in literature



### 2.1.3 Terminal recognition units with two chelating sites

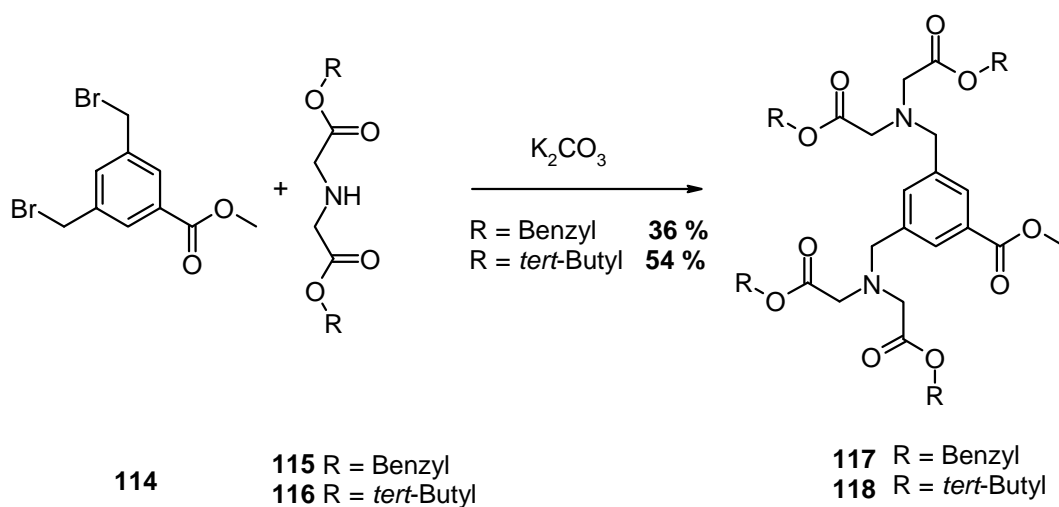
As shown in the introduction, receptors having two metal complexes can bind to suitable substrates with very high affinities. However, most of these published receptors have no additional functionality, which can be used for extension of the receptor molecule.

In this chapter, the synthesis of terminal recognition units with two chelating arms bearing an additional functionality for receptor ligation is reported.

#### 2.1.3.1 Bidentate IDA-units

Starting from 3,5-bis-(bromomethyl)-benzoic acid methylester, terminal bidentate IDA receptors were synthesised. *tert*-Butyl- (**116**)<sup>8</sup> and benzyl-protected (**115**)<sup>9</sup> IDA-units were introduced in the benzylic position of **114** via nucleophilic substitution. The recognition units **117** and **118** were obtained in poor yields.

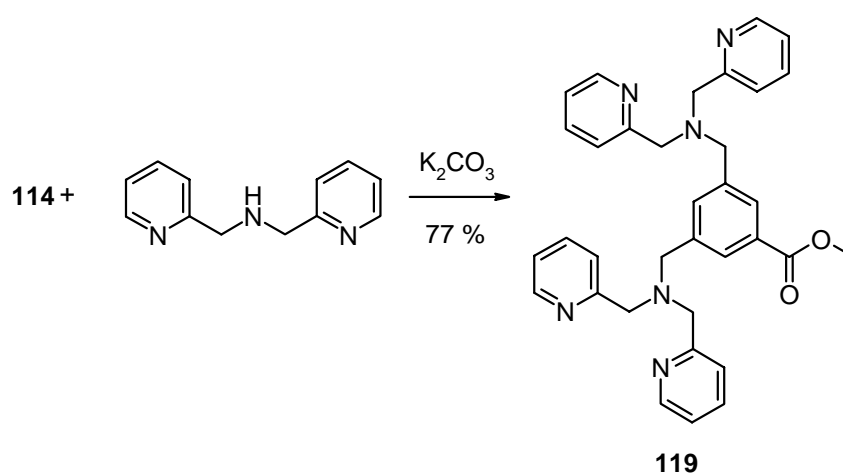
**Scheme 39.** Synthesis of the IDA-sandwich receptors **117** and **118**



**2.1.3.2 Bidentate BPA-units**

Starting from *Hamachi* phosphate receptor (see introduction), **114** was substituted with two BPA-units.

**Scheme 40.** Synthesis of the BPA sandwich receptor **119**



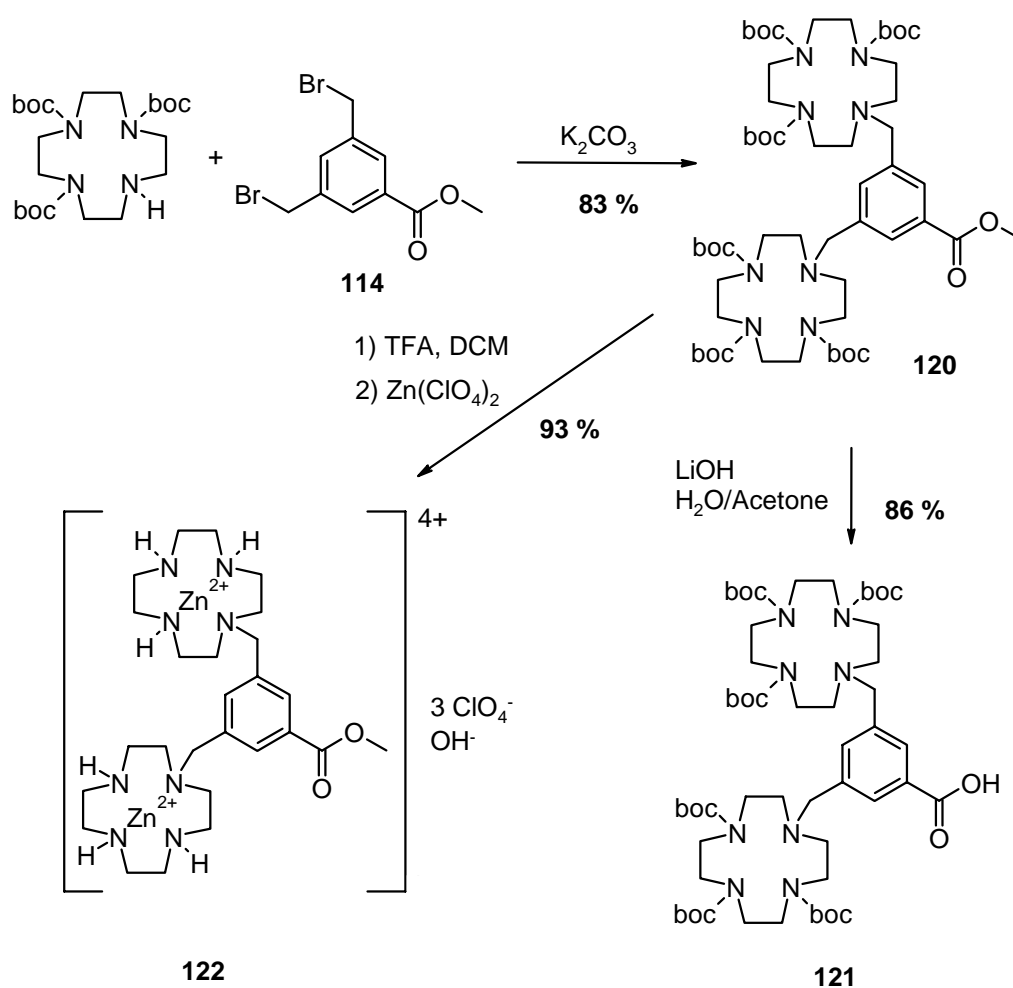
While the synthesis of **119** was accomplished in good yields, the ester cleavage was not successful until now. *Vomasta* is currently further investigating this molecule.<sup>ii</sup>

<sup>ii</sup> Vomasta, D. Diploma Thesis, University of Regensburg, *ongoing*.

### 2.1.3.3 Bidentate Cyclen-units

Under identical conditions, the terminal receptor containing two tris-Boc-Cyclen units **120** were synthesised in good yields. The ester of this molecule was cleaved in good yields resulting in **121**. *Grauer* is currently further investigating this carbonic acid.<sup>iii</sup> Scheme 41 also shows the synthesis of the bis-Zn(II) complex **122**, which was synthesised in good yields over two steps.

**Scheme 41.** Synthesis of the N-terminal cyclen building block **120** and its conversion to the bis-Zn(II)-cyclen complex **122** or to its free acid **121**



**122** was analysed using X-Ray crystallography. Figure 88 shows the structure of the compound in the solid-state binding one anion ( $OH^-$ ).

<sup>iii</sup> Grauer, A. Diploma Thesis, University of Regensburg, *ongoing*.

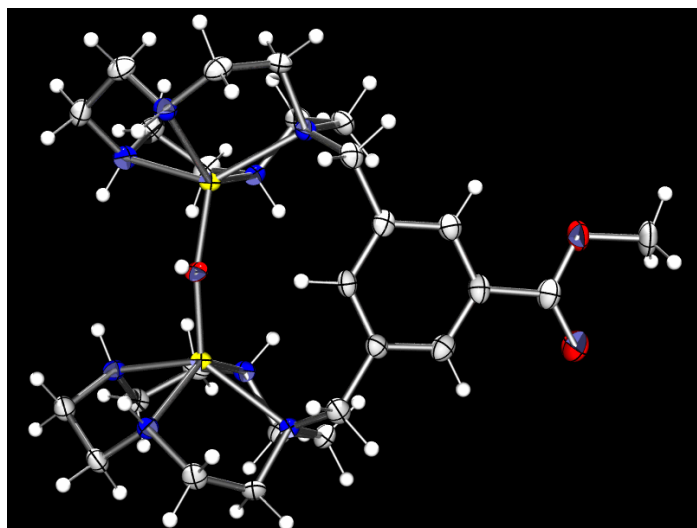


**Figure 88.** X-Ray structure of **122**.

The ability of this dinuclear complex to bind phosphates was examined by microcalorimetric titration and  $^{31}\text{P}$ -NMR.

For this purpose a solution of the Zn(II)-complex **122** ( $c = 1 \text{ mM}$ ) in HEPES buffer (50 mM, pH 7.5) was titrated with a solution of sodium phenyl phosphate ( $c = 35 \text{ mM}$ ). The data were analysed assuming a 1:1 binding stoichiometry between substrate and receptor (figure 89).

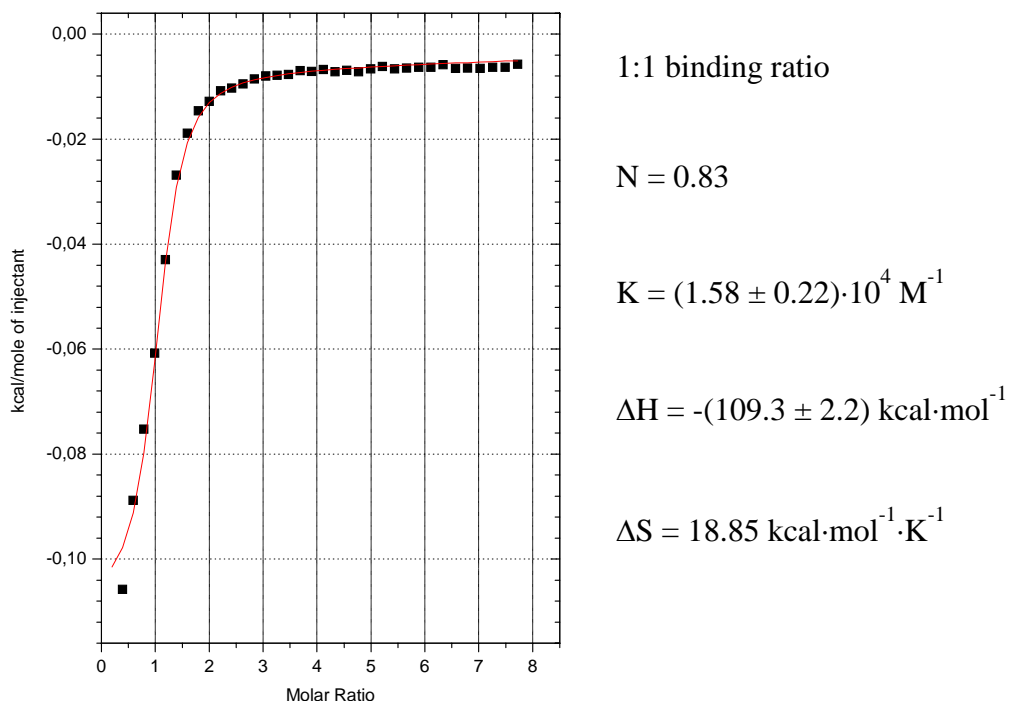


**Figure 89.** Microcalorimetric titration of **122** ( $c = 1 \text{ mM}$ ) and phenyl phosphate ( $c = 35 \text{ mM}$ ) in HEPES buffer ( $T = 298 \text{ K}$ , pH 7.5, 50 mM).

The high binding constant demonstrates a strong affinity of phosphate towards **122**. Therefore, this binding process was examined using  $^{31}\text{P}$ -NMR experiments (162.0 MHz,  $\text{D}_2\text{O}$ ,  $c = 65.5 \text{ mM}$ , 294 K). Solution of pure phenyl phosphate (A) and a 1:1 mixture of **122** and phenyl phosphate (B) were measured and showed a shift of the phosphate signal of  $\Delta\text{ppm} = -0.91$ . This fits very well to the chemically induced shift, which was observed by *Hamachi* examining his phosphate receptors.

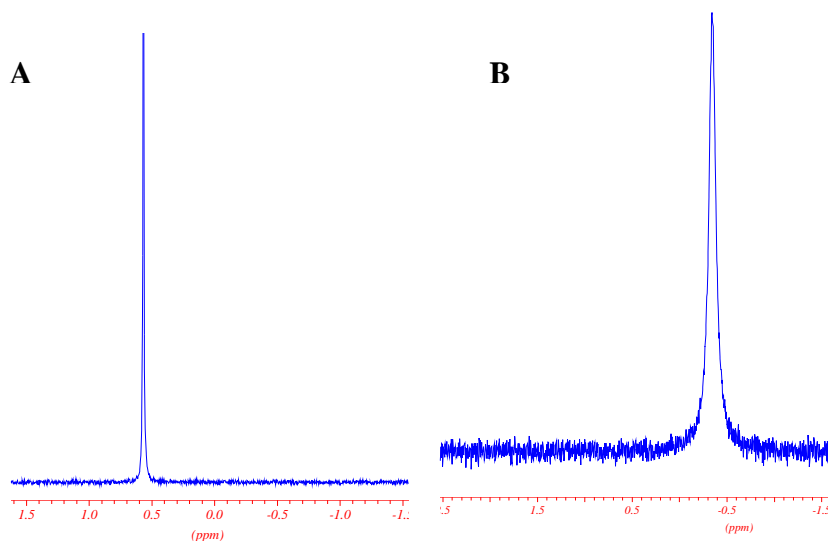


**Figure 90.**  $^{31}\text{P}$ -NMR of pure phenyl phosphate (A) and a 1:1 mixture of **122** and phenyl phosphate (B).

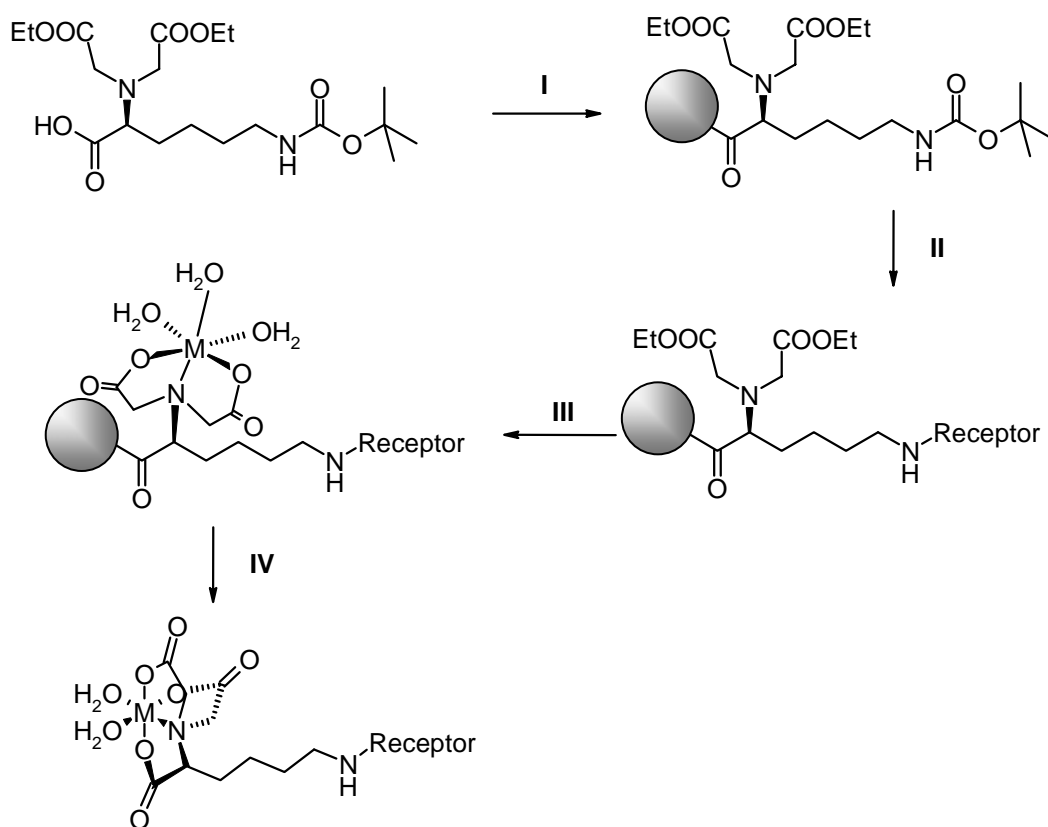
Additionally only one signal was observed in the NMR solution of the mixture. This indicates complete phosphate ion binding by the receptor molecule.

#### 2.1.4 SPRS (Solid Phase Receptor Synthesis)

In addition to the established concept of peptide based receptor synthesis in solution, a solid phase synthesis needed to be established. The aim was the synthesis of a receptor oligoamide using Boc-strategy on a solid support. Because of the high polarity of final receptor molecules (consisting of several metal complexes), the synthesis of the metal complex on solid support was desired. In a first series of experiments a C-terminal NTA unit was used to preload a resin (scheme 42, **I**). After successful loading, a Boc-protected primary amine was used for solid phase receptor synthesis (**II**). The loading process converted the NTA motif into an IDA binding site. Therefore it is possible to generate a  $\text{M(II)}$ -IDA metal complex on the solid support (**III**). The cleavage of the receptor, which has to be done under basic conditions generates a  $\text{M(II)}$ -NTA complex (**IV**). This amplifies

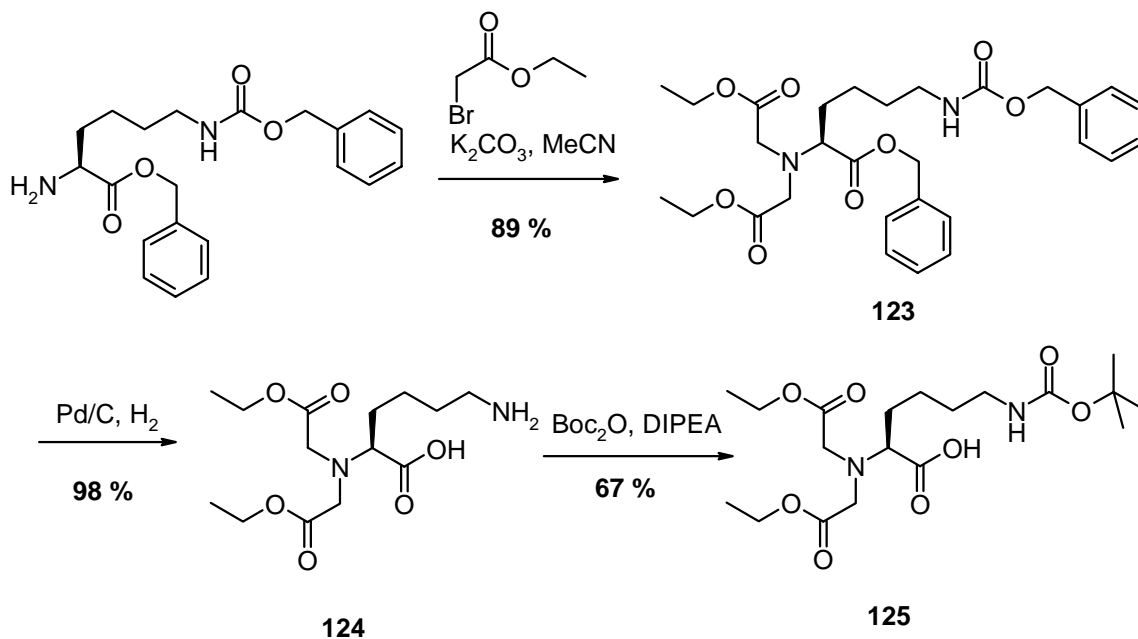
the metal binding towards the chelator. The synthesis of the metal complex can be performed without loss of the metal ion.

**Scheme 42.** Schematic depiction of a planned SPRS



The first challenge was the synthesis of a C-terminal NTA building block, which contains one acid orthogonally protected to the other two remaining acids. Starting from commercially available H-Lys(Z)-OBzl, the  $\alpha$ -amine was double alkylated with ethylbromoacetate resulting in **123**. The following hydrogenolytical cleavage of the amino and carboxy protecting groups gave the zwitterion **124**. This zwitterion was extracted with water. Lyophilisation gave **124** in good purity. The necessary Boc-protection did not work well and gave **125** in only moderate yields (scheme 43).

**Scheme 43.** Synthesis of a terminal NTA building block **125** with a free carbonic acid for SPRs



This building block was used for loading of a safety-catch-resin<sup>10</sup> (*procedure see experimental part*). This resin allows solid phase synthesis under acidic and basic conditions. The cleavage from the resin is possible with NaOH only after initial activation of the sulfonamide giving N-methyl acylsulfonamide using iodoacetonitrile.

The success of the loading experiments was verified by gravimetric analysis and FT-IR spectroscopy. Figure 91 shows the changed IR resonance in the region of carbonyl vibrations of esters (new peaks at  $\tilde{\nu} = 1716\text{ cm}^{-1}$  and  $1747\text{ cm}^{-1}$ ) and sulfonamides (new peak at  $\tilde{\nu} = 1342\text{ cm}^{-1}$ ) after resin loading.



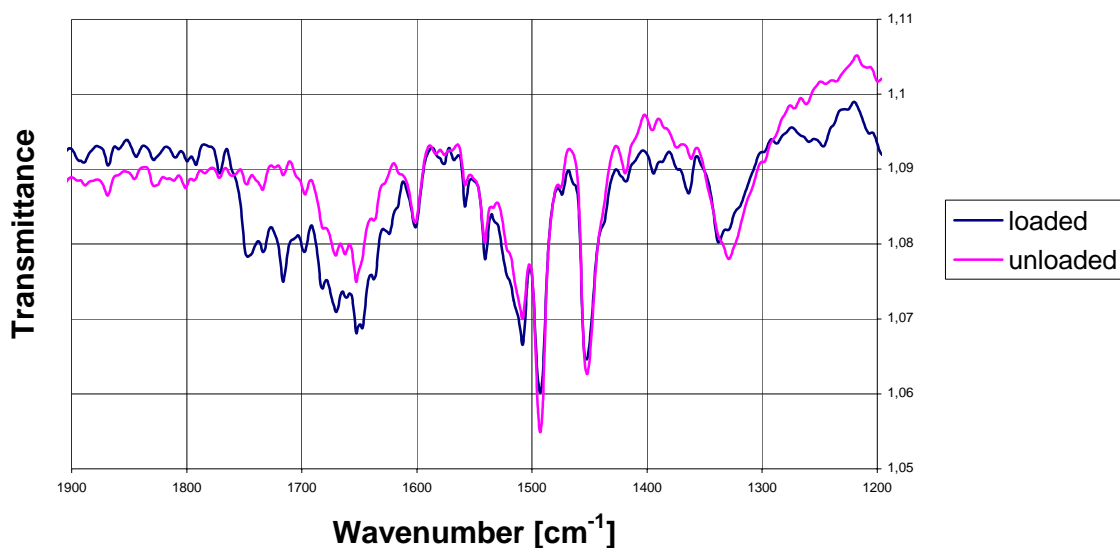
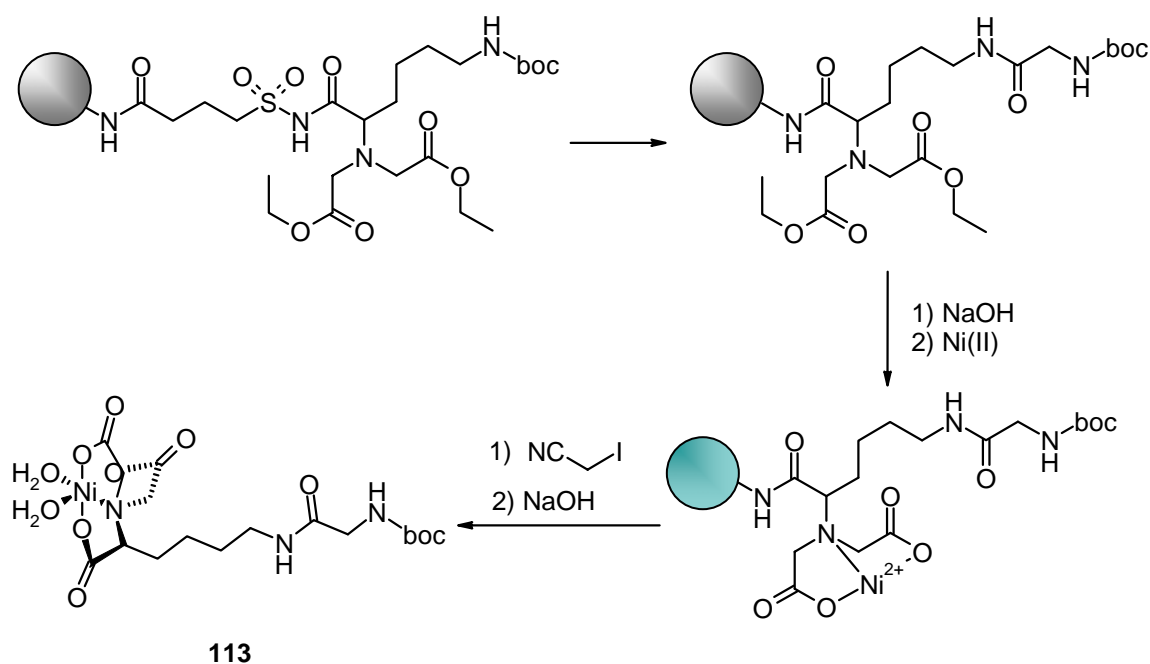


**Figure 91.** IR-Spectra of the carbonyl region of unloaded und loaded safety-catch-resin.

The preloaded resin was used for a simple coupling experiment with Boc-Gly-OH. After ester hydrolysis, Ni(II) complexation (the colour of the resin changed to bluish green) and cleavage, the receptor molecule **113** was obtained (scheme 44). This compound was analysed with mass-spectroscopy and gave nearly the same results as **113** synthesised in solution (see scheme37).

**Scheme 44.** SPRS with NTA preloaded safety-catch-resin



## 2.2 Receptors as Side Chains of Amino Acids

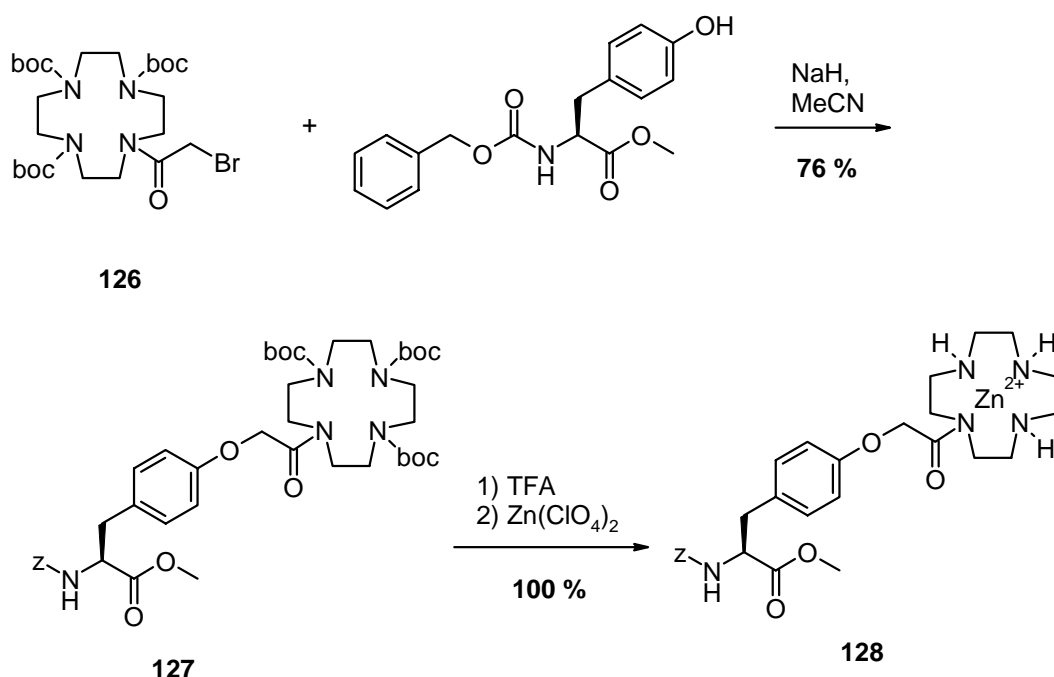
In addition to the already discussed terminal receptors, the synthesis of molecular recognition building blocks by amino acid side chain functionalisation was aspired.

Metal chelating units are introduced into the side chains of natural amino acids. One possibility is a coupling reaction of the terminal recognition units from the previous chapters with aspartic acid, glutamic acid or lysine. This is desirable, if the distance between receptor backbone and binding site should be large. For receptors with recognition units very close to the receptor backbone, the design of new unnatural amino acids is necessary. The following chapters demonstrate such syntheses using *Williamson* ether synthesis and *Negishi* coupling of iodoalanines.

### 2.2.1 Tyrosine based Receptor

Starting from the natural amino acid tyrosine, the side chain was modified via nucleophilic substitution. Starting from the literature known compound **126**,<sup>11</sup> a *Williamson* ether synthesis was used to attach this protected cyclen **126** to the phenol side chain of Z-Tyr-OMe in good yields (scheme 45). To prove the ability to form a metal complex out of this chelator precursor, the Boc-groups were cleaved quantitatively in TFA/DCM. The following complexation reaction with Zn(II) gave the Zn(II) cyclen derivative **128**.

**Scheme 45.** *Williamson* ether synthesis of **127** and synthesis of the corresponding Zn(II) complex **128**



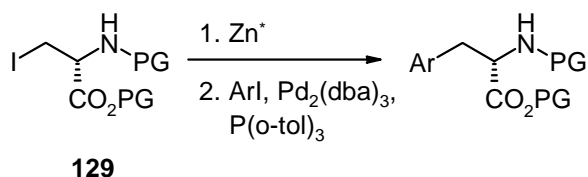
## 2.2.2 Phenylalanine based Receptors<sup>iv</sup>

The function of peptides and proteins is strongly correlated with their secondary and tertiary structure,<sup>12</sup> which is induced by side chain interactions determined through the amino acid sequence. Non-proteinogenic amino acids<sup>13,14,15</sup> and amino acid mimics are widely used to define,<sup>16</sup> modulate<sup>17</sup> or switch<sup>18</sup> the structure of peptides, which may result in changes of their biological properties. One concept<sup>19</sup> to control a peptide structure is the inter- or intramolecular formation of a metal complex, whereby parts of the peptide function as donor ligands. This requires modified amino acids bearing a strong metal ion chelating ligand for stable complex formation for incorporation into a peptide sequence.<sup>20</sup> Different research groups used alkylation reactions of lysine or diaminopropionic acid to generate IDA<sup>21</sup> or BPA<sup>22</sup> chelates directly on protein surfaces.

As this modification of amino acid side chains is limited to a certain kind of chelates, a more general solution to transform natural amino acids into metal ion chelating amino acids is desired.

*Jackson* already showed that palladium-catalysed coupling of the organozinc compound derived from **129** with aryl iodides is a feasible route to derivatives of phenylalanine.<sup>23</sup> The scope of this reaction is now extended to phenylalanine derivatives bearing *p*-NH<sub>2</sub> (**132**), *p*-NH-Boc (**133**), and *p*-Me (**131**) aryl substituents. The efficient synthesis of the non-natural chiral amino acids **134** and **135** having protected IDA and cyclen metal ion chelating ligands in their side chain is reported in this chapter.

### Scheme 46. Palladium-catalysed coupling of aryl iodides with **129**

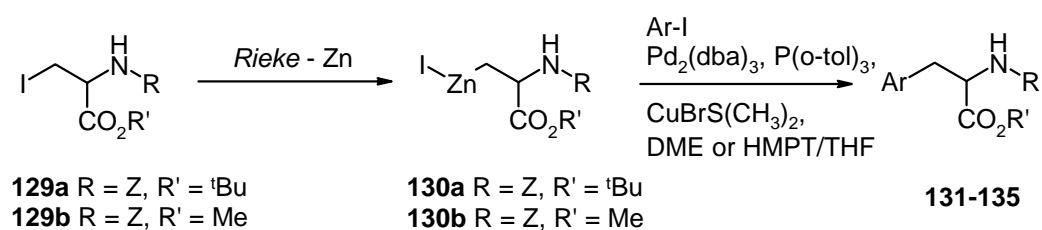


So far, no *Negishi* coupling<sup>24</sup> reaction has been reported for alkenyl organozinc compounds with *p*-iodoaniline derivatives as reactants. Previous preparations of the unnatural amino acid H-*p*-NH<sub>2</sub>-Phe-OH and protected derivatives of it used either the reduction of *p*-nitrophenyl alanine<sup>25</sup> or *Staudinger* reactions<sup>26</sup> of *p*-azidophenyl alanine. The necessary iodide precursors **129a**<sup>27</sup> and **129b**<sup>28</sup> were synthesised from commercially available serine.

<sup>iv</sup> Kruppa, M.; Imperato, G.; König, B. *Adv. Cat. Synth.* **2005**, in preparation.

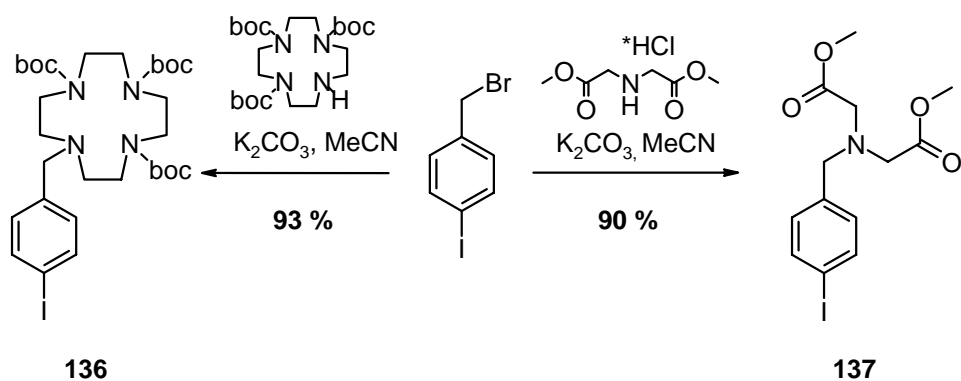
The corresponding organozinc reagents **130a** and **130b** were obtained by direct insertion of freshly prepared *Rieke* zinc.<sup>29</sup> The alternative method of zinc dust activation by Me<sub>3</sub>SiCl in DMF was not as efficient as the use of *Rieke* zinc. The disappearance of the black zinc indicates the complete conversion by insertion reaction. The quantitative formation of the organozinc compounds **130a** and **130b** was confirmed by quenching the reaction with water giving alanine derivatives.

**Scheme 47.** Preparation of the organozinc reagents **130a** and **130b**



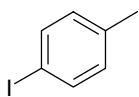
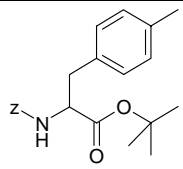
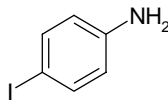
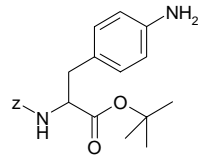
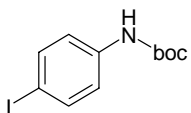
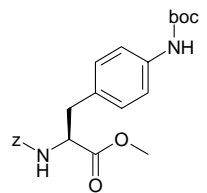
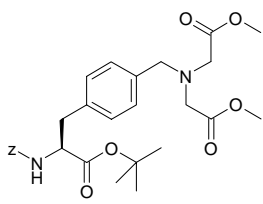
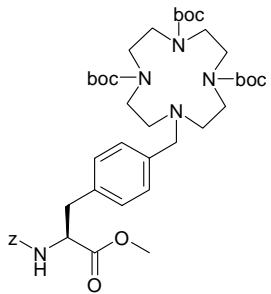
The reaction conditions of the palladium-catalysed coupling reaction were optimised using organozinc reagent **130a** and *p*-iodotoluene and *p*-iodoaniline as aryl iodides. While *p*-iodotoluene gave 66 % yield of the coupling product (table 23, entry 1) using DME as solvent with 0.1 eq CuBr·SMe<sub>2</sub>, the more electron rich *p*-iodoaniline requires a solvent mixture of HMPT and THF (1:1) to give 73 % of *Z*-*p*-NH<sub>2</sub>-Phe-O<sup>t</sup>Bu **132** (table 23, entry 2). To apply the method to the synthesis of metal chelating chiral amino acids, aryl iodide substituted protected metal chelates were prepared starting from *p*-iodobenzyl bromide. Methyl imino diacetate and threefold Boc-protected cyclen<sup>30</sup> were alkylated in good yield giving aryl iodides **136** and **137**.

**Scheme 48.** Synthesis of aryl iodides **136** and **137**



Applying the same conditions as used for the coupling of *p*-iodoaniline, IDA derivative **134** was obtained in moderate yield of 42 % (table 23, entry 4). *Negishi* coupling of aryl iodide **136** with iodoalanine **130a** gave cyclen-modified amino acid **135** in good yield of 86 % (table 23, entry 5).

**Table 23.** Palladium-catalysed synthesis of the phenylalanine derivatives **131-135**

Entry	Iodoalanine	Ar-I	Solvent	Yield [%]	Product
1	<b>130a</b>		DME	66	 <b>131</b>
2	<b>130a</b>		HMPT:THF = 1:1	73	 <b>132</b>
3	<b>130b</b>		HMPT:THF = 1:1	75	 <b>133</b>
4	<b>130a</b>	<b>137</b>	HMPT:THF = 1:1	65	 <b>134</b>
5	<b>130b</b>	<b>136</b>	HMPT:THF = 1:1	86	 <b>135</b>

## 2.3 Conclusion

The synthesis of C- and N-terminal receptor building blocks could be achieved by simple  $S_N2$  reactions of mono protected diamines and amino acids. The ligation of these building blocks was optimised using the active ester formed out of EDC/HOBt. The synthesis of **113** showed the deprotection and metal complexation of the binding site. This receptor proved high affinity towards a pentapeptide containing a terminal histidine. The binding process was examined by microcalorimetric titration.

Furthermore the synthesis of bidentate recognition units possessing an additional carboxylate for receptor ligation yielded the new receptor precursors **117**, **118**, **119** and **120**. The Zn(II) complex **122** synthesised by Boc-deprotection of **120** showed high affinity towards phenylphosphate which was examined by  $^{31}\text{P}$ -NMR and microcalorimetric titration.

In a first attempt a solid phase receptor synthesis was performed using a safety-catch resin.

To create binding sites in the side chains of natural amino acids the functionalisation of tyrosine was used for cyclen ligation.

The scope of the Negishi cross coupling reaction of organozinc compounds derived from chiral amino acids was extended to electron rich iodoanilines as coupling reagents. This now allows the direct modification of serine into phenylalanine derivatives bearing metal ion chelating ligand in their side chain. This concept was illustrated by the synthesis of the amino esters **134** and **135**. Such and similar modified chiral amino acids are useful for the preparation of peptides labelled with metal complexes as binding sites or probes, for the construction of synthetic receptors and hybrid materials having a peptide backbone and metal complex functionality.

## References:

- <sup>1</sup> Choi, K.-Y.; Jeon, Y.-M.; Ryu, H.; Oh, J.; Lim, H.-H.; Kim, M.-W. *Polyhedron* **2004**, *23*, 903.
- <sup>2</sup> Li, C.; Wong, W.-T.. *Tet. Lett.* **2002**, *43*, 3217.
- <sup>3</sup> Eisenfuhr, A.; Arora, P.S.; Sengle, G.; Takaoka, L.R.; Nowick, J.S.; Famulok, M. *Bioorg. Med. Chem.* **2003**, *11*, 235.
- <sup>4</sup> Dijols, S.; Boucher, J.-L.; Lepoivre, M.; Lefevre-Groboillot, D.; Moreau, M.; Frapart, Y.; Rekka, E.; Meade, A.L.; Stuehr, D.J.; Mansuy, D. *Biochem.* **2002**, *41*, 9286.
- <sup>5</sup> (a) Hart, B.R.; Shea, K.J. *J. Am. Chem. Soc.* **2001**, *123*, 2072. (b) Hart, B.R.; Shea, K.J. *Macromol.* **2002**, *124*, 12999.
- <sup>6</sup> Reichenbach-Klinke, R.; Kruppa, M.; König, B. *J. Am. Chem. Soc.* **2002**, *124*, 12999.
- <sup>7</sup> (a) Kawabata, E.; Kikuchi, K.; Urano, Y.; Kojima, H.; Odani, A.; Nagano, T.. *J. Am. Chem. Soc.* **2005**, *127*, 818. (b) Kim, T.W.; Park, J.; Hong, J. *J. Chem. Soc., Perkin Trans.* **2002**, 923.
- <sup>8</sup> Commercial available at Aldrich.
- <sup>9</sup> Hagemann, J.P.; Kaye, P.T. *Synth. Commun.* **1997**, *27*, 2539.
- <sup>10</sup> Backes, B.J.; Virgilio, A.A.; Ellman, J. *J. Am. Chem. Soc.* **1996**, *118*, 3055.
- <sup>11</sup> Wiest, O.; Harrison, C.B.; Saettel, N.J.; Cibulka, R.; Sax, M.; König, B. *J. Org. Chem.* **2004**, *69*, 8183.
- <sup>12</sup> Typical examples: 1) Prion-beta sheet structures, see: (a) Gasset, M.; Baldwin, M.A.; Fletterick, R.J.; Prusiner, S.B. *Proc. Nat. Acad. Sci.* **1993**, *90*, 1. (b) Inouye, H.; Kirschner, D.A. *J. Mol. Biol.* **1997**, *268*, 375. (c) Liu, H.; Farr-Jones, S.; Ulyanov, N.B.; Llinas, M.; Marqusee, S.; Groth, D.; Cohen, F.E.; Prusiner, S.B.; James, T. *Biochem.* **1999**, *38*, 5362. (d) Laws, D.D.; Bitter, H.-M.L.; Liu, K.; Ball, H.L.; Kaneko, K.; Wille, H.; Cohen, F.E.; Prusiner, S.B.; Pines, A.; Wemmer, D.E.; *Proc. Nat. Acad. Sci.* **2001**, *98*, 11686. 2) Seven helix transmembrane bundles, see: (a) Cronet, P.; Sander, C.; Vriend, G. *Prot. Eng.* **1993**, *6*, 59. (b) Elling, C.E.; Schwartz, T.W. *EMBO Journal* **1996**, *15*, 6213. (c) Son, H.S.; Sansom, M.S.P. *Eur. Biophys. J.* **1999**, *28*, 489.
- <sup>13</sup> Duthaler, R.O. *Tetrahedron* **1994**, *50*, 1539.
- <sup>14</sup> Taylor, P.P.; Pantaleone, D.P.; Senkpeil, R.F.; Fotheringham, I.G. *Trends in Biotech.* **1998**, *16*, 412.
- <sup>15</sup> Jun-An Ma, *Angew. Chem. Int. Ed.* **2003**, *42*, 4290.
- <sup>16</sup> Examples of typical peptide mimics, see: (a) Lai, J.R.; Gellman, S.H. *Prot. Sci.* **2003**, *12*, 560. (b) Gardner, R.R.; Liang, G.-B.; Gellman, S.H. *J. Am. Chem. Soc.* **1999**, *121*, 1806.
- <sup>17</sup> Example of peptide beta-sheet binders: (a) Bonauer, C.; Zabel, M.; König, B. *Org. Lett.* **2004**, *6*, 1349. (b) Nowick, J.S.; Chung, D.M.; Maitra, K.; Maitra, S.; Stigers, K.D.; Sun, Y. *J. Am. Chem. Soc.* **2000**, *122*, 7654. (c) Nowick, J.S.; Smith, E.M.; Ziller, J.W.;

- 
- Shaka, A.J. *Tetrahedron* **2002**, 58, 727. (d) Tsai, J.H.; Waldman, A.S.; Nowick, J.S. *Bioorg. Med. Chem.* **1999**, 7, 29.
- <sup>18</sup>Aemissegger, A.; Kraeutler, V.; van Gunsteren, W.F.; Hilvert, D. *J. Am. Chem. Soc.* **2005**, 127, 2929.
- <sup>19</sup>Examples of other concepts to control a peptide structure by 1) hydrogen bonds: Loughlin, W.A.; Tyndall, J.D.A.; Glenn, M.P.; Fairlie, D.P. *Chem. Rev.* **2004**, 104, 6085; 2) salt bridges: Schug, K.A.; Lindner, W. *Chem. Rev.* **2005**, 105, 67.
- <sup>20</sup>For an example of a cyclen-modified amino acid, see: Miltschitzky, S.; König, B. *Syn. Commun.* **2004**, 34, 2077.
- <sup>21</sup>(a) Ruan, F.; Chen, Y.; Hopkins, P.B. *J. Am. Chem. Soc.* **1990** 112, 9403. (b) Ruan, F.; Chen, Y.; Itoh, K.; Sasaki, T.; Hopkins, P.B. *J. Org. Chem.* **1991**, 56, 4347. (c) Hutschenreiter, S.; Neumann, L.; Räder, U.; Schmitt, L.; Tampé, R. *ChemBioChem* **2003**, 4, 1340. (d) Futaki, S.; Kiwada, T.; Sugiura, Y. *J. Am. Chem. Soc.* **2004**, 126, 15762.
- <sup>22</sup>Banerjee, S.R.; Wie, L.; Levadala, M.K.; Lazarova, N.; Golub, V.O.; O'Connor, C.J.; Stephenson, K.A.; Valliant, J.F.; Babich, J.W.; Zubietta, J. *Inorg. Chem.* **2002**, 41, 5795.
- <sup>23</sup>(a) Jackson, R.F.W.; Wythes, M.J.; Wood, A. *Tet. Lett.* **1989**, 30, 5941. (b) Jackson, R.F.W.; Moore, R.J.; Dexter, C.S. *J. Org. Chem.* **1998**, 63, 7875 (and references therein). (c) Deboves, H.J.C.; Montalbetti, C.A.G.N.; Jackson, R.F.W. *J. Chem. Soc., Perkin Trans. 1* **2001**, 1876. (d) Oates, L.J.; Jackson, R.F.W.; Block, M.H. *Org. Biomol. Chem.* **2003**, 1, 140.
- <sup>24</sup>Negishi, E.; Xu C. in *Handbook of Organopalladium Chemistry for Organic synthesis*, (Ed.: E. Negishi), Wiley, New York, **2002**, pp 229.
- <sup>25</sup>(a) Landis, G.; Lui, G.; Shook, J.E.; Yamamura, H.I. *J. Med. Chem.* **1989**, 32, 638. (b) Lai, J.H.; Pham, H.; Hanauer, D.G. *J. Org. Chem.* **1996**, 61, 1872. (c) Sidduri, A.; Jefferson, J.W.; Lou, J.P.; Chen, L.; Kaplan, G.; Mennona, F.; Campbell, R.; Guthrie, R.; Huang, T.N.; Rowan, K.; Schwinge, V.; Renzetti, L.M. *Bioorg. Med. Chem. Lett.* **2002**, 12, 2479.
- <sup>26</sup>Lindsley, C.W.; Zhao, Z.; Newton, R.C.; Leister, W.H.; Strauss, K.A. *Tet. Lett.* **2002**, 43, 4467.
- <sup>27</sup>Anderson, J.T.; Toogood, P.T.; Marsh, E.N.G. *Org. Lett.* **2002**, 4, 4281.
- <sup>28</sup>Trost, B.M.; Rudd, M.T. *Org. Lett.* **2003**, 5, 4599.
- <sup>29</sup>Rieke, R.D.; Hanson, M.V. *Tetrahedron* **1997**, 53, 1925.
- <sup>30</sup>Brandes, S.; Gros, C.; Denat, F.; Pullumbi, P.; Guillard, R. *Bull. Soc. Chim. Fr.* **1996**, 133, 65.



## 2.4 Experimental Section

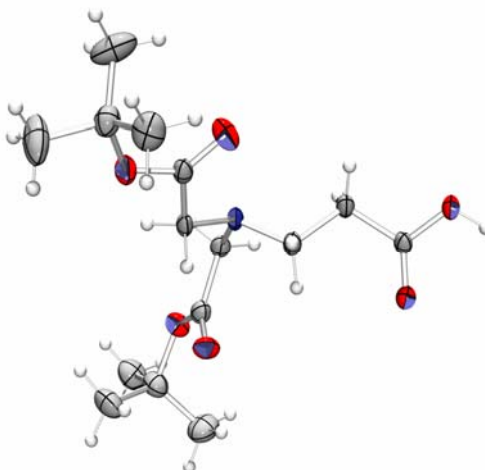
### 2.4.1 Instruments and general techniques

See experimental part of chapter 1 (page 131).

#### X-Ray Data:

**94:**

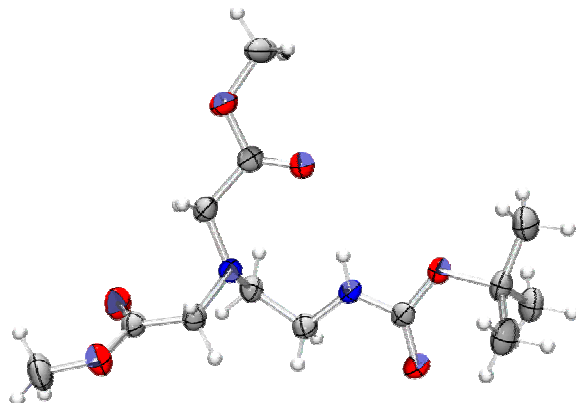
$C_{15}H_{27}NO_6$ ,  $M_r = 317.38$ , colourless translucent plates, orthorhombic, Space group  $Pnca$ ,  $a = 6.7622(5) \text{ \AA}$ ,  $b = 10.3093(9) \text{ \AA}$ ,  $c = 25.479(3) \text{ \AA}$ ,  $\alpha = \beta = \gamma = 90^\circ$ ,  $Z = 4$ ,  $V = 1776.2(3) \text{ \AA}^3$ ,  $D_x = 1.185 \text{ mg/m}^3$ ,  $\mu = 0.091 \text{ mm}^{-1}$ ,  $F(000) = 688$ , Crystal size  $0.620 \times 0.540 \times 0.120 \text{ mm}$ ,  $\theta$ -range for data collections  $3.12$  to  $25.81^\circ$ , Index ranges  $-8 \leq h \leq 8$ ,  $-12 \leq k \leq 12$ ,  $-31 \leq l \leq 31$ , Reflections collected/unique  $10900/3388$  [ $R_{\text{int}} = 0.0662$ ], Data/restraints/parameters  $3388/1/203$ , Goodness-of-fit on  $F^2$   $1.035$ , Final  $R$  indices [ $I > 2\sigma(I)$ ]  $R_1 = 0.0419$ ,  $wR_2 = 0.0998$   $R$  indices (all data)  $R_1 = 0.0445$ ,  $wR_2 = 0.1017$ , Absolute structure parameter  $-0.1(8)$ , largest diff. peak and hole  $0.298$  and  $-0.161 \text{ e. \AA}^{-3}$ .



**98:**

$C_{13}H_{24}N_2O_6$ ,  $M_r = 304.34$ , colourless translucent prism, monoclinic, Space group  $P2_1/a$ ,  $a = 9.0953(8) \text{ \AA}$ ,  $b = 19.1113(13) \text{ \AA}$ ,  $c = 9.7889(9) \text{ \AA}$ ,  $\alpha = \gamma = 90^\circ$ ,  $\beta = 109.062(10)^\circ$ ,  $Z = 4$ ,  $V = 1608.2(3) \text{ \AA}^3$ ,  $D_x = 1.257 \text{ mg/m}^3$ ,  $\mu = 0.099 \text{ mm}^{-1}$ ,  $F(000) = 656$ , Crystal size  $0.400 \times 0.260 \times 0.240 \text{ mm}$ ,  $\theta$ -range for data collections  $2.13$  to  $25.78^\circ$ , Index ranges  $-11 \leq h \leq 11$ ,  $-23 \leq k \leq 23$ ,  $-11 \leq l \leq 11$ , Reflections collected/unique  $11159/3077$  [ $R_{\text{int}} =$

0.0674], Data/restraints/parameters 3077/0/194, Goodness-of-fit on  $F^2$  0.881, Final R indices [ $I > 2\sigma(I)$ ]  $R_1 = 0.0383$ ,  $wR_2 = 0.0877$  R indices (all data)  $R_1 = 0.0637$ ,  $wR_2 = 0.0948$ , largest diff. peak and hole 0.195 and -0.193 e.  $\text{\AA}^{-3}$ .

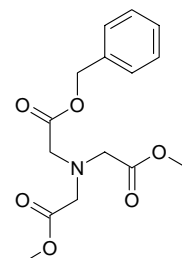


## 122:

$C_{26}H_{49}N_8O_3Zn_2 \cdot 3(ClO_4)$ ,  $M_r = 950.86$ , colourless translucent stick, orthorhombic, Space group  $Pb21a$ ,  $a = 12.5672(7) \text{ \AA}$ ,  $b = 18.5822(10) \text{ \AA}$ ,  $c = 32.298(3) \text{ \AA}$ ,  $\alpha = \beta = \gamma = 90^\circ$ ,  $Z = 8$ ,  $V = 1776.2(3) \text{ \AA}^3$ ,  $D_x = 1.675 \text{ mg/m}^3$ ,  $\mu = 1.562 \text{ mm}^{-1}$ ,  $F(000) = 936$ , Crystal size  $0.60 \times 0.20 \times 0.12 \text{ mm}$ ,  $\theta$ -range for data collections  $2.05$  to  $25.79^\circ$ , Index ranges  $-15 \leq h \leq 14$ ,  $-21 \leq k \leq 22$ ,  $-39 \leq l \leq 39$ , Reflections collected/unique 52151/13872 [ $R_{int} = 0.0384$ ], Data/restraints/parameters 13872/1/979, Goodness-of-fit on  $F^2$  0.618, Final R indices [ $I > 2\sigma(I)$ ]  $R_1 = 0.0327$ ,  $wR_2 = 0.0793$  R indices (all data)  $R_1 = 0.0519$ ,  $wR_2 = 0.0897$ , Absolute structure parameter  $-0.009(7)$ , largest diff. peak and hole 2.050 and -0.285 e.  $\text{\AA}^{-3}$ .

## 2.4.2 Synthesis

**108**,<sup>v</sup> and 3,5-Bis-(bromomethyl)-benzoic acid methylester<sup>vi</sup> were synthesised according to literature known procedures.



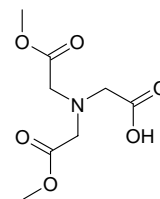
(*Benzyloxycarbonylmethyl-methoxycarbonylmethyl-amino*)-acetic acid methyl ester (**80**):

Dimethyl iminodiacetic acid hydrogenschloride (3.00 g, 15.2 mmol) was dissolved in MeCN (40 mL). Benzyloxycarbonylmethyl bromide (2.38 mL, 15.2 mmol), a spatula tip KI and K<sub>2</sub>CO<sub>3</sub> (4.20 g, 30.4 mmol) were added to the reaction mixture. The suspension was stirred at 60 °C for 3 days, filtered, mixed with water (25 mL) and extracted with EtOAc. The organic layers were dried over Na<sub>2</sub>SO<sub>4</sub> and concentrated under reduced pressure. The crude oil was purified using column chromatography on silica gel (PE:EtOAc = 1:1, *R<sub>f</sub>* = 0.36). **80** (13.9 mmol, 4.31 g, 92 %) is a colourless oil.

<sup>1</sup>H-NMR (300 MHz; [D<sub>6</sub>]-Acetone): δ = 3.63 (s, 6 H, O-CH<sub>3</sub>), 3.68 (s, 4 H, CH<sub>2</sub>-COOMe), 3.74 (s, 2 H, CH<sub>2</sub>-COOBzl), 5.14 (s, 2 H, CH<sub>2</sub>-Ph), 7.31-7.41 (m, 5 H, H-Ar). – <sup>13</sup>C-NMR (75 MHz; [D<sub>6</sub>]-Acetone): δ = 30.1, 51.7 (+, 2 C, CH<sub>3</sub>), 55.0 (–, 2 C, CH<sub>2</sub>), 55.2 (–, 2 C, CH<sub>2</sub>), 66.5 (–, CH<sub>2</sub>), 128.3 (+, 2 C, C-Ar), 128.4 (+, C-Ar), 128.6 (+, 2 C, C-Ar), 135.5 (C<sub>quat</sub>, C-Ar), 170.6 (C<sub>quat</sub>, COOBzl), 171.2 (C<sub>quat</sub>, 2 C, COOMe). – IR (KBr) [cm<sup>–1</sup>]:  $\tilde{\nu}$  = 3478, 3032, 2956, 1740, 1004. – MS (CI-MS, NH<sub>3</sub>): *m/z* (%) = 310 (100) [MH<sup>+</sup>], 327 (7) [M + NH<sub>4</sub><sup>+</sup>]. – Elemental analysis calcd. (%) for C<sub>15</sub>H<sub>19</sub>NO<sub>6</sub> (309.32): C 58.25, H 6.19, N 4.53; found C 58.03, H 6.27, N 4.24.

<sup>v</sup> Beck-Piotraschke, K.; Jakubke, H.D. *Tet. Asym.* **1998**, 9, 1505.

<sup>vi</sup> Kurz, K.; Göbel, M.W. *Helvet. Chim. Acta* **1996**, 79, 1967.

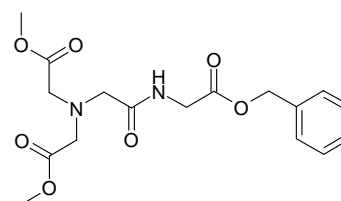


*(Bis-methoxycarbonylmethyl-amino)-acetic acid (81):*

Literature known compound BRNr: 8055366 but improved synthesis

**80** (1.00 g, 3.2 mmol) was dissolved in EtOH (25 mL) and mixed with a spatula tip 10 % Pd/C. The reaction mixture was stirred for 12 h in an autoclave under 10 bar H<sub>2</sub> pressure. The suspension was filtered using celite and the filtrate concentrated under reduced pressure. **81** (3.1 mmol, 682 mg, 96 %) was isolated as a yellowish oil without further purification.

<sup>1</sup>H-NMR (300 MHz; CDCl<sub>3</sub>): δ = 3.54 (s, 2 H, CH<sub>2</sub>), 3.62 (s, 4 H, CH<sub>2</sub>), 3.76 (s, 6 H, O-CH<sub>3</sub>). – MS (CI, NH<sub>3</sub>): *m/z* (%) = 237 (23) [M+NH<sub>4</sub><sup>+</sup>], 220 (100) [MH<sup>+</sup>]. – C<sub>8</sub>H<sub>13</sub>NO<sub>6</sub> (219.20).

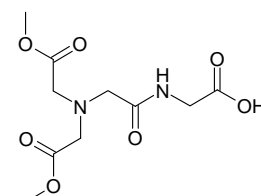


*[[ (Benzyloxycarbonylmethyl-carbamoyl)-methyl]-methoxycarbonylmethyl-amino]-acetic acid methyl ester (82):*

H-Gly-OBzl-HOTos (0.32 g, 0.9 mmol) was dissolved in DCM (15 mL) and DIPEA (0.48 mL, 2.8 mmol) was added. After 5 min, **81** (0.23 g, 1.0 mmol), EDC (0.20 mL, 1.2 mmol), and HOBT (0.16 g, 1.2 mmol) were added to the solution. The reaction process was monitored by TLC (EtOAc). Once the reaction was completed, the reaction mixture was added to water (25 mL) and extracted with DCM. The organic layers were washed twice with brine (30 mL each) and dried over Na<sub>2</sub>SO<sub>4</sub>. After evaporation of the solvent, the crude product was purified by column chromatography on silica gel (EtOAc, *R<sub>f</sub>* = 0.44). **82** (0.7 mmol, 246 mg, 71 %) is a colourless oil.

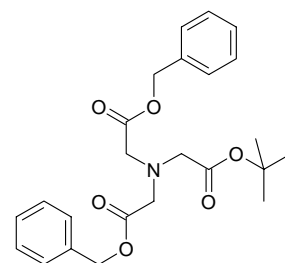
<sup>1</sup>H-NMR (300 MHz; CDCl<sub>3</sub>): δ = 3.45 (s, 2 H, CH<sub>2</sub>), 3.57 (s, 4 H, N-CH<sub>2</sub>), 3.71 (s, 6 H, O-CH<sub>3</sub>), 4.12 (d, <sup>3</sup>*J* = 6.0 Hz, 2 H, CH<sub>2</sub>-Gly), 5.17 (s, 2 H, CH<sub>2</sub>-Ph), 7.29-7.40 (m, 5 H, H-Ar), 8.20 (t, <sup>3</sup>*J* = 5.5 Hz, 1 H, NH). – <sup>13</sup>C-NMR (75 MHz; CDCl<sub>3</sub>): δ = 41.0 (–, CH<sub>2</sub>), 51.9

(+, 2 C, CH<sub>3</sub>), 55.4 (–, 2 C, CH<sub>2</sub>), 58.7 (–, CH<sub>2</sub>), 67.1 (–, CH<sub>2</sub>), 128.3 (+, 2 C, C-Ar), 128.5 (+, C-Ar), 128.6 (+, 2 C, C-Ar), 135.3 (C<sub>quat</sub>, C-Ar), 169.7 (C<sub>quat</sub>, CONH), 171.3 (C<sub>quat</sub>, COOBzl), 171.6 (C<sub>quat</sub>, 2 C, COOMe). – IR (KBr) [cm<sup>–1</sup>]:  $\tilde{\nu}$  = 3478, 3034, 2946, 2935, 1742, 1646, 1030. – MS (CI, NH<sub>3</sub>):  $m/z$  (%) = 384 (8) [MNa<sup>+</sup>], 367 (100) [MH<sup>+</sup>]. – C<sub>17</sub>H<sub>22</sub>N<sub>2</sub>O<sub>7</sub> (366.27).



[2-(Bis-methoxycarbonylmethyl-amino)-acetylamino]-acetic acid (**83**):

**82** (0.25 g, 0.7 mmol) was dissolved in EtOH (25 mL) and mixed with a spatula tip 10 % Pd/C. The reaction mixture was stirred for 12 h in an autoclave under 10 bar H<sub>2</sub> pressure. The suspension was filtered using celite and the filtrate concentrated under reduced pressure. **83** (0.6 mmol, 169 mg, 91 %) was isolated as a yellowish oil without purification. <sup>1</sup>H-NMR (600 MHz; CDCl<sub>3</sub>):  $\delta$  = 3.47 (s, 2 H, CH<sub>2</sub>), 3.58 (s, 4 H, N-CH<sub>2</sub>), 3.72 (s, 6 H, O-CH<sub>3</sub>), 4.10 (d, <sup>3</sup> $J$  = 5.5 Hz, 2 H, CH<sub>2</sub>-Gly), 8.32 (t, <sup>3</sup> $J$  = 5.6 Hz, 1H, NH). – <sup>13</sup>C-NMR (75 MHz; CDCl<sub>3</sub>):  $\delta$  = 41.0 (–, CH<sub>2</sub>-Gly), 52.0 (+, 2 C, O-CH<sub>3</sub>), 55.5 (–, 2 C, CH<sub>2</sub>), 58.5 (–, CH<sub>2</sub>), 171.7 (C<sub>quat</sub>, 2 C, COOMe), 172.3 (C<sub>quat</sub>, COOH), 172.5 (C<sub>quat</sub>, CONH). – IR (KBr) [cm<sup>–1</sup>]:  $\tilde{\nu}$  = 3397, 2958, 1738, 1659, 1414. – MS (CI, NH<sub>3</sub>):  $m/z$  (%) = 294 (68) [M + NH<sub>4</sub><sup>+</sup>], 277 (100) [MH<sup>+</sup>]. – Elemental analysis calcd. (%) for C<sub>10</sub>H<sub>16</sub>N<sub>2</sub>O<sub>7</sub> (276.25): C 43.48, H 5.84, N 10.14; found C 43.81, H 6.07, N 5.49.

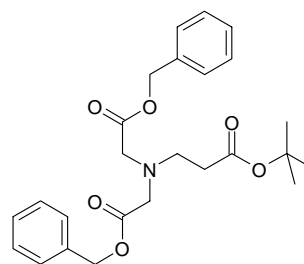


(Bis-benzyloxycarbonylmethyl-amino)-acetic acid tert-butylester (**84**):

H-Gly-OtBu·HCl (0.50 g, 3.0 mmol), benzyloxycarbonyl bromide (1.03 mL, 6.6 mmol), K<sub>2</sub>CO<sub>3</sub> (1.81 g, 13.1 mmol), and a spatula tip of KI were dissolved in MeCN (25 mL). The suspension was stirred at 60 °C for 2 days und monitored via TLC (EtOAc). The finished

reaction was filtered, mixed with water (25 mL) and extracted with EtOAc. The organic layers were dried over Na<sub>2</sub>SO<sub>4</sub> and evaporated. The crude product was purified using column chromatography on silica gel (EtOAc,  $R_f$  = 0.84) giving the colourless oil **84** (2.4 mmol, 1.01 g, 79 %).

<sup>1</sup>H-NMR (300 MHz; CDCl<sub>3</sub>):  $\delta$  = 1.44 (s, 9 H, CH<sub>3</sub>), 3.57 (s, 2 H, N-CH<sub>2</sub>-COO<sup>t</sup>Bu), 3.72 (s, 4 H, N-CH<sub>2</sub>-COOBzl), 5.14 (s, 4 H, CH<sub>2</sub>-Ph), 7.29-7.39 (m, 10 H, H-Ar). – <sup>13</sup>C-NMR (75 MHz; CDCl<sub>3</sub>):  $\delta$  = 28.1 (+, 3 C, CH<sub>3</sub>), 55.1 (–, 2 C, CH<sub>2</sub>), 55.8 (–, CH<sub>2</sub>), 66.4 (–, 2 C, CH<sub>2</sub>), 81.4 (C<sub>quat</sub>, C-Boc), 128.3 (+, 6 C, C-Ar), 128.6 (+, 4 C, C-Ar), 135.6 (C<sub>quat</sub>, 2 C, C-Ar), 170.0 (C<sub>quat</sub>, COO<sup>t</sup>Bu), 170.8 (C<sub>quat</sub>, 2 C, COOBzl). – IR [cm<sup>–1</sup>]:  $\tilde{\nu}$  = 3455, 3034, 2978, 1746, 1145. – MS (CI-MS, NH<sub>3</sub>):  $m/z$  (%) = 428 (100) [MH<sup>+</sup>], 372 (19) [MH<sup>+</sup> – C<sub>4</sub>H<sub>8</sub>]. – Elemental analysis calcd. (%) for C<sub>24</sub>H<sub>29</sub>NO<sub>6</sub> (427.5): C 67.43, H 6.84, N 3.28; found C 66.95, H 6.59, N 3.01.

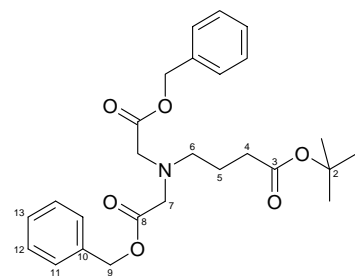


### 3-(Bis-benzoyloxycarbonylmethyl-amino)-propionic acid tert-butylester (**85**):

H- $\beta$ -Ala-O<sup>t</sup>Bu·HCl (1.00 g, 5.5 mmol), benzylbromoacetate (1.73 mL, 11.0 mmol), K<sub>2</sub>CO<sub>3</sub> (3.04 g, 22.0 mmol), and a spatula tip of KI were dissolved in MeCN (30 mL). The suspension was stirred at 60 °C for 2 days und monitored by TLC (EtOAc). The finished reaction was filtered, mixed with water (25 mL) and extracted with EtOAc. The organic layers were dried over Na<sub>2</sub>SO<sub>4</sub> and evaporated. The crude product was purified using column chromatography on silica gel (EtOAc,  $R_f$  = 0.84) giving the colourless oil **85** (5.5 mmol, 2.43 g, 100 %).

<sup>1</sup>H-NMR (300 MHz; CDCl<sub>3</sub>):  $\delta$  = 1.42 (s, 9 H, CH<sub>3</sub>), 2.41 (t, <sup>3</sup> $J$  = 7.3 Hz, 2 H, N-CH<sub>2</sub>), 3.05 (t, <sup>3</sup> $J$  = 7.3 Hz, 2 H, N-CH<sub>2</sub>-COO<sup>t</sup>Bu), 3.63 (s, 4 H, N-CH<sub>2</sub>-COOBzl), 5.13 (s, 4 H, CH<sub>2</sub>-Ph), 7.31-7.39 (m, 10 H, H-Ar). – <sup>13</sup>C-NMR (75 MHz; CDCl<sub>3</sub>):  $\delta$  = 28.1 (+, 3 C, CH<sub>3</sub>), 34.9 (–, CH<sub>2</sub>), 50.3 (–, CH<sub>2</sub>), 55.0 (–, 2 C, CH<sub>2</sub>), 66.3 (–, 2 C, CH<sub>2</sub>), 80.5 (C<sub>quat</sub>, C-Boc), 128.3 (+, 6 C, C-Ar), 128.6 (+, 4 C, C-Ar), 135.7 (C<sub>quat</sub>, 2 C, C-Ar), 171.1 (C<sub>quat</sub>, 2 C, COOBzl), 171.5 (C<sub>quat</sub>, COO<sup>t</sup>Bu). – IR [cm<sup>–1</sup>]:  $\tilde{\nu}$  = 3445, 3034, 2976, 1730, 1164. –

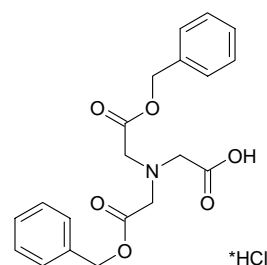
MS (CI-MS, NH<sub>3</sub>):  $m/z$  (%) = 442 (100) [MH<sup>+</sup>]. – Elemental analysis calcd. (%) for C<sub>25</sub>H<sub>31</sub>NO<sub>6</sub> (441.53): C 68.01, H 7.08, N 3.17; found C 67.99, H 7.14, N 3.02.



*4-(Bis-benzyloxycarbonylmethyl-amino)-butyric acid tert-butylester (86):*

H- $\gamma$ -Abu-OtBu-HCl (0.50 g, 2.6 mmol), benzyloxycarbonyl bromide (0.88 mL, 5.6 mmol), K<sub>2</sub>CO<sub>3</sub> (1.55 g, 11.3 mmol), and a spatula tip of KI were dissolved in MeCN (25 mL). The suspension was stirred at 60 °C for 2 days und monitored by TLC (EtOAc). The finished reaction was filtered, mixed with water (25 mL) and extracted with EtOAc. The organic layers were dried over Na<sub>2</sub>SO<sub>4</sub> and evaporated. The crude product was purified using column chromatography on silica gel (EtOAc,  $R_f$  = 0.83) giving the colourless oil **86** (2.6 mmol, 1.17 g, 100 %).

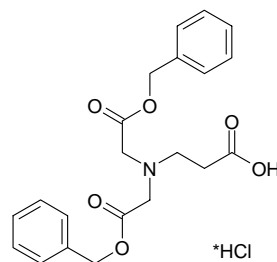
<sup>1</sup>H-NMR (400 MHz; CDCl<sub>3</sub>):  $\delta$  = 1.43 (s, 9 H, HSQC: H(1)), 1.73 (quin, <sup>3</sup> $J$  = 7.3 Hz, 2 H, HSQC: H(5)), 2.25 (t, <sup>3</sup> $J$  = 7.4 Hz, 2 H, HMBC: H(4)), 2.75 (t, <sup>3</sup> $J$  = 7.4 Hz, 2 H, HMBC: H(6)), 3.60 (s, 4 H, HSQC: H(7)), 5.13 (s, 4 H, HSQC: H(9)), 7.30-7.38 (m, 10 H, H-Ar). – <sup>13</sup>C-NMR (100 MHz; CDCl<sub>3</sub>; HSQC, HMBC):  $\delta$  = 23.3 (–, C(5)), 28.1 (+, 3 C, C(1)), 32.9 (–, C(4)), 53.5 (–, C(6)), 55.0 (–, 2 C, C(7)), 66.3 (–, 2 C, C(9)), 80.1 (C<sub>quat</sub>, C(2)), 128.3 (+, 4 C, C(11)), 128.4 (+, 2 C, C(13)), 128.6 (+, 4 C, C(12)), 135.7 (C<sub>quat</sub>, C(10)), 171.1 (C<sub>quat</sub>, 2 C, C(8)), 172.8 (C<sub>quat</sub>, C(3)). – IR [cm<sup>–1</sup>]:  $\tilde{\nu}$  = 3442, 3034, 2974, 1729, 1154. – MS (CI-MS, NH<sub>3</sub>):  $m/z$  (%) = 456 (100) [MH<sup>+</sup>]. – Elemental analysis calcd. (%) for C<sub>26</sub>H<sub>33</sub>NO<sub>6</sub> (455.56): C 68.55, H 7.30, N 3.07; found C 68.20, H 7.24, N 2.96.



(*Bis-benzyloxycarbonylmethyl-amino*)-acetic acid hydrogenchloride (**87**):

**84** (0.39 g, 0.9 mmol) was dissolved in Et<sub>2</sub>O (10 mL) and HCl/Et<sub>2</sub>O was added to the solution under ice cooling. After 30 min the Et<sub>2</sub>O was evaporated and the product dried under high vacuum. **87** (0.6 mmol, 0.24 g, 66 %) is a colourless very hygroscopic solid.

<sup>1</sup>H-NMR (300 MHz; [D<sub>6</sub>]-DMSO): δ = 3.65 (s, 2 H, CH<sub>2</sub>-COOH), 3.79 (s, 4 H, CH<sub>2</sub>-COOBzl), 5.11 (s, 2 H, CH<sub>2</sub>-Ph), 7.29-7.41 (s, 10 H, H-Ar), 10.00-11.00 (bs, 2 H, COOH + NH<sup>+</sup>). – <sup>13</sup>C-NMR (75 MHz; [D<sub>6</sub>]-DMSO): δ = 54.3 (–, 2 C, CH<sub>2</sub>), 62.7 (–, CH<sub>2</sub>), 65.5 (–, 2 C, CH<sub>2</sub>), 127.3 (+, 6 C, C-Ar), 128.2 (+, 4 C, C-Ar), 135.8 (C<sub>quat</sub>, 2 C, C-Ar), 169.7 (C<sub>quat</sub>, 2 C, COOBzl), 171.2 (C<sub>quat</sub>, COOH). – IR (KBr) [cm<sup>–1</sup>]:  $\tilde{\nu}$  = 3385, 2962, 1746, 1201. – MS (ESI, MeCN/MeOH + 10 mmol/L NH<sub>4</sub>Ac): *m/z* (%) = 372 (100) [MH<sup>+</sup>]. – Elemental analysis calcd. (%) for C<sub>20</sub>H<sub>22</sub>NO<sub>6</sub>Cl (407.85) x 2 H<sub>2</sub>O: C 54.21, H 5.90, N 3.16; found C 54.69, H 5.22, N 3.38.



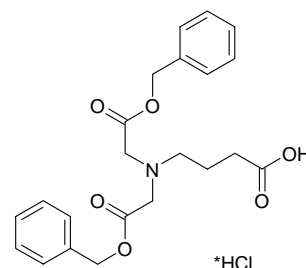
3-(*Bis-benzyloxycarbonylmethyl-amino*)-propionic acid hydrogenchloride (**88**):

**85** (0.50 g, 1.1 mmol) was dissolved in Et<sub>2</sub>O (10 mL) and HCl/Et<sub>2</sub>O was added to the solution under ice cooling. After 30 min the Et<sub>2</sub>O was evaporated and the product dried under high vacuum. **88** (1.0 mmol, 0.42 g, 88 %) is a colourless very hygroscopic solid.

<sup>1</sup>H-NMR (300 MHz; [D<sub>6</sub>]-DMSO): δ = 2.70 (t, <sup>3</sup>*J* = 7.3 Hz, 2 H, N-CH<sub>2</sub>), 3.34 (t, <sup>3</sup>*J* = 6.7 Hz, 2 H, CH<sub>2</sub>-COOH), 4.15 (s, 4 H, CH<sub>2</sub>-COOBzl), 5.19 (s, 2 H, CH<sub>2</sub>-Ph), 7.31-7.42 (s, 10 H, H-Ar), 9.00-11.50 (bs, 2 H, COOH + NH<sup>+</sup>). – <sup>13</sup>C-NMR (75 MHz; [D<sub>6</sub>]-DMSO): δ = 30.1 (–, CH<sub>2</sub>), 50.3 (–, CH<sub>2</sub>), 54.0 (–, 2 C, CH<sub>2</sub>), 66.5 (–, 2 C, CH<sub>2</sub>), 128.2 (+, 4 C, C-Ar), 128.4 (+, 2 C, C-Ar), 128.8 (+, 4 C, C-Ar), 135.2 (C<sub>quat</sub>, C-Ar), 167.5 (C<sub>quat</sub>, COOH),



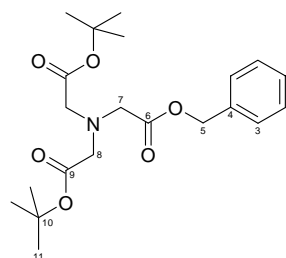
171.9 ( $C_{\text{quat}}$ , 2 C, COOBzl). – IR (KBr) [ $\text{cm}^{-1}$ ]:  $\tilde{\nu}$  = 3380, 2957, 1740, 1196, 742, 698. – MS (ESI, DCM/MeOH + 10 mmol/L  $\text{NH}_4\text{Ac}$ ):  $m/z$  (%) = 386 (100) [ $\text{MH}^+$ ]. – Elemental analysis calcd. (%) for  $\text{C}_{21}\text{H}_{23}\text{NO}_6$  (385.42) +  $\text{H}_2\text{O}$ : C 62.52, H 6.25, N 3.47; found C 62.57, H 6.00, N 3.45.



*4-(Bis-benzyloxycarbonylmethyl-amino)-butyric acid hydrogenchloride (89):*

**86** (0.29 g, 0.7 mmol) was dissolved in  $\text{Et}_2\text{O}$  (10 mL) and  $\text{HCl}/\text{Et}_2\text{O}$  was added to the solution under ice cooling. After 30 min the  $\text{Et}_2\text{O}$  was evaporated and the product dried under high vacuum. **89** (0.6 mmol, 0.24 g, 86 %) is a colourless very hygroscopic solid.

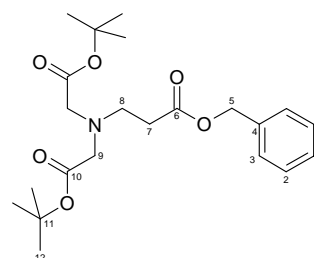
mp 41-42 °C. –  $^1\text{H}$ -NMR (300 MHz;  $[\text{D}_6]$ -DMSO):  $\delta$  = 1.78 (quin,  $^3J$  = 7.1 Hz, 2 H,  $\text{CH}_2$ ), 2.27 (t,  $^3J$  = 7.3 Hz, 2 H, N- $\text{CH}_2$ ), 3.01-3.13 (m, 2 H,  $\text{CH}_2$ -COOH), 4.01-4.19 (m, 4 H,  $\text{CH}_2$ -COOBzl), 5.19 (s, 2 H,  $\text{CH}_2$ -Ph), 7.31-7.42 (s, 10 H, H-Ar). –  $^{13}\text{C}$ -NMR (75 MHz;  $[\text{D}_6]$ -DMSO):  $\delta$  = 20.0 (–,  $\text{CH}_2$ ), 30.5 (–,  $\text{CH}_2$ ), 53.9 (–,  $\text{CH}_2$ ), 54.4 (–, 2 C,  $\text{CH}_2$ ), 66.5 (–, 2 C,  $\text{CH}_2$ ), 128.1 (+, 4 C, C-Ar), 128.4 (+, 2 C, C-Ar), 128.8 (+, 4 C, C-Ar), 135.2 ( $C_{\text{quat}}$ , 2 C, C-Ar), 167.5 ( $C_{\text{quat}}$ , COOH), 171.9 ( $C_{\text{quat}}$ , 2 C, COOBzl). – IR (KBr) [ $\text{cm}^{-1}$ ]:  $\tilde{\nu}$  = 3419, 2957, 1748, 1211, 748, 698. – MS (ESI, MeCN/MeOH):  $m/z$  (%) = 400 (100) [ $\text{MH}^+$ ], 422 (32) [ $\text{MNa}^+$ ]. – Elemental analysis calcd. (%) for  $\text{C}_{22}\text{H}_{25}\text{NO}_6$  (399.44) +  $\text{H}_2\text{O}$ : C 63.30, H 6.51, N 3.35; found C 63.32, H 6.09, N 3.47.



*(Bis-tert-butoxycarbonylmethyl-amino)-acetic acid benzylester (90):*

H-Gly-OBzl-HOTos (1.00 g, 3.0 mmol) was dissolved in MeCN (25 mL). *tert*-Butylbromoacetate (0.96 mL, 6.5 mmol), K<sub>2</sub>CO<sub>3</sub> (1.80 g, 13.0 mmol), and a spatula tip of KI were added. The suspension was stirred at 60 °C for 2 days and monitored by TLC (EtOAc). After filtration the filtrate was mixed with water (30 mL) and extracted with EtOAc. The organic layers were dried over Na<sub>2</sub>SO<sub>4</sub> and concentrated under reduced pressure. The crude product was purified using column chromatography on silica gel (EtOAc, *R<sub>f</sub>* = 0.84) yielding **90** (2.5 mmol, 1.00 g, 86 %) as a colourless oil.

<sup>1</sup>H-NMR (300 MHz; CDCl<sub>3</sub>): δ = 1.44 (s, 18 H, CH<sub>3</sub>), 3.55 (s, 4 H, CH<sub>2</sub>-COO<sup>t</sup>Bu), 3.70 (s, 2 H, CH<sub>2</sub>-COOBzl), 5.16 (s, 2 H, CH<sub>2</sub>-Ph), 7.31-7.37 (m, 5 H, H-Ar). – <sup>13</sup>C-NMR (150 MHz; CDCl<sub>3</sub>; HSQC, HMBC): δ = 28.1 (+, 6 C, C(11)), 55.0 (–, C(7)), 55.9 (–, 2 C, C(8)), 66.3 (–, 2 C, C(5)), 81.2 (C<sub>quat</sub>, 2 C, C(10)), 128.2 (+, C(1)), 128.2 (+, 2 C, C(2)), 128.5 (+, 2 C, C(3)), 135.8 (C<sub>quat</sub>, C(4)), 170.1 (C<sub>quat</sub>, 2 C, C(9)), 170.9 (C<sub>quat</sub>, C(6)). – IR (KBr) [cm<sup>–1</sup>]:  $\tilde{\nu}$  = 3445, 2979, 2934, 1733, 1159. – MS (CI-MS, NH<sub>3</sub>): *m/z* (%) = 394 (100) [MH<sup>+</sup>], 338 (65) [MH<sup>+</sup> – C<sub>4</sub>H<sub>8</sub>]. – Elemental analysis calcd. (%) for C<sub>21</sub>H<sub>31</sub>NO<sub>6</sub> (393.48): C 64.10, H 7.94, N 3.56; found C 63.17, H 7.43, N 3.60.



*3-(Bis-tert-butoxycarbonylmethyl-amino)-propionic acid benzyl ester (91):*

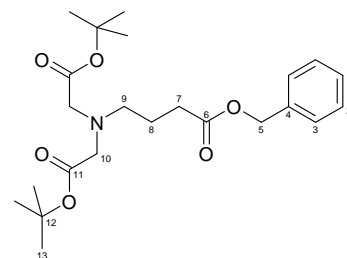
Literature known compound BRNr: 7314298<sup>vii</sup> but improved synthesis

H-β-Ala-OBzl-HOTos (2.00 g, 5.7 mmol) was dissolved in MeCN (40 mL). *tert*-Butylbromoacetate (1.85 mL, 12.5 mmol), K<sub>2</sub>CO<sub>3</sub> (3.46 g, 25.0 mmol), and a spatula tip of

<sup>vii</sup> Sunagawa, M.; Matsumura, H.; Sumita, Y.; Nouda, H. *J. Antibiot.* **1995**, 48, 408.

KI were added. The suspension was stirred at 60 °C for 2 days and monitored by TLC (EtOAc). After filtration the filtrate was mixed with water (30 mL) and extracted with EtOAc. The organic layers were dried over Na<sub>2</sub>SO<sub>4</sub> and concentrated under reduced pressure. The crude product was purified using column chromatography on silica gel (EtOAc, *R<sub>f</sub>* = 0.84) yielding **91** (3.5 mmol, 1.42 g, 86 %) as a colourless oil.

<sup>1</sup>H-NMR (400 MHz; CDCl<sub>3</sub>): δ = 1.44 (s, 18 H, CH<sub>3</sub>), 2.58 (t, <sup>3</sup>*J* = 7.2 Hz, 2 H, N-CH<sub>2</sub>), 3.07 (t, <sup>3</sup>*J* = 7.4 Hz, 2 H, CH<sub>2</sub>-COOBzl), 3.44 (s, 4 H, CH<sub>2</sub>-COO<sup>t</sup>Bu), 5.12 (s, 2 H, CH<sub>2</sub>-Ph), 7.28-7.39 (m, 5 H, H-Ar). – <sup>13</sup>C-NMR (100 MHz; CDCl<sub>3</sub>; HSQC, HMBC): δ = 28.2 (+, 6 C, C(12)), 33.9 (–, C(8)), 50.0 (–, C(7)), 56.0 (–, 2 C, C(9)), 66.2 (–, C(5)), 81.0 (C<sub>quat</sub>, 2 C, C(11)), 128.2 (+, C(1)), 128.2 (+, 2 C, C(2)), 128.5 (+, 2 C, C(3)), 136.0 (C<sub>quat</sub>, C(4)), 170.6 (C<sub>quat</sub>, 2 C, C(10)), 172.1 (C<sub>quat</sub>, C(6)). – IR (KBr) [cm<sup>–1</sup>]:  $\tilde{\nu}$  = 3446, 2977, 2940, 1738, 1157. – MS (CI-MS, NH<sub>3</sub>): *m/z* (%) = 408 (100) [MH<sup>+</sup>], 352 (8) [MH<sup>+</sup> – C<sub>4</sub>H<sub>8</sub>]. – C<sub>22</sub>H<sub>33</sub>NO<sub>6</sub> (407.51).

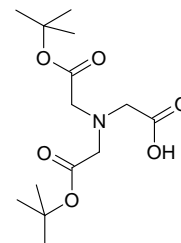


*4-(Bis-tert-butoxycarbonylmethyl-amino)-butyric acid benzyl ester (92):*

H-γ-Abu-OBzl-HOTos (2.00 g, 5.5 mmol) was dissolved in MeCN (40 mL). *tert*-Butylbromoacetate (1.78 mL, 12.0 mmol), K<sub>2</sub>CO<sub>3</sub> (3.33 g, 24.1 mmol), and a spatula tip of KI were added. The suspension was stirred at 60 °C for 2 days and monitored by TLC (EtOAc). After filtration the filtrate was mixed with water (30 mL) and extracted with EtOAc. The organic layers were dried over Na<sub>2</sub>SO<sub>4</sub> and concentrated under reduced pressure. The crude product was purified using column chromatography on silica gel (EtOAc, *R<sub>f</sub>* = 0.80) yielding **92** (3.5 mmol, 1.42 g, 63 %) as a colourless oil.

<sup>1</sup>H-NMR (400 MHz; CDCl<sub>3</sub>): δ = 1.44 (s, 18 H, HSQC: H(13)), 1.81 (quin, <sup>3</sup>*J* = 7.2 Hz, 2 H, HSQC: H(8)), 2.45 (t, <sup>3</sup>*J* = 7.4 Hz, 2 H, HMBC: H(7)), 2.74 (t, <sup>3</sup>*J* = 7.1 Hz, 2 H, HMBC: H(9)), 3.41 (s, 4 H, HSQC: H(10)), 5.11 (s, 2 H, HSQC: H(5)), 7.28-7.38 (m, 5 H, H-Ar). – <sup>13</sup>C-NMR (100 MHz; CDCl<sub>3</sub>; HSQC, HMBC): δ = 23.2 (–, C(8)), 28.2 (+, 6 C, C(13)), 31.7 (–, C(7)), 53.3 (–, C(9)), 55.8 (–, 2 C, C(10)), 66.1 (–, C(5)), 81.0 (C<sub>quat</sub>, 2 C, C(12)), 128.1 (+, C(1)), 128.2 (+, 2 C, C(2)), 128.5 (+, 2 C, C(3)), 136.2 (C<sub>quat</sub>, C(4)),

170.6 (C<sub>quat</sub>, 2 C, C(11)), 173.5 (C<sub>quat</sub>, C(6)). – IR [cm<sup>-1</sup>]:  $\tilde{\nu}$  = 3447, 2976, 2934, 1738, 1156. – MS (CI-MS, NH<sub>3</sub>):  $m/z$  (%) = 422 (100) [MH<sup>+</sup>]. – Elemental analysis calcd. (%) for C<sub>22</sub>H<sub>33</sub>NO<sub>6</sub> (421.54): C 64.84, H 8.16, N 3.44; found C 64.97, H 8.53, N 3.32.

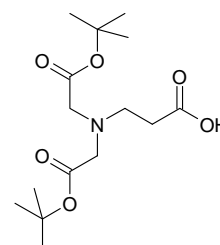


*(Bis-tert-butoxycarbonylmethyl-amino)-acetic acid (93):*

Literature known compound BRNr: 7547231 but improved synthesis

**90** (0.20 g, 0.50 mmol) was dissolved in EtOH (25 mL), to which two drops acetic acid and a spatula tip 10 % Pd/C were added. The reaction mixture was stirred 18 h in an autoclave under 10 bar H<sub>2</sub> pressure. The suspension was filtered using celite and the filtrate concentrated under reduced pressure. **93** (0.47 mmol, 0.14 g, 93 %) was isolated as a colourless solid without further purification.

mp 88-89 °C. – <sup>1</sup>H-NMR (300 MHz; [D<sub>6</sub>]-Acetone):  $\delta$  = 1.36-1.44 (m, 18 H, CH<sub>3</sub>), 1.47-1.50 (m, 2 H, CH<sub>2</sub>-COOH), 3.47-3.54 (m, 4 H, CH<sub>2</sub>-COO<sup>t</sup>Bu), 10.35 (bs, 1 H, COOH). – <sup>13</sup>C-NMR (75 MHz; [D<sub>6</sub>]-Acetone):  $\delta$  = 28.3 (+, 6 C, CH<sub>3</sub>), 57.4 (–, 2 C, CH<sub>2</sub>-COO<sup>t</sup>Bu), 57.6 (–, CH<sub>2</sub>-COOH), 81.9 (C<sub>quat</sub>, 2 C, C<sub>Boc</sub>), 171.7 (C<sub>quat</sub>, 2 C, COO<sup>t</sup>Bu), 171.7 (C<sub>quat</sub>, COOH). – IR (KBr) [cm<sup>-1</sup>]:  $\tilde{\nu}$  = 2984, 2936, 1747, 1370, 1223, 1155, 995. – MS (-ESI, DCM/MeOH + 10 mmol/L NH<sub>4</sub>Ac):  $m/z$  (%) = 362 (100) [M+Ac<sup>-</sup>], 302 (85) [M – H<sup>+</sup>]. – C<sub>14</sub>H<sub>25</sub>NO<sub>6</sub> (303.36).

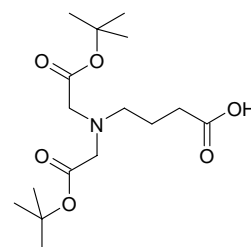


*3-(Bis-tert-butoxycarbonylmethyl-amino)-propionic acid (94):*

**91** (0.40 g, 1.0 mmol) was dissolved in EtOH (25 mL) and mixed with a spatula tip 10 % Pd/C. The reaction mixture was stirred for 12 h in an autoclave under 10 bar H<sub>2</sub> pressure.

The suspension was filtered using celite and the filtrate concentrated under reduced pressure. **94** (1.0 mmol, 0.32 g, 100 %) was isolated as a colourless crystalline solid.

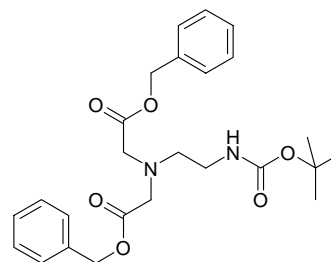
mp 60-61 °C. –  $^1\text{H-NMR}$  (300 MHz;  $\text{CDCl}_3$ ):  $\delta$  = 1.48 (s, 18 H,  $\text{CH}_3$ ), 2.51 (t,  $^3J$  = 6.2 Hz, 2 H, N- $\text{CH}_2$ ), 3.09 (t,  $^3J$  = 6.3 Hz, 2 H,  $\text{CH}_2\text{-COOH}$ ), 3.50 (s, 4 H,  $\text{CH}_2\text{-COO}^t\text{Bu}$ ). –  $^{13}\text{C-NMR}$  (75 MHz;  $\text{CDCl}_3$ ):  $\delta$  = 28.1 (+, 6 C,  $\text{CH}_3$ ), 31.5 (–,  $\text{CH}_2$ ), 49.8 (–,  $\text{CH}_2$ ), 55.3 (–, 2 C,  $\text{CH}_2$ ), 82.5 ( $\text{C}_{\text{quat}}$ , 2 C, C-Boc), 169.3 ( $\text{C}_{\text{quat}}$ , 2 C,  $\text{COO}^t\text{Bu}$ ), 173.2 ( $\text{C}_{\text{quat}}$ , COOH). – IR (KBr) [ $\text{cm}^{-1}$ ]:  $\tilde{\nu}$  = 2980, 2932, 2534, 1735, 1706, 1370, 1158. – MS (CI-MS,  $\text{NH}_3$ ):  $m/z$  (%) = 318 (100) [ $\text{MH}^+$ ]. –  $\text{C}_{16}\text{H}_{29}\text{NO}_6$  (317.39).



*4-(Bis-tert-butoxycarbonylmethyl-amino)-butyric acid (95):*

**92** (0.40 g, 1.0 mmol) was dissolved in MeOH (25 mL) and mixed with a spatula tip 10% Pd/C. The reaction mixture was stirred for 12 h in an autoclave under 10 bar  $\text{H}_2$  pressure. The suspension was filtered using celite and the filtrate concentrated under reduced pressure. **95** (0.9 mmol, 0.29 g, 93 %) was isolated as a colourless oil without further purification.

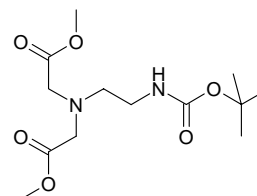
$^1\text{H-NMR}$  (300 MHz;  $\text{CDCl}_3$ ):  $\delta$  = 1.46 (s, 18 H,  $\text{CH}_3$ ), 1.82 (quin, 2 H,  $^3J$  = 6.7 Hz,  $\text{CH}_2$ ), 2.51 (t,  $^3J$  = 6.7 Hz, 2 H, N- $\text{CH}_2$ ), 2.88 (t,  $^3J$  = 6.7 Hz, 2 H,  $\text{CH}_2\text{-COOH}$ ), 3.52 (s, 4 H,  $\text{CH}_2\text{-COO}^t\text{Bu}$ ). –  $^{13}\text{C-NMR}$  (75 MHz;  $\text{CDCl}_3$ ):  $\delta$  = 22.0 (–,  $\text{CH}_2$ ), 28.1 (+, 6 C,  $\text{CH}_3$ ), 33.0 (–,  $\text{CH}_2$ ), 53.8 (–,  $\text{CH}_2$ ), 55.1 (–, 2 C,  $\text{CH}_2$ ), 82.1 ( $\text{C}_{\text{quat}}$ , 2 C, C-Boc), 169.1 ( $\text{C}_{\text{quat}}$ , 2 C,  $\text{COO}^t\text{Bu}$ ), 177.0 ( $\text{C}_{\text{quat}}$ , COOH). – IR [ $\text{cm}^{-1}$ ]:  $\tilde{\nu}$  = 2978, 2621, 1732, 1251, 1158, 843. – MS (CI-MS,  $\text{NH}_3$ ):  $m/z$  (%) = 332 (100) [ $\text{MH}^+$ ]. – Elemental analysis calcd. (%) for  $\text{C}_{16}\text{H}_{29}\text{NO}_6$  (331.41) + MeOH: C 56.34, H 9.18, N 3.86; found C 55.92, H 9.18, N 3.86.



*[Benzyloxycarbonylmethyl-(2-tert-butoxycarbonylamino-ethyl)-amino]-acetic acid benzyl ester (97):*

Mono-Boc-Ethylendiamine (0.50 g, 3.1 mmol) was dissolved in DMF (15 mL). Benzylbromoacetate (1.08 mL, 6.9 mmol),  $K_2CO_3$  (1.90 g, 13.7 mmol), and a spatula tip of KI were added. The suspension was stirred at r.t. for 6 h and then at 60 °C for 2 days and monitored by TLC (EtOAc). After filtration the filtrate was mixed with water (30 mL) and extracted with EtOAc. The organic layers were dried over  $Na_2SO_4$  and concentrated under reduced pressure. The crude product was purified using column chromatography on silica gel (EtOAc,  $R_f$  = 0.80) yielding **97** (2.7 mmol, 1.24 g, 87 %) as a colourless oil.

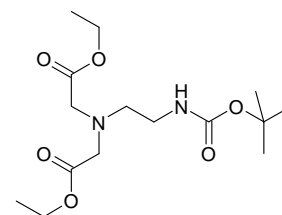
$^1H$ -NMR (300 MHz;  $CDCl_3$ ):  $\delta$  = 1.43 (s, 9 H,  $CH_3$ ), 2.73 (t,  $^3J$  = 5.4 Hz, 2 H,  $CH_2$ ), 3.17-3.22 (m, 2 H,  $CH_2$ ), 3.44 (s, 4 H,  $CH_2$ ), 5.03 (bs, 1 H, NH), 5.16 (s, 4 H,  $CH_2$ -Ph), 7.27-7.40 (m, 10 H, H-Ar). –  $^{13}C$ -NMR (75 MHz;  $CDCl_3$ ):  $\delta$  = 28.5 (+, 3 C,  $CH_3$ ), 38.4 (–,  $CH_2$ ), 53.6 (–, 2 C,  $CH_2$ ), 66.5 (–, 2 C,  $CH_2$ -Ph), 79.0 ( $C_{quat}$ , C-Boc), 128.3 (+, 4 C, C-Ar), 128.3 (+, 2 C, C-Ar), 128.6 (+, 4 C, C-Ar), 135.5 ( $C_{quat}$ , 2 C, C-Ar), 156.2 ( $C_{quat}$ , COON), 171.3 ( $C_{quat}$ , 2 C, COOBzl). – IR [ $cm^{-1}$ ]:  $\tilde{\nu}$  = 3396, 3034, 2974, 1742, 1709, 1169, 740, 698. – MS (CI,  $NH_3$ ):  $m/z$  (%) = 457 (100) [ $MH^+$ ]. – Elemental analysis calcd. (%) for  $C_{25}H_{32}N_2O_6$  (456.54): C 65.77, H 7.07, N 6.14; found C 65.46, H 7.02, N 6.23.



*[(2-tert-Butoxycarbonylamino-ethyl)-methoxycarbonylmethyl-amino]-acetic acid methyl ester (98):*

Mono-Boc-Ethylendiamine (0.50 g, 3.1 mmol) was dissolved in MeCN (40 mL). Methylbromoacetate (0.64 mL, 6.9 mmol),  $K_2CO_3$  (1.90 g, 13.7 mmol), and a spatula tip of KI were added. The suspension was stirred at r.t. for 6 h and then at 60 °C for 2 days and

monitored by TLC (EtOAc). After filtration the filtrate was mixed with water (30 mL) and extracted with EtOAc. The organic layers were dried over Na<sub>2</sub>SO<sub>4</sub> and concentrated under reduced pressure. The crude product was purified using column chromatography on silica gel (PE:EtOAc 1:1,  $R_f$  = 0.40) yielding **98** (1.8 mmol, 1.06 g, 63 %) as a colourless solid. mp 73-74 °C. – <sup>1</sup>H-NMR (300 MHz; CDCl<sub>3</sub>): δ = 1.44 (s, 9 H, CH<sub>3</sub>), 2.84 (t, <sup>3</sup> $J$  = 5.6 Hz, 2 H, N-CH<sub>2</sub>), 3.13-3.18 (m, 2 H, NH-CH<sub>2</sub>), 3.54 (s, 4 H, N-CH<sub>2</sub>), 3.71 (s, 6 H, O-CH<sub>3</sub>), 5.50 (bs, 1 H, NH). – <sup>13</sup>C-NMR (75 MHz; CDCl<sub>3</sub>): δ = 28.4 (+, 3 C, CH<sub>3</sub>), 51.6 (+, 2 C, CH<sub>3</sub>), 53.5 (–, CH<sub>2</sub>), 54.9 (–, 2 C, CH<sub>2</sub>), 60.7 (–, CH<sub>2</sub>), 78.9 (C<sub>quat</sub>, C-Boc), 156.1 (C<sub>quat</sub>, 2 C, COOMe), 171.8 (C<sub>quat</sub>, COON). – IR (KBr) [cm<sup>–1</sup>]:  $\tilde{\nu}$  = 3358, 2977, 2872, 1739, 1699, 1524, 861, 581. – MS (ESI, CH<sub>2</sub>Cl<sub>2</sub>/MeOH + 10 mmol/L NH<sub>4</sub>Ac):  $m/z$  (%) = 647 (2) [2 M + K<sup>+</sup>], 631 (8) [2 M + Na<sup>+</sup>], 609 (11) [2 M + H<sup>+</sup>], 343 (9) [MK<sup>+</sup>], 327 (20) [M + Na<sup>+</sup>], 305 (100) [MH<sup>+</sup>], 249 (50) [MH<sup>+</sup> – C<sub>4</sub>H<sub>8</sub>], 205 (21) [MH<sup>+</sup> – Boc]. – Elemental analysis calcd. (%) for C<sub>13</sub>H<sub>24</sub>N<sub>2</sub>O<sub>6</sub> (304.35): C 51.31, H 7.95, N 9.20; found C 51.04, H 7.30, N 8.93.



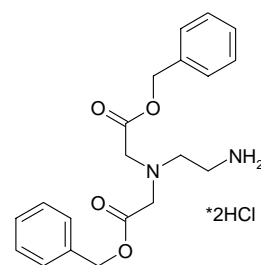
*[(2-tert-Butoxycarbonylamino-ethyl)-ethoxycarbonylmethyl-amino]-acetic acid ethyl ester* (**99**):

Literature known compound BRNr: 7651262<sup>viii</sup> but improved synthesis

Mono-Boc-Ethylendiamine (0.50 g, 3.1 mmol) was dissolved in MeCN (40 mL). Ethyl-bromoacetate (0.76 mL, 6.9 mmol), K<sub>2</sub>CO<sub>3</sub> (1.90 g, 13.7 mmol), and a spatula tip of KI were added. The suspension was stirred at r.t. for 6 h and then at 60 °C for 2 days and monitored via TLC (EtOAc). After filtration the filtrate was mixed with water (30 mL) and extracted with EtOAc. The organic layers were dried over Na<sub>2</sub>SO<sub>4</sub> and concentrated under reduced pressure. The crude product was purified using column chromatography on silica gel (EtOAc,  $R_f$  = 0.72) yielding **99** (2.2 mmol, 0.74 g, 72 %) as a colourless solid.

<sup>1</sup>H-NMR (300 MHz; CDCl<sub>3</sub>): δ = 1.27 (t, <sup>3</sup> $J$  = 7.1 Hz, 6 H, CH<sub>3</sub>), 1.44 (s, 9 H, CH<sub>3</sub>-Boc), 2.84 (t, <sup>3</sup> $J$  = 5.3 Hz, 2 H, CH<sub>2</sub>), 3.13-3.18 (m, 2 H, CH<sub>2</sub>), 3.52 (s, 4 H, CH<sub>2</sub>), 4.17 (q, <sup>3</sup> $J$  = 7.1 Hz, 4 H, O-CH<sub>2</sub>). – C<sub>15</sub>H<sub>28</sub>N<sub>2</sub>O<sub>6</sub> (332.4).

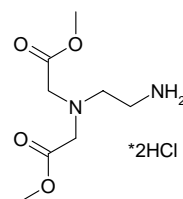
<sup>viii</sup> Hamachi, I.; Matsugi, T.; Shinkai, S. *Tet. Lett.* **1996**, 37, 9233.



*[(2-Amino-ethyl)-benzyloxycarbonylmethyl-amino]-acetic acid benzyl ester di-hydrogen-chloride (100):*

**97** (1.24 g, 2.7 mmol) was dissolved in Et<sub>2</sub>O (10 mL) and HCl/Et<sub>2</sub>O was added to the solution under ice cooling. After 30 min the Et<sub>2</sub>O is evaporated and the product dried under high vacuum. **100** (2.7 mmol, 1.16 g, 99 %) is a colourless very hygroscopic solid.

<sup>1</sup>H-NMR (300 MHz; [D<sub>6</sub>]-DMSO): δ = 2.84-2.95 (m, 4 H, CH<sub>2</sub>), 3.69 (s, 4 H, N-CH<sub>2</sub>), 5.13 (s, 4 H, CH<sub>2</sub>-Ph), 7.31-7.42 (m, 10 H, H-Ar), 7.80 (bs, 3 H, NH<sub>3</sub><sup>+</sup>). – <sup>13</sup>C-NMR (75 MHz; [D<sub>6</sub>]-DMSO): δ = 36.7 (–, CH<sub>2</sub>), 51.2 (–, CH<sub>2</sub>), 54.7(–, 2 C, CH<sub>2</sub>), 65.6 (–, 2 C, CH<sub>2</sub>), 127.9 (+, 4 C, C-Ar), 128.0 (+, 2 C, C-Ar), 128.3 (+, 4 C, C-Ar), 135.7 (C<sub>quat</sub>, 2 C, C-Ar), 170.9 (C<sub>quat</sub>, 2 C, COOBzl). – MS (ESI, H<sub>2</sub>O/MeOH + 10 mmol/L NH<sub>4</sub>Ac): *m/z* (%) = 577 (100) [MH<sup>+</sup>], 521 (65) [MH<sup>+</sup> – C<sub>4</sub>H<sub>8</sub>]. – C<sub>20</sub>H<sub>26</sub>N<sub>2</sub>O<sub>4</sub>Cl<sub>2</sub> (429.34).

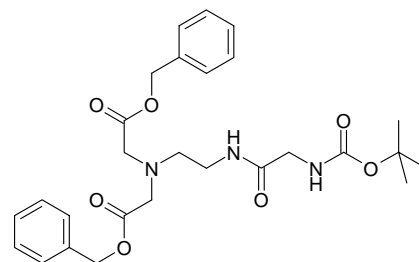


*[(2-Amino-ethyl)-methoxycarbonylmethyl-amino]-acetic acid methyl ester di-hydrogen-chloride (101):*

**98** (0.68 g, 2.2 mmol) was dissolved in Et<sub>2</sub>O (10 mL) and HCl/Et<sub>2</sub>O was added to the solution under ice cooling. After 30 min the Et<sub>2</sub>O is evaporated and the product dried under high vacuum. **101** (2.0 mmol, 542 mg, 88 %) is a colourless very hygroscopic solid.

mp 83-85 °C. – <sup>1</sup>H-NMR (300 MHz; [D<sub>6</sub>]-DMSO): δ = 2.83-2.93 (m, 4 H, CH<sub>2</sub>), 3.61 (s, 10 H, O-CH<sub>3</sub> + CH<sub>2</sub>), 7.89 (bs, 3 H, NH<sub>3</sub><sup>+</sup>). – <sup>13</sup>C-NMR (75 MHz; [D<sub>6</sub>]-DMSO): δ = 36.4 (–, CH<sub>2</sub>), 51.2 (–, CH<sub>2</sub>), 51.5 (+, 2 C, CH<sub>3</sub>), 54.4 (–, 2 C, CH<sub>2</sub>-N), 171.0 (C<sub>quat</sub>, 2 C, COOMe). – IR (KBr) [cm<sup>–1</sup>]:  $\tilde{\nu}$  = 3420, 3303, 2959, 2537 1745, 1709, 1252. – MS (CI, NH<sub>3</sub>): *m/z* (%) = 457 (100) [MH<sup>+</sup>]. – C<sub>25</sub>H<sub>32</sub>N<sub>2</sub>O<sub>6</sub> (456.54).

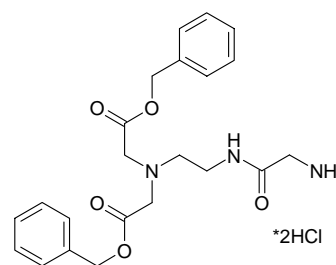




*{Benzyloxycarbonylmethyl-[2-(2-tert-butoxycarbonylamino-acetylamino)-ethyl]-amino}-acetic acid benzyl ester (**102**):*

Boc-Gly-OH (207 mg, 1.2 mmol), DIPEA (0.37 mL, 2.2 mmol), EDC (0.23 mL, 1.3 mmol), and HOBt (176 mg, 1.3 mmol) were dissolved in DCM (10 mL) under ice cooling. **100** (100 mg, 0.2 mmol) dissolved in a little DCM was added slowly via syringe. The reaction was allowed to warm to r.t.. The reaction progress was monitored by TLC (EtOAc). After completion the solution was mixed with water (25 mL) and extracted with DCM. The combined organic layers were washed with brine and dried over Na<sub>2</sub>SO<sub>4</sub>. The solvent was evaporated and the product purified using column chromatography on silica gel (EtOAc, *R<sub>f</sub>* = 0.48) yielding **102** (0.15 mmol, 76 mg, 64 %) as a colourless oil.

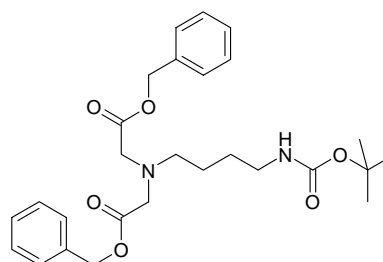
<sup>1</sup>H-NMR (300 MHz; CDCl<sub>3</sub>): δ = 1.40 (s, 9 H, CH<sub>3</sub>), 2.85 (t, <sup>3</sup>*J* = 5.5 Hz, 2 H, CH<sub>2</sub>), 3.20-3.25 (m, 2 H, CH<sub>2</sub>), 3.52 (s, 4 H, N-CH<sub>2</sub>), 3.81 (d, <sup>3</sup>*J* = 5.2 Hz, 2 H, CH<sub>2</sub>-Gly), 5.09 (s, 4 H, CH<sub>2</sub>-Ph), 5.19 (bs, 1 H, NH), 7.30-7.35 (m, 10 H, H-Ar). – <sup>13</sup>C-NMR (75 MHz; CDCl<sub>3</sub>): δ = 28.4 (+, 3 C CH<sub>3</sub>), 37.3 (–, CH<sub>2</sub>), 43.9 (–, CH<sub>2</sub>-Gly), 52.8 (–, CH<sub>2</sub>), 66.7 (–, 2 C, CH<sub>2</sub>), 79.7 (C<sub>quat</sub>, C-Boc), 128.3 (+, 4 C, C-Ar), 128.5 (+, 2 C, C-Ar), 128.7 (+, 4 C, C-Ar), 135.4 (C<sub>quat</sub>, 2 C, C-Ar), 155.8 (C<sub>quat</sub>, COON), 169.3 (C<sub>quat</sub>, CONR), 171.5 (C<sub>quat</sub>, 2 C, COOBzl). – IR (KBr) [cm<sup>–1</sup>]:  $\tilde{\nu}$  = 3253, 3032, 2969, 1732, 1580. – MS (ESI, CH<sub>2</sub>Cl<sub>2</sub>/MeOH + 10 mmol/L NH<sub>4</sub>Ac): *m/z* (%) = 536 (13) [MNa<sup>+</sup>], 514 (100) [MH<sup>+</sup>]. – Elemental analysis calcd. (%) for C<sub>27</sub>H<sub>35</sub>N<sub>3</sub>O<sub>7</sub> (513.59) + EtOH: C 62.24, H 7.38, N 7.51; found C 62.01, H 7.36, N 7.93.



*{[2-(2-Amino-acetyl-amino)-ethyl]-benzyloxycarbonylmethyl-amino}-acetic acid benzyl ester di-hydrogenchloride (**103**):*

**102** (76 mg, 0.15 mmol) was dissolved in Et<sub>2</sub>O (10 mL) and HCl/Et<sub>2</sub>O was added to the solution under ice cooling. After 150 min the Et<sub>2</sub>O is evaporated and the product dried under high vacuum. **103** (0.14 mmol, 66 mg, 90 %) is a yellowish very hygroscopic solid.

<sup>1</sup>H-NMR (300 MHz; [D<sub>6</sub>]-DMSO): δ = 2.96 (t, <sup>3</sup>J = 6.4 Hz, 2 H, CH<sub>2</sub>), 3.27-3.33 (m, 2 H, CH<sub>2</sub>), 3.47-3.53 (m, 2 H, CH<sub>2</sub>-Gly), 3.85 (s, 4 H, N-CH<sub>2</sub>), 5.14 (s, 4 H, CH<sub>2</sub>-Ph), 7.31-7.41 (m, 10 H, H-Ar), 8.21 (bs, 3 H, NH<sub>3</sub><sup>+</sup>), 8.51 (t, <sup>3</sup>J = 5.3 Hz 1 H, NH). – <sup>13</sup>C-NMR (75 MHz; [D<sub>6</sub>]-DMSO): δ = 35.7 (–, CH<sub>2</sub>), 39.8 (–, CH<sub>2</sub>), 53.3 (–, CH<sub>2</sub>), 54.1 (–, 2 C, CH<sub>2</sub>), 66.2 (–, 2 C, CH<sub>2</sub>), 128.0 (+, 4 C, C-Ar), 128.2 (+, 4 C, C-Ar), 128.4 (+, 2 C, C-Ar), 135.4 (C<sub>quat</sub>, 2 C, C-Ar), 166.1 (C<sub>quat</sub>, CONH), 168.5 (C<sub>quat</sub>, 2 C, COOBzl). – IR (KBr) [cm<sup>–1</sup>]:  $\tilde{\nu}$  = 3252, 3030, 2954, 1732, 1570. – MS (ESI, H<sub>2</sub>O/MeOH + 10 mmol/L NH<sub>4</sub>Ac): *m/z* (%) = 414 (100) [MH<sup>+</sup>]. – C<sub>22</sub>H<sub>29</sub>N<sub>3</sub>O<sub>5</sub>Cl (486.40).

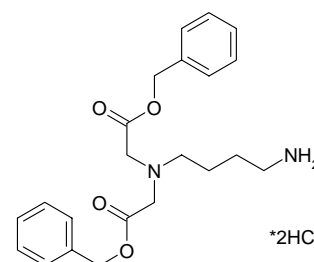


*[Benzyloxycarbonylmethyl-(4-tert-butoxycarbonylamino-butyl)-amino]-acetic acid-benzyl-ester (**105**):*

Mono-Boc-diaminobutane (0.20 g, 1.1 mmol) was dissolved in MeCN (20 mL). Benzyloxycarbonylmethylbromide (0.37 mL, 2.3 mmol), K<sub>2</sub>CO<sub>3</sub> (0.64 g, 4.7 mmol) and a spatula tip of KI were added. The suspension was stirred at r.t. for 6 h and then at 60 °C for 2 days and monitored by TLC (EtOAc). After filtration the filtrate was mixed with water (30 mL) and extracted with EtOAc. The organic layers were dried over Na<sub>2</sub>SO<sub>4</sub> and concentrated under

reduced pressure. The crude product was purified using column chromatography on silica gel (PE:EtOAc 1:1,  $R_f$  = 0.54) yielding **105** (0.8 mmol, 356 mg, 71 %) as a colourless oil.

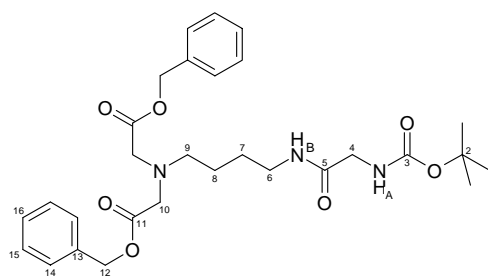
$^1\text{H-NMR}$  (600 MHz;  $\text{CDCl}_3$ ):  $\delta$  = 1.39-1.46 (m, 11 H,  $\text{CH}_2$  +  $\text{CH}_3\text{-Boc}$ ), 1.60-1.65 (m, 2 H,  $\text{CH}_2$ ), 2.65-2.70 (m, 2 H,  $\text{CH}_2$ ), 2.97-3.09 (m, 2 H,  $\text{CH}_2$ ), 3.55 (s, 4 H,  $\text{N-CH}_2$ ), 4.52 (bs, 1 H, NH), 5.09 (s, 4 H,  $\text{CH}_2\text{-Ph}$ ), 7.25-7.35 (m, 10 H, H-Ar). –  $^{13}\text{C-NMR}$  (75 MHz;  $\text{CDCl}_3$ ):  $\delta$  = 25.2 (–,  $\text{CH}_2$ ), 27.4 (–,  $\text{CH}_2$ ), 28.4 (+, 3 C,  $\text{CH}_3$ ), 40.3 (–,  $\text{CH}_2$ ), 53.9 (–,  $\text{CH}_2$ ), 55.0 (–, 2 C,  $\text{CH}_2$ ), 66.3 (–, 2 C,  $\text{CH}_2$ ), 79.0 ( $\text{C}_{\text{quat}}$ , C-Boc), 128.1 (+, 4 C, C-Ar), 128.4 (+, 2 C, C-Ar), 128.6 (+, 4 C, C-Ar), 135.6 ( $\text{C}_{\text{quat}}$ , 2 C, C-Ar), 156.0 ( $\text{C}_{\text{quat}}$ , COON), 171.1 ( $\text{C}_{\text{quat}}$ , 2 C, COOBzl). – IR (KBr) [ $\text{cm}^{-1}$ ]:  $\tilde{\nu}$  = 3250, 3032, 2962, 1730, 1581, 876. – MS (ESI,  $\text{H}_2\text{O}/\text{MeCN}$ ):  $m/z$  (%) = 507 (11) [ $\text{MNa}^+$ ], 485 (100) [ $\text{MH}^+$ ], 429 (36) [ $\text{MH}^+ - \text{C}_4\text{H}_8$ ]. – Elemental analysis calcd. (%) for  $\text{C}_{27}\text{H}_{36}\text{N}_2\text{O}_6$  (484.60): C 66.92, H 7.49, N 5.78; found C 66.53, H 7.04, N 5.49.



*[(4-Amino-butyl)-benzyloxycarbonylmethyl-amino]-acetic acid benzyl ester di-hydrogen-chloride (106):*

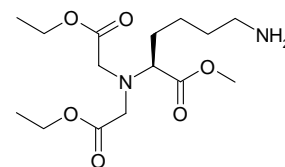
**105** (125 mg, 0.26 mmol) was dissolved in  $\text{Et}_2\text{O}$  (10 mL) and  $\text{HCl}/\text{Et}_2\text{O}$  was added to the solution under ice cooling. After 60 min the  $\text{Et}_2\text{O}$  is evaporated and the product dried under high vacuum. **106** (0.25, 114 mg, 96 %) is a colourless hygroscopic solid.

mp 63-65 °C. –  $^1\text{H-NMR}$  (300 MHz;  $[\text{D}_6]\text{-DMSO}$ ):  $\delta$  = 1.57-1.59 (m, 4 H,  $\text{CH}_2$ ), 2.74-2.75 (m, 2 H,  $\text{CH}_2$ ), 2.91-3.05 (m, 2 H,  $\text{CH}_2$ ), 3.99 (m, 4 H,  $\text{N-CH}_2$ ), 5.17 (s, 4 H,  $\text{CH}_2\text{-Ph}$ ), 7.31-7.42 (m, 10 H, H-Ar), 8.06 (bs, 3 H,  $\text{NH}_3^+$ ). –  $^{13}\text{C-NMR}$  (75 MHz;  $[\text{D}_6]\text{-DMSO}$ ):  $\delta$  = 23.9 (–,  $\text{CH}_2$ ), 37.9 (–,  $\text{CH}_2$ ), 53.9 (–, 2 C,  $\text{CH}_2$ ), 54.5 (–,  $\text{CH}_2$ ), 64.8 (–,  $\text{CH}_2$ ), 66.6 (–, 2 C,  $\text{CH}_2$ ), 128.1 (+, 4 C, C-Ar), 128.2 (+, 4 C, C-Ar), 128.4 (+, 2 C, C-Ar), 135.2 ( $\text{C}_{\text{quat}}$ , 2 C, C-Ar), 167.2 ( $\text{C}_{\text{quat}}$ , 2 C, COOBzl). – IR (KBr) [ $\text{cm}^{-1}$ ]:  $\tilde{\nu}$  = 3252, 3025, 2952, 1734, 1593. – MS (ESI,  $\text{MeOH} + 10 \text{ mmol/L } \text{NH}_4\text{Ac}$ ):  $m/z$  (%) = 385 (100) [ $\text{MH}^+$ ]. – Elemental analysis calcd. (%) for  $\text{C}_{22}\text{H}_{30}\text{N}_2\text{O}_4\text{Cl}_2$  (457.40) +  $\text{H}_2\text{O}$ : C 55.68, H 6.80, N 5.91; found C 55.65, H 6.98, N 5.80.



*{Benzyloxycarbonylmethyl-[4-(2-tert-butoxycarbonylamino-acetylamino)-butyl]-amino}-acetic acid benzyl ester (**107**):*

Boc-Gly-OH (0.10 g, 0.4 mmol), DIPEA (0.15 mL, 0.9 mmol), EDC (0.09 mL, 0.5 mmol), and HOBt (66 mg, 0.5 mmol) were dissolved in DCM (15 mL) under ice cooling. **106** (0.10 g, 0.2 mmol) dissolved in a little DCM was added slowly via syringe. The reaction was allowed to warm to r.t.. The reaction progress was monitored by TLC (EtOAc). After completion the solution was mixed with water (25 mL) and extracted with DCM. The combined organic layers were washed with brine and dried over Na<sub>2</sub>SO<sub>4</sub>. The solvent was evaporated and the crude product purified using column chromatography on silica gel (EtOAc, *R<sub>f</sub>* = 0.56) yielding **107** (0.15 mmol, 81 mg, 68 %) as a colourless hygroscopic oil. <sup>1</sup>H-NMR (600 MHz; CDCl<sub>3</sub>): δ = 1.45 (s, 9 H, CH<sub>3</sub>), 1.46-1.57 (m, 4 H, CH<sub>2</sub>), 2.72 (t, <sup>3</sup>*J* = 6.5 Hz, 2 H, CH<sub>2</sub>), 3.23-3.26 (m, 2 H, CH<sub>2</sub>), 3.59 (s, 4 H, N-CH<sub>2</sub>), 3.76 (d, <sup>3</sup>*J* = 5.3 Hz, 2 H, CH<sub>2</sub>-Gly), 5.14 (s 4 H, CH<sub>2</sub>-Ph), 5.31 (bs, 1 H, NH<sub>B</sub>), 6.54 (m, 1 H, NH<sub>A</sub>), 7.32-7.38 (m, 10 H, H-Ar). – <sup>13</sup>C-NMR (150 MHz; CDCl<sub>3</sub>; HSQC): δ = 25.2 (–, C(7)), 26.9 (–, C(8)), 28.3 (+, 3 C, C(1)), 39.1 (–, C(6)), 53.9 (–, C(9)), 55.1 (–, 2 C, C(10)), 66.4 (–, 2 C, C(12)), 80.0 (C<sub>quat</sub>, C(2)), 128.3 (+, 4 C, C-Ar), 128.4 (+, 2 C, C-Ar), 128.6 (+, 4 C, C-Ar), 135.6 (C<sub>quat</sub>, 2 C, C(13)), 169.3 (C<sub>quat</sub>, C(5)), 171.1 (C<sub>quat</sub>, 2 C, C(11)). – IR (KBr) [cm<sup>–1</sup>]:  $\tilde{\nu}$  = 3242, 3030, 2969, 1730, 1658, 1580. – MS (ESI, CH<sub>2</sub>Cl<sub>2</sub>/MeOH + 10 mmol/l NH<sub>4</sub>Ac): *m/z* (%) = 564 (21) [MNa<sup>+</sup>], 542 (100) [MH<sup>+</sup>]. – Elemental analysis calcd. (%) for C<sub>29</sub>H<sub>39</sub>N<sub>3</sub>O<sub>7</sub> (541.28) + H<sub>2</sub>O: C 62.24, H 7.38, N 7.51; found C 61.59, H 7.19, N 7.42.

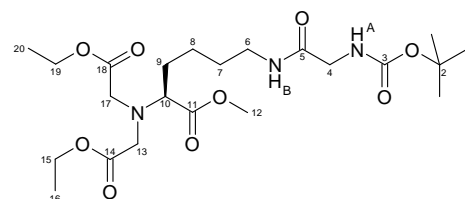


*Nα-Bis(2-ethoxy-2-oxoethyl)-L-lysine methylester (109):*

Literature known compound<sup>ix</sup> but improved procedure.

H-Lys(Z)-OMe·HCl (1.12 g, 3.4 mmol) was dissolved in MeCN (25 mL). After addition of K<sub>2</sub>CO<sub>3</sub> (9.40 g, 68.0 mmol) the suspension was stirred at r.t. over night. Ethylbromoacetate (3.79 mL, 34.0 mmol) was added and the reaction mixture was refluxed over night. The suspension was filtered and the obtained filtrate concentrated under reduced pressure. The crude product was purified using column chromatography on silica gel (PE → PE:EtOAc 2:1, *R<sub>f</sub>* = 0.2) yielding Z-protected **109** (3.2 mmol, 1.47 g, 93 %) as a colourless oil. This oil was dissolved in EtOH (25 mL), mixed with a spatula tip 10 % Pd/C and stirred for 10 h in an autoclave under 10 bar H<sub>2</sub> atmosphere yielding **109** (3.2 mmol, 1.06 g, 100 %) as a colourless oil.

<sup>1</sup>H-NMR (300 MHz; [D<sub>6</sub>]-Acetone): δ = 1.22 (t, <sup>3</sup>*J* = 7.1 Hz, 6 H, CH<sub>3</sub>), 1.31-1.64 (m, 4 H, CH<sub>2</sub>), 1.65-1.75 (m, 2 H, CH<sub>2</sub>), 3.16-3.29 (m, 2 H, CH<sub>2</sub>), 3.47 (t, <sup>3</sup>*J* = 7.3 Hz, 1 H, CH), 3.60-3.68 (m, 7 H, CH<sub>2</sub> + O-CH<sub>3</sub>), 4.09 (q, <sup>3</sup>*J* = 7.1 Hz, 4 H, O-CH<sub>2</sub>). – <sup>13</sup>C-NMR (75 MHz; [D<sub>6</sub>]-Acetone): δ = 14.2 (+, CH<sub>3</sub>), 22.9 (–, CH<sub>2</sub>), 29.3 (–, CH<sub>2</sub>), 29.9 (–, CH<sub>2</sub>), 40.8 (–, CH<sub>2</sub>), 51.4 (+, CH<sub>3</sub>), 52.6 (–, 2 C, CH<sub>2</sub>), 60.6 (–, 2 C, CH<sub>2</sub>), 64.5 (+, CH), 156.4 (C<sub>quat</sub>, COOMe), 171.4 (C<sub>quat</sub>, 2 C, COOEt). – MS (ESI, MeOH + 10 mmol/L NH<sub>4</sub>Ac): *m/z* (%) = 355 (17) [MNa<sup>+</sup>], 333 (100) [MH<sup>+</sup>]. – C<sub>15</sub>H<sub>38</sub>N<sub>2</sub>O<sub>6</sub> (332.19).



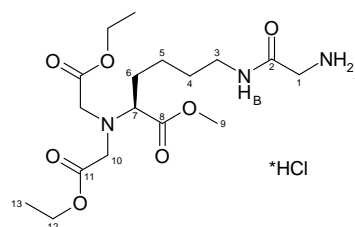
*2-(Bis-ethoxycarbonylmethyl-amino)-6-(2-tert-butoxycarbonylamino-acetylamino)-hexanoic acid methylester (Boc-Gly-NTAL-OMe/Et)(110):*

Boc-Gly-OH (0.21 g, 1.2 mmol), DIPEA (0.37 mL, 2.2 mmol), EDC (0.23 mL, 1.3 mmol) and HOBt (0.18 g, 1.3 mmol) were dissolved in DCM under ice cooling **109** (0.37 g, 1.1 mmol) dissolved in few DCM was added slowly via syringe. The reaction was allowed

<sup>ix</sup> Hart, B.R.; Shea, K.J. *J. Am. Chem. Soc.* **2001**, *123*, 2072.

to warm to r.t.. The reaction progress was monitored by TLC (EtOAc). After completion the solution was mixed with water (25 mL) and extracted with DCM. The combined organic layers were washed with brine and dried over Na<sub>2</sub>SO<sub>4</sub>. The solvent was evaporated and the crude product purification using column chromatography on silica gel (EtOAc, *R<sub>f</sub>* = 0.36) yielding **110** (0.4 mmol, 188 mg, 71 %) as a colourless oil.

<sup>1</sup>H-NMR (400 MHz; CDCl<sub>3</sub>): δ = 1.28 (t, <sup>3</sup>*J* = 7.1 Hz, 6 H, COSY: H(16)), 1.47 (s, 9 H, COSY: H(1)), 1.48-1.67 (m, 4 H, COSY: H(7), H(8)), 1.70-1.74 (m, 2 H, COSY: H(9)), 3.28-3.31 (m, 2 H, COSY: H(6)), 3.45 (t, <sup>3</sup>*J* = 7.6 Hz, 1 H, COSY: H(10)), 3.61 (s, 2 H, COSY: H(13)), 3.62 (s, 2 H, COSY: H(17)), 3.71 (s, 3 H, COSY: H(12)), 3.81-3.85 (m, 2 H, COSY: H(4)), 4.17 (q, <sup>3</sup>*J* = 7.1 Hz, 4 H, COSY: H(15)), 5.42 (bs, 1 H, COSY: H(A)), 6.51 (bs, 1 H, COSY: H(B)). – <sup>13</sup>C-NMR (100 MHz; CDCl<sub>3</sub>; HSQC): δ = 14.2 (+, 2 C, C(16), C(20)), 22.5 (–, C(8)), 28.2 (–, C(7)), 28.3 (+, 3 C, C(1)), 29.3 (–, C(9)), 39.1 (–, C(6)), 44.2 (–, C(4)), 51.4 (+, C(12)), 52.7 (–, 2 C, C(13), C(17)), 60.7 (–, 2 C, C(15), C(19)), 64.1 (+, C(10)), 79.9 (C<sub>quat</sub>, C(2)), 156.0 (C<sub>quat</sub>, C(3)), 169.5 (C<sub>quat</sub>, C(5)), 171.5 (C<sub>quat</sub>, 2 C, C(14), C(18)), 173.3 (C<sub>quat</sub>, C(11)). – IR [cm<sup>–1</sup>]:  $\tilde{\nu}$  = 3362, 2981, 2938, 2251, 1740, 1670, 1166. – MS (ESI, H<sub>2</sub>O/MeCN): *m/z* (%) = 528 (9) [MK<sup>+</sup>], 512 (36) [MNa<sup>+</sup>], 490 (100) [MH<sup>+</sup>], 434 (77) [MH<sup>+</sup> – C<sub>4</sub>H<sub>8</sub>], 390 (13) [MH<sup>+</sup> – Boc]. – HRMS (C<sub>22</sub>H<sub>39</sub>N<sub>3</sub>O<sub>9</sub>): calcd. 489.2686, found 489.2680 ± 0.01 ppm.

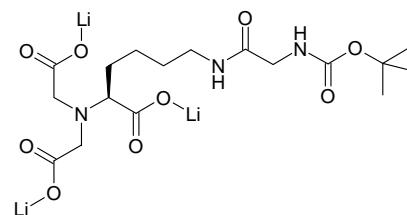


*6-(2-Amino-acetyl-amino)-2-(bis-ethoxycarbonylmethyl-amino)-hexanoic acid methyl ester hydrogenchloride (111):*

**110** (0.38 g, 0.8 mmol) was dissolved in Et<sub>2</sub>O (10 mL) and HCl/Et<sub>2</sub>O was added to the solution under ice cooling. After 60 min the Et<sub>2</sub>O is evaporated and the product dried under high vacuum. **111** (0.8 mmol, 332 mg, 100 %) is a colourless hygroscopic solid.

mp 73-74 °C. – <sup>1</sup>H-NMR (400 MHz; [D<sub>6</sub>]-DMSO; COSY): δ = 1.18 (t, <sup>3</sup>*J* = 7.3 Hz, 6 H, H<sub>13</sub>), 1.23-1.50 (m, 4 H, H<sub>4</sub> + H<sub>5</sub>), 1.57-1.60 (m, 2 H, H<sub>6</sub>), 3.05-3.11 (m, 2 H, H<sub>3</sub>), 3.39 (t, <sup>3</sup>*J* = 7.5 Hz, 1 H, H<sub>7</sub>), 3.41-3.52 (m, 2 H, H<sub>1</sub>), 3.52-3.77 (m, 7 H, H<sub>9</sub> + H<sub>10</sub>), 4.05 (q, <sup>3</sup>*J* = 7.0 Hz, 4 H, H<sub>12</sub>), 8.12 (bs, 3 H, H<sub>A</sub>), 8.40 (t, <sup>3</sup>*J* = 5.4 Hz, 1 H, H<sub>B</sub>). – <sup>13</sup>C-NMR (100 MHz;

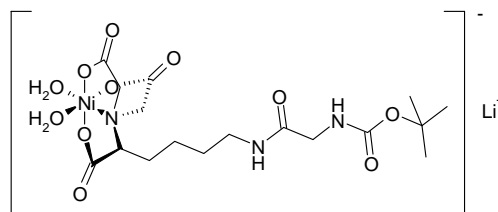
[D<sub>6</sub>]-DMSO; HSQC, HMQC):  $\delta$  = 14.0 (+, 2 C, C(13)), 22.6 (–, C(5)), 28.4 (–, C(4)), 29.2 (–, C(6)), 38.5 (–, C(3)), 39.8 (–, C(1)), 51.0 (+, C(9)), 52.1 (–, 2 C, C(10)), 59.8 (–, 2 C, C(12)), 63.7 (+, C(7)), 165.5 (C<sub>quat</sub>, C(2)), 170.8 (C<sub>quat</sub>, 2 C, C(11)), 172.3 (C<sub>quat</sub>, C(8)). – IR (KBr) [cm<sup>–1</sup>]:  $\tilde{\nu}$  = 3226, 3074, 2951, 1744, 1680, 1218, 1025. – MS (ESI, MeOH + 10 mmol/L NH<sub>4</sub>Ac):  $m/z$  (%) = 412 (33) [MNa<sup>+</sup>], 390 (100) [MH<sup>+</sup>]. – Elemental analysis calcd. (%) for C<sub>17</sub>H<sub>32</sub>N<sub>3</sub>O<sub>7</sub>Cl (425.91) + H<sub>2</sub>O: (M + H<sub>2</sub>O) C 46.00, H 7.72, N 9.47; found C 46.05, H 7.37, N 9.42.



***Boc-Gly-NTAL-OLi (112):***

**110** (0.11 g, 0.22 mmol) and LiOH·H<sub>2</sub>O (27.8 mg, 0.66 mmol) were dissolved in 25 % water/acetone (10 mL). The mixture was stirred at r.t. for 12 h. The remaining acetone was evaporated and the remaining solution freeze dried. The resulting solid was redissolved in water and extracted with DCM. The aqueous solution was freeze dried again yielding **112** (0.22 mmol, 96 mg, 100 %) as a colourless solid.

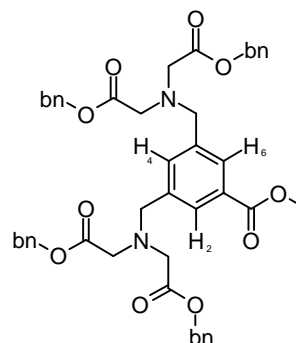
mp 97-99 °C. – <sup>1</sup>H-NMR (300 MHz; D<sub>2</sub>O):  $\delta$  = 1.30-1.65 (m, 15 H, CH<sub>3</sub> + CH<sub>3</sub>), 2.86-3.10 (m, 7 H, CH + CH<sub>2</sub> + N-CH<sub>2</sub>), 3.56-3.59 (m, 2 H, CH<sub>2</sub>-Gly). – <sup>13</sup>C-NMR (75 MHz; D<sub>2</sub>O; HMQC):  $\delta$  = 24.3 (–, CH<sub>2</sub>), 27.5 (+, 3 C, CH<sub>3</sub>), 28.1 (–, CH<sub>2</sub>), 28.4 (–, CH<sub>2</sub>), 39.0 (–, CH<sub>2</sub>), 39.0 (–, CH<sub>2</sub>), 43.4 (–, CH<sub>2</sub>), 56.8 (–, 2 C, CH<sub>2</sub>), 68.0 (+, CH), 81.5 (C<sub>quat</sub>, C-Boc), 172.3 (C<sub>quat</sub>, CONH), 181.0 (C<sub>quat</sub>, 2C, COO<sup>–</sup>), 182.3 (C<sub>quat</sub>, COO<sup>–</sup>). – IR (KBr) [cm<sup>–1</sup>]:  $\tilde{\nu}$  = 3354, 2969, 1739, 1539, 1512. – MS (ESI, H<sub>2</sub>O/MeOH + 10 mmol/L NH<sub>4</sub>Ac):  $m/z$  (%) = 285 (100) [A<sup>3–</sup> – Boc – Gly + NH<sub>4</sub><sup>+</sup> + 2 H<sup>+</sup> Li<sup>+</sup>], 420 (50) [A<sup>3–</sup> + 4 H<sup>+</sup>], 426 (71) [A<sup>3–</sup> + 3 H<sup>+</sup> + Li<sup>+</sup>], 432 (30) [A<sup>3–</sup> + 2 H<sup>+</sup> + 2 Li<sup>+</sup>]. – C<sub>17</sub>H<sub>26</sub>Li<sub>3</sub>N<sub>3</sub>O<sub>9</sub> (437.23).



*Li[Ni(Boc-Gly-NTAL)(H<sub>2</sub>O)<sub>2</sub>] (113):*

**112** (122 mg, 0.28 mmol) and NiCO<sub>3</sub>·2Ni(OH)<sub>2</sub>·4H<sub>2</sub>O (35 mg, 0.09 mmol) were dissolved in water (20 mL). The solution was stirred 30 min at r.t. and 30 min at 60 °C. The resulting suspension was filtered and the filtrate freeze dried. The product **113** (0.28 mmol, 145 mg, 100 %) could be obtained as a green-blue solid after recrystallisation in EtOH/water.

IR (KBr) [cm<sup>-1</sup>]:  $\tilde{\nu}$  = 3253, 3032, 2969, 1732, 1580. – MS (ESI(–), H<sub>2</sub>O/MeOH): *m/z* (%) = 474 (100) [A<sup>-</sup> – 2 H<sub>2</sub>O]. – C<sub>17</sub>H<sub>30</sub>LiN<sub>3</sub>NiO<sub>11</sub> (518.07).



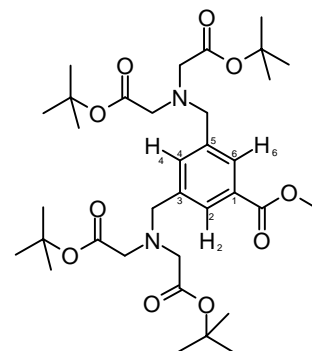
*3,5-Bis-[(bis-benzyloxycarbonylmethylamino)-methyl]-benzoic acid methylester (117):*

3,5-Bis-(bromomethyl)-benzoic acid methylester (1.00 g, 3.1 mmol), iminodiacetic acid-di-benzylester (1.92 g, 6.2 mmol), and K<sub>2</sub>CO<sub>3</sub> (1.72 g, 12.4 mmol) were dissolved in MeCN (50 mL). The suspension was stirred at 60 °C for 2 d. The remaining solid was filtered off and the filtrate acidified with 1N HCl. The mixture was separated between water and EtOAc. The organic layers were dried over Na<sub>2</sub>SO<sub>4</sub> and concentrated under reduced pressure. The crude product was purified using column chromatography on silica gel. (PE:EtOAc = 5:1, *R<sub>f</sub>* = 0.4). The product **117** (1.1 mmol, 0.89 g, 36 %) is a yellow oil.

<sup>1</sup>H-NMR (300 MHz; CDCl<sub>3</sub>): δ = 3.59 (s, 8 H, N-CH<sub>2</sub>), 3.87 (s, 3 H, O-CH<sub>3</sub>), 3.93 (s, 4 H, CH<sub>2</sub>-Ar), 5.12 (s, 8 H, CH<sub>2</sub>-Ph), 7.27-7.38 (m, 20 H, Ph), 7.57 (s, 1 H, H(4)-Ar), 7.94 (d, <sup>4</sup>*J* = 1.5 Hz, 2 H, H(2)-Ar + H(6)-Ar). – <sup>13</sup>C-NMR (75 MHz; CDCl<sub>3</sub>): δ = 52.1 (+, O-CH<sub>3</sub>), 54.3 (–, 4 C, CH<sub>2</sub>), 57.4 (–, 2 C, CH<sub>2</sub>), 66.2 (–, 4 C, CH<sub>2</sub>), 128.2 (+, 8 C, C-Ar), 128.3 (+, 4 C, C-Ar), 128.6 (+, 8 C, C-Ar), 129.3 (+, 2 C, C-Ar), 130.6 (C<sub>quat</sub>, C(1)), 134.2 (+, C-Ar),



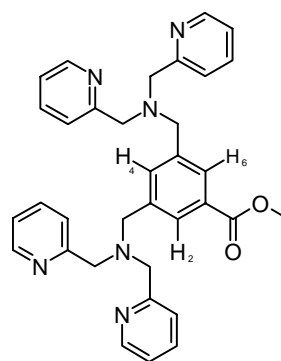
135.7 (C<sub>quat</sub>, C-Ar), 138.9 (C<sub>quat</sub>, 4 C, C-Ar), 167.0 (C<sub>quat</sub>, Ar-COOCH<sub>3</sub>), 170.8 (C<sub>quat</sub>, 4 C, COOBn). – IR [cm<sup>-1</sup>]:  $\tilde{\nu}$  = 3463, 3065, 3034, 2951, 1734, 1605, 1002. – MS (ESI, CH<sub>2</sub>Cl<sub>2</sub>/MeOH + 10 mmol/L NH<sub>4</sub>Ac):  $m/z$  (%) = 787 (100) [MH<sup>+</sup>] – C<sub>46</sub>H<sub>46</sub>N<sub>2</sub>O<sub>10</sub> (786.89).



**3,5-Bis-[(bis-tert-butoxycarbonylamino)-methyl]-benzoic acid methylester (**118**):**

3,5-Bis-(bromomethyl)-benzoic acid methylester (0.50 g, 1.6 mmol), iminodiacetic acid-di-*tert*-butylester (0.76 g, 3.1 mmol), and K<sub>2</sub>CO<sub>3</sub> (0.86 g, 6.2 mmol) were dissolved in MeCN (50 mL). The suspension was stirred at 60 °C for 2 d. The remaining solid was filtered off and the filtrate acidified with 1N HCl. The mixture was separated between water and EtOAc. The organic layers were dried over Na<sub>2</sub>SO<sub>4</sub> and concentrated under reduced pressure. The crude product was purified using column chromatography on silica gel. (PE:EtOAc = 5:1,  $R_f$  = 0.4). The product **118** (0.8 mmol, 0.55 g, 54 %) is a yellow solid.

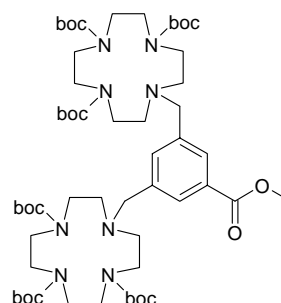
<sup>1</sup>H-NMR (300 MHz; CDCl<sub>3</sub>):  $\delta$  = 1.41 (s, 36 H, CH<sub>3</sub>), 3.36 (s, 8 H, CH<sub>2</sub>), 3.83 (s, 3 H, OCH<sub>3</sub>), 3.88 (s, 4 H, CH<sub>2</sub>-Ar), 7.56 (s, 1 H, H(4)-Ar), 7.91 (d, <sup>4</sup> $J$  = 1.4 Hz, 2 H, H(2)-Ar + H(6)-Ar). – <sup>13</sup>C-NMR (150 MHz; CDCl<sub>3</sub>):  $\delta$  = 28.2 (+, 12 C, CH<sub>3</sub>), 51.9 (+, CH<sub>3</sub>), 55.2 (–, 4 C, CH<sub>2</sub>), 57.1 (–, 2 C, CH<sub>2</sub>), 81.0 (C<sub>quat</sub>, 4 C, C-Boc), 129.2 (+, 2 C, C(2) + C(6)), 130.4 (C<sub>quat</sub>, C(1)), 134.3 (+, C(4)), 139.2 (C<sub>quat</sub>, 2 C, C(3)+C(5)), 167.2 (C<sub>quat</sub>, COOCH<sub>3</sub>), 170.4 (C<sub>quat</sub>, 4 C, COO<sup>t</sup>Bu). – IR (KBr) [cm<sup>-1</sup>]:  $\tilde{\nu}$  = 3368, 2979, 2932, 1740, 1369. – UV/Vis (MeCN)  $\lambda_{max}$  [nm] (lg  $\epsilon$ ): 282 (3.150). – MS (ESI, CH<sub>2</sub>Cl<sub>2</sub>/MeOH + 10 mmol/L NH<sub>4</sub>Ac):  $m/z$  (%) = 651 (100) [MH<sup>+</sup>], 595 (6) [MH<sup>+</sup> – C<sub>4</sub>H<sub>8</sub>]. – C<sub>34</sub>H<sub>54</sub>N<sub>2</sub>O<sub>10</sub> (650.82).



**3,5-Bis-[(bis-pyridine-2-ylmethyl-amino)-methyl]-benzoic acid methylester (**119**):**

3,5-Bis-(bromomethyl)-benzoic acid methylester (0.50 g, 1.6 mmol), BPA (0.93 g, 4.7 mmol), and  $K_2CO_3$  (1.29 g, 9.3 mmol) were dissolved in MeCN (50 mL). The suspension was stirred at 60 °C for 2 d. The remaining solid was filtered off and the filtrate acidified with 1N HCl. The mixture was separated between water and EtOAc. The organic layers were dried over  $Na_2SO_4$  and concentrated under reduced pressure. The product **119** (1.2 mmol, 0.67 g, 77 %) is a yellow solid.

mp 75-77 °C.  $^1H$ -NMR (300 MHz;  $[D_6]$ -Acetone):  $\delta$  = 3.65-4.14 (m, 15 H,  $OCH_3$ ,  $NCH_2$ ), 7.11-7.30 (m, 4 H, H-Py), 7.46-7.55 (m, 1 H, H-Ar), 7.59-7.78 (m, 8 H, H-Py), 7.89-7.96 (m, 2 H, H-Ar), 8.41-8.57 (m, 4 H, H-Py). –  $^{13}C$ -NMR (75 MHz;  $[D_6]$ -Acetone):  $\delta$  = 52.3 (+,  $CH_3$ ), 58.8 (–, 2 C,  $CH_2$ ), 60.6 (–, 4 C,  $CH_2$ ), 122.9 (+, C-Ar), 123.6 (+, 2 C, C-Ar), 129.4 (+, 4 C, C-Py), 131.1 ( $C_{quat}$ , C-Ar), 134.7 (+, 4 C, C-Py), 137.2 (+, 4 C, C-Py), 139.2 ( $C_{quat}$ , 2 C, C-Ar), 140.9 ( $C_{quat}$ , 4 C, C-Py), 149.8 (+, 4 C, C-Py), 160.5 ( $C_{quat}$ ,  $COOCH_3$ ). – MS (EI, 70 eV):  $m/z$  (%) = 558 (3) [ $M^{+\bullet}$ ], 527 (3) [ $M^{+\bullet} - \bullet O-CH_3$ ], 466 (100) [ $M^{+\bullet} - \bullet CH_2-Py$ ]. –  $C_{34}H_{34}N_6O_2$  (558.69).

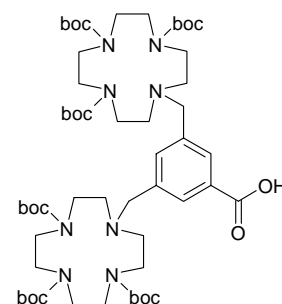


**3,5-Bis-(tri-Boc-Cyc-aminomethyl)-benzoic acid methylester (**120**):**

Tri-Boc-Cyc (1.00 g, 2.1 mmol),  $K_2CO_3$  (1.17 g, 8.5 mmol) and a spatula tip of KI were dissolved in MeCN (40 mL). 3,5-Bis(bromomethyl)-benzoic acid methylester (0.32 g,

1.0 mmol) was added in little portions over a period of 15 min. The suspension was stirred at 60 °C for 2 d. The remaining solid was filtered off and the filtrate acidified with 1N HCl. The mixture was separated between water and EtOAc. The organic layers were dried over Na<sub>2</sub>SO<sub>4</sub> and concentrated under reduced pressure. The crude product was purified using column chromatography on silica gel. (PE:EtOAc = 1:1, *R<sub>f</sub>* = 0.74). **120** (1.7 mmol, 1.93 g, 83 %) is a colourless solid.

mp 107-110 °C. – <sup>1</sup>H-NMR (300 MHz; CDCl<sub>3</sub>): δ = 1.25-1.47 (m, 54 H, CH<sub>3</sub>), 2.60-2.69 (m, 8 H, CH<sub>2</sub>-Cyc), 3.27-3.80 (m, 24 H, CH<sub>2</sub>-Cyc), 3.78-3.81 (m, 4 H, CH<sub>2</sub>-Ph), 3.88 (s, 3 H, O-CH<sub>3</sub>), 7.27 (s, 1 H, H-Ar), 7.84 (bs, 2 H, H-Ar). – <sup>13</sup>C-NMR (75 MHz; CDCl<sub>3</sub>): δ = 28.4 (+, 12 C, CH<sub>3</sub>), 28.7 (+, 6 C, CH<sub>3</sub>), 48.0 (–, 4 C, CH<sub>2</sub>), 49.8 (–, 4 C, CH<sub>2</sub>), 52.0 (+, CH<sub>3</sub>), 54.0 (–, 4 C, CH<sub>2</sub>), 55.4 (–, 4 C, CH<sub>2</sub>), 56.2 (–, 2 C, CH<sub>2</sub>), 79.4 (C<sub>quat</sub>, 4 C, C-Boc), 79.5 (C<sub>quat</sub>, 2 C, C-Boc), 124.1 (+, C-Ar), 125.2 (+, 2 C, C-Ar), 130.0 (C<sub>quat</sub>, C-Ar), 130.3 (C<sub>quat</sub>, 2 C, C-Ar), 155.7 (C<sub>quat</sub>, 4 C, NCOO<sup>t</sup>Bu), 156.1 (C<sub>quat</sub>, 2 C, NCOO<sup>t</sup>Bu), 166.5 (C<sub>quat</sub>, COOMe). – IR (KBr) [cm<sup>–1</sup>]:  $\tilde{\nu}$  = 3013, 2976, 2932, 1690, 1169, 772. – MS (ESI, DCM/MeOH + 10 mmol/L NH<sub>4</sub>Ac): *m/z* (%) = 1106 (100) [MH<sup>+</sup>]. – C<sub>56</sub>H<sub>96</sub>N<sub>8</sub>O<sub>14</sub> (1105.43).

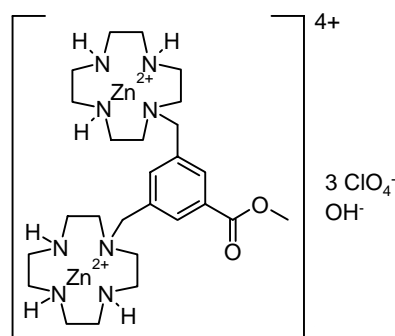


*3,5-Bis-(tri-Boc-Cyc-aminomethyl)-benzoic acid (121):*

**120** (0.30 g, 0.3 mmol) and LiOH·H<sub>2</sub>O (0.13 g, 0.3 mmol) were dissolved in water/acetone = 3:1 (25 mL). The solution was stirred at r.t for 12 h. The remaining acetone was evaporated. The aqueous solution was neutralised with saturated ammonium chloride solution and extracted with DCM. The organic layers were dried over Na<sub>2</sub>SO<sub>4</sub> and concentrated. The crude product was purified using column chromatography on silica (EtOAc → MeOH:EtOAc = 5:1, *R<sub>f</sub>* = 0.34). **121** (0.26 mmol, 0.28 g, 86 %) is a colourless solid.

mp 136-138 °C. – <sup>1</sup>H-NMR (300 MHz; CDCl<sub>3</sub>): δ = 1.19-1.49 (m, 54 H, CH<sub>3</sub>), 2.39-2.68 (m, 8 H, CH<sub>2</sub>-Cyc), 3.12-3.81 (m, 28 H, CH<sub>2</sub>-Cyc + CH<sub>2</sub>-Ph) 7.15 (bs, 1 H, H-Ar), 8.79

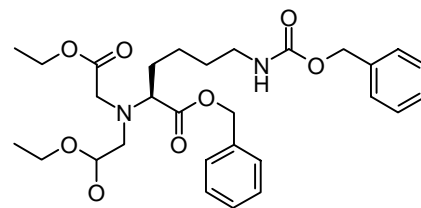
(bs, 2 H, H-Ar). –  $^{13}\text{C}$ -NMR (75 MHz;  $\text{CDCl}_3$ ):  $\delta$  = 28.3 (+, 12 C,  $\text{CH}_3$ ), 28.6 (+, 6 C,  $\text{CH}_3$ ), 48.2 (–, 4 C,  $\text{CH}_2$ ), 49.8 (–, 4 C,  $\text{CH}_2$ ), 54.1 (–, 4 C,  $\text{CH}_2$ ), 55.5 (–, 4 C,  $\text{CH}_2$ ), 56.1 (–, 2 C,  $\text{CH}_2$ ), 79.4 ( $\text{C}_{\text{quat}}$ , 4 C, C-Boc), 79.5 ( $\text{C}_{\text{quat}}$ , 2 C, C-Boc), 124.1 (+, C-Ar), 125.2 (+, 2 C, C-Ar), 130.0 ( $\text{C}_{\text{quat}}$ , C-Ar), 130.3 ( $\text{C}_{\text{quat}}$ , C-Ar), 155.7 ( $\text{C}_{\text{quat}}$ , 4 C,  $\text{NCOO}^t\text{Bu}$ ), 156.1 ( $\text{C}_{\text{quat}}$ , 2 C,  $\text{NCOO}^t\text{Bu}$ ), 166.5 ( $\text{C}_{\text{quat}}$ ,  $\text{COOH}$ ). – IR (KBr) [ $\text{cm}^{-1}$ ]:  $\tilde{\nu}$  = 3473, 2977, 2933, 2821, 1685, 1251, 1167, 773. – MS (ESI,  $\text{DCM}/\text{MeOH}$  + 10 mmol/L  $\text{NH}_4\text{Ac}$ ):  $m/z$  (%) = 1092 (52) [ $\text{MH}^+$ ], 547 (100) [ $\text{M} + 2 \text{H}^+$ ]. –  $\text{C}_{55}\text{H}_{94}\text{N}_8\text{O}_{14}$  (1091.41).



[ $\text{Zn}_2(\text{bis}-(\text{Cyc-methyl})\text{-benzoic acid methylester})(\text{OH})](\text{ClO}_4)_3$  (**122**):

**120** (0.62 g, 0.6 mmol) was dissolved in few DCM and mixed with TFA (3.6 mL, 47 mmol). The solution was stirred over night at r.t.. After evaporation of the solvents the completion of the reaction was controlled via  $^1\text{H}$ -NMR. The resulting triflate salt was dissolved in water and freeze dried. The obtained solid was dissolved in EtOH and neutralised with  $\text{NaHCO}_3$ . In EtOH (5 mL) predissolved zinc(II) perchlorate hexahydrate (0.22 g, 0.6 mmol) was added to the reaction mixture. The resulting suspension was refluxed over night. Insoluble particles were filtered off and the filtrate concentrated. The resulting crude product was recrystallised in water/MeCN. **122** (0.53 g, 0.56 mmol, 93 %) is obtained as colourless needles.

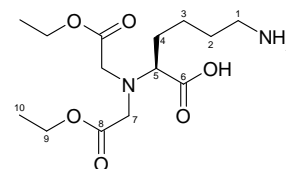
mp > 200 °C. –  $^1\text{H}$ -NMR (300 MHz;  $\text{CDCl}_3$ ):  $\delta$  = 2.52-2.87 (m, 16 H,  $\text{CH}_2\text{-Cyc}$ ), 2.89-3.05 (m, 8 H,  $\text{CH}_2\text{-Cyc}$ ), 3.09-3.21 (m, 4 H,  $\text{CH}_2\text{-Ph}$ ), 3.22-3.49 (m, 4 H,  $\text{CH}_2\text{-Ph}$ ), 3.85 (s, 2 H,  $\text{CH}_2\text{-Ar}$ ), 3.91 (s, 3 H, O- $\text{CH}_3$ ), 4.01 (s, 2 H,  $\text{CH}_2\text{-Ar}$ ), 7.42 (s, 1 H, H-Ar), 7.95 (d,  $^3J$  = 6.8 Hz, 2 H, H-Ar). –  $^{13}\text{C}$ -NMR (75 MHz;  $\text{CD}_3\text{CN}$ ):  $\delta$  = 47.5 (–, 4 C,  $\text{CH}_2$ ), 48.9 (–, 4 C,  $\text{CH}_2$ ), 51.4 (+,  $\text{CH}_3$ ), 53.6 (–, 4 C,  $\text{CH}_2$ ), 55.7 (–, 4 C,  $\text{CH}_2$ ), 55.9 (–, 2 C,  $\text{CH}_2$ ), 123.8 (+, 2 C, C-Ar), 124.1 (+, C-Ar), 130.4 ( $\text{C}_{\text{quat}}$ , 2 C, C-Ar), 130.2 ( $\text{C}_{\text{quat}}$ , C-Ar), 166.5 ( $\text{C}_{\text{quat}}$ ,  $\text{COOMe}$ ). – IR (KBr) [ $\text{cm}^{-1}$ ]:  $\tilde{\nu}$  = 3005, 2986, 2966, 2930, 1734, 1169. – MS (ESI, MeCN):  $m/z$  (%) = 431 (100) [ $\text{K}^{4+} + 2 \text{TFA}^-$ ]. –  $\text{C}_{26}\text{H}_{49}\text{N}_8\text{O}_{15}\text{Cl}_3\text{Zn}_2$  (946.10).



*Nε-Benzylloxycarbonyl-Nα-bis(2-ethoxy-2-oxoethyl)-L-lysine-benzylester (123):*

H-Lys(Z)-OBzl·HCl (1.26 g, 3.4 mmol), K<sub>2</sub>CO<sub>3</sub> (9.40 g, 68.0 mmol) were dissolved in MeCN (25 mL) and stirred for 8 h. Ethylbromoacetate (3.8 mL, 34.0 mmol) was added and the suspension refluxed for 18 h. The suspension was filtered and the solution concentrated. The resulting crude product was purified using column chromatography on silica gel (PE → PE:EtOAc = 1:1, *R<sub>f</sub>* = 0.51). **123** (3.0 mmol, 1.64 g, 89 %) is a yellow liquid.

<sup>1</sup>H-NMR (300 MHz; CDCl<sub>3</sub>): δ = 1.21 (t, <sup>3</sup>*J* = 7.1 Hz, 6 H, CH<sub>3</sub>), 1.39-1.58 (m, 2 H, CH<sub>2</sub>), 1.64-1.76 (m, 4 H, CH<sub>2</sub>), 3.08-3.22 (m, 2 H, CH<sub>2</sub>), 3.46 (t, <sup>3</sup>*J* = 7.5 Hz, 1 H, CH), 3.62 (s, 4 H, N-CH<sub>2</sub>), 4.10 (q, <sup>3</sup>*J* = 7.1 Hz, 4 H, O-CH<sub>2</sub>), 4.91 (bs, 1 H, NH), 5.05-5.12 (m, 4 H, CH<sub>2</sub>-Ph), 7.28-7.39 (m, 10 H, H-Ar). – C<sub>29</sub>H<sub>38</sub>N<sub>2</sub>O<sub>8</sub> (542.63).

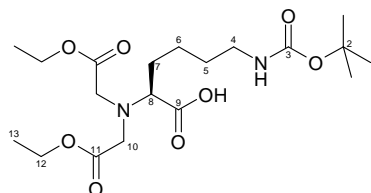


*6-Amino-2-(bis-ethoxycarbonylmethylamino)-hexanoic acid (124):*

**123** (0.80 g, 1.5 mmol) and a spatula tip of 10 % Pd/C were suspended in EtOH (25 mL). The reaction mixture was stirred over night in a autoclave under 10 bar H<sub>2</sub> atmosphere. After hydrogenolysis the suspension was filtered over celite and concentrated under reduced pressure. The crude product was dissolved in water and washed with DCM and EtOAc. The aqueous solution was freeze dried. **124** (1.4 mmol, 0.46 g, 98 %) was isolated as a colourless solid.

mp 141-142 °C. – <sup>1</sup>H-NMR (400 MHz; D<sub>2</sub>O): δ = 1.18 (t, <sup>3</sup>*J* = 7.2 Hz, 6 H, COSY: H(10)), 1.20-1.39 (m, 2 H, COSY: H(3)), 1.50-1.65 (m, 4 H, COSY: H(2) + H(4)), 2.92 (t, <sup>3</sup>*J* = 7.4 Hz, 2 H, COSY: H(1)), 3.17 (dd, <sup>3</sup>*J* = 5.8, 9.1 Hz, 1 H, COSY: H(5)), 3.42 (d, <sup>2</sup>*J* = 17.5 Hz, 2 H, COSY: H(7)), 3.60 (d, <sup>2</sup>*J* = 17.5 Hz, 2 H, COSY: H(7)), 4.10 (q, <sup>3</sup>*J* = 7.3 Hz, 4 H, COSY: H(9)). – <sup>13</sup>C-NMR (100 MHz; D<sub>2</sub>O; HSQC, HMQC): δ = 13.3 (+, 2 C,

C(10)), 22.7 (–, C(3)), 26.6 (–, C(2)), 29.8 (–, C(4)), 39.3 (–, C(1)), 53.9 (–, 2 C, C(7)), 61.9 (–, 2 C, C(9)), 68.2 (+, C(5)), 173.7 (C<sub>quat</sub>, 2 C, C(8)), 179.6 (C<sub>quat</sub>, C(6)). – IR (KBr) [cm<sup>–1</sup>]:  $\tilde{\nu}$  = 3430, 2940, 1744, 1561, 1397. – MS (ESI, H<sub>2</sub>O/MeOH + 10 mmol/L NH<sub>4</sub>Ac):  $m/z$  (%) = 319 (100) [MH<sup>+</sup>]. – Elemental analysis calcd. (%) for C<sub>14</sub>H<sub>26</sub>N<sub>2</sub>O<sub>6</sub> (318.37): C 52.82, H 8.23, N 8.80; found C 52.40, H 7.91, N 8.61.



*2-(Bis-ethoxycarbonylmethyl-amino)-6-tert-butoxycarbonylamino-hexanoic acid (125):*

**124** (0.50 g, 1.6 mmol) and NEt<sub>3</sub> (0.3 mL, 2.1 mmol) were dissolved in MeOH (25 mL). The solution was cooled in an ice bath and was drop wise mixed with Boc<sub>2</sub>O (0.41 g, 1.88 mmol) dissolved in DCM. The mixture was allowed to warm to r.t. and stirred over night. The solution was concentrated and purified using column chromatography (EtOAc → EtOAc:MeOH = 5:1,  $R_f$  (EE) = 0.3). The resulting product **125** (0.45 g, 1.1 mmol, 67 %) is a colourless solid.

mp 71–74 °C. – <sup>1</sup>H-NMR (400 MHz; CDCl<sub>3</sub>; HSQC):  $\delta$  = 1.22 (t, <sup>3</sup> $J$  = 7.1 Hz, 6 H, H(13)), 1.37–1.49 (m, 11 H, H(1) + H(6)), 1.52–1.80 (m, 2 H, H(7)), 3.05–3.07 (m, 2 H, H(4)), 3.28 (t, <sup>3</sup> $J$  = 7.1 Hz, 1 H, H(8)), 3.50 + 3.60 (2s, 4 H, H(10)), 5.47 (q, <sup>3</sup> $J$  = 7.1 Hz, 4 H, H(12)), 4.60 (bs, 1 H, H<sub>A</sub>), 10.71 (bs, 1 H, H<sub>B</sub>). – <sup>13</sup>C-NMR (100 MHz; CDCl<sub>3</sub>; HSQC):  $\delta$  = 14.1 (+, 2 C, C(13)), 23.9 (–, C(6)), 28.4 (+, 3 C, C(1)), 28.7 (–, C(5)), 29.8 (–, C(7)), 40.2 (–, C(4)), 53.4 (–, C(10)), 61.2 (–, 2 C, C(12)), 66.1 (+, C(8)), 67.0 (–, 2 C, C(10)), 78.9 (C<sub>quat</sub>, C(2)), 156.0 (C<sub>quat</sub>, C(3)), 172.4 (C<sub>quat</sub>, 2 C, C(11)), 176.0 (C<sub>quat</sub>, C(9)). – IR (KBr) [cm<sup>–1</sup>]:  $\tilde{\nu}$  = 3320, 2967, 2945, 1732, 1624, 1555. – MS (ESI, H<sub>2</sub>O/MeOH + 10 mmol/L NH<sub>4</sub>Ac):  $m/z$  (%) = 441 (39) [MNa<sup>+</sup>], 419 (100) [MH<sup>+</sup>], 363 (53) [MH<sup>+</sup> – C<sub>4</sub>H<sub>8</sub>]. – C<sub>19</sub>H<sub>34</sub>N<sub>2</sub>O<sub>8</sub> (418.49).

### **SPRS Protocol:**

- Loading:

The resin was suspended in DMF. Four equivalents (based on resin substitution) of the carboxylic acid and 4 equivalents of PyBOP (based on resin substitution) were dissolved in DMF. This mixture was added to the resin. Eight equivalents (based on resin substitution) of DIPEA were added and the mixture was shaken for 18 h.

- Capping

The resin was preswelled in DMF (15 min) and DCM (10 min). After removal of the solvents the resin was mixed with a solution of Ac<sub>2</sub>O (47 µL, 0.5 mmol) and pyridine (81 µL, 1.0 mmol) in DCM (2 mL). The solution was removed after 15 min and the resin washed with DCM and DMF. The acetylation step was repeated twice.

- Boc-Deprotection

The resin was preswelled in DCM (2 mL). The deprotection was performed using a mixture of TFA (4 mL), anisole (0.2 mL) and DCM (1 mL) and a reaction time of 15 min. The deprotection step was repeated for three times. After completion the resin was washed with DCM and dried.

- Coupling

The Boc-AA (0.5 mmol), HOBt (68 mg, 0.5 mmol) and HBTU (186 mg, 0.49 mmol) were dissolved in DMF (2 mL). After addition of DIPEA (171 µL, 1.0 mmol) the coupling mixture was added to the resin (preswollen in DMF). The resin filtered off after 1 h and the coupling step repeated for three times. The completion of the coupling step was monitored using the *Kaiser* test. The resin was washed with DCM and DMF and dried.

- Ester Cleavage

The resin was preswelled in water/DMF and mixed with 1 M LiOH. The deprotection was repeated three times. The resin was washed with water/DMF.

- Complexation

The resin was preswelled in water/MeCN and mixed with a Ni(II)-solution (NiCl<sub>2</sub> and Ni(OAc)<sub>2</sub>). After 1 h the complexation was repeated. The resin was washed several times with water, DMF, MeCN and DCM. Additionally the resin was extracted with water using a soxlet apparatus. After drying of the resin the Ni(II) loading was determined gravimetrically (97 % Ni(II)-loading).

- Activation of safety-catch-resin

The resin was mixed with NMP (8 mL/g resin). DIPEA (5 eq.) and iodoacetonitrile (23.5 eq.) were added and stirred for 24 h at r.t..

- Cleavage

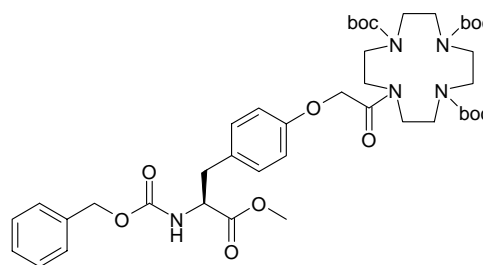
The resin was filled in a syringe and washed with DMSO and THF. The resin was preswelled in THF and mixed for 20 h with 2 N NaOH (10 mL/500 mg resin). Filtration and washing of the resin delivers the free acid. The Ni(II)-NTA complex was obtained after freeze drying.

Kaiser test:

Preparation of the following solutions:

*Sol-1*: 5 g of Ninhydrin in 100 mL of EtOH. *Sol-2*: 80 g of liquefied phenol in 20 mL of EtOH. *Sol-3*: 2 mL of a 0.001 M aqueous solution of KCN in 98 mL of pyridine.

Place a few resin beads in a glass vial and rinse several times with EtOH. Add two drops of each of the solutions above. Mix well and heat to 120 °C for 4-6 min. Positive test is indicated by blue/purple resin beads. Negative test is indicated by pale yellow/brown colour.

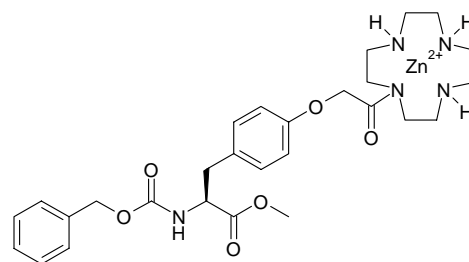


*Z*-L-Tyr[Ac-(Tri-Boc-Cyc)]-OMe (**127**)

*Z*-L-Tyr-OMe (0.15 g, 0.5 mmol), **126** (0.32 g, 0.6 mmol), and K<sub>2</sub>CO<sub>3</sub> (0.12 g, 0.9 mmol) were suspended in MeCN (25 mL). After refluxing for 12 h the mixture was filtered. Concentration of the filtrate delivered the crude product which was purified using column chromatography on silica gel (PE:EtOAc = 2:3, *R<sub>f</sub>* = 0.33). **127** (0.32 g, 0.4 mmol, 76 %) is a colourless solid.

mp 93-96 °C. – <sup>1</sup>H-NMR (300 MHz; CDCl<sub>3</sub>): δ = 1.32-1.42 (m, 27 H, Boc-CH<sub>3</sub>), 2.93-3.01 (m, 2 H, CH<sub>2</sub>), 3.25-3.56 (m, 16 H, CH<sub>2</sub>-Cyc), 3.64 (s, 3 H, O-CH<sub>3</sub>), 4.49-4.59 (m, 3 H, CH<sub>2</sub>-Ar + CH), 5.02 (s, 2 H, CH<sub>2</sub>-Ar), 5.18 (d, <sup>3</sup>*J* = 8.2 Hz, 1 H, NH), 6.78 (d, <sup>3</sup>*J* = 8.5 Hz, 2 H, H-Ar), 6.92 (d, <sup>3</sup>*J* = 8.5 Hz, 2 H, H-Ar), 7.22-7.30 (m, 5 H, H-Ar). – <sup>13</sup>C-NMR (75 MHz; CDCl<sub>3</sub>): δ = 28.4 (+, 3 C, CH<sub>3</sub>), 28.5 (+, 3 C, CH<sub>3</sub>), 28.5 (+, 3 C, CH<sub>3</sub>), 37.2 (–, CH<sub>2</sub>) 49.7 (–, 4 C, CH<sub>2</sub>), 49.9 (–, 2 C, CH<sub>2</sub>), 50.4 (–, 2 C, CH<sub>2</sub>), 51.4 (–, CH<sub>2</sub>), 52.3 (+, CH<sub>3</sub>), 54.9 (+, CH), 66.9 (–, CH<sub>2</sub>), 80.3 (C<sub>quat</sub>, C-Boc), 80.4 (C<sub>quat</sub>, C-Boc), 80.5 (C<sub>quat</sub>, C-Boc), 115.0 (+, 2 C, C-Ar), 128.1 (+, 2 C, C-Ar), 128.2 (+, C-Ar), 128.5 (+, C-Ar), 128.7 (C<sub>quat</sub>, C-Ar), 130.3 (+, 2 C, C-Ar), 136.2 (C<sub>quat</sub>, 2 C, C-Ar), 155.6 (C<sub>quat</sub>, NCOO<sup>t</sup>Bu), 157.1 (C<sub>quat</sub>, NCOO<sup>t</sup>Bu), 157.3 (C<sub>quat</sub>, NCOO<sup>t</sup>Bu), 168.6 (C<sub>quat</sub>, COOMe), 171.1 (C<sub>quat</sub>, COOR), 172.0 (C<sub>quat</sub>, CONH). – MS (ESI, DCM/MeOH + 10 mmol/L NH<sub>4</sub>Ac): *m/z* (%) = 859 (57) [M+NH<sub>4</sub><sup>+</sup>], 843 (28) [MH<sup>+</sup>], 742 (100) [MH<sup>+</sup> - Boc]. – C<sub>43</sub>H<sub>63</sub>N<sub>5</sub>O<sub>12</sub> (842.01).





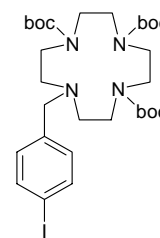
*[Zn(Z-L-Tyr(Ac-Cyc)-OMe)](ClO<sub>4</sub>)<sub>2</sub> (**128**):*

**127** (0.15 g, 0.2 mmol) was dissolved in TFA (5 mL) and stirred at r.t. over night. <sup>1</sup>H-NMR-control showed completion of the Boc-deprotection. TFA was removed under reduced pressure. The resulting slurry was dissolved in water and freeze dried. The triflate salt was dissolved in water and neutralised with NaHCO<sub>3</sub>. This solution was mixed with Zn(ClO<sub>4</sub>)<sub>2</sub>·6 H<sub>2</sub>O (75 mg, 0.2 mmol). After 1 h warming to 40 °C the insoluble particles were filtered off and the filtrate concentrated. **128** (0.12 g, 0.2 mmol, 100 %) was obtained as a colourless solid after crystallisation in water/MeCN.

mp > 200 °C. – MS (ESI, H<sub>2</sub>O/MeOH + 10 mmol/L NH<sub>4</sub>Ac): *m/z* (%) = 664 (75) [K<sup>2+</sup> + Ac<sup>-</sup>], 590 (100) [K<sup>2+</sup> - Me]. – IR (KBr) [cm<sup>-1</sup>]:  $\tilde{\nu}$  = 3204, 3007, 2986, 2966, 1734, 1716, 1655, 1320, 1169, 837. – C<sub>28</sub>H<sub>39</sub>N<sub>5</sub>O<sub>6</sub>Zn (605.22).

#### General procedure for the generation of organozinc reagents **130a** and **130b**.

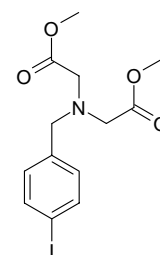
The *Rieke* zinc was prepared from ZnCl<sub>2</sub> using a catalytic amount of naphthalene: To a *Schlenk* tube charged with finely divided lithium (1% Na) (3.0 mmol), naphthalene (0.3 mmol) and anhydrous THF (2 mL) (distilled from benzophenone-sodium ketyl under N<sub>2</sub>) or DME (in case of *Z-p-Me-Phe-O<sup>t</sup>Bu* **131**) under argon a solution of anhydrous zinc chloride (1.5 mmol in 2 mL of THF or DME (in case of *Z-p-Me-Phe-O<sup>t</sup>Bu* **131**)) was transferred via syringe. The mixture was stirred vigorously until all lithium was consumed (30 min). To the *Rieke* zinc suspension under argon a solution of iodoalanine (1.28 mmol) in DME (3 mL) (in case of *Z-p-Me-Phe-O<sup>t</sup>Bu* **131**) or THF was added via syringe. The exothermic reaction was completed in 5 min (the end of reaction is indicated when the black zinc disappeared). The mixture was stirred for additional 30 min.



*10-(p-Iodo-benzyl)-1,4,7,10-tetraaza cyclododecane-1,4,7-tricarboxylic acid-tri-tert-butylester (136):*

*p*-Iodobenzylbromide (0.5 g, 1.7 mmol) was dissolved in MeCN (35 mL). Trifold-Boc protected cyclen (1.03 g, 2.2 mmol) and K<sub>2</sub>CO<sub>3</sub> (1.21 g 8.8 mmol) were added, and after completion of the reaction the reaction mixture was filtered and concentrated. The crude product was purified by chromatography on silica gel (PE:DCM = 5:1 → EtOAc, *R<sub>f</sub>*(EtOAc) = 0.84) giving **136** (1.58 mmol, 1.09 g, 93 %) as a colourless solid.

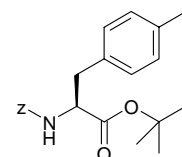
mp = 75-77 °C. – <sup>1</sup>H-NMR (300 MHz, CDCl<sub>3</sub>): δ = 1.25-1.56 (m, 27H), 2.39-2.78 (m, 4H), 3.11-3.73 (m, 14H), 7.00 (d, <sup>3</sup>*J* = 8.2 Hz, 2H), 7.61 (d, <sup>3</sup>*J* = 8.2 Hz, 2H). – <sup>13</sup>C-NMR (75 MHz, CDCl<sub>3</sub>): δ = 28.5 (+, 6 C, CH<sub>3</sub>), 28.7 (+, 3 C, CH<sub>3</sub>), 47.9 (–, 2 C, CH<sub>2</sub>), 50.0 (–, 2 C, CH<sub>2</sub>), 54.8 (–, 2 C, CH<sub>2</sub>), 55.5(–, 2 C, CH<sub>2</sub>), 56.7(–, CH<sub>2</sub>), 79.5 (C<sub>quat</sub>, 3 C, C-Boc), 92.8 (C<sub>quat</sub>, C-Ar), 132.2 (+, 2 C, C-Ar), 136.7 (C<sub>quat</sub>, C-Ar), 137.2 (+, 2 C, C-Ar), 155.4 (C<sub>quat</sub>, NCOO<sup>t</sup>Bu), 155.7 (C<sub>quat</sub>, NCOO<sup>t</sup>Bu), 156.1 (C<sub>quat</sub>, NCOO<sup>t</sup>Bu). – MS (ESI/DCM/MeOH + 10 mmol/L NH<sub>4</sub>OAc): *m/z* = 689 [(M+H)<sup>+</sup>]. – C<sub>30</sub>H<sub>49</sub>IN<sub>4</sub>O<sub>6</sub> (688.65).



*[(4-Iodo-benzyl)-methoxycarbonylmethyl-amino]-acetic acid methylester (137):*

Dimethyl iminodiacetate hydrochloride (0.87 g, 4.4 mmol) and NaH (60 % suspension) (0.18 g, 4.4 mmol) were dissolved in MeCN (35 mL) and stirred for 5 min. K<sub>2</sub>CO<sub>3</sub> (2.42 g, 17.5 mmol) and *p*-iodobenzylbromide (1.00 g, 3.4 mmol) were added to this suspension. After completion of the reaction the mixture was filtered and concentrated. The crude product was purified by chromatography on silica gel (PE:DCM = 5:1 → EtOAc, *R<sub>f</sub>* = 0.44) yielding **137** (3.1 mmol, 1.49 g, 90 %) as a colourless oil.

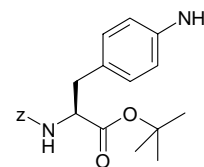
$^1\text{H}$ -NMR (300 MHz,  $\text{CDCl}_3$ ):  $\delta$  = 3.52 (s, 4H), 3.68 (s, 6H), 3.84 (s, 2H), 7.13 (d,  $^3J$  = 8.2 Hz, 2H), 7.62 (d,  $^3J$  = 8.2 Hz, 2H). –  $^{13}\text{C}$ -NMR (75 MHz,  $\text{CDCl}_3$ ):  $\delta$  = 51.6 (+, 2 C,  $\text{CH}_3$ ), 54.1 (–, 2 C,  $\text{CH}_2$ ), 57.3 (–,  $\text{CH}_2$ ), 92.9 ( $\text{C}_{\text{quat}}$ , C-Ar), 130.7 (+, 2 C, C-Ar), 137.2 ( $\text{C}_{\text{quat}}$ , C-Ar), 137.8 (+, 2 C, C-Ar), 171.5 ( $\text{C}_{\text{quat}}$ , 2 C, COOMe). – MS ( $\text{CI}/\text{NH}_3$ ):  $m/z$  = 378  $[(\text{M}+\text{H})^+]$ . –  $\text{C}_{13}\text{H}_{16}\text{INO}_4$  (377.18).



***Z*-*p*-Me-Phe-*O*<sup>t</sup>Bu (**131**):**

A *Schlenk* flask was charged with *p*-iodotoluene (0.34 g, 1.5 mmol),  $\text{Pd}_2(\text{dba})_3$  (40 mg, 2.5 mol%),  $\text{P}(\text{o-tol})_3$  (47 mg, 10 mol%),  $\text{CuBr}\cdot\text{DMS}$  (32 mg, 0.1 eq) and DME (4 mL). At  $-10\text{ }^\circ\text{C}$  a solution of the organozinc derivate of *Z*-*I*-Ala-*O*<sup>t</sup>Bu (1.2 mmol) in DME (4 mL) was added. The reaction mixture was slowly allowed to warm to r.t. over night. The reaction mixture was concentrated under argon and the solvent was removed in vacuum. EtOAc was added and the organic phase was washed twice with water and brine, the combined organic layers were dried over  $\text{MgSO}_4$  and concentrated. The crude resulting oil was purified by chromatography on silica gel (PE:EtOAc = 4:1,  $R_f$  = 0.28) affording **131** (0.79 mmol, 0.31 g, 66 %) as a colourless solid.

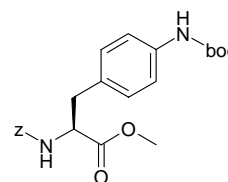
mp = 51-52  $^\circ\text{C}$ . –  $^1\text{H}$ -NMR (300 MHz,  $\text{CDCl}_3$ ):  $\delta$  = 1.41 (s, 9H), 2.31 (s, 3H), 3.04 (d,  $^3J$  = 5.5 Hz, 2H), 4.51 (dt,  $^3J$  = 5.9, 8.1 Hz, 1H), 5.10 (s, 2H), 5.21 (d,  $^3J$  = 8.2 Hz, 1H), 7.00-7.11 (m, 4H), 7.30-7.39 (m, 5H). –  $^{13}\text{C}$ -NMR (75 MHz,  $\text{CDCl}_3$ ):  $\delta$  = 21.1 (+,  $\text{CH}_3$ ), 28.0 (+, 3 C,  $\text{CH}_3$ ), 37.9 (–,  $\text{CH}_2$ ), 52.2 (+, CH), 66.8 (–,  $\text{CH}_2$ ), 82.3 ( $\text{C}_{\text{quat}}$ , C), 128.1 (+, 3 C, C-Ar), 128.5 (+, 2 C, C-Ar), 129.1 (+, 2 C, C-Ar), 129.4 (+, 2 C, C-Ar), 132.9 ( $\text{C}_{\text{quat}}$ , C-Ar), 136.4 ( $\text{C}_{\text{quat}}$ , C-Ar), 136.5 ( $\text{C}_{\text{quat}}$ , C-Ar), 143.4 (+, C-Ar), 155.6 ( $\text{C}_{\text{quat}}$ , COOBzl), 170.7 ( $\text{C}_{\text{quat}}$ , COO<sup>t</sup>Bu). – MS (ESI/ DCM/MeOH + 10 mmol/L  $\text{NH}_4\text{OAc}$ ):  $m/z$  = 756  $[(2\text{M}+\text{NH}_4)^+]$ , 387  $[(\text{M}+\text{NH}_4)^+]$ , 370  $[(\text{M}+\text{H})^+]$ . – Elemental anal. calcd. (%) for  $\text{C}_{22}\text{H}_{27}\text{NO}_4$  (369.46): C 71.52, H 7.37, N 3.79; found C 71.60, H 7.14, N 3.60.



***Z-p-NH<sub>2</sub>-Phe-O<sup>t</sup>Bu (132):***

A *Schlenk* flask was charged with *p*-iodoaniline (0.34 g, 1.5 mmol), Pd<sub>2</sub>(dba)<sub>3</sub> (40 mg, 2.5 mol%), P(o-tol)<sub>3</sub> (47 mg, 10 mol%), CuBr·DMS (32 mg, 0.1 eq), and DME (4 mL). At -10 °C a solution of the organozinc derivate of *Z-I-Ala-O<sup>t</sup>Bu* (1.2 mmol) in DME (4 mL) was added. The reaction mixture was slowly allowed to warm to r.t. over night. The reaction mixture was concentrated under argon and the solvent was removed under vacuum. EtOAc was added and the organic phase was washed twice with water and brine. The collected organic layers were dried over MgSO<sub>4</sub> and concentrated. The crude resulting oil was purified via chromatography on silica gel (PE:EtOAc = 3:2, *R<sub>f</sub>* = 0.2) affording the pure product **132** (0.88 mmol, 0.35 g, 73 %) as a glass.

<sup>1</sup>H-NMR (300 MHz, CDCl<sub>3</sub>): δ = 1.37 (s, 9H), 2.92 (d, <sup>3</sup>*J* = 5.8 Hz, 2H), 3.56 (bs, 2H), 4.41 (dt, <sup>3</sup>*J* = 5.9, 8.1 Hz, 1H), 5.05 (s, 2H), 5.15 (d, <sup>3</sup>*J* = 8.0 Hz, 1H), 6.54 (d, <sup>3</sup>*J* = 8.2 Hz, 2H), 6.87 (d, <sup>3</sup>*J* = 8.2 Hz, 2H), 7.25-7.35 (m, 5H). – <sup>13</sup>C-NMR (75 MHz, CDCl<sub>3</sub>): δ = 28.0 (+, 3 C, CH<sub>3</sub>), 37.5 (–, CH<sub>2</sub>), 55.3 (+, CH), 66.8 (–, CH<sub>2</sub>), 82.1 (C<sub>quat</sub>, C), 115.2 (+, 2 C, C-Ar), 125.8 (C<sub>quat</sub>, C-Ar), 128.1 (+, 3 C, C-Ar), 128.5 (+, 2 C, C-Ar), 128.6 (C<sub>quat</sub>, C-Ar), 130.4 (+, 2 C, C-Ar), 136.5 (C<sub>quat</sub>, C-Ar), 146.3 (C<sub>quat</sub>, C-Ar), 155.7 (C<sub>quat</sub>, COOBzl), 170.8 (C<sub>quat</sub>, COO<sup>t</sup>Bu). – MS (ESI DCM/MeOH + 10 mmol/L NH<sub>4</sub>OAc): *m/z* = 388 [(M+NH<sub>4</sub>)<sup>+</sup>], 371 [(M+H)<sup>+</sup>]. – Elemental anal. calcd. (%) for C<sub>21</sub>H<sub>26</sub>N<sub>2</sub>O<sub>4</sub> (370.45): C 68.09, H 7.07, N 7.56; found C 68.23, H 7.20, N 7.38.

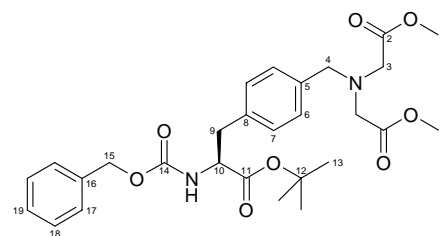


***Z-p-Boc-NH-L-Phe-OMe (133):***

A *Schlenk* flask was charged with (4-Iodo-phenyl)-carbamic acid *tert*-butylester (0.38 g, 1.2 mmol), Pd<sub>2</sub>(dba)<sub>3</sub> (40 mg, 2.5 mol%), P(o-tol)<sub>3</sub> (47 mg, 10 mol%), CuBr·DMS (32 mg, 0.1 eq), HMPT (2 mL), and THF (2 mL). At -10 °C a solution of the organozinc derivate of *Z-I-L-Ala-OMe* (1.1 mmol) in THF (2 mL) was added. The reaction mixture was slowly

allowed to warm to r.t. over night. The reaction mixture was concentrated under argon and the solvent was removed under vacuum. EtOAc was added and the organic phase was washed twice with water and brine. The collected organic layers were dried over  $\text{MgSO}_4$  and concentrated. The crude resulting oil was purified via chromatography on silica gel (PE:EtOAc = 2:1,  $R_f$  = 0.2) affording the pure product **133** (0.83 mmol, 0.39 g, 75 %) as a solid.

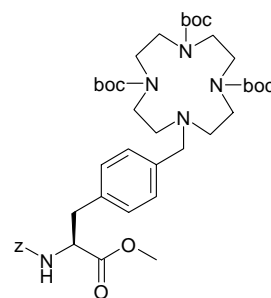
mp = 65-67 °C. –  $[\alpha]_D^{20}$  = + 3.0 (c 0.5 in  $\text{CHCl}_3$ ). –  $^1\text{H-NMR}$  (300 MHz,  $\text{CDCl}_3$ ):  $\delta$  = 1.51 (s, 9H), 2.97-3.13 (m, 2H), 3.71 (s, 3H), 4.57-4.68 (m, 1H), 5.09 (s, 2H), 5.21 (d,  $^3J$  = 8.2 Hz, 1H), 7.00 (d,  $^3J$  = 8.5 Hz, 2H), 7.27 (d,  $^3J$  = 8.2 Hz, 2H), 7.30-7.44 (m, 5H), 7.30-7.39 (m, 5H). –  $^{13}\text{C-NMR}$  (75 MHz,  $\text{CDCl}_3$ ):  $\delta$  = 28.3 (+, 3 C,  $\text{CH}_3$ ), 37.5 (–,  $\text{CH}_2$ ), 52.4 (+,  $\text{CH}_3$ ), 54.8 (+, CH), 67.0 (–,  $\text{CH}_2$ ), 80.6 ( $\text{C}_{\text{quat}}$ , C), 118.6 (+, 2 C, C-Ar), 128.1 (+, 3 C, C-Ar), 128.2 (+, C-Ar), 128.6 (+, 2 C, C-Ar), 129.9 (+, 2 C, C-Ar), 130.1 ( $\text{C}_{\text{quat}}$ , C-Ar), 136.2 ( $\text{C}_{\text{quat}}$ , C-Ar), 137.4 ( $\text{C}_{\text{quat}}$ , C-Ar), 152.7 ( $\text{C}_{\text{quat}}$ ,  $\text{COOBzl}$ ), 155.6 ( $\text{C}_{\text{quat}}$ ,  $\text{NCOO}^t\text{Bu}$ ), 172.0 ( $\text{C}_{\text{quat}}$ ,  $\text{COOMe}$ ). – MS (ESI DCM/MeOH + 10 mmol/L  $\text{NH}_4\text{OAc}$ ):  $m/z$  = 446  $[(\text{M}+\text{NH}_4)^+]$ , 429  $[(\text{M}+\text{H})^+]$ , 373  $[(\text{M}+\text{H}-\text{C}_4\text{H}_8)^+]$ , 329  $[(\text{M}+\text{H}-\text{Boc})^+]$ . – Elemental anal. calcd. (%) for  $\text{C}_{23}\text{H}_{28}\text{N}_2\text{O}_6$  (428.49): C 64.47, H 6.59, N 6.54; found C 64.30, H 6.27, N 6.19.



#### *Z-p-Me(IDA-OMe)-Phe-O<sup>t</sup>Bu (134):*

A *Schlenk* flask was charged with **137** (0.30 g, 1.2 mmol),  $\text{Pd}_2(\text{dba})_3$  (40 mg, 2.5 mol%),  $\text{P}(\text{o-tol})_3$  (47 mg, 10 mol%),  $\text{CuBr}\cdot\text{DMS}$  (32 mg, 0.1 eq), HMPT (2 mL), and THF (2 mL). At -10 °C a solution of the organozinc derivate of *Z-I-Ala-O<sup>t</sup>Bu* (1.2 mmol) in THF (4 mL) was added. The reaction mixture was slowly allowed to warm to r.t. over night. The reaction mixture was concentrated under argon and the solvent was removed under vacuum. EtOAc was added and the organic phase was washed twice with water and brine. The collected organic layers were dried over  $\text{MgSO}_4$  and concentrated. The crude resulting oil was purified via chromatography on silica gel (PE:EtOAc = 7:3,  $R_f$  = 0.18) affording the pure product **134** (0.78 mmol, 0.41 g, 65 %) as a glass.

$[\alpha]_D^{20} = + 14.6$  (c 0.5 in  $\text{CHCl}_3$ ).  $^1\text{H-NMR}$  (600 MHz,  $\text{CDCl}_3$ , HSQC):  $\delta = 1.42$  (s, 9H, H(13)), 3.09 (d,  $^3J = 5.7$  Hz, 2H, H(9)), 3.57 (s, 4H, H(3)), 3.72 (s, 6H, H(1)), 3.91 (s, 2H, H(4)), 4.51-4.57 (m, 1H, H(10)), 5.12 (s, 2H, H(15)), 5.25 (d,  $^3J = 7.7$  Hz, 1H, NH), 7.13 (d,  $^3J = 7.5$  Hz, 2H, H(6)), 7.31 (d,  $^3J = 7.6$  Hz, 2H, H(7)), 7.32-7.40 (m, 5H, H(17-19)). –  $^{13}\text{C-NMR}$  (150 MHz,  $\text{CDCl}_3$ , HSQC):  $\delta = 27.9$  (+, 3 C, C(13)), 38.1 (–, C(9)), 51.5 (+, 2 C, C(1)), 53.9 (–, C(3)), 55.2 (+, C(10)), 60.4 (–, C(4)), 66.8 (–, C(15)), 82.3 ( $\text{C}_{\text{quat}}$ , C(12)), 128.1 (+, 2 C, C(17)), 128.2 (+, C(19)), 128.5 (+, 2 C, C(7)), 129.1 (+, 2 C, C(18)), 129.6 (+, 2 C, C(6)), 135.3 ( $\text{C}_{\text{quat}}$ , C(8)), 136.0 ( $\text{C}_{\text{quat}}$ , C(16)), 136.4 ( $\text{C}_{\text{quat}}$ , C(5)), 155.6 ( $\text{C}_{\text{quat}}$ , C(14)), 170.5 ( $\text{C}_{\text{quat}}$ , C(11)), 171.5 ( $\text{C}_{\text{quat}}$ , 2 C, C(2)). – MS (ESI DCM/MeOH + 10 mmol/L  $\text{NH}_4\text{OAc}$ ):  $m/z = 529$  [(M+H) $^+$ ], 473 [(M+H-C $_4$ H $_8$ ) $^+$ ]. – Elemental anal. calcd. (%) for  $\text{C}_{28}\text{H}_{36}\text{N}_2\text{O}_8$  (528.61): C 63.62, H 6.86, N 5.30; found C 63.79, H 6.91, N 5.20.



***Z-p-Me(3-Boc-Cyc)-L-Phe-OMe (135):***

A *Schlenk* flask was charged with **136** (0.19 g, 0.28 mmol),  $\text{Pd}_2(\text{dba})_3$  (10 mg, 2.5 mol%),  $\text{P}(\text{o-tol})_3$  (12 mg, 10 mol%),  $\text{CuBr}\cdot\text{DMS}$  (8 mg, 0.1 eq), HMPT (2 mL), and THF (2 mL). At  $-10\text{ }^\circ\text{C}$  a solution of the organozinc derivate of *Z-I-L-Ala-OMe* (0.35 mmol) in of THF (2 mL) was added. The reaction mixture was slowly allowed to warm to r.t. over night. The reaction mixture was concentrated under argon and the solvent was removed under vacuum. EtOAc was added and the organic phase was washed twice with water and brine. The collected organic layers were dried over  $\text{MgSO}_4$  and concentrated. The crude resulting oil was purified via chromatography on silica gel (PE:EtOAc = 3:2,  $R_f = 0.16$ ) affording the pure product **135** (0.30 mmol, 0.19 g, 86 %) as a solid.

mp =  $56\text{--}57\text{ }^\circ\text{C}$ . –  $[\alpha]_D^{20} = + 40.4$  (c 0.5 in  $\text{CHCl}_3$ ). –  $^1\text{H-NMR}$  ( $\text{CDCl}_3$ , 300 MHz):  $\delta = 1.42$  (s, 9H), 1.47 (s, 18H), 2.53-2.79 (m, 4H), 3.03-3.11 (m, 2 H), 3.11-3.50 (m, 8H), 3.57 (bs, 4H), 3.69 (s, 3H), 4.57-4.70 (m, 1H), 5.08 (s, 2H), 5.21 (d,  $^3J = 7.7$  Hz, 1H), 7.02 (d,  $^3J = 8.0$  Hz, 2H), 7.16 (d,  $^3J = 8.0$  Hz, 2H), 7.30-7.44 (m, 5H), 7.30-7.38 (m, 5H). –  $^{13}\text{C-NMR}$  (75 MHz,  $\text{CDCl}_3$ ):  $\delta = 28.5$  (+, 6 C,  $\text{CH}_3$ ), 28.7 (+, 3 C,  $\text{CH}_3$ ), 37.9 (–,  $\text{CH}_2$ ), 47.3 (–,

2 C, CH<sub>2</sub>), 48.9 (–, 2 C, CH<sub>2</sub>), 49.5 (–, 2 C, CH<sub>2</sub>), 50.0 (–, 2 C, CH<sub>2</sub>), 52.3 (+, CH<sub>3</sub>), 54.8 (+, CH), 56.9 (–, CH<sub>2</sub>), 67.0 (–, CH<sub>2</sub>), 79.3 (C<sub>quat</sub>, 2 C, C-Boc), 79.4 (C<sub>quat</sub>, C-Boc), 128.1 (+, 2 C, C-Ar), 128.2 (+, C-Ar), 128.6 (+, 2 C, C-Ar), 129.1 (+, 2 C, C-Ar), 130.3 (C<sub>quat</sub>, C-Ar), 130.6 (+, C-Ar), 134.7 (C<sub>quat</sub>, C-Ar), 136.7 (C<sub>quat</sub>, 2 C, C-Ar), 155.6 (C<sub>quat</sub>, NCOO<sup>t</sup>Bu), 155.8 (C<sub>quat</sub>, NCOO<sup>t</sup>Bu), 156.1 (C<sub>quat</sub>, COOBzl), 171.9 (C<sub>quat</sub>, COOME). – HR-MS (EI/70 eV):  $m/z$  = calcd. for C<sub>42</sub>H<sub>63</sub>N<sub>5</sub>O<sub>10</sub> 797.4575; found 797.4559 ± 0.62 ppm.

### 3. Enhanced Peptide $\beta$ -Sheet Affinity by Metal to Ligand Coordination<sup>i</sup>

This chapter deals with the application of a C-terminal NTA recognition unit which is bound to MOPAS (= methoxy-pyrrole amino acids) units.<sup>ii</sup> These MOPAS building blocks bind to oligoamides inducing a  $\beta$ -sheet conformation. The resulting receptor oligopeptide was used to bind a pentapeptide. Within the receptor-peptide assembly the peptide backbone was forced to adapt a  $\beta$ -sheet conformation. The induced secondary structure of the peptide was examined by NMR-techniques.<sup>iii</sup>

---

<sup>i</sup> Kruppa, M.; Bonauer, C.; Michlova, V.; König, B, *J. Org. Chem.* **2005**, *Web Release Date: 25.05.2005*.

<sup>ii</sup> MOPAS building blocks were synthesised by C. Bonauer.

<sup>iii</sup> NMR measurements were performed by V. Michlova.



### 3.1 Introduction

Intramolecular processes are typically more favourable than intermolecular processes.<sup>1</sup> This includes the formation of weak reversible interactions such as hydrogen bonds. Recent studies on hydrogen bonding patterns complementary to peptide  $\beta$ -sheet structures<sup>2</sup> by Nowick,<sup>3</sup> Gellman,<sup>4</sup> and others<sup>5</sup> have taken advantage of this.<sup>6</sup> The peptide and its complementary binding sites are covalently linked by a turn structure allowing intramolecular hydrogen bond formation.<sup>7</sup> The selective binding of amino acid side chain functional groups, such as carboxyl-, ammonium-, phosphate- or imidazole-groups is an alternative way of peptide binding, which has been thoroughly investigated.<sup>8</sup> Schmuck *et al.*<sup>9</sup> recently reported the combination of a carboxyl-binding pyrrole guanidinium group with pyrazoles, which provides hydrogen bond donor and acceptor sites complementary to a peptide structure.<sup>10</sup> We report here a compound, which combines strong intermolecular coordination, with hydrogen bonds to create a synthetic peptide binding site. The concept is illustrated using a histidine-coordinating nitrilotriacetic acid (NTA) complex<sup>11</sup> and methoxy pyrrole amino acids (MOPAS) with peptide  $\beta$ -sheet binding ability. After complex formation the subsequent process of peptide backbone binding becomes intramolecular, facilitating hydrogen bond formation and control of the small peptide conformation in DMSO.

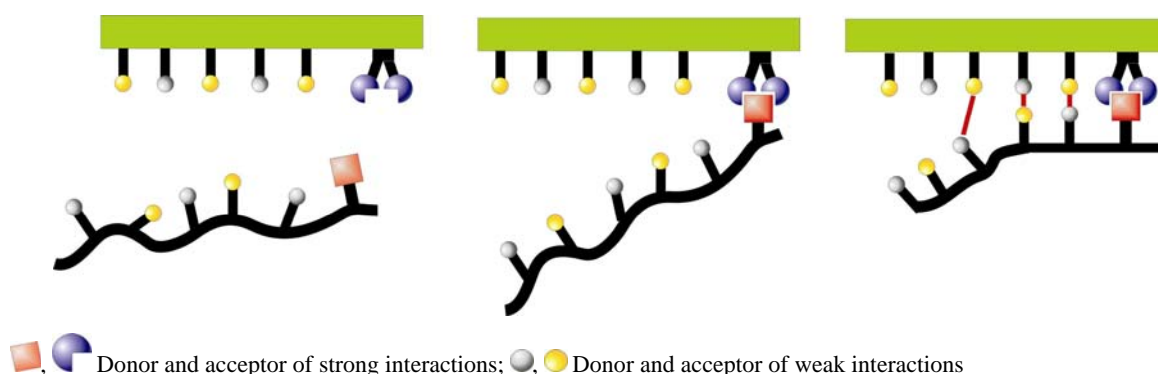
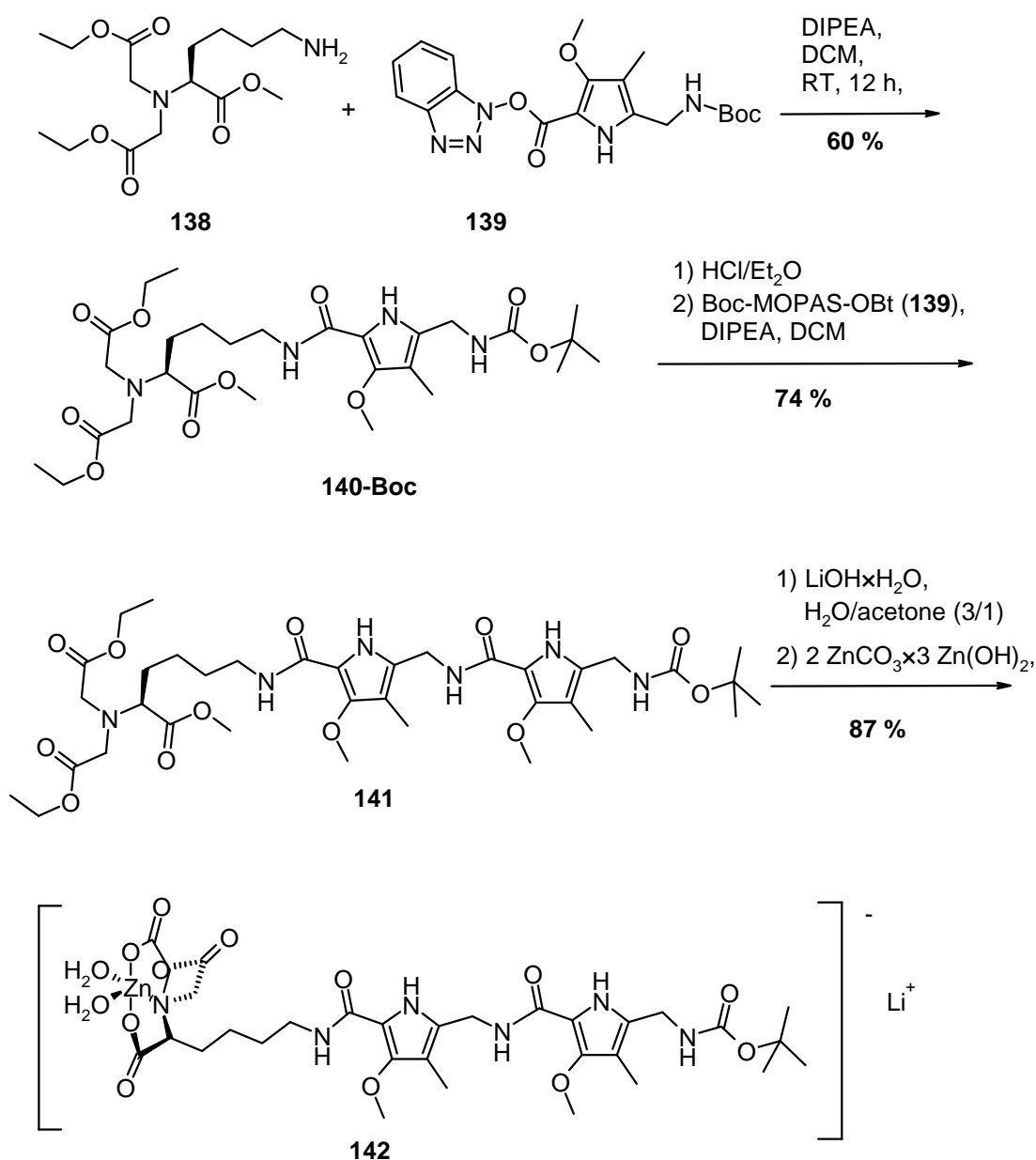


**Figure 92.** Schematic illustration of a binding process combining strong metal to ligand coordination and weaker interactions.

### 3.2 Results and Discussion

Scheme 49 shows the synthesis of the peptide binding complex **142**. Compound **138**,<sup>12</sup> obtained from lysine methyl ester, was coupled to activated ester **139**, which we have reported recently.<sup>5</sup> After Boc-deprotection a second MOPAS unit was introduced, again using compound **139**. Cleavage of the methyl/ethyl-ester under basic conditions generated the NTA ligand, from which the zinc complex **142** was obtained in good yield.

**Scheme 49.** Synthesis of complex **142**



Although Ni(II) or Cu(II) NTA complexes show higher affinities to *N*-terminal histidine, Zn(II) was chosen as metal ion for complex formation to obtain a diamagnetic compound, which allows spectroscopic investigation of the supramolecular structure with a bound peptide. The affinity of the Zn(II)-NTA complex to *N*-terminal histidine in DMSO<sup>13</sup> is still sufficiently high ( $K > 10^4$  L/mol) to ensure complete complex formation in a millimolar solution, which is necessary for NMR investigations. Pentapeptide H<sub>2</sub>N-His-Leu-Leu-Val-Phe-OMe<sup>14</sup> was used to investigate the binding properties of **142**. The NMR spectra of **142**-H<sub>2</sub>N-His-Leu-Leu-Val-Phe-OMe ( $c = 2.22 \cdot 10^{-2}$  mol/L), obtained by dissolving equimolar amounts of the receptor and the pentapeptide in DMSO [D<sub>6</sub>], shows a single set of resonances, which were structurally assigned. The temperature dependence of the chemical shifts confirmed the expected hydrogen bond interaction of the MOPAS amide NH to methoxy groups, which should keep the structure planar.<sup>15</sup>

**Table 24.** Temperature dependence of NH Signal shifts

	[ppb/K]
NH A	-4.1
NH B	-4.6*
NH C	-2.3
NH D	-5.4*
NH E	-2.3
NH F	-1.1
NH G	-5.4
NH H	-4.0
NH I	-2.8
NH J	-4.1
NH K	-5.6

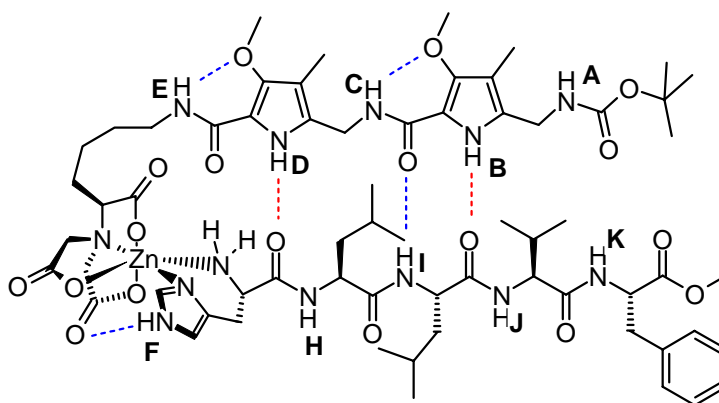


**Figure 93.** Hydrogen bonds as suggested from temperature dependence of chemical shifts (blue dotted lines). Red hydrogen bonds are expected, but without reference value for temperature dependence of chemical shift of hydrogen bound pyrrole NH no support can be derived from the experiment.

\* For NH B and NH D pyrrole hydrogen atoms, which are expected to form intrastrand hydrogen bonds to the pentapeptide, and for NH F imidazole hydrogen atom no reference values are known. So no conclusions can be derived from the temperature dependence.

A small ppb/K value for one of the central peptide amide protons indicates a possible hydrogen bond to a MOPAS carbonyl group. 2D NOESY spectra (see experimental

section) revealed four intrastrand contacts, which are indicated in figure 94.<sup>16</sup> This proves strong interactions between the bound pentapeptide and the MOPAS units.

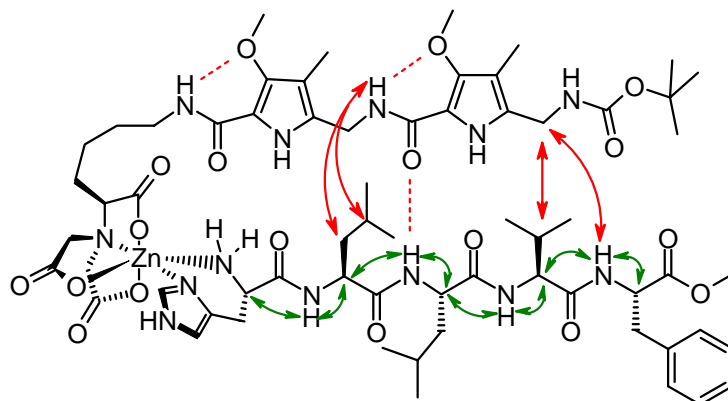


**Figure 94.** Spectroscopically detected interactions of **142** and H<sub>2</sub>N-His-Leu-Leu-Val-Phe-OMe in DMSO solution. Red dotted lines: Hydrogen bonding suggested from temperature dependence of chemical shift. Red arrows: Intrastrand NOE contacts. Green arrows: Intramolecular distances within the pentapeptide used for the determination of its conformation.

The interactions of the conformationally restricted MOPAS units with the bound pentapeptide induce a conformational preference of the peptide. To show this, intramolecular distances of the bound pentapeptide were derived from integrated NOESY spectra and used as constraints to calculate the solution structure of the pentapeptide bound to MOPAS complex **142** (see experimental section). Figure 95 shows the resulting pentapeptide structures, which have a  $\beta$ -sheet like conformation.<sup>17</sup> Distances of the derived structure correspond well with the experimental NOE values (see table 25).<sup>18</sup> As control experiments an equimolar mixture of the ligand of **142** without NTA-unit and the pentapeptide were investigated under identical conditions (see experimental section). No crosspeaks indicating close interactions between the peptide and the MOPAS units could be detected. Intramolecular NOE's within the peptide were of low intensity, again showing a flexible conformation.<sup>19</sup>

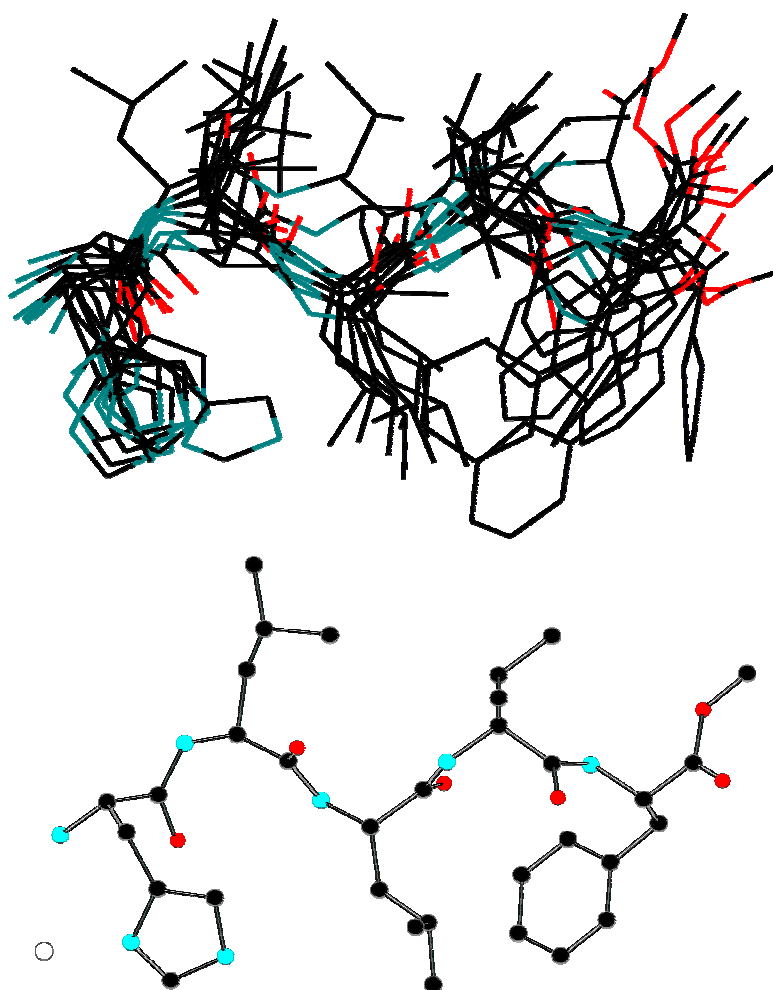


**Figure 95.** Structure of H<sub>2</sub>N-His-Leu-Leu-Val-Phe-OMe bound to **142**. Top: Overlaid structures from MD simulation; bottom: Minimized average structure.

**Table 25.** Distances within the assembly of H<sub>2</sub>N-His-Leu-Leu-Val-Phe-OMe and **142**

Interacting protons	distance from NOE [Å]	distance of average structure
NH G – 24'	2.8	2.5
NH H – 24'	2.1	2.3
NH H – 19'	2.8	2.9
NH I – 19'	2.1	2.2
NH I – 14'	2.8	2.9
NH J – 14'	2.0	2.2
NH J – 10'	2.9	3.0
NH K – 10'	2.1	2.2
NH K – 3'	2.8	3.0

### 3.3 Conclusion

*Mallik and Srivastava*<sup>20</sup> recently reported the significantly enhanced binding affinity of an inhibitor of carbonic anhydrase II by attaching a metal complex tether, which interacts with surface-exposed histidine residues. Our experiments have now shown that by combining a Zn-NTA tether with a heterocyclic peptide  $\beta$ -sheet binder, it is possible to restrict the conformation of a small flexible pentapeptide in DMSO solution. Intermolecular interactions of the MOPAS units with the pentapeptide in DMSO would be too weak to induce a conformational preference. The principle of “two-prong” binders is applicable to other peptide receptors, which suffer from competing solvent interactions. Exchanging Zn(II) in **142** by Cu(II) or Ni(II) leads to peptide-binding compounds with an affinity to H<sub>2</sub>N-His-Leu-Leu-Val-Phe-OMe in the lower micromolar range<sup>21</sup> under aqueous physiological conditions. Other amino acid residues than imidazole can be targeted using other transition metal ion conjugates.<sup>22</sup> This allows selective recognition and conformational control of small peptides in biological environment.

## References:

---

- <sup>1</sup> Typical examples are cycloadditions or cyclisation reactions and intramolecular folding.
- <sup>2</sup> One important motivation to develop synthetic binding sites for peptide  $\beta$ -sheets is the interception of prion protein aggregation. (a) Kirsten, C.N.; Schrader, T.H. *J. Am. Chem. Soc.* **1997**, *119*, 1206. (b) Wehner, M.; Schrader, T. *Angew. Chem. Int. Ed.* **2002**, *41*, 1751. (c) Cernovska, K.; Kemter, M.; Gallmeier, H.-C.; Rzepecki, P.; Schrader, T.H.; König, B. *Org. Biomol. Chem.* **2004**, *2*, 1603.
- <sup>3</sup> (a) Nowick, J.S.; Chung, D.M. *Angew. Chem., Intl. Ed.* **2003**, *42*, 1765. (b) Chung, D.M.; Nowick, J.S. *J. Am. Chem. Soc.* **2004**, *126*, 3062. (c) Nowick, J.S.; Lam, S.K.; Khasanova, T.V.; Kemnitzer, W.E.; Maitra, S.; Mee, H. T.; Liu, R. *J. Am. Chem. Soc.* **2002**, *124*, 4972. (d) Chung, D.M.; Nowick, J.S. *J. Am. Chem. Soc.* **2004**, *126*, 3062.
- <sup>4</sup> (a) Woll, M.G.; Lai, J.R.; Guzei, I.A.; Taylor, S.J.C.; Smith, M.E.B.; Gellman, S.H. *J. Am. Chem. Soc.* **2001**, *123*, 11077. (b) Fisk, J.D.; Gellman, S.H. *J. Am. Chem. Soc.* **2001**, *123*, 343. (c) Huck, B.R.; Fisk, J.D.; Gellman, S.H. *Org. Lett.* **2000**, *2*, 2607.
- <sup>5</sup> Bonauer, C.; Zabel, M.; König, B. *Org. Lett.* **2004**, *9*, 1349.
- <sup>6</sup> Many examples of intermolecular  $\beta$ -sheet binders based on complementary hydrogen bonding patterns have been reported, but their use is mostly restricted to non-polar solvents, which do not intercept the hydrogen bonds.
- <sup>7</sup> Nowick, J.S.; Brower, J.O. *J. Am. Chem. Soc.* **2003**, *125*, 876.
- <sup>8</sup> Such ionic interactions provide much higher affinity than hydrogen bonds and allow peptide binding in polar solvents. Examples of carboxyl group binding: (a) Peczuh, M.W.; Hamilton, A.D.; Sánchez-Quesada, J.; de Mendoza, J.; Haack, T.; Giralt, E. *J. Am. Chem. Soc.* **1997**, *119*, 9327. Example of phosphate-binding: (b) Ojida, A.; Mito-oka, Y.; Sada, K.; Hamachi, I. *J. Am. Chem. Soc.* **2004**, *126*, 2454. Examples of ammonium-group binding: (c) Hossain, M.A.; Schneider, H.-J. *J. Am. Chem. Soc.* **1998**, *120*, 11208. (d) Herm, M.; Molt, O.; Schrader, T.H. *Chem. Eur. J.* **2002**, *8*, 1485. Examples of binding to hydrophobic groups or areas: (e) Breslow, R.; Yang, Z.; Ching, R.; Trojandt, G.; Odobel, F. *J. Am. Chem. Soc.* **1998**, *120*, 3536. (f) Baldini, L.; Wilson, A.J.; Hong, J.; Hamilton, A.D. *J. Am. Chem. Soc.* **2004**, *126*, 5656. (g) Jain, R.K.; Hamilton, A.D. *Org. Lett.* **2000**, *2*, 1721. (h) Ernst, J.T.; Kutzki, O.; Debnath, A.K.; Jiang, S.; Lu, H.; Hamilton, A.D. *Angew. Chem. Int. Ed.* **2002**, *41*, 117. (i) Jasper, C.; Schrader, T.; Panitzky, J.; Klärner, F.-G. *Angew. Chem. Int. Ed.* **2002**, *41*, 1355. (k) Malinovski, V.; Tumir, L.; Piantanida, I.; Zinic, M.; Schneider, H.-J. *Eur. J. Org. Chem.* **2002**, 3785.
- <sup>9</sup> Schmuck, C.; Geiger, L. *J. Am. Chem. Soc.* **2004**, *126*, 8898.
- <sup>10</sup> Other examples of combined use of different reversible interaction: Ligand to metal coordination and ionic interaction: (a) Wright, A.T.; Anslyn, E.V. *Org. Lett.* **2004**, *6*, 1341. Ligand to metal coordination and hydrogen bonding: (b) Tobey, S.L.; Anslyn, E.V. *J. Am. Chem. Soc.* **2003**, *125*, 14807. Guanidinium ion and boronic acid: (c) Wiskur, S.L.; Lavigne, J.J.; Metzger, A.; Tobey, S.L.; Lynch, V.; Anslyn, E.V. *Chem. Eur. J.* **2004**, *10*, 3792. (d) Tobey, S.L.; Anslyn, E.V. *J. Am. Chem. Soc.* **2003**, *125*, 14807. (e) Shirin, Z.; Hammes, B.S.; Young, V.G.; Borovik, A.S. *J. Am. Chem. Soc.* **2000**, *122*, 1836. (f) MacBeth, E.C.; Hammes, B.S.; Young, V.G.; Borovik, A.S. *Inorg. Chem.* **2001**, *40*, 4733.

- 
- <sup>11</sup>(a) Beauchamp, A.L.; Israeli, J.; Saulnier, H. *Can. J. Chem.* **1969**, *47*, 1269. (b) Hopgood, D.; Angelici, R.J. *J. Am. Chem. Soc.* **1968**, *90*, 2508.
- <sup>12</sup>Hart, B. R.; Shea, K. J. *J. Am. Chem. Soc.* **2001**, *123*, 2072.
- <sup>13</sup>In neutral aqueous solution the affinity of **142** to the pentapeptide is too small to be accurately determined by microcalorimetry, which has its limit at about 10<sup>3</sup> L/mol with our apparatus.
- <sup>14</sup>The methyl ester was used to avoid any additional ionic interactions of the carboxylate group.
- <sup>15</sup>This concept of using intramolecular hydrogen bonds to planarise  $\beta$ -sheet mimic was extensively used by Nowick in methoxy-substituted hydrazine benzoic acids.
- <sup>16</sup>Overlap of resonance signals restricts the number of detectable cross peaks.
- <sup>17</sup>Due to signal broadening and overlap with receptor resonance signals it was not possible to determine  $^3J_{\text{NHH}\alpha}$  coupling constants of the aggregate. The  $^3J_{\text{NHH}\alpha}$  coupling constants of the non-bound pentapeptide are given in the supporting information.
- <sup>18</sup>The importance to compare modeling results with primary derived data was recently described. Glättli, A.; van Gunsteren, W. F. *Angew. Chem.* **2004**, *116*, 6472.
- <sup>19</sup>The absence of intermolecular contacts shows that no aggregates are formed between peptides or peptide and MOPAS under the experimental conditions.
- <sup>20</sup>(a) Banerjee, A.L.; Swanson, M.; Roy, B.C.; Jia, X.; Haldar, M.K.; Mallik, S.; Srivastava, D.K. *J. Am. Chem. Soc.* **2004**, *126*, 10875. (b) Roy, B.C.; Banerjee, A.L.; Swanson, M.; Jia, X.G.; Haldar, M.K.; Mallik, S.; Srivastava, D.K. *J. Am. Chem. Soc.* **2004**, *126*, 13206.
- <sup>21</sup>The affinity was determined by microcalorimetry. Paramagnetism of the copper complex and substantial line broadening in the nickel complex, so far prevent a detailed investigation of the structure inducing effect of the receptor on the pentapeptide in water.
- <sup>22</sup>Ojida, A.; Miyahara, Y.; Kohira, T.; Hamachi, I. *Biopolymers* **2004**, *76*, 177.



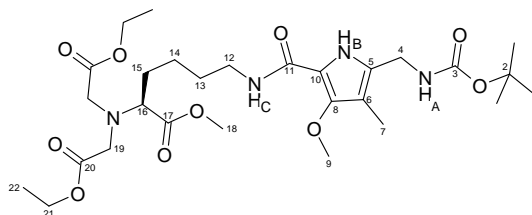
## 3.4 Experimental Section

### 3.4.1 Instruments and general techniques

See experimental section of chapter 1 (page 131).

### 3.4.2 Synthesis

Compounds **138**<sup>iv</sup> and Boc-MOPAS-OBt (**139**)<sup>v</sup> were prepared as previously reported.



#### *Et/Me-NTA-MOPAS-BOC (140-Boc):*

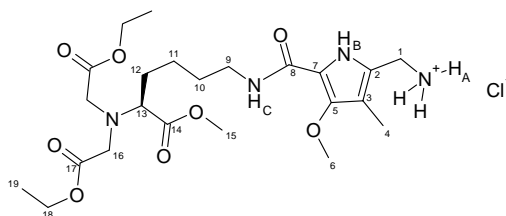
Boc-MOPAS-OBt (72 mg, 0.18 mmol) was dissolved in DCM (15 mL). After the solution was cooled to 0 °C, **138** (55 mg, 0.15 mmol) and DIPEA (0.07 mL, 0.4 mmol) were added. The ice bath was removed and the reaction mixture was stirred for 24 h. The resulting product was extracted twice with 5% aqueous KHSO<sub>4</sub> (25 mL), once with water (25 mL) and twice with 0.5 M aqueous NaHCO<sub>3</sub> (25 mL) solution. After drying over Na<sub>2</sub>SO<sub>4</sub>, evaporation of the solvent and subsequent column chromatography on silica (EtOAc, *R<sub>f</sub>* = 0.64) gave **140-Boc** (0.09 mmol, 54 mg, 60 %) as a yellow oil.

<sup>1</sup>H-NMR (400 MHz, CDCl<sub>3</sub>, COSY): δ = 1.18 (t, <sup>3</sup>*J* = 7.2 Hz, 6 H; H(22)), 1.29-1.50 (m, 11 H; H(1) + H(14)), 1.51-1.60 (m, 2 H; H(13)), 1.62-1.74 (m, 2 H; H(15)), 2.01 (s, 3 H; H(7)), 3.30-3.38 (m, 2 H; H(12)), 3.37 (t, <sup>3</sup>*J* = 7.4 Hz, 1 H; H(16)), 3.54-3.59 (m, 4 H; H(19)), 3.61 (s, 3 H; H(18)), 3.79 (s, 3 H; H(9)), 4.07 (q, <sup>3</sup>*J* = 7.2 Hz, 4 H; H(21)), 4.11-4.20 (m, 2 H; H(4)), 5.74-5.84 (m, 1 H; H<sub>A</sub>), 6.91-7.01 (m, 1 H; H<sub>C</sub>), 10.25 (bs, 1 H; H<sub>B</sub>). –  
<sup>13</sup>C-NMR (150 MHz, CDCl<sub>3</sub>, HSQC, HMBC): δ = 8.1 (+, C(7)), 14.2 (+, 2 C, C(22)), 23.4 (–, C(14)), 28.4 (+, C(1)), 29.6 (–, C(3)), 30.2 (–, C(15)), 35.4 (–, C(4)), 38.8 (–, C(11)), 51.4 (+, C(18)), 52.6 (–, 2 C, C(19)), 60.5 (–, 2 C, C(21)), 61.4 (–, C(9)), 64.7 (+, C(16)), 79.2 (C<sub>quat</sub>, C(2)), 107.9 (C<sub>quat</sub>, C(6)), 112.4 (C<sub>quat</sub>, C(10)), 128.7 (C<sub>quat</sub>, C(5)), 147.0 (C<sub>quat</sub>, C(8)), 155.9 (C<sub>quat</sub>, C(3)), 161.5 (C<sub>quat</sub>, C(11)), 171.3 (C<sub>quat</sub>, 2 C, C(20)), 173.0 (C<sub>quat</sub>,

<sup>iv</sup> Hart, B.R.; Shea, K.J. *J. Am. Chem. Soc.* **2001**, *123*, 2072.

<sup>v</sup> Bonauer, C.; Zabel, M.; König, B. *Org. Lett.* **2004**, *9*, 1349.

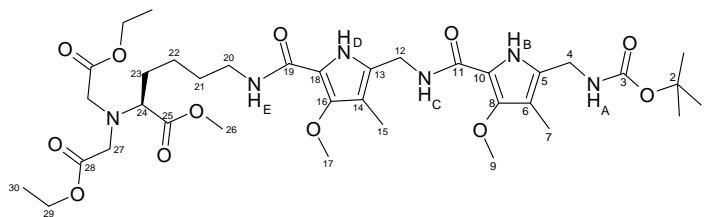
C(17)). – IR (KBr) [ $\text{cm}^{-1}$ ]:  $\tilde{\nu}$  = 3426, 3074, 2951, 1744, 1680, 1534, 1218, 1025. – MS (ESI,  $\text{H}_2\text{O}/\text{MeOH}$  + 10 mmol/L  $\text{NH}_4\text{Ac}$ ):  $m/z$  (%) = 637 (12) [ $\text{MK}^+$ ], 621 (22) [ $\text{MNa}^+$ ], 599 (100) [ $\text{MH}^+$ ] – Elemental analysis calcd (%) for  $\text{C}_{28}\text{H}_{46}\text{N}_4\text{O}_{10}$  (598.7): C 56.17, H 7.74, N 9.36; found C 55.68, H 7.66, N 9.27.



***Et/Me-NTA-MOPAS-NH<sub>2</sub>·HCl (140-H):***

Compound **140-Boc** (81 mg, 0.14 mmol) was dissolved in  $\text{Et}_2\text{O}$  (5 mL) and cooled to 0 °C in ice. To deprotect the Boc-group HCl saturated  $\text{Et}_2\text{O}$  was added drop wise until the product started to precipitate. The ice bath was removed and the reaction progress monitored by TLC ( $\text{EtOAc}$ ). After 90 min the solvent was evaporated. Compound **140-H** (0.14 mmol, 75 mg, 100 %) was isolated as a very hygroscopic colourless solid.

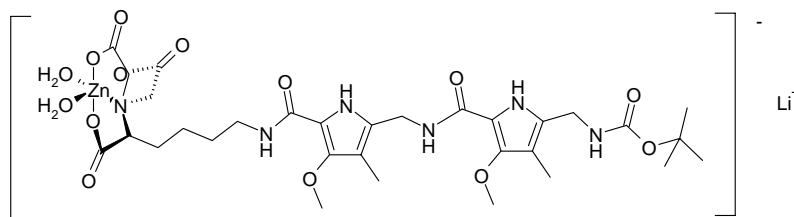
mp 81-83 °C. –  $^1\text{H-NMR}$  (400 MHz,  $[\text{D}_6]\text{-DMSO}$ , COSY, HMBC, HSQC):  $\delta$  = 1.17 (t,  $^3J$  = 7.1 Hz, 6 H; H(19)), 1.21-1.41 (m, 2 H; H(11)), 1.49 (m, 2 H; H(10)), 1.60 (m, 2 H; H(12)), 2.01 (s, 3 H; H(4)), 3.23 (m, 2 H; H(9)), 3.39 (m, 1 H; H(13)), 3.50-3.65 (m, 7 H; H(16), H(15)), 3.75 (s, 3 H; H(6)), 3.88 (m, 2 H; H(1)), 4.04 (q,  $^3J$  = 7.1 Hz, 4 H; H(18)), 6.35 (bs, 6 H), 7.14 (m, 1 H;  $\text{H}_\text{C}$ ), 8.29 (m, 3 H;  $\text{H}_\text{A}$ ), 10.93 (s, 1 H;  $\text{H}_\text{B}$ ). –  $^{13}\text{C-NMR}$  (100 MHz,  $[\text{D}_6]\text{-DMSO}$ , HMBC, HSQC):  $\delta$  = 7.7 (+, C(4)), 13.9 (+, 2 C, C(19)), 22.6 (–, C(11)), 29.1 (–, C(10)), 29.3 (–, C(12)), 33.1 (–, C(1)), 37.9 (–, C(9)), 51.0 (+, C(15)), 52.1 (–, 2 C, C(16)), 59.8 (–, 2 C, C(18)), 61.3 (+, C(6)), 63.7 (+, C(13)), 110.1 ( $\text{C}_{\text{quat}}$ , C(3)), 113.8 ( $\text{C}_{\text{quat}}$ , C(7)), 121.8 ( $\text{C}_{\text{quat}}$ , C(2)), 145.7 ( $\text{C}_{\text{quat}}$ , C(5)), 159.5 ( $\text{C}_{\text{quat}}$ , C(8)), 170.7 ( $\text{C}_{\text{quat}}$ , C(8)), 170.7 ( $\text{C}_{\text{quat}}$ , 2 C, C(17)), 172.3 ( $\text{C}_{\text{quat}}$ , C(14)). – IR (KBr) [ $\text{cm}^{-1}$ ]:  $\tilde{\nu}$  = 3429, 3010, 2928, 1744, 1631, 1547, 1227. – MS (ESI,  $\text{CH}_2\text{Cl}_2/\text{MeOH}$  + 10 mmol/L  $\text{NH}_4\text{Ac}$ ):  $m/z$  (%) = 521 (64) [ $\text{MNa}^+$ ], 499 (100) [ $\text{MH}^+$ ]. – Elemental analysis calcd. (%) for  $\text{C}_{23}\text{H}_{39}\text{N}_4\text{O}_8\text{Cl}$  (534.25) +  $\text{H}_2\text{O}$ : C 49.98, H 7.48, N 10.14; found C 49.92, H 7.37, N 10.08.



*Et/Me-NTA-MOPAS-MOPAS-Boc (141):*

Compound **140-H** (0.14 g, 0.27 mmol) was dissolved in DCM (15 mL). After the solution was cooled to 0 °C Boc-*MOPAS*-OBt (0.16 g, 0.40 mmol) and DIPEA (0.12 mL, 0.7 mmol) were added. The ice bath was removed and the reaction mixture was stirred for 24 h. The resulting product was extracted twice with 5% aqueous KHSO<sub>4</sub> (25 mL), once with water (25 mL) and twice with 0.5 M aqueous NaHCO<sub>3</sub> (25 mL) solution. After drying over Na<sub>2</sub>SO<sub>4</sub>, the solvent was evaporated in vacuum and column chromatography on silica gel (PE:EtOAc = 1:1, *R<sub>f</sub>* (EtOAc) = 0.60) yielded **141** (0.20 mmol, 153 mg, 74 %) as a slightly yellow oil.

<sup>1</sup>H-NMR (400 MHz, CDCl<sub>3</sub>, COSY): δ = 1.23 (t, <sup>3</sup>*J* = 7.0 Hz, 6 H; H(30)), 1.34-1.55 (m, 11 H; H(1) + H(22)), 1.57-1.67 (m, 2 H; H(21)), 1.72-1.86 (m, 2 H; H(23)), 2.00 (s, 3 H; H(7)), 2.13 (s, 3 H; H(15)), 3.38-3.47 (m, 3 H; H(24) + H(20)), 3.61 (s, 3 H; H(17)), 3.62 (s, 4 H; H(27)), 3.65 (s, 3 H; H(26)), 3.88 (s, 3 H; H(9)), 4.12 (q, <sup>3</sup>*J* = 7.0 Hz, 4 H; H(29)), 4.19 (d, <sup>3</sup>*J* = 5.6 Hz, 2 H; H(12)), 4.72 (d, <sup>3</sup>*J* = 4.8 Hz, 2 H; H(4)), 6.14-6.21 (m, 1 H; H<sub>C</sub>), 6.96 (t, <sup>3</sup>*J* = 4.9 Hz, 1 H; H<sub>A</sub>), 7.12 (t, <sup>3</sup>*J* = 5.7 Hz, 1 H; H<sub>E</sub>), 11.1 (bs, 1 H; H<sub>B</sub>), 11.46 (bs, 1 H; H<sub>D</sub>). – <sup>13</sup>C-NMR (100 MHz, CDCl<sub>3</sub>, HSQC + HMBC): δ = 7.9 (+, C(7)), 8.2 (+, C(15)), 14.2 (+, 2 C, C(30)), 23.4 (–, C(22)), 28.4 (+, C(1)), 29.5 (–, C(21)), 30.3 (–, C(23)), 34.3 (–, C(4)), 35.3 (–, C(12)), 38.8 (–, C(20)), 51.4 (+, C(26)), 52.6 (–, 2 C, C(27)), 60.5 (–, 2 C, C(29)), 61.2 (+, C(17)), 61.4 (+, C(9)), 64.7 (+, C(24)), 78.9 (C<sub>quat</sub>, C(2)), 107.6 (C<sub>quat</sub>, C(6)), 108.3 (C<sub>quat</sub>, C(14)), 112.2 (C<sub>quat</sub>, C(10) + C(18)), 128.0 (C<sub>quat</sub>, C(13)), 129.1 (C<sub>quat</sub>, C(5)), 147.1 (C<sub>quat</sub>, C(16)), 147.5 (C<sub>quat</sub>, C(8)), 155.8 (C<sub>quat</sub>, C(11)), 160.8 (C<sub>quat</sub>, C(3)), 161.9 (C<sub>quat</sub>, C(19)), 171.3 (C<sub>quat</sub>, 2 C, C(28)), 173.0 (C<sub>quat</sub>, C(25)). – IR (KBr) [cm<sup>–1</sup>]:  $\tilde{\nu}$  = 3425, 3032, 2960, 1731, 1679, 1580, 1012. – MS (ESI, CH<sub>2</sub>Cl<sub>2</sub>/MeOH + 10 mmol/L NH<sub>4</sub>Ac): *m/z* (%) = 803 (15) [MK<sup>+</sup>], 787 (43) [MNa<sup>+</sup>], 766 (100) [MH<sup>+</sup>].



*Li[Zn(NTA-MOPAS-MOPAS-Boc)(H<sub>2</sub>O)<sub>2</sub>] (142):*

To a solution of **141** (0.12 g, 0.15 mmol) in 25% water/acetone (20 mL) was added LiOH·H<sub>2</sub>O (19 mg, 0.45 mmol). The reaction mixture was stirred for 12 h at r.t., acetone was removed in vacuum and the remaining solvent lyophilised. The crude carboxylate and basic zinc carbonate (27 mg, 0.05 mmol) were dissolved in water (20 mL). After stirring for 30 min at r.t. the suspension was heated to 60 °C for 1 d. Insoluble particles were filtered off and the filtrate was lyophilised. The raw product was suspended in ethanol followed by the addition of ether. The precipitated material was separated from solution by centrifugation to give **142** (0.13 mmol, 103 mg, 86 %), as a colorless solid.

mp > 200 °C. – MS (ESI, H<sub>2</sub>O/MeOH + 10 mmol/l NH<sub>4</sub>Ac): *m/z* (%) = 755 (100) [M-2H<sub>2</sub>O]<sup>-</sup>, 757 (100) [MH<sub>2</sub>-2H<sub>2</sub>O]<sup>+</sup>. – IR (KBr) [cm<sup>-1</sup>]:  $\tilde{\nu}$  = 3384, 2972, 2932, 1701, 1624, 1537. FAB NI-LSIMS (MeOH/glycerine) HRMS (C<sub>31</sub>H<sub>45</sub>N<sub>6</sub>O<sub>12</sub>Zn [A- + 2H<sup>+</sup>]<sup>+</sup>) calcd. 757.2387; found 757.2381+/- 0.0015.

### 3.4.3 Structure determination

#### Preparation of the assembly:

The MOPAS receptor (**142**) and the pentapeptide were mixed in a molar ratio 1:1 and dissolved in approx. 0.7 mL of [D<sub>6</sub>]-DMSO to reach a concentration of 22 mmol/L. The NMR experiments were performed in a tube with an inside diameter of 5 mm. To remove oxygen the sample was degassed in three freeze-thaw cycles in liquid nitrogen.

#### Assignment of resonance signals

Complete <sup>1</sup>H and <sup>13</sup>C resonance assignments were done using conventional 2D techniques (COSY, HMQC and HMBC experiments).

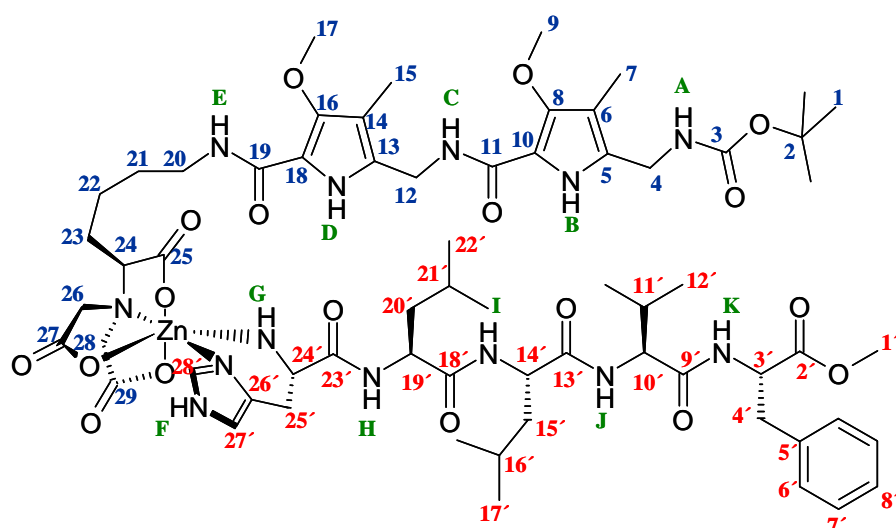


**Figure 96.** Numbering of **142**-His-Leu-Leu-Val-Phe-OMe used for NMR assignments.

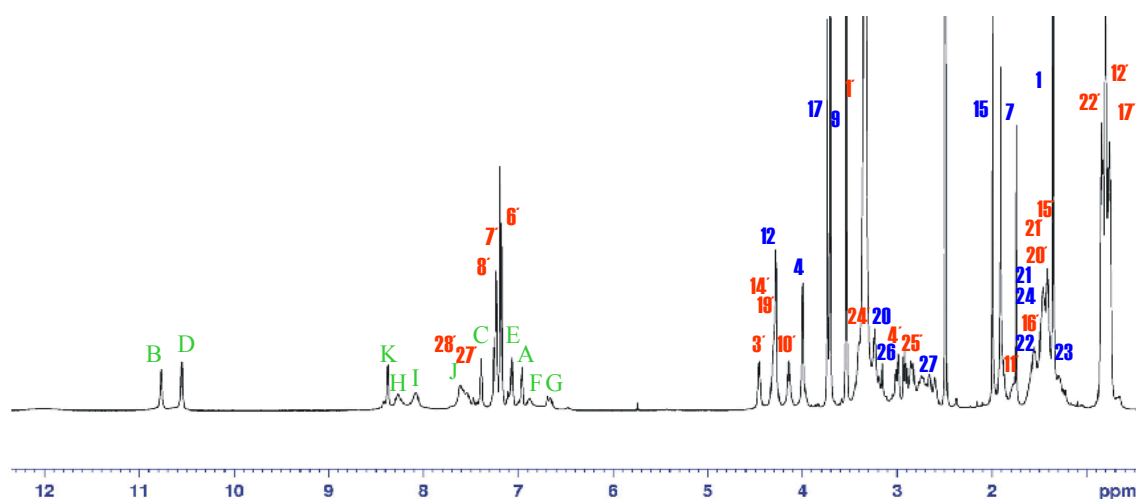


**Figure 97.** <sup>1</sup>H NMR spectrum of **142**-His-Leu-Leu-Val-Phe-OMe in [D<sub>6</sub>]-DMSO.

**142-His-Leu-Leu-Val-Phe-OMe:**  $^1\text{H}$  NMR (600 MHz;  $[\text{D}_6]$ -DMSO; COSY):  $\delta$  = 0.77 (m, 6H, H(22')), 0.79/0.84 (m, 6H, H(12')), 0.82 (m, 6H, H(17')), 1.28 (m, 2H, H(23)), 1.35 (s, 9H, H(1)), 1.42 (m, 2H, H(15')), 1.45 (m, 2H, H(20')), 1.47 (q, 2H, H(21)), 1.48 (m, 2H, H(21')), 1.55 (d, 2H, H(16')), 1.58 (m, 2H, H(24)), 1.77 (m, 2H, H(22)), 1.88 (m, 1H, H(11')), 1.9 (s, 3H, H(7)), 1.99 (s, 3H, H(15)), 2.59/2.85 (dd, 2H, H(25')), 2.92/2.99 (dd, 2H, H(4')), 2.78/3.08 (m, 2H, H(26)), 2.7/3.17 (m, 2H, H(28)), 3.23 (m, 2H, H(20)), 3.38 (m, 1H, H(24')), 3.53 (s, 3H, H(1')), 3.70 (s, 3H, H(17)), 3.73 (s, 3H, H(9)), 3.99 (d, 2H, H(4)), 4.14 (d, 1H, H(10')), 4.27 (d, 2H, H(12)), 4.29 (m, 1H, H(19')), 4.30 (m, 1H, H(14')), 4.45 (q, 1H, H(3')), 6.48/6.67 (bs, 1H, H<sub>G</sub>), 6.89 (bs, 1H, H<sub>F</sub>), 6.96 (bs, 1H, H<sub>A</sub>), 7.06 (bs, 1H, H<sub>E</sub>), 7.18 (d, 1H, H(6')), 7.22 (m, 1H, H(8')), 7.24 (d, 1H, H(7')), 7.39 (bs, 1H, H<sub>C</sub>), 7.47 (m, 1H, H(27')), 7.54 (bs, 1H, H<sub>I</sub>), 7.61 (m, 1H, H(28')), 8.07 (bs, 1H, H<sub>I</sub>), 8.30 (bs, 1H, H<sub>H</sub>), 8.38 (d, 1H, H<sub>K</sub>), 10.45 (s, 1H, H<sub>B</sub>), 10.54 (s, 1H, H<sub>D</sub>).  $^{13}\text{C}$ -NMR (150 MHz;  $[\text{D}_6]$ -DMSO; HMQC + HMBC):  $\delta$  = 7.4 (C(7)), 7.6 (C(15)), 17.8 + 18.8 (C(12')), 21.4 (C(17')), 21.7 (C(22')), 23.9 (C(21')), 23.9 (C(16')), 25.5 (C(23)), 25.6 (C(24)), 27.9 (C(1)), 29.6 (C(21)), 26.3 (C(22)), 30.5 (C(11')), 33.0 (C(12)), 36.8 (C(4')), 36.8 (C(25')), 37.8 (C(20)), 34.9 (C(4)), 40.1 (C(15')), 40.8 (C(20')), 50.3 (C(19')), 50.7 (C(14')), 51.5 (C(1')), 53.1 (C(3')), 54.6 (C(24')), 56.5 (C(26)), 56.8 (C(28)), 56.9 (C(10')), 61.5 (C(9)), 61.6 (C(17)), 78.2 (C(2)), 107.4 (C(6)), 107.6 (C<sub>quat</sub>, C(14)), 125.7 (C<sub>quat</sub>, C(7')), 127.2 (C<sub>quat</sub>, C(6')), 127.3 (C<sub>quat</sub>, C(8')), 128.0 (C<sub>quat</sub>, C(27')), 128.4 (C<sub>quat</sub>, C(5')), 128.4 (C<sub>quat</sub>, C(13)), 128.7 (C<sub>quat</sub>, C(5)), 129.1 (C<sub>quat</sub>, C(18)), 134.9 (C<sub>quat</sub>, C(28')), 126.6 (C<sub>quat</sub>, C(26')), 146.3 (C<sub>quat</sub>, C(16)), 146.8 (C<sub>quat</sub>, C(8)), 155.7 (C<sub>quat</sub>, C(3)), 159.9 (C<sub>quat</sub>, C(11)), 171.2 (C<sub>quat</sub>, C(9')), 171.6 (C<sub>quat</sub>, C(27)), 171.9 (C<sub>quat</sub>, C(29)), 172.2 (C<sub>quat</sub>, C(2')), 174.2 (C<sub>quat</sub>, C(18')), 179.6 (C<sub>quat</sub>, C(13')), 182.1 (C<sub>quat</sub>, C(23')), 211.4 (C<sub>quat</sub>, C(25)).

### Temperature dependence of chemical shifts

Temperature dependence of chemical shifts was measured to identify possible hydrogen bonds. The  $^1\text{H}$ -NMR spectra were recorded at various temperatures on a Bruker DRX-600 spectrometer. Table 26 shows the determined chemical shift values (Hz) for each NH group of the examined compound in the range of 285 - 325 K.

**Table 26.** Determined  $^1\text{H}$  resonance chemical shift in Hz for NH protons at various temperatures in  $[\text{D}_6]$ -DMSO

NH[Hz] / T[K]	285	290	295	300	305	310	315	320	325
<b>NH A</b>	4214.63	4202.44	4190.05	4177.77	4165.03	4151.79	4139.81	4126.57	4113.96
<b>NH B</b>	6502.40	6488.74	6474.66	6460.99	6448.6	6434.09	6420.22	6405.3	6390.17
<b>NH C</b>	4458.44	4451.08	4443.52	4435.62	4429.22	4421.14	4415.56	4408.42	4401.90
<b>NH D</b>	6382.60	6366.84	6349.81	6332.22	6317.45	6300.63	6285.08	6268.69	6253.13
<b>NH E</b>	4261.71	4255.83	4247.00	4240.68	4233.97	4226.19	4218.42	4212.53	4205.39
<b>NH F</b>	4136.66	4133.93	4131.19	4128.19	4125.31	4121.74	4118.12	4113.98	4109.40
<b>NH G</b>	4043.13	4028.21	4012.23	3996.66	3977.77	3961.37	3946.03	3928.58	3912.40
<b>NH H</b>	4997.54	4988.08	4972.74	4960.53	4948.36	4935.96	4924.40	4912.21	4902.54
<b>NH I</b>	4869.96	4863.66	4854.41	4846.95	4838.23	4828.98	4820.78	4811.32	4802.08
<b>NH J</b>	4566.05	4549.87	4538.94	4524.64	4509.30	4495.07	4488.70	4476.09	4465.37
<b>NH K</b>	5076.36	5062.91	5044.81	5028.06	5008.26	4991.87	4977.78	4958.66	4943.74

The resonance values from table 26 were used to calculate the temperature dependence of the chemical shift. The measured values were plotted and fitted in EXCEL using a linear correlation function. The obtained coefficient in Hz/K is converted into the corresponding values in ppb/K (see table 24). These values are used to estimate the possibility of hydrogen bonds, using the following boundaries:

Hydrogen bond very likely	less than -2 ppb/K
Intermediate range	-2 to -3 ppb/K
No hydrogen bonding	more than -4 ppb/K

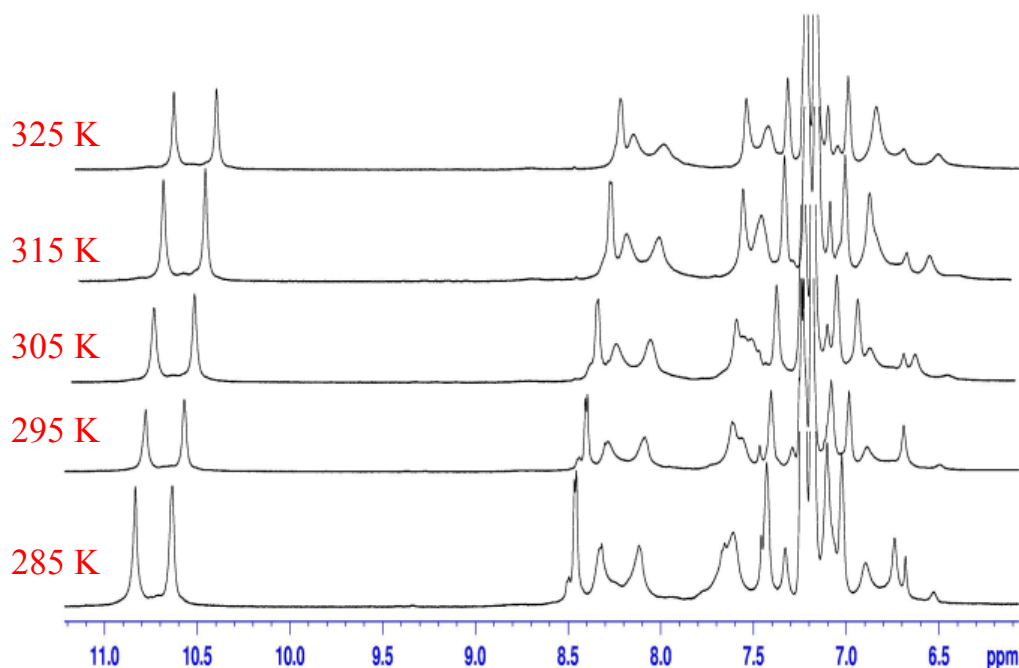


**Figure 98.**  $^1\text{H}$ -NMR spectra in  $[\text{D}_6]$ -DMSO at different temperatures.

### NMR NOE experiments

1D-NOE measurements in  $[\text{D}_6]$ -DMSO were performed at 300 K on a Bruker DRX-600 spectrometer with working frequency 600.13 MHz. The difference NOE experiment with selective excitation using the modified DPFGE pulse sequence (q3 gaussian cascade Double Pulsed Field Gradient Spin Echo) has been used. For every proton, which has been irradiated a series of 5 experiments with different mixing times (from 10 ms to 1 s) and with a relaxation delay of 2 s were acquired. An exponential window function with 4 Hz line broadening was applied before the Fourier transformation (FT) and a baseline correction was conducted after the FT.

2D-NOESY experiments with a mixing time of 500 ms were performed for structural calculations. Signal overlap restricts the number of observable intrastrand contacts. At least four NOE interactions between the bound peptide and the MOPAS heterocycles can be clearly detected. The measurements have been repeated with mixing times of 100, 200, 300, 400 and 500 ms giving the same structural parameter for the intramolecular distances. Cross peaks from intermolecular interactions are best seen at 500 ms.



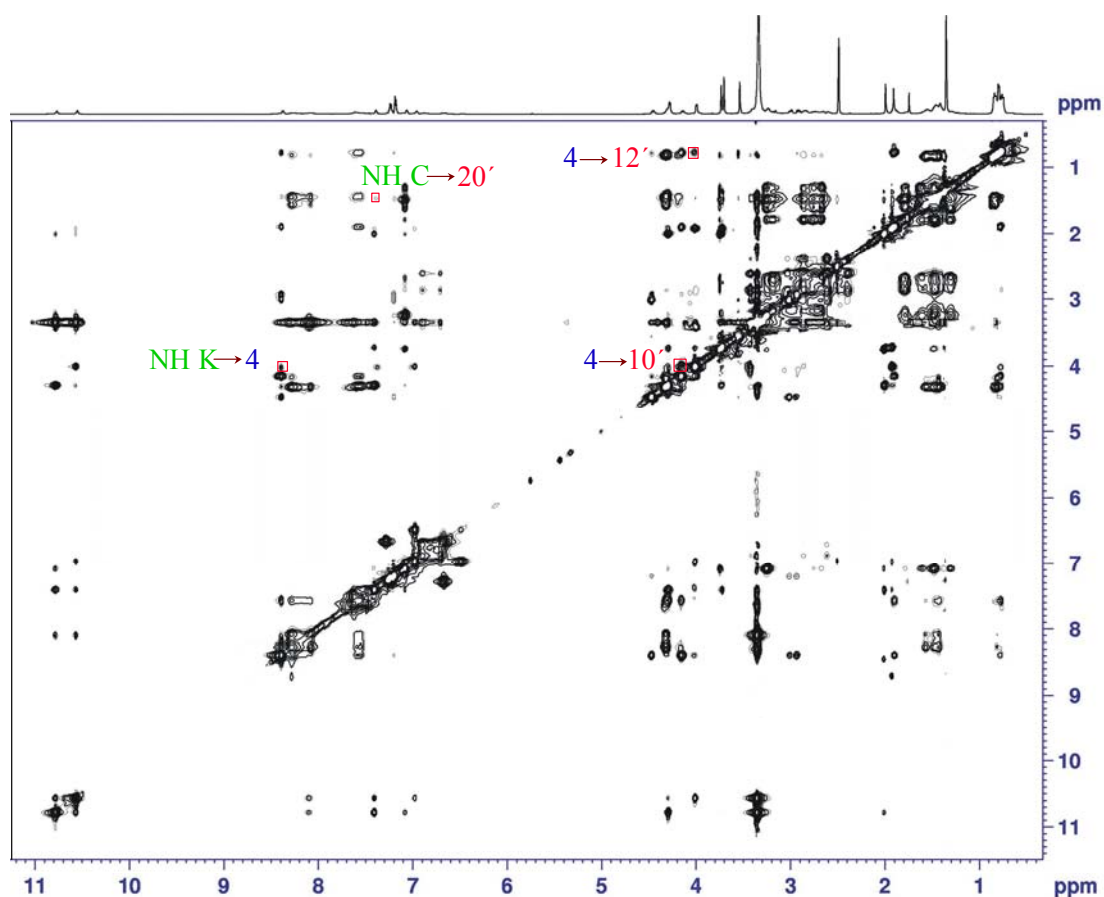


**Figure 99.** NOESY spectrum at 300 K with mixing time 500ms. Interactions between the pentapeptide and the **142** units are labelled.

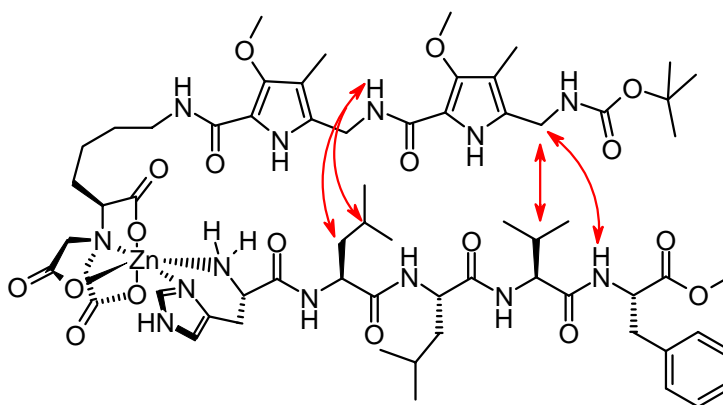


**Figure 100.** Interactions between the pentapeptide and the MOPAS units as detected by the NOESY spectrum.

### Structure of the bound pentapeptide unit

The intramolecular cross peaks of the bound pentapeptide in the 2D NOESY spectrum were integrated to obtain the distances<sup>vi</sup> describing the structure of the pentapeptide. The value of the integral of the methylene hydrogens (number 25') was used as the reference distance for these calculations. The value of the integral intensity is 293.85. Table 27 summarises the derived distances within the bound peptide. The distances were calculated using the following standard and known equations.

$$\sigma_{IS} = \left( \frac{\mu_0}{4\pi} \right)^2 \frac{\hbar^2 \gamma^4}{10} r_{IS}^{-6} \left( \frac{6\tau_C}{1 + 4\omega^2 \tau_C^2} - \tau_C \right) \Longrightarrow \sigma_{kl} = k r_{kl}^{-6} \Longrightarrow r_{IS} = r_{ref} \sqrt[6]{\frac{\sigma_{ref}}{\sigma_{kl}}}$$

**Table 27.** Intramolecular distances for the bound pentapeptide derived from the integrals of NOE crosspeak intensity

Interacting protons	Intensity	Distance [Å]
NH G – 24'	21.82	2.79
NH H – 24'	105.4	2.07
NH H – 19'	77.59	2.85
NH I – 19'	19.83	2.24
NH I – 14'	18.2	2.78
NH J – 14'	76.69	2.08
NH J – 10'	13.2	2.93
NH K – 10'	72.34	2.21
NH K – 3'	13.95	2.90

The distances were used as constraints to calculate the molecular structure of the pentapeptide (Hyperchem, NH-CH distance constraints as in Table S2; force field MM+). A subsequent MD simulation at 300 K for 10 ps and 10 times for 10 ps with 0.001 ps step size gave 10 structures, which are shown as overlay in figure 95, top. The average structure from these ten conformers was again energy minimised with MM+ to give the structure shown in figure 95, bottom.

<sup>vi</sup> Neuhaus, D.; Williamson, M.P. *The Nuclear Overhauser Effect in Structural and Conformational Analysis*, Wiley-VCH, New York, 2<sup>nd</sup> Ed, **2000**.

### Measurements in the absence of the Zn-NTA-unit

To prove the importance of the complex for the intermolecular interactions NMR measurements of mixtures of Boc-MOPAS-MOPAS-OEt<sup>y</sup> and the pentapeptide were done. In the absence of the Zn(II)-NTA complex two tautomeric forms of the histidine residue were observed, while in the presence of the Zn(II)-NTA complex only one was present. The second tautomer was observable in the proton spectrum (figure 102). All signals were less broad in comparison to **142**-His-Leu-Leu-Val-Phe-OMe, which indicated that both parts do not interact and show unrestricted motion on the NMR time scale.

The 2D-NOESY experiment (figure 103) for a mixture of Boc-MOPAS-MOPAS-OEt and His-Leu-Leu-Val-Phe-OMe showed different dynamic behaviour of the pentapeptide and the MOPAS unit. The intramolecular cross peaks in the 2D-NOESY spectrum are due to fast movement of very low intensity. No cross peaks, which indicate interstrand interactions were observed. Strong chemical exchange is observed for all NH groups in the 2D-NOESY spectrum.

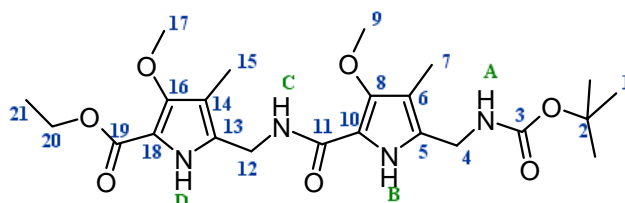


**Figure 101.** Boc-MOPAS-MOPAS-OEt.

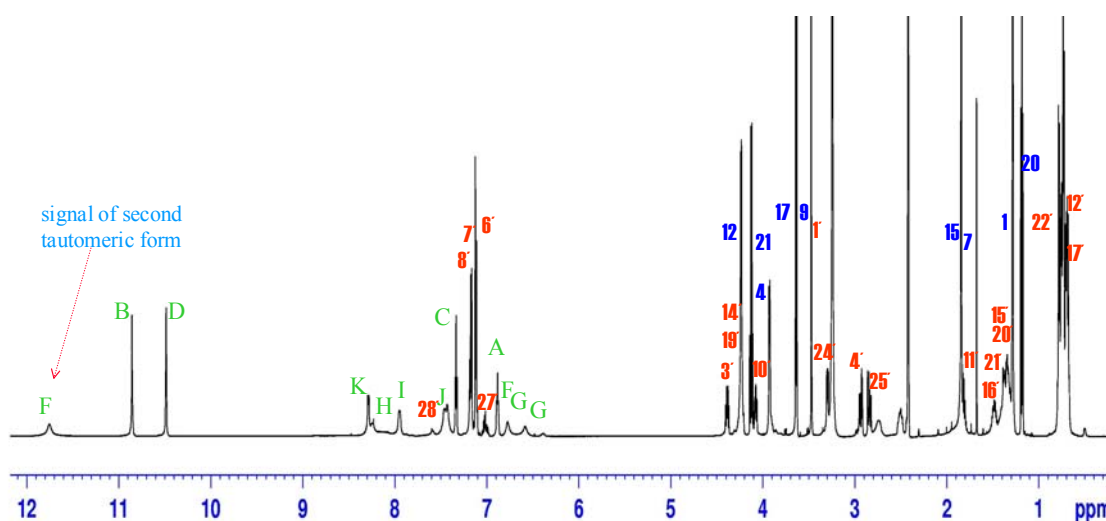


**Figure 102.** <sup>1</sup>H-NMR spectrum of Boc-MOPAS-MOPAS-OEt and His-Leu-Leu-Val-Phe-OMe measured under identical conditions as before.

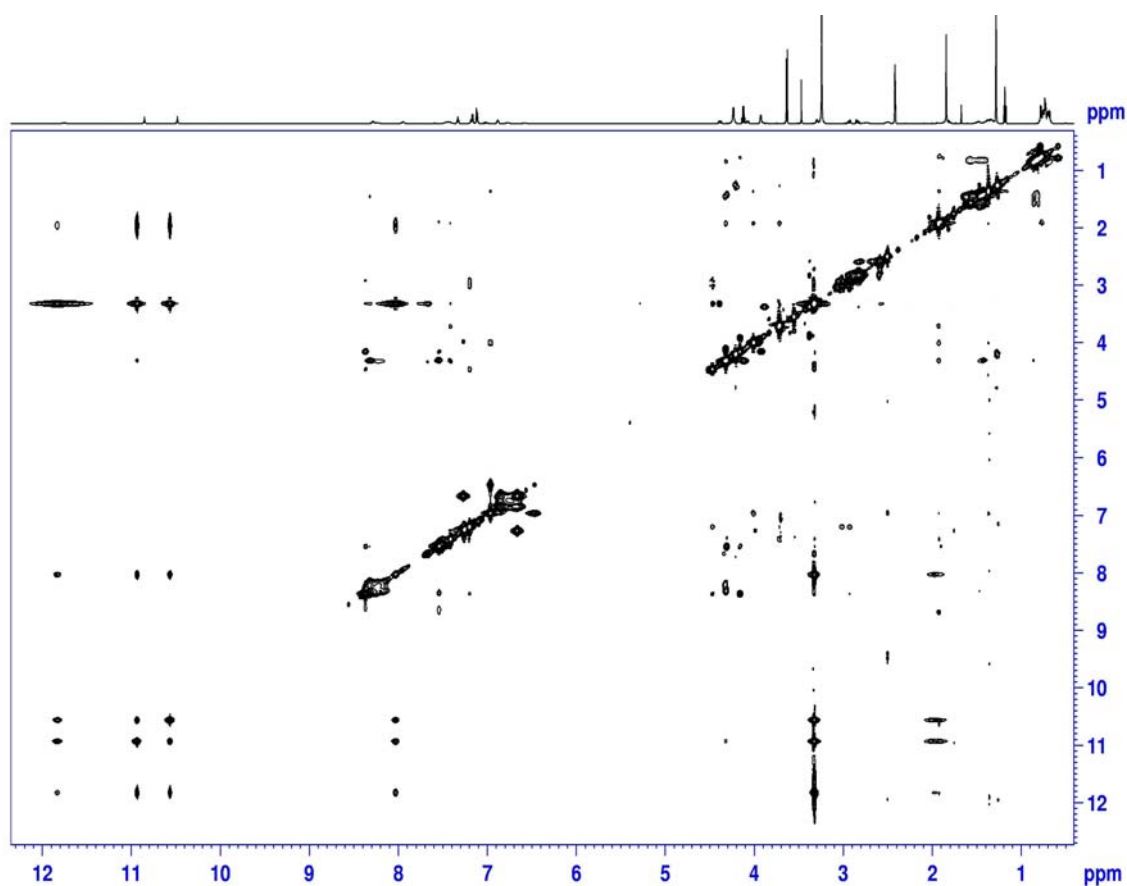


**Figure 103.** NOESY spectrum of Boc-MOPAS-MOPAS-OEt and His-Leu-Leu-Val-Phe-OMe measured at 300 K with a mixing time of 500 ms.

**$^3J_{\text{NHH}\alpha}$  coupling constants:**

Phe:  $^3J_{\text{NHH}\alpha} = 6.88$

Val:  $^3J_{\text{NHH}\alpha} = 6.59$

Leu:  $^3J_{\text{NHC}\alpha} = 6.86$

Leu:  $^3J_{\text{NHH}\alpha} = 5.69$

**$C_{\alpha}/H_{\alpha}$  coupling constants:**

Phe: 137 Hz

Val: 140 Hz

Leu: 136 Hz

Leu: 138 Hz

His: 137 Hz

**Parameters of the NMR experiments**

$^1\text{H}$ -NMR spectra

Spectral width: 14 kHz

Size: 16k of data points

Relaxation period: 2 s

Number of pass: 32

### 1D $^1\text{H}$ -DPFGSE-NOE

Spectral width: 14 kHz

Size: 16k of data points

Mixing time: 100 to 1000 ms

Length of gaussian cascade: 79.2 ms

Relaxation period: 2 s

Number of pass: 4 – 6k

### $^1\text{H}$ - $^1\text{H}$ NOESY

Spectral width: 14 kHz for both domains

Size: 512 (f1) and 2k (f2) of data points

Mixing time: 500 ms

Relaxation period: 2 s

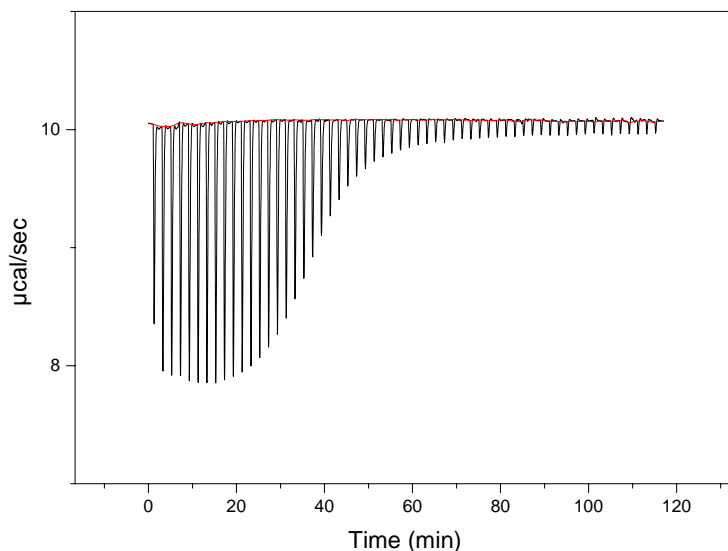
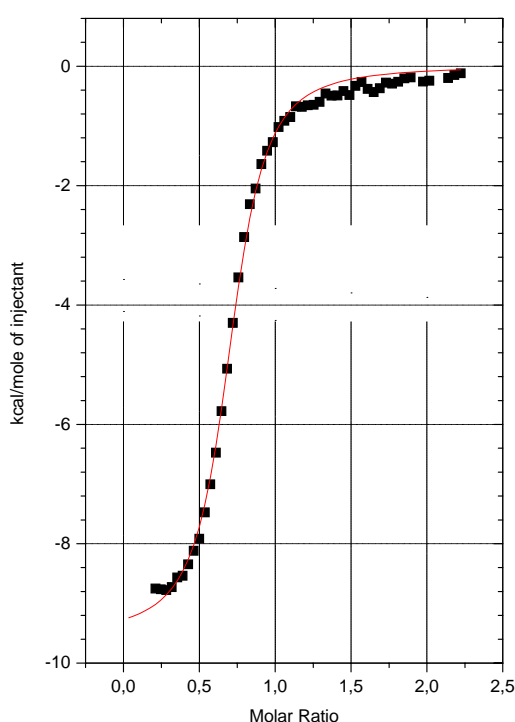
Number of pass: 32

### Calculation of the pentapeptide structure:

2D-NOESY spectrum at 300 K was measured for the calculation of the distances. The apodization function  $\cos^2(x)$  was applied on the measured data. After Fourier transformation in both domains the phase shift was corrected in the spectrum and the baseline was corrected using the multinomial of fifth degree.

### **Example of microcalorimetric titration**

Titration of nickel complex of Ni(II)-**142** with pentapeptide in buffered aqueous solution



$$N = 0.71$$

$$K = (4.7 \pm 0.29) \cdot 10^5 \text{ M}^{-1}$$

$$\Delta H = -(9.53 \pm 0.09) \cdot 10^3 \text{ kcal} \cdot \text{mol}^{-1}$$

$$\Delta S = -6.03 \text{ kcal} \cdot \text{K}^{-1} \cdot \text{mol}^{-1}$$

**Figure 104.** Microcalorimetric titration of Ni(II)-**142** ( $c = 0.1 \text{ mM}$ ) with analysed pentapeptide ( $c = 1 \text{ mM}$ ) in DMSO ( $T = 293 \text{ K}$ ).

## 4. A Luminescent Receptor with Imidazole and Ammonium Ion Affinity for Peptide Binding in Aqueous Solution<sup>i</sup>

This chapter deals with the application of a C-terminal IDA recognition building block. The free amine is linked to a precursor of a fluorescent crown ether by a double S<sub>N</sub>2 reaction.<sup>ii</sup> The available ditopic receptor was used to bind to small peptides containing a terminal histidine in aqueous buffered solutions.<sup>iii</sup> In a final screening, the receptor proved the selectivity to bind histidine among all natural amino acids exclusively.

---

<sup>i</sup> Kruppa, M.; Mandl, C.; Miltschitzky, S.; König, B. *J. Am. Chem. Soc.* **2005**, *127*, 3362.

<sup>ii</sup> Precursor **145** and crown ether **148** were synthesised by C. Mandl.

<sup>iii</sup> Microcalorimetric measurements were carried out by S. Miltschitzky.

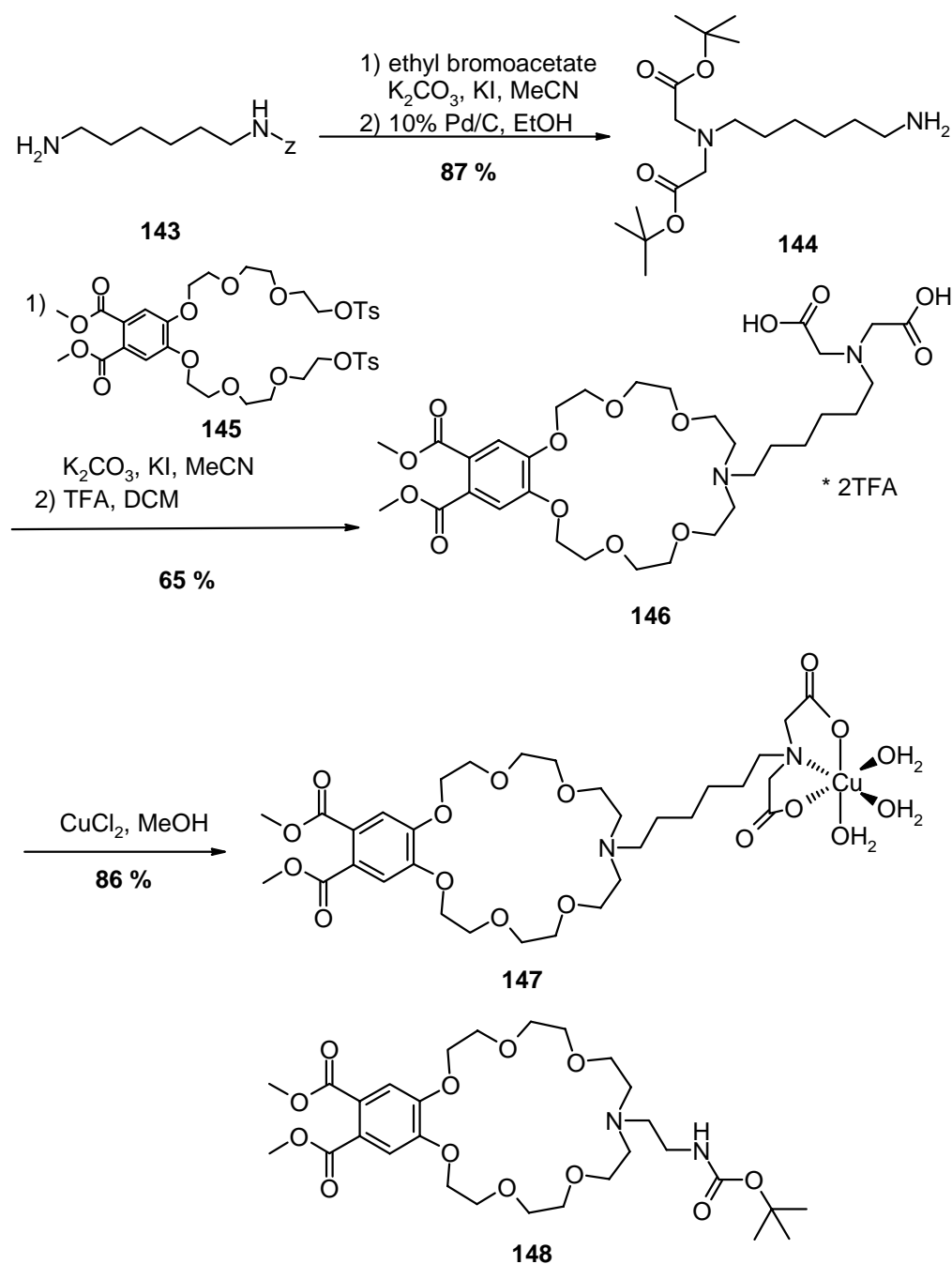
## 4.1 Introduction

Ammonium ions are present in many compounds of biological or pharmaceutical interest, ranging from simple amino acids, neurotransmitters, amino sugars to peptides and proteins. The classic hosts for the ammonium ion binding<sup>1</sup> are crown ethers of appropriate size, however high binding affinities are only observed in organic solvents, such as methanol.<sup>2</sup> At physiological conditions in water or DMSO as solvent, the binding constants are usually smaller than  $\log K = 2$ . A more favourable intramolecular hydrogen bond formation between crown ether and ammonium ion<sup>3</sup> is achieved by combining it with a stronger ionic or reversible covalent intermolecular interaction creating di- or polytopic receptors.<sup>4</sup> Recent examples used the combination of crown ethers with boronic acids<sup>5</sup> to bind glucoseamine, with guanidinium<sup>6,7</sup> ammonium and non-polar groups<sup>8</sup> to bind amino acids.<sup>9,10,11</sup> Reversible coordination to metal complexes can provide high affinity and selectivity in aqueous solution, but it has not been used to amplify crown ether – ammonium ion binding.<sup>12</sup> We report here the preparation and peptide binding properties of the luminescent crown ether<sup>13</sup> **147** which contains a pendant copper(II) imino diacetic acid (Cu(II)-IDA) complex.<sup>14,15</sup>

## 4.2 Results and Discussion

The Cu(II)-IDA motif is well known for its binding ability to imidazole and histidine.<sup>16,17,18,19,20,21</sup> To combine this property with the ammonium ion affinity of a crown ether, amine **144** was allowed to react with bis-tosylate **145** followed by deprotection to give the aza crown **146** (scheme 50). The phthalic-ester moiety of **146** allows one to monitor the binding of an ammonium ion to the crown ether by an increase in its emission intensity (excitation:  $\lambda = 305$  nm; detection:  $\lambda \approx 377$  nm). Upon addition of Cu(II) ions a stable complex (**147**) is formed with the IDA ligand. Compound **148** was prepared for comparison from **145** by reaction with mono-Boc-protected 1,2-ethylenediamine to investigate the response of the crown ether emission to an ammonium ion binding.

**Scheme 50.** Synthesis of luminescent benzocrown ethers **146**, **147** and **148**



To investigate the photophysical properties of the crown ether part, absorption and emission spectra of compound **148** were recorded in methanol and their response to the presence of ammonium ions tested. Upon excitation at the absorption maximum around  $\lambda_{max} = 268$  nm an emission with a maximum at 385 nm was observed. The quantum yield of  $\Phi = 0.09$  is rather low.<sup>22</sup> Upon addition of KSCN or *n*-BuNH<sub>3</sub>Cl, the emission intensity



increases significantly by a factor of 2.2 or 3.7, respectively. Table 28 summarises the binding constants derived from the titration data.

**Table 28.** Binding affinities and emission response of compound **148** in methanol to the addition of potassium or ammonium ions

guest	$K [M^{-1}]$	log $K$	$I_{\max}/I_o$
KSCN	4790	3.68	2.22
<i>n</i> -BuNH <sub>3</sub> Cl	178	2.25	3.68

As expected, no response of the emission properties is observed for **147**<sup>23</sup> or **148** if treated with KSCN or *n*-BuNH<sub>3</sub>Cl in buffered aqueous solution (50 mM HEPES, pH 7.5,  $c = 10^{-5}$  mol/L, up to 1000 equiv. ammonium ion), even with a large excess of the salts. The aqueous solvent competes with the crown ether for the cation binding and the ammonium - crown ether interaction is intercepted. The situation changes if the dipeptide His-Lys-OMe is added to a solution of **147**. Coordination of the *N*-terminal histidine to the Cu(II)-IDA complex<sup>24</sup> of **147** makes the crown ether - ammonium ion binding intramolecularly and much more favourable. Titration of **147** with His-Lys-OMe in HEPES buffer (50 mM, pH 7.5)<sup>25</sup> resulted in a 1:1 complex (scheme 51) as shown by a Job's plot analysis (figure 105). With a binding constant of  $\log K = 4.22 \pm 0.05$  compound **147** binds the ammonium group of His-Lys-OMe with high affinity in buffered water. Calorimetric titrations confirmed the strong interaction of **147** and His-Lys-OMe. Calorimetric titrations confirmed the strong interactions of **147** and His-Lys-OMe. The emission intensity change of **147** in the presence of His-Lys-OMe can even be observed with the naked eye (figure 106). No emission response is detected under the same conditions with the *N*-terminal acylated dipeptide Ac-His-Lys-OMe, which proves the importance of an *N*-terminal histidine for the overall binding process.

**Scheme 51.** Proposed mode of binding of luminescent crown ether **147** and His-Lys-OMe

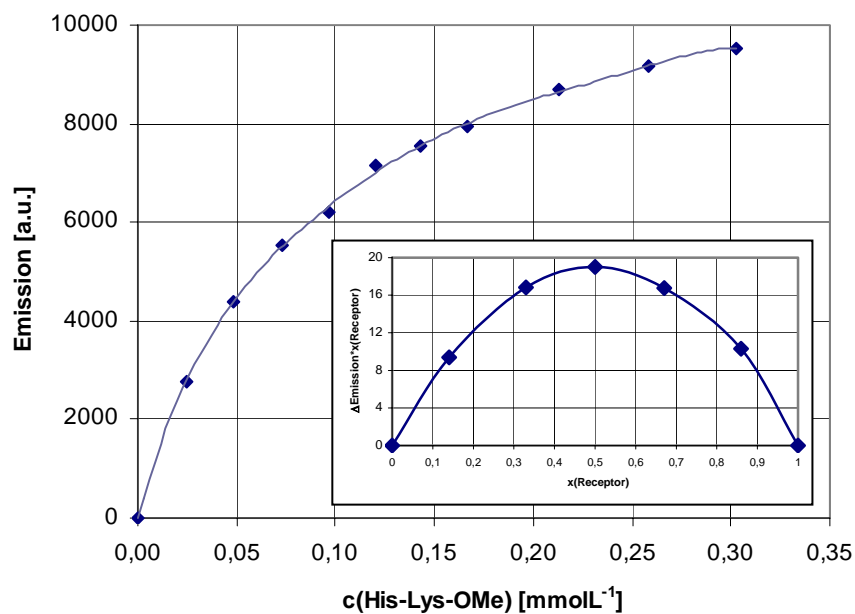
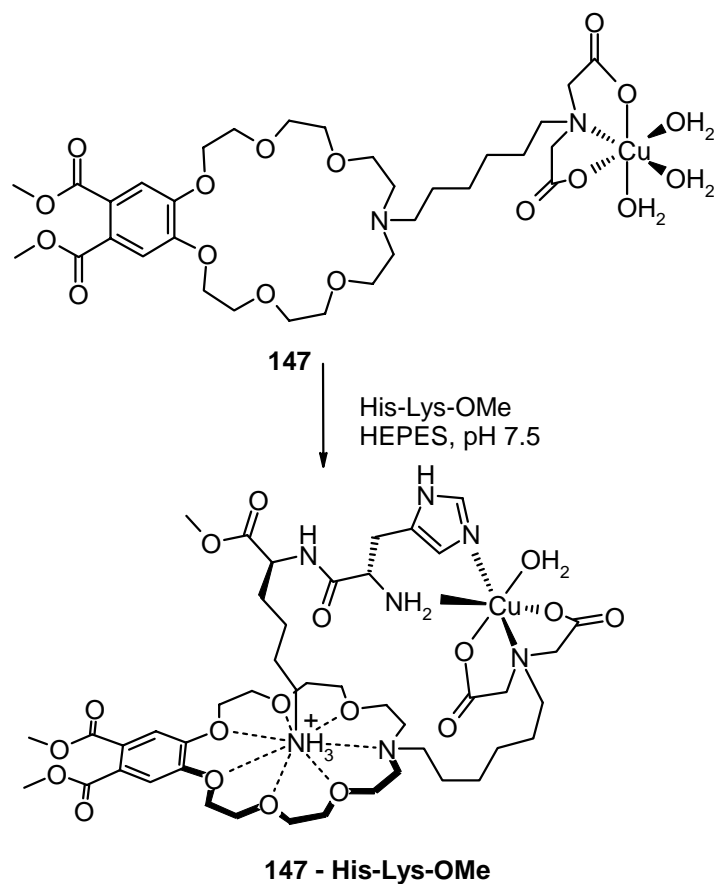


**Figure 105.** Emission titration of **147** ( $c = 10^{-5}$  mol/L) with His-Lys-OMe in buffered aqueous solution (50 mM HEPES, pH 7.5). Insert: Job's plot analysis.

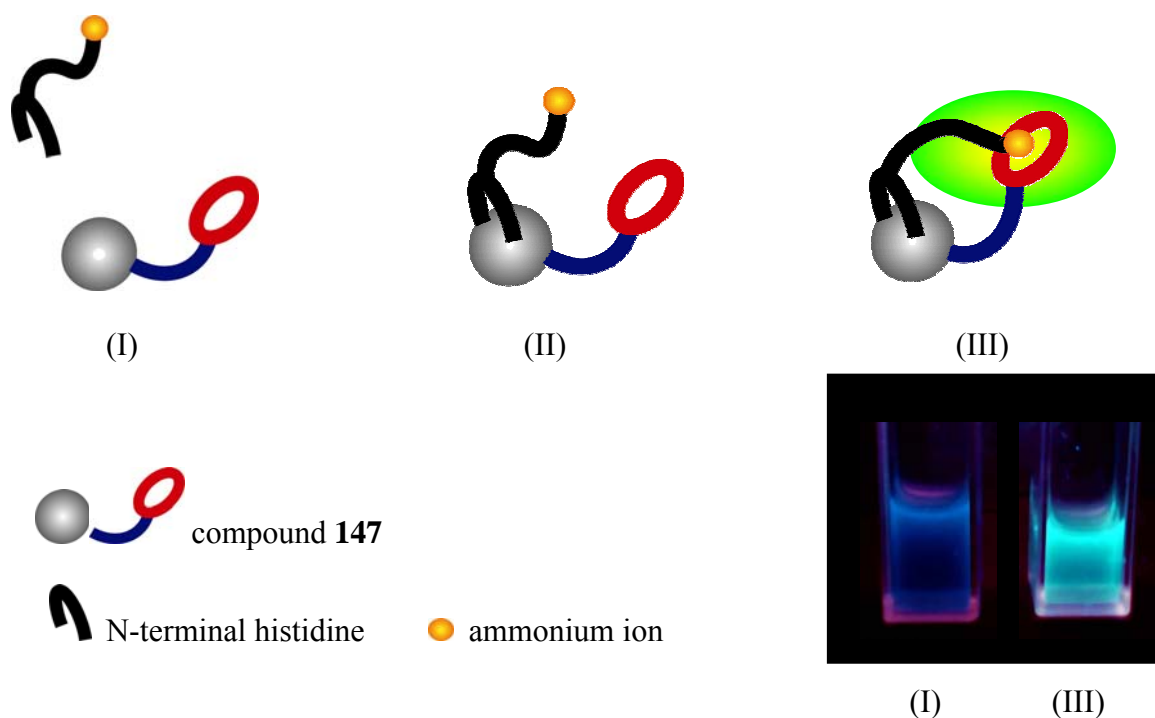
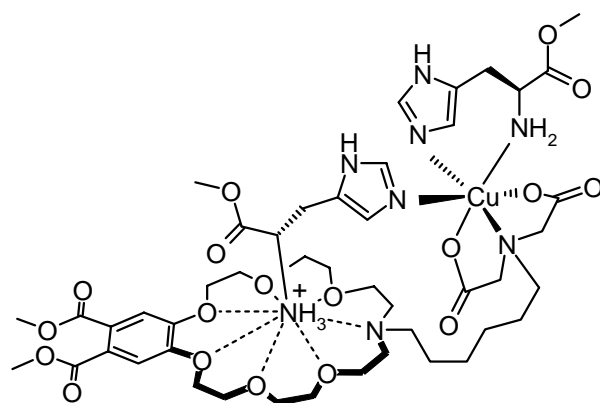


**Figure 106.** Schematic binding process and emission intensity changes of solutions of **147** in buffered water in the presence of His-Lys-OMe.

Surprisingly, using His-OMe as an added guest molecule, nearly the same enhancement of emission intensity is observed as with His-Lys-OMe. Job's plot analysis shows a stoichiometry of 2:1 for the His-OMe – **147** aggregate (figures 107 and 108). The coordination chemistry of the Cu(II)- IDA complex provides a likely rationale for this observation: After the binding of one His-OMe to Cu(II)-IDA, one coordination site remains, which can accommodate the imidazole moiety of a second His-OMe while its ammonium group is bound by the crown ether, leading to an increased emission intensity.<sup>26</sup> The overall binding constant of His-OMe to **147** was determined to be  $\log K = 3.8 \pm 0.1$ . The binding motif allows the selective detection of N-terminal His groups, which is illustrated by the binding of the tripeptide H-His-Gly-Gly-OH. This peptide binds to **147** with the same 2:1 stoichiometry as observed for histidine and an overall affinity of  $\log K = 3.71 \pm 0.05$ .



**147 - 2His-OMe**

**Figure 107.** Proposed structure of the assembly of two His-OMe with **147**.

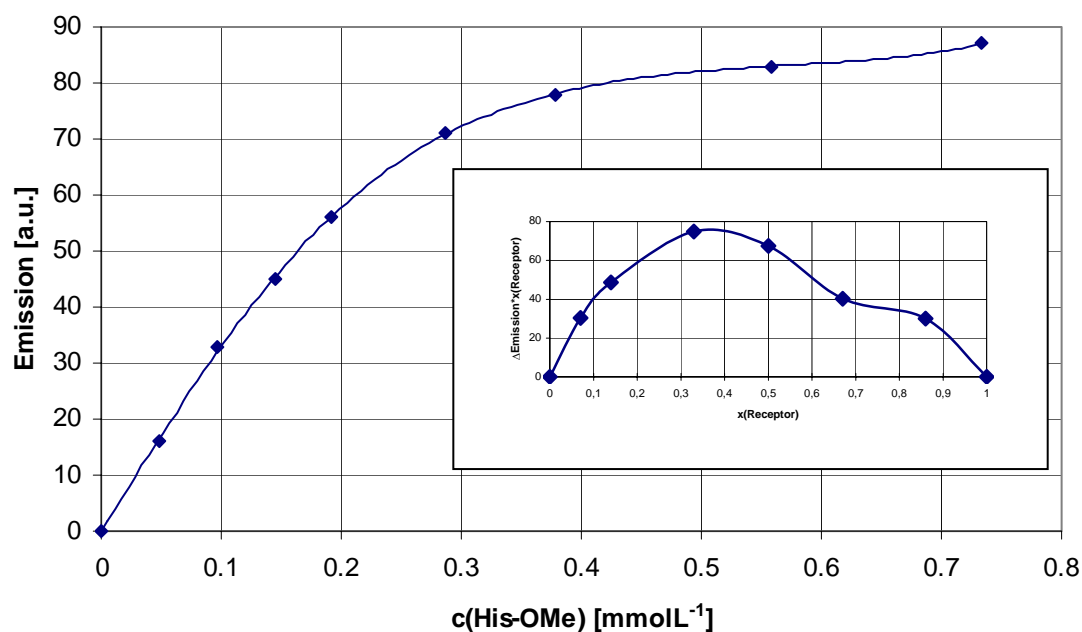


**Figure 108.** Emission titration curve of **147** with His-OMe in buffered aqueous solution at pH 7.5. Insert: Job's plot analysis.

The binding studies show that compound **147** has the ability to detect the simultaneous presence of an imidazole and an ammonium ion in one molecule. The stoichiometry of the resulting assembly with **147** depends on their geometrical arrangement. A simple illustration of an application of such a property is the selective detection of the amino acid histidine among 20 natural  $\alpha$ -amino acids.<sup>27</sup> Only histidine with imidazole and ammonium group leads to emission enhancement, while the presence of all other amino acids does not induce significant emission changes.

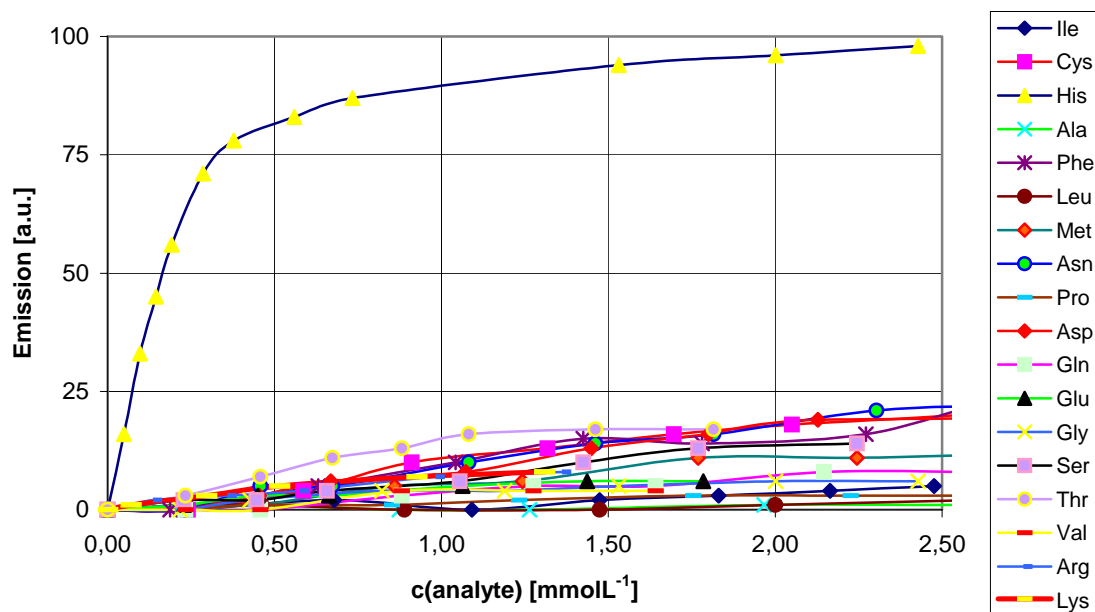


**Figure 109.** Response of the emission intensity of **147** to the presence of 20 natural  $\alpha$ -amino acids in aqueous buffered solution (50 mM HEPES, pH 7.5).

Side chain functionalities of amino acids, such as Lys, Cys, Ser or Met are known to coordinate to the Cu(II)-IDA complex, but only this interaction alone does not trigger the emission response. The interaction of the ammonium group with the benzo crown, which only becomes possible intramolecularly,<sup>28</sup> is the necessary second process to signal the binding event.

### 4.3 Conclusion

The combination of an imidazole coordinating metal complex with a luminescent ammonium-binding crown ether results in a simple synthetic receptor with high affinity in buffered water for molecules bearing *both* functional groups. The emission response is triggered by the weak ammonium ion binding which only becomes possible intramolecularly within the assembly. Only the presence of an ammonium group, even in large excess, does not trigger an optical output. Binding selectivities, which are different from the present one, may be accomplished by other combinations of strongly coordinating metal complexes and binding sites of weak affinity.

## References:

---

- <sup>1</sup> For a comprehensive overview on receptors for cationic guests, see: *Comprehensive Supramolecular Chemistry* (Ed.: Lehn, J.-M.; Attwood, J.L.; Davies, J.E.D.; Macnicol, D.D.; Vögtle, F.), Vol. 1, 1996, Oxford.
- <sup>2</sup> Rüdiger, V.; Schneider, H.-J.; Solov'ev, V.P.; Kazachenko, V.P.; Raevsky, O.A. *Eur. J. Org. Chem.* **1999**, 1847.
- <sup>3</sup> Examples of intramolecular crown ether – ammonium ion interactions: (a) Al-Sayah, M.H.; Branda, N.R. *Org. Lett.* **2002**, 4, 881. (b) Shinkai, S.; Ishihara, M.; Ueda, K.; Manabe, O. *J. Chem. Soc. Perkin Trans. II* **1985**, 511.
- <sup>4</sup> Examples for ditopic receptors: (a) Cheng, Y.; Suenaga, T.; Still, W.C. *J. Am. Chem. Soc.* **1996**, 118, 1813. (b) Wennemers, H.; Conza, M.; Nold, M.; Krattinger, P. *Chem. – Eur. J.* **2001**, 7, 3342.
- <sup>5</sup> Cooper, C.R.; James, T.D. *Chem. Commun.* **1997**, 15, 1419.
- <sup>6</sup> Metzger, A.; Gloe, K.; Stephan, H.; Schmidtchen, F.P. *J. Org. Chem.* **1996**, 61, 2051.
- <sup>7</sup> de Silva, A.P.; Gunaratne, H.Q.N.; McVeigh, C.; Maguire, G.E.M.; Maxwell, P.R.S.; O'Hanlon, E. *Chem. Commun.* **1996**, 2191.
- <sup>8</sup> Hossain, M.A.; Schneider, H.-J. *J. Am. Chem. Soc.* **1998**, 120, 11208.
- <sup>9</sup> Receptor for binding of *N*-acylated dipeptides in water: Schmuck, C.; Geiger, L. *J. Am. Chem. Soc.* **2004**, 126, 8898.
- <sup>10</sup> For a recent example of cooperative metal coordination and ion pairing in peptide recognition, see: Wright, A.T.; Anslyn, E.V. *Org. Lett.* **2004**, 6, 1341.
- <sup>11</sup> Aspartic acid receptor using reversible coordination: Ait-Haddou, H.; Wiskur, S.L.; Lynch, V.M.; Anslyn, E.V. *J. Am. Chem. Soc.* **2001**, 123, 11296.
- <sup>12</sup> For lanthanide complex – crown ether conjugates which show emission response to potassium or sodium, see: Gunnlaugson, T.; Leonard, J.P. *Chem. Commun.* **2003**, 2424.
- <sup>13</sup> Otsuki, J.; Yamagata, T.; Ohmuro, K.; Araki, K.; Takido, T.; Seno, M. *Bull. Chem. Soc. Jpn.* **2001**, 74, 333.
- <sup>14</sup> For a recent example of pyridine-substituted crown ether and its coordination to a metal complex, see: Chi, K.-W.; Addicott, C.; Stang, P.J. *J. Org. Chem.* **2004**, 69, 2910.
- <sup>15</sup> For a recent report of crown ether based luminescent metal ion sensor, see: Kim, H.M.; Jeong, M.-J.; Ahn, H.C.; Jeon, S.-J.; Cho, B. R. *J. Org. Chem.* **2004**, 69, 5749.
- <sup>16</sup> A major application of this binding process is found in the purification of His-tagged proteins by affinity chromatography techniques.
- <sup>17</sup> Examples for the use of metal IDA complexes in synthetic receptors: (a) Sun, S.; Fazal, M.A.; Roy, B. C.; Mallik, S. *Org. Lett.* **2000**, 2, 911. (b) Sun, S.; Fazal, M. A.; Roy, B. C.; Chandra, B.; Mallik, S. *Inorg. Chem.* **2002**, 41, 1584. (c) Roy, B. C.; Fazal, M. A.; Sun, S.; Mallik, S. *J. Chem. Soc., Chem. Commun.* **2000**, 547. (d) Fazal, M. A.; Roy, B.

- 
- C.; Sun, S.; Mallik, S.; Rodgers, K. R. *J. Am. Chem. Soc.* **2001**, *123*, 6283. (e) Banerjee, A. L.; Swanson, M.; Roy, B. C.; Jia, X.; Haldar, M. K.; Mallik, S.; Srivatava, D. K. *J. Am. Chem. Soc.* **2004**, *126*, 13206.
- <sup>18</sup>Use of metal-NTA complexes in imprinting studies: Hart, B.R.; Shea, K.J. *Macromolecules*, **2002**, *35*, 6192.
- <sup>19</sup>For Metal IDA fluorophore conjugates as sensors for histidine-tagged proteins see: (a) Dorn, I.T.; Neumaier, K.R.; Tampe, R. *J. Am. Chem. Soc.* **1998**, *120*, 2753. (b) Hutschenreiter, S.; Neumann, L.; Rädler, U.; Schmitt L.; Tampe, R. *ChemBioChem* **2003**, *4*, 1340.
- <sup>20</sup>Cu(II)-based receptor for imidazole and histidine: Fabbrizzi, L.; Francese, G.; Licchelli, M.; Perotti, A.; Taglietti, A. *Chem. Commun.* **1997**, 581.
- <sup>21</sup>Fluorescent sensor for histidine based on a Co(II)-free base porphyrin dimmer: Yang, R.; Wang, K.; Long, L.; Xiao, D.; Yang, X.; Tan, W. *Anal. Chem.* **2002**, *74*, 1088.
- <sup>22</sup>All quantum yields were determined with quinine disulfate in 1 N H<sub>2</sub>SO<sub>4</sub> as the reference compound ( $\Phi = 0.546$ ).
- <sup>23</sup>Upon incorporation of Cu(II) ions the quantum yield of the emission of **147** decreases to  $\Phi = 0.0045$  compared to that of **146** ( $\Phi = 0.62$ , all quantum yields relative to quinine sulfate in 1 N H<sub>2</sub>SO<sub>4</sub>). The presence of the paramagnetic transition-metal ion may quench the emission of the crown ether. Binding of His-containing peptides restores parts of the emission intensity, presumably by part suppression of the quenching mechanism.
- <sup>24</sup>Hopgood, D.; Angelici, R.J. *J. Am. Chem. Soc.* **1968**, *90*, 2508.
- <sup>25</sup>At this pH the IDA-metal complex is stable, imidazole is not protonated and coordinates to the metal complex, and the lysine side chain bears an ammonium ion, which can bind to the crown ether.
- <sup>26</sup>A rapid exchange of bound histidines within the dynamic assembly is expected.
- <sup>27</sup>Only Tyr and Trp could not be used in this assay. Tyr is not soluble in HEPES-buffer and the indole emission of Trp interferes with the emission of **147**. However, calorimetric titration showed no binding of the amino acids to **147**.
- <sup>28</sup>All amino acids bear an ammonium group under the experimental conditions. But in aqueous solution the affinity of the ammonium group to the benzo crown ether is too weak to give any emission response.

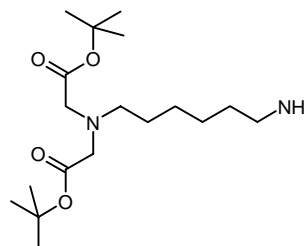
## 4.4 Experimental Section

### 4.4.1 Instruments and general techniques

See experimental section of chapter 1 (page 131)

### 4.4.2 Synthesis

*N*-Z-1,6-diamino-hexane (**143**)<sup>iv</sup>, 4,5-bis-(2-{2-[2-(toluol-4-sulfonyloxy)-ethoxy]-ethoxy}-ethoxy)-phthalic acid dimethylester (**145**)<sup>v</sup>



*tert*-Butyl-[(6-aminohexyl)-*tert*-butoxycarbonylmethylamino]-acetate (**144**):

**143** (0.21 g, 4.9 mmol) was dissolved in MeCN (20 mL) and mixed with *tert*-butyl bromoacetate (1.56 mL, 10.6 mmol), K<sub>2</sub>CO<sub>3</sub> (2.92 g, 21.1 mmol) and a spatula tip of potassium iodide. The suspension was stirred 2 days at 60 °C and monitored by TLC (EtOAc). The mixture was filtered, diluted with water (20 mL) and extracted twice with EtOAc. After drying over Na<sub>2</sub>SO<sub>4</sub> the organic solvents were evaporated to yield the crude product. Purification using column chromatography on silica gel (EtOAc, *R*<sub>f</sub> = 0.9) gave the *Z*-protected IDA-intermediate as a colourless oil.

To deprotect the *Z*-group, the oil was dissolved in EtOH (25 mL) and mixed with a spatula tip of 10% Pd/C. Hydrogenolytical cleavage was performed in an autoclave at 10 bar H<sub>2</sub> pressure for 12 h at r.t.. After filtration, the ethanol was evaporated to yield **144** (4.3 mmol, 1.46 g, 87 %) as a colourless oil.

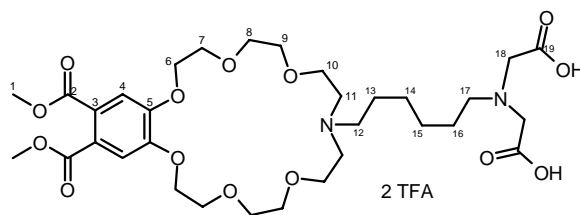
<sup>1</sup>H-NMR (300 MHz; CDCl<sub>3</sub>): δ = 1.24-1.29 (m, 4 H, CH<sub>2</sub>), 1.38-1.49 (m, 20 H, CH<sub>3</sub>-Boc + CH<sub>2</sub>), 2.62-2.69 (m, 4 H, CH<sub>2</sub>), 3.16-3.18 (m, 2 H, CH<sub>2</sub>), 3.40 (s, 4 H, N-CH<sub>2</sub>), 4.82 ppm (bs, 1 H, NH). – <sup>13</sup>C-NMR (75 MHz; CDCl<sub>3</sub>): δ = 26.6 (–, CH<sub>2</sub>), 26.8 (–, CH<sub>2</sub>), 27.8 (–, CH<sub>2</sub>), 28.2 (+, 6 C, CH<sub>3</sub>), 40.9 (–, CH<sub>2</sub>), 54.0 (–, CH<sub>2</sub>), 55.9 (–, 2 C, CH<sub>2</sub>), 66.6 (–, CH<sub>2</sub>), 80.9 (C<sub>quat</sub>, 2 C, C-Boc), 170.8 ppm (C<sub>quat</sub>, 2 C, COO<sup>t</sup>Bu). – IR [cm<sup>–1</sup>]:  $\tilde{\nu}$  = 2930, 1740, 1714, 1209. – MS (CI-MS, NH<sub>3</sub>): *m/z* (%) = 345 (100) [MH<sup>+</sup>]. – HRMS (C<sub>18</sub>H<sub>36</sub>N<sub>2</sub>O<sub>4</sub><sup>+</sup>):

<sup>iv</sup> Atwell, G. J.; Denny, W. A. *Synthesis* **1984**, 12, 1032.

<sup>v</sup> Mandl, C.P.; König, B. *J. Org. Chem.* **2005**, 70, 670.



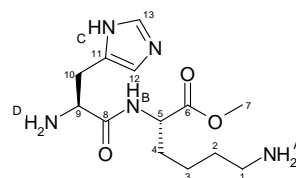
calcd. 344.2675, found 344.2671  $\pm$  0.72 ppm. – Elemental analysis calcd. (%) for C<sub>18</sub>H<sub>36</sub>N<sub>2</sub>O<sub>4</sub> (344.27) + EtOAc: C 58.36, H 9.97, N 6.93; found C 58.29, H 9.92, N 6.98.



*14-[6-(Bis-carboxymethyl-amino)-hexyl]-6,7,9,10,13,14,15,16,18,19,21,22-dodecahydro-12H-5,8,11,17,20,23-hexaoxa-14-aza-benzocyclohenicosene-2,3-dicarboxylic acetic acid dimethylester ditriflate (146):*

Compound **144** (0.3 g, 0.9 mmol) was dissolved in MeCN (14 mL) and mixed with **145** (0.67 g, 0.8 mmol), K<sub>2</sub>CO<sub>3</sub> (1.29 g, 9.3 mmol) and KI (0.14 g, 0.9 mmol). The suspension was refluxed for 2 d and the reaction progress monitored by TLC (CHCl<sub>3</sub>:MeOH = 6:1). After cooling to r.t. the mixture was filtered over celite, washed with MeCN and CHCl<sub>3</sub> and the filtrate was evaporated to dryness. Purification using column chromatography on silica gel (CHCl<sub>3</sub> : MeOH = 20:1  $\rightarrow$  15:1, *R<sub>f</sub>* (CHCl<sub>3</sub>:MeOH = 6:1) = 0.33) gave bis-*tert*-butyl protected **146** as a light yellow oil. This diester was dissolved in TFA (5 mL) and stirred for 2 h at r.t.. After evaporating the TFA, the slurry was suspended in Et<sub>2</sub>O and decanted. Compound **146** (0.5 mmol, 0.44 g, 65 %) is a colourless hygroscopic solid.

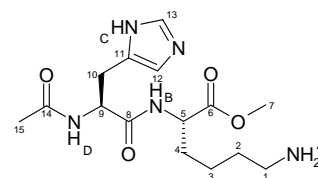
mp 38-40 °C. – <sup>1</sup>H- NMR (600 MHz; D<sub>2</sub>O; COSY, HSQC):  $\delta$  = 0.93-0.98 (m, 2 H, H(15)), 1.01-1.04 (m, 2 H, H(14)), 1.41-1.46 (m, 4 H, H(13), H(16)), 2.99-3.02 (m, 2 H, H(12)), 3.07-3.10 (m, 2 H, H(17)), 3.23-3.27 (m, 2 H, H(11)), 3.29-3.33 (m, 2 H, H(11)), 3.58-3.63 (m, 6 H, H(10), H(8/9)), 3.66-3.74 (m, 6 H, H(8/9)), 3.78 (s, 6 H, H(1)), 3.77-3.80 (m, 2 H, H(7)), 3.86-3.89 (m, 2 H, H(7)), 4.05 (s, 4 H, H(18)), 4.05-4.08 (m, 2 H, H(6)), 4.17-4.20 (m, 2 H, H(6)), 7.18 (s, 2 H, H(4)). – <sup>13</sup>C- NMR (100 MHz; D<sub>2</sub>O; HSQC, HMBC):  $\delta$  = 22.6 + 23.0 (–, 2 C, C(14), C(15)), 25.0 & 25.1 (–, 2 C, C(13), C(16)), 53.2 (–, C(12)), 53.2 (+, 2 C, C(1)), 53.7 (–, 2 C, C(11)), 54.4 (–, 2 C, C(18)), 56.4 (–, C(17)), 63.7 (–, 2 C, C(10)), 68.2 (–, 2 C, C(6)), 68.9 (–, 2 C, C(7)), 69.8 (–, 4 C, C(8), C(9)), 112.6 (+, 2 C, C(4)), 124.7 (C<sub>quat</sub>, 2 C, C(3)), 149.6 (C<sub>quat</sub>, 2 C, C(5)), 168.1 (C<sub>quat</sub>, 2 C, C(2)), 169.3 (C<sub>quat</sub>, 2 C, C(19)) [TFA signals are not listed]. – IR (KBr) [cm<sup>–1</sup>]:  $\tilde{\nu}$  = 3450, 2930, 2890, 1732, 1294, 1196 – MS ((–)ESI, DCM/MeOH + 10 mmol/L NH<sub>4</sub>Ac): *m/z* (%) = 685 (100) [M – H<sup>+</sup>]. – HRMS (C<sub>32</sub>H<sub>51</sub>N<sub>2</sub>O<sub>14</sub><sup>+</sup>): calcd. 687.3339, found 687.3340  $\pm$  0.64 ppm.



### *H-His-Lys-OMe · 3 TFA*

H-Lys(Boc)-OMe·HCl (0.25 g, 0.8 mmol) was dissolved in DCM (15 mL) and DIPEA (0.43 mL, 2.5 mmol) added under nitrogen atmosphere. Boc-His(Boc)-OH-dicyclohexylamine (0.49 g, 0.9 mmol), EDC (0.18 mL, 1.0 mol) and HOBt (0.14 g, 1.0 mmol) were added and the reaction was monitored by TLC (EtOAc). After 12 h the solution was mixed with water (15 mL), diluted with DCM (20 mL) and extracted twice with brine (20 mL). The combined organic layers were dried over Na<sub>2</sub>SO<sub>4</sub> and the solvent evaporated. The crude product was purified using column chromatography on silica gel (EtOAc, *R<sub>f</sub>* = 0.4) resulting in a colourless solid. The protected dipeptide was dissolved in a small amount of DCM and mixed with TFA (1.46 mL, 18.9 mmol). After 12 h the mixture was evaporated to dryness and completion of the reaction controlled by <sup>1</sup>H-NMR. The triflate salt was redissolved in water, washed with DCM and lyophilised. H-His-Lys-OMe·3TFA (0.29 g, 0.5 mmol, 58 %) is a colourless, hygroscopic solid.

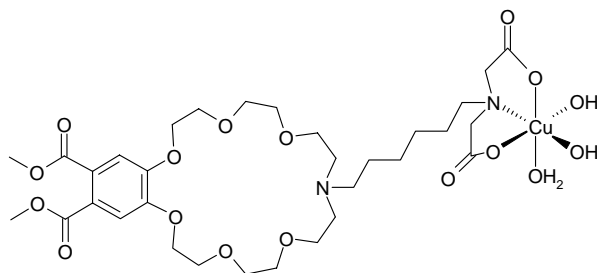
mp 62–63 °C. – <sup>1</sup>H-NMR (600 MHz; [D<sub>6</sub>]-DMSO): δ = 1.16–1.18 (m, 2 H, COSY: H(3)), 1.34–1.59 (m, 2 H, HSQC: H(2)), 1.60–1.76 (m, 2 H, COSY: H(4)), 2.76 (m, 2 H, COSY: H(1)), 3.19 (2 x dd, <sup>2</sup>*J* = 15.4 Hz, <sup>3</sup>*J* = 7.2 Hz, 2 H, COSY: H(10)), 3.62 (s, 3 H, HSQC: H(7)), 4.22 (t, <sup>3</sup>*J* = 6.9 Hz, 1 H, COSY: H(9)), 4.29 (dt, <sup>3</sup>*J* = 5.4, 7.8 Hz, 1 H, COSY: H(5)), 7.41 (s, 1 H, HMBC: H(12)), 7.90 (bs, 3 H, HMBC: H<sub>A</sub>), 8.11–8.80 (bs, 1 H, HMBC: H<sub>D</sub>), 8.92 (d, <sup>3</sup>*J* = 7.3 Hz, 1 H, HMBC: H<sub>B</sub>), 8.98 (s, 1 H, HMBC: H(13)), 13.50–15.45 ppm (bs, 2 H, H<sub>C</sub>). – <sup>13</sup>C-NMR (150 MHz; [D<sub>6</sub>]-DMSO; HSQC, HMQC): δ = 22.0 (–, C(3)), 26.4 (–, C(10)), 26.5 (–, C(2)), 30.4 (–, C(4)), 38.4 (–, C(1)), 51.2 (+, C(9)), 52.0 (+, C(5)), 52.1 (+, C(7)), 117.8 (+, C(12)), 127.2 (C<sub>quat</sub>, C(11)), 134.3 (+, C(13)), 167.5 (C<sub>quat</sub>, C(8)), 171.7 ppm (C<sub>quat</sub>, C(6)) [TFA signals are not listed]. – IR (KBr) [cm<sup>–1</sup>]:  $\tilde{\nu}$  = 3431, 3123, 3049 2965, 1676, 1204, 1135, 723. – MS (ESI, H<sub>2</sub>O/MeOH + 10 mmol/L NH<sub>4</sub>Ac): *m/z* (%) = 298 (100) [MH<sup>+</sup>], 170 (10) [M + 2H<sup>+</sup> + MeCN]. – Elemental analysis calcd. (%) for C<sub>19</sub>H<sub>26</sub>N<sub>5</sub>O<sub>9</sub>F<sub>9</sub> (639.16) + H<sub>2</sub>O: C 34.71, H 4.29, N 10.65; found: C 34.17, H 4.28, N 10.55.



### *Ac-His-Lys-OMe · 2 TFA*

H-Lys(Boc)-OMe·HCl (0.25 g, 0.8 mmol) was dissolved in DCM (15 mL) and DIPEA (0.43 mL, 2.5 mmol) added under nitrogen atmosphere. Ac-His(1-Trt)-OH (0.4 g, 0.9 mmol), EDC (0.18 mL, 1.0 mol) and HOBt (0.14 g, 1.0 mmol) were added thereafter and the reaction was monitored by TLC (EtOAc). After 12 h the solution was mixed with water (15 mL), diluted with DCM (20 mL) and extracted twice with brine (20 mL). The combined organic layers were dried over Na<sub>2</sub>SO<sub>4</sub> and the solution evaporated. The crude product was purified using column chromatography on silica gel (EtOAc → EtOAc/MeOH = 1/1, R<sub>f</sub> (EtOAc) = 0.1) resulting in a colourless solid. The protected dipeptide was dissolved in a small amount of DCM and mixed with TFA (1.06 mL, 13.7 mmol). After 12 h the mixture was evaporated to dryness and completion of the reaction was controlled by <sup>1</sup>H-NMR. The triflate salt was redissolved in water, washed with DCM and lyophilised. Ac-His-Lys-OMe·2TFA (0.42 g, 0.7 mmol, 93 %) is a colourless, hygroscopic solid.

<sup>1</sup>H-NMR (600 MHz; [D<sub>6</sub>]-DMSO): δ = 1.28-1.41 (m, 2 H, COSY: H(3)), 1.45-1.58 (m, 2 H, HSQC: H(2)), 1.59-1.78 (m, 2 H, COSY: H(4)), 1.83 (s, 3 H, HSQC: H(15)), 2.70-2.82 (m, 2 H, COSY: H(1)), 2.85-3.11 (2 x dd, <sup>2</sup>J = 14.9 Hz, <sup>3</sup>J = 5.5 Hz, 2 H, COSY: H(10)), 3.62 (s, 3 H, HSQC: H(7)), 4.17-4.28 (m, 1 H, COSY: H(9)), 4.57-4.67 (m, 1 H, COSY: H(5)), 7.31 (s, 1 H, HMBC: H(12)), 7.81 (bs, 3 H, HMBC: H<sub>A</sub>), 8.23 (d, <sup>3</sup>J = 7.9 Hz, 1 H, HMBC: H<sub>D</sub>) 8.41 (d, <sup>3</sup>J = 7.5 Hz, 1 H, HMBC: H<sub>B</sub>), 8.94-8.98 (m, 1 H, HMBC: H(13)), 14.01-14.73 (bs, 2 H, H<sub>C</sub>). – <sup>13</sup>C-NMR (150 MHz; [D<sub>6</sub>]-DMSO; HSQC, HMQC): δ = 22.1 (–, C(3)), 22.4 (+, C(15)), 26.3 (–, C(2)), 27.0 (–, C(10)), 30.0 (–, C(4)), 38.4 (–, C(1)), 51.3 (+, C(5)), 51.7 (+, C(9)), 51.8 (+, C(7)), 116.6 (+, C(12)), 129.3 (C<sub>quat</sub>, C(11)), 133.6 (+, C(13)), 169.4 (C<sub>quat</sub>, C(14)), 170.3 (C<sub>quat</sub>, C(8)), 172.1 (C<sub>quat</sub>, C(6)). – IR (KBr) [cm<sup>–1</sup>]:  $\tilde{\nu}$  = 3431, 3122, 3050 2965, 2913, 1676, 1204, 1130. – MS (ESI, H<sub>2</sub>O/MeCN): *m/z* (%) = 340 (100) [MH<sup>+</sup>].



[Cu(**146**)(H<sub>2</sub>O)<sub>3</sub>] (**147**)

To a solution of the diacid **146** (90 mg, 0.1 mmol) in water (5 mL), CuCl<sub>2</sub> (13 mg, 0.1 mmol) in MeOH (10 mL) was added. Stirring was continued at r.t. for 2 h. The solvent was evaporated and the residue dissolved in a small amount of water. MeOH was added until a precipitate had formed and the solid was removed by filtration. MeOH was evaporated and the crude product was recrystallised from methanol yielding compound **147** (73 mg, 0.09 mmol, 86 %) as a blue solid.

mp > 200 °C. – MS (ESI, MeOH + 10 mmol/L NH<sub>4</sub>Ac): *m/z* (%) = 847 (34) [MH<sup>+</sup> + 2 MeCN + H<sub>2</sub>O], 830 (50) [MH<sup>+</sup> + 2 MeCN], 825 (65) [MH<sup>+</sup> + H<sub>2</sub>O + HAc], 808 (35) [MH<sup>+</sup> + HAc], 748 (100) [MH<sup>+</sup>].

### Spectra and emission titration in methanol

Procedure:

The cuvette with 2.5 mL of receptor **147** in HEPES buffer was titrated stepwise with small amounts of the analyte solution.

Cary Eclipse Spectrometer

Spectrometer setup:

Excitation wavelength  $\lambda = 305$  nm

Detection wavelength  $\lambda = 377 - 380$  nm

Temperature: T = 298 K

Titration conditions:

Solvent: 50 mM HEPES buffer, pH 7.5,

Starting volume: 2.5 mL

*c* (receptor) = 5.04·10<sup>-5</sup> M

*c* (analyte) = 1.1 – 1.2·10<sup>-2</sup> M

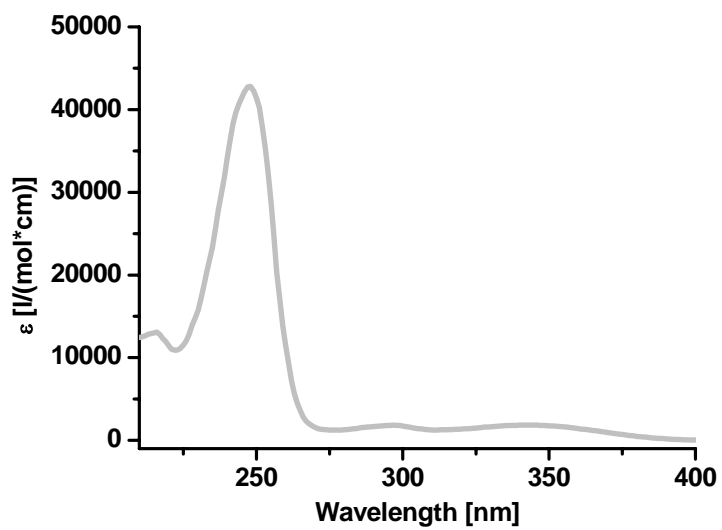


**Figure 110.** Absorption spectra of compound **148** in methanol.

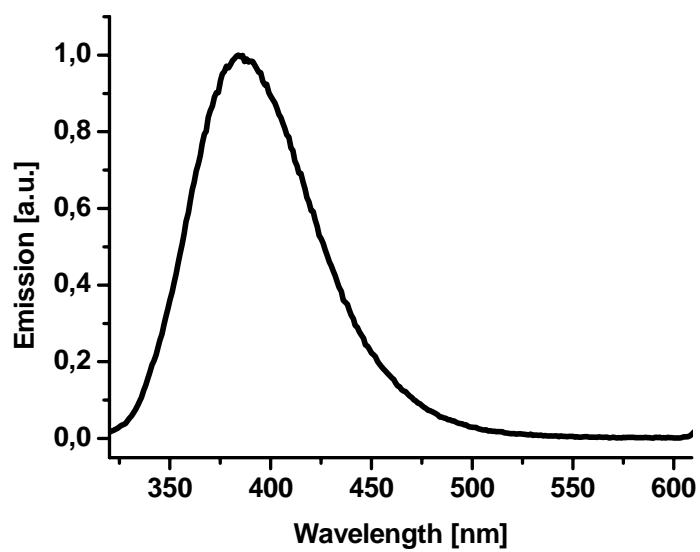


**Figure 111.** Emission spectra of compound **148** in methanol (excitation at 270 nm).

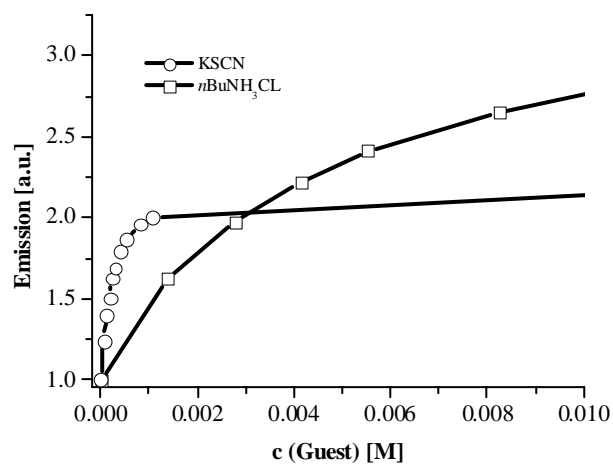


**Figure 112.** Change in emission intensity of compound **148** at 384 nm upon titration with KSCN or nBuNH<sub>3</sub>Cl in methanol.

#### Receptor **147** vs. H-His-Gly-Gly-OH

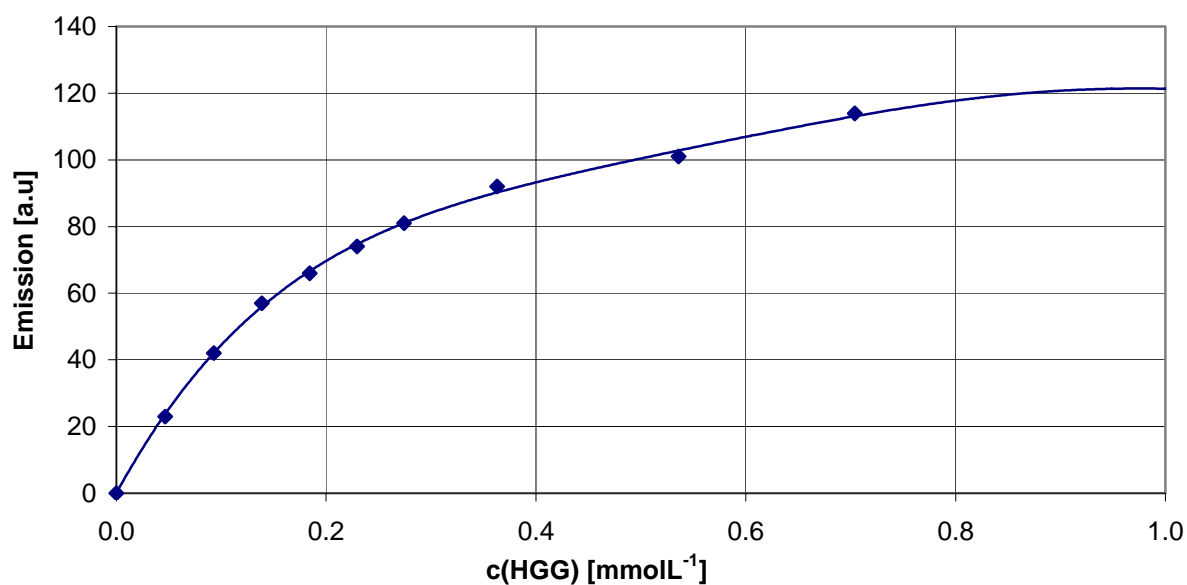


**Figure 113.** Fluorescence titration of **147** vs. H-His-Gly-Gly-OH in HEPES buffer ( $\log K = 3.7 \pm 0.05$ ).

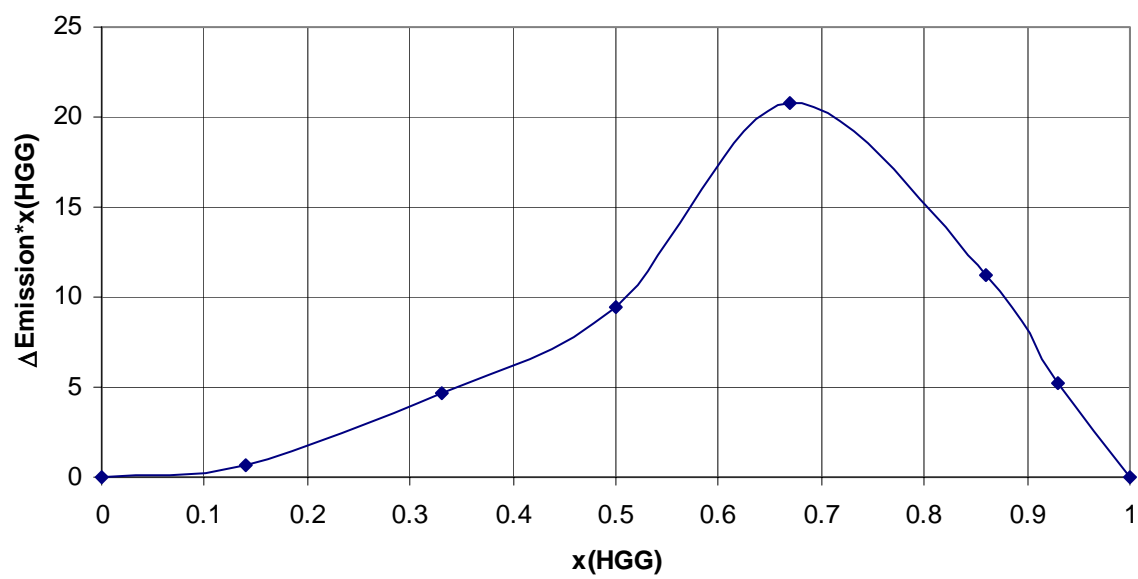


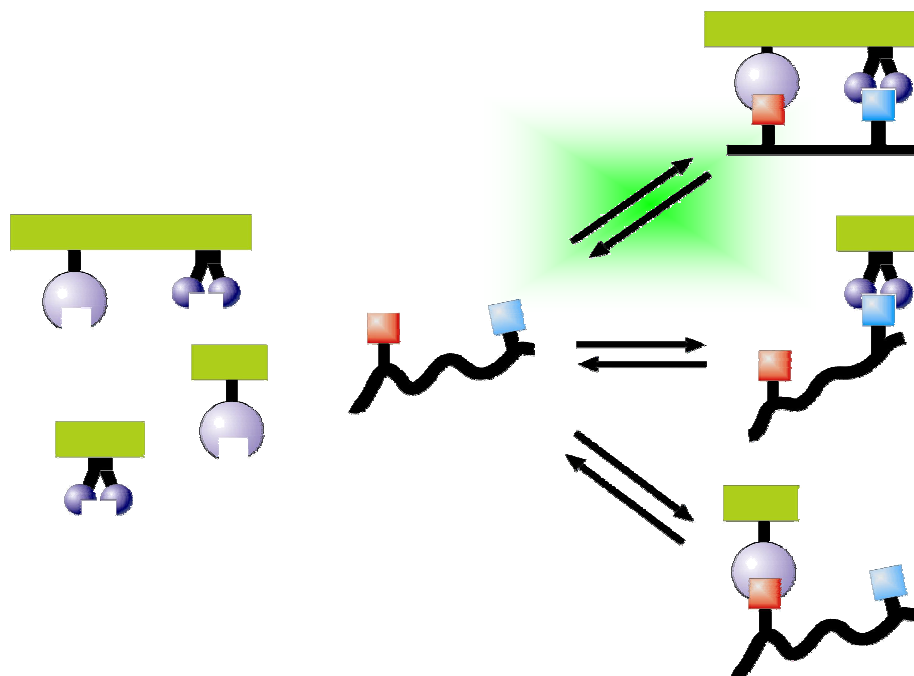
**Figure 114.** Job`s plot analysis of **147** - H-His-Gly-Gly-OH binding.

## 5. Receptor for Protein Surfaces with Affinity to Histidine and phosphorylated Amino acids

High binding constants under physiological conditions turn metal complexes into essential components of peptide receptor molecules (see previous chapters). The possibility to boost weaker molecule interactions (like hydrogen bonds) by metal complex support was demonstrated in chapter 3 and chapter 4. The maximal binding constant ( $K = 10^4 - 10^5 \text{ M}^{-1}$ ) reached by these polytopic receptors were equivalent with the binding constants of the corresponding pure metal complexes. The incorporation of several metal complexes in one receptor molecule might lead to increased binding affinities.

For this purpose a histidine recognition unit (🟡) is combined with a phosphate binder (🟢). The new receptor molecule (🟡🟢) which combines both affinities should bind in a superior way to a peptide (🟡🟢) containing phosphate (🟢) and histidine (🟡). As all binding events are reversible (scheme 52) a receptor mixture in the presence of this peptide should lead to the formation of one main assembly of peptide and receptor molecule.

**Scheme 52.** Schematic depiction of a binding experiment



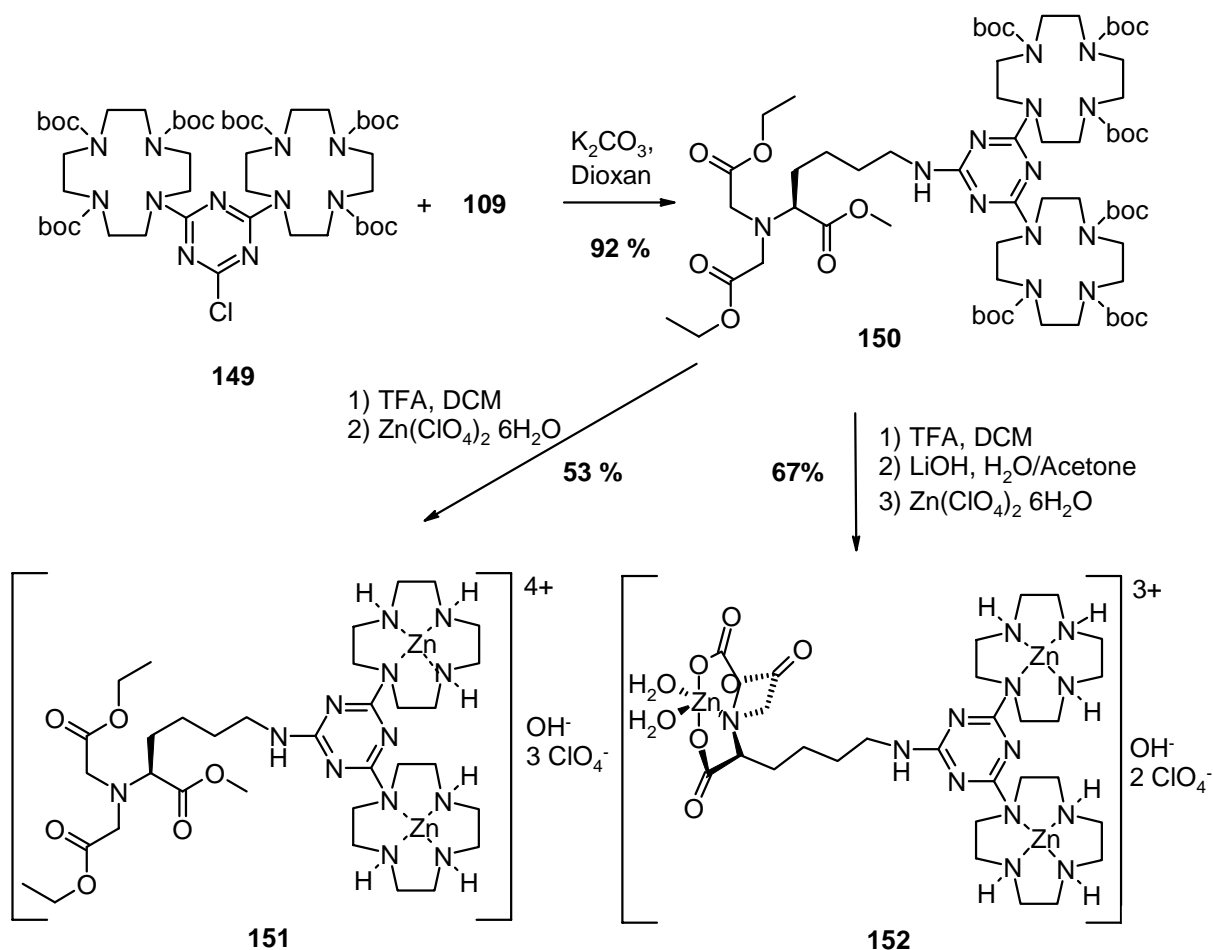
In a first synthesis the C-terminal NTA recognition unit **109** was linked with bis-cyclen receptor **149**.<sup>i</sup> Using a nucleophilic aromatic substitution reaction the cyclen functionalised

<sup>i</sup> Subat, M. PhD Thesis, University of Regensburg.



triazin was bound to the primary amine in good yields giving **150**. This Boc- and ester-protected precursor **150** was stepwise deprotected and used for metal complexations yielding the Zn(II)-complexes **151** and **152** in moderate yields.

**Scheme 53.** Synthesis of the Zn(II)-complexes **151** and **152**



The metal complexes **151** and **152** are presently used by Grauer<sup>ii</sup> to determine the binding ability to histidine and phosphorylated peptides.

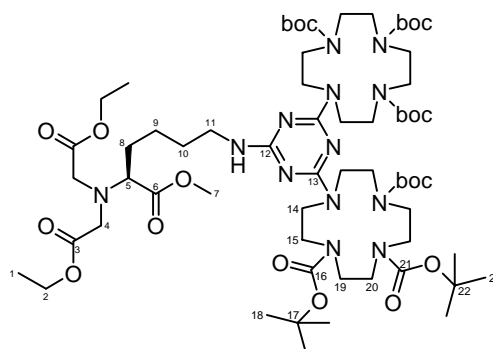
<sup>ii</sup> Grauer, A. Diploma Thesis, University of Regensburg, *ongoing*.

## 5.1 Experimental Part

### 5.1.1 Instruments and general techniques

See experimental section chapter 1 (page 131)

### 5.1.2 Synthesis

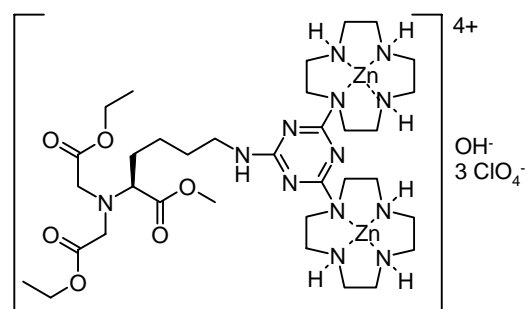


*Bis-(tri-Boc-cyc)-triazin-NTAL-OEt/Me (150):*

**149**<sup>iii</sup> (0.60 g, 0.57 mmol), **109** (0.20 g, 0.6 mmol) and K<sub>2</sub>CO<sub>3</sub> (1.44 g, 1.2 mmol) were dissolved in dioxan (20 mL). The mixture was heated to 95 °C and stirred for 3 days. The suspension was filtered and the filtrate concentrated under reduced pressure. The crude product was purified using column chromatography on silica gel (EtOAc, *R<sub>f</sub>* = 0.8) yielding **150** (0.52 mmol, 700 mg, 92 %) as a colourless solid.

mp 48-49 °C. – <sup>1</sup>H-NMR (600 MHz; CDCl<sub>3</sub>; COSY, HMBC, HSQC): δ = 1.25 (t, <sup>3</sup>*J* = 7.2 Hz, 6 H, H(1)), 1.28-1.51 (m, 56 H, H(9) + H(18) + H(23)), 1.52-1.54 (m, 2 H, H(11)), 1.66-1.73 (m, 2 H, H(8)), 3.33-3.59 (m, 35 H, H(10) + H(14) + H(15) + H(19) + H(20) + H(5)), 3.63 (d, <sup>3</sup>*J* = 4.8 Hz, 4 H, H(4)), 3.67 (s, 3 H, H(7)), 4.13 (q, <sup>3</sup>*J* = 7.1 Hz, 4 H, H(2)), 4.74 (bs, 1 H, NH). – <sup>13</sup>C-NMR (150 MHz; CDCl<sub>3</sub>; HMBC, HSQC): δ = 14.2 (+, 2 C, C(1)), 23.4 (–, C(9)), 28.5 (+, 18 C, C(18) + C(23)), 29.6 (–, C(11)), 30.3 (–, C(8)), 40.9 (–, C(10)), 49.2-51.3 (–, 16 C, C(14) + C(15) + C(19) + C(20)), 51.4 (+, C(7)), 52.8 (–, 2 C, C(4)), 60.3 (–, 2 C, C(2)), 64.8 (+, C(5)), 80.0 (C<sub>quat</sub>, 4 C, C(17)), 80.2 (C<sub>quat</sub>, 2 C, C(22)), 156.3 (C<sub>quat</sub>, 6 C, C(16) + C(21)), 164.7 (C<sub>quat</sub>, 2 C, C(13)), 168.0 (C<sub>quat</sub>, C(12)), 171.4 (C<sub>quat</sub>, 2 C, C(3)), 172.9 (C<sub>quat</sub>, C(6)). – IR (KBr) [cm<sup>–1</sup>]:  $\tilde{\nu}$  = 3341, 2980, 2940, 1741, 1687, 1165, 730. – MS (ESI, MeCN/MeOH): *m/z* (%) = 1353 (100) [MH<sup>+</sup>], 677 (32) [M+2H<sup>+</sup>], 649 (23) [M-C<sub>4</sub>H<sub>8</sub>+2H<sup>+</sup>], 627 (20) [M+2H<sup>+</sup>-Boc]. – C<sub>64</sub>H<sub>113</sub>N<sub>13</sub>O<sub>18</sub> (1351.80).

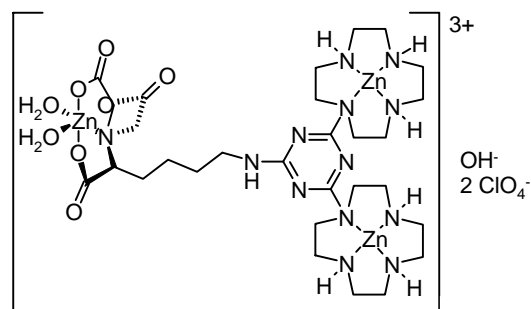
<sup>iii</sup> Subat, M. PhD Thesis, University of Regensburg.



$[Zn_2(\text{Bis-cyc-triazin-NTAL-OEt/Me})(OH)](ClO_4)_3$  (**151**):

**150** (0.13 g, 0.1 mmol) was dissolved in TFA (10 mL) and stirred at r.t.. The reaction progress was monitored by  $^1H$ -NMR. After all Boc protons disappeared the reaction mixture was evaporated. The obtained triflate was dissolved in water and freeze dried. The residue was redissolved in water (10 mL) and neutralised with  $NaHCO_3$  followed by the addition of  $Zn(ClO_4)_2 \cdot 6H_2O$  (75 mg, 0.2 mmol). The mixture was refluxed over night. Undissolved particles were filtered off and the filtrate freeze dried. Crystallisation in MeOH yielded **151** (0.08 mmol, 96 mg, 53 %) as a colourless solid.

mp > 200 °C. – IR (KBr)  $[cm^{-1}]$ :  $\tilde{\nu} = 3249, 3242, 2993, 2977, 2944, 1732, 1714, 1687, 1570, 1084, 623$ . – MS (ESI, MeCN/ $H_2O$ ):  $m/z$  (%) = 485 (100)  $[K^{4+} + OH^- + ClO_4^-]$ . –  $C_{34}Cl_3H_{66}N_{13}O_{19}Zn_2$  (1193.22).



$[Zn_2(\text{Bis-cyc-triazin-NTAL})(OH)(H_2O)_2](ClO_4)_2$  (**152**):

**150** (0.25 g, 0.18 mmol) was dissolved in TFA (10 mL) and stirred at r.t.. The reaction progress was monitored by  $^1H$ -NMR. After all Boc protons disappeared the reaction mixture was evaporated. The obtained triflate was dissolved in water and freeze dried. The residue was redissolved in water (10 mL) and neutralised with LiOH. To this neutral solution LiOH· $H_2O$  (25 mg, 0.6 mmol) was added and the mixture refluxed for 2 d. The mixture was freeze dried, redissolved in water (10 mL) and  $Zn(ClO_4)_2 \cdot 6H_2O$  (0.22 g,

0.6 mmol) was added. The mixture was refluxed over night. Undissolved particles were filtered off and the filtrate freeze dried. Crystallisation in MeOH yielded **152** (0.12 mmol, 135 mg, 67 %) as a colourless solid.

mp > 200 °C. – IR (KBr) [ $\text{cm}^{-1}$ ]:  $\tilde{\nu}$  = 3249, 3242, 2993, 2977, 2944, 1687, 1570, 1084, 623. – MS (ESI, MeCN/H<sub>2</sub>O):  $m/z$  (%) = 443 (100) [ $\text{K}^{3+} + \text{OH}^-$ ]. – C<sub>29</sub>Cl<sub>2</sub>H<sub>57</sub>N<sub>13</sub>O<sub>17</sub>Zn<sub>3</sub> (1121.12).

## C. Appendix

### Abbreviations

Ar	Aryl
BOC	<i>tert</i> -Butoxycarbonyl
BPA	Bis-(2-picolyl)-amine
Bzl	Benzyl
c	Concentration
CI	Chemical Ionisation
d	Day(s)
DCM	Dichloromethane
DIPEA	Diisopropyl-ethyl-amine
DME	1,2-Dimethoxyethane
DMF	Dimethylformamide
DSMO	Dimethylsulfoxide
EDC	<i>N</i> -(3-Dimethylaminopropyl)- <i>N'</i> -ethyl-carbodiimide
EI	Electronic Ionisation
EtOAc	Ethylacetat
EtOH	Ethanol
ESI	Electronspray Ionisation
Et	Ethyl
FAB	Fast-Atom Bombardement
FT-IR	Fourier Transformation Infrared
h	Hour(s)
HEPES	<i>N</i> -2-Hydroxyethylpiperazine- <i>N'</i> -2-ethansulfonic acid
HMPT	Hexamethyl phosphor acid triamide
HOBt	1-Hydroxybenzotriazole
HRMS	High Resolution Mass Spectroscopy
IDA	Iminodiacetic acid
IR	Infrared Spectroscopy
<i>J</i>	Coupling Constant
K	Molecule cation
Me	Methyl

MeOH	Methanol
min	minutes
MOPAS	Methoxy-pyrrol-amino acid
mp	Melting Point
MS	Mass Spectroscopy
NMR	Nuclear Magnetic Resonanz Spectroscopy
NTA	Nitrilotriacetic acid
PE	Petrol Ether (Hexanes)
Ph	Phenyl
Py	Pyridine
PyBOP	(Benzotriazol-1-yloxy)-tripyrrolidinophosphonium-hexfluorophosphate
$R_f$	Retention Factor
r.t.	Room Temperatur
TEAOH	Tetraethylammonium hydroxide
TEAP	Tetraethylammonium perchloride
TFA	Trifluoroacetic acid
THF	Tetrahydrofuran
TLC	Thin Layer Chromatography
Tos	<i>p</i> -Toluol-sulfonyl
x	Mole Fraction
Z	Benzyloxycarbonyl

## Publications

- Synthesis of Chiral Amino Acids with Metal Ion Chelating Side Chains from L-Serine using Negishi Cross-Coupling Reaction  
Kruppa, M.; Imperato, G.; König, B. *Adv. Cat. Synth.* **2005**, *in preparation*.
- Screening of Metal Complex-Amino Acid Side Chain Interactions  
Kruppa, M.; Frank, D.; Leffler-Schuster, H.; König, B. *Inorg. Chem.* **2005**, *submitted*.
- Reversible Coordinative Bonds in Molecular Recognition  
Kruppa, M.; Walenzyk, T.; König, B. *Chem. Rev.* **2005**, *under revision*.
- Peptide Recognition by a Combination of Intermolecular Coordinative Interactions and Intramolecular Hydrogen Bonds  
Kruppa, M.; Bonauer, C.; Michlova, V.; König, B. *J. Org. Chem.* **2005**, *Web Release Date: 25.05.2005..*
- A Luminescent Receptor with Affinity for N-Terminal Histidine in Peptides in Aqueous Solution  
Kruppa, M.; Mandl, C.; Miltschitzky, S.; König, B. *J. Am. Chem. Soc.* **2005**, *127*, 3362.
- Mol4D – Moleküle in der 4. Dimension, Engel, E.; Kruppa, M.; König, B. *Angew. Chem.* **2004**, *116*, 6744.
- Mol4D – Molecules in the 4<sup>th</sup> Dimension, Engel, E.; Kruppa, M.; König, B. *Angew. Chem. Int. Ed.* **2004**, *43*, 6582.
- CombiChem and Solid Phase Synthesis teaching lab course, K. Agoston, A. Geyer, B. König, M. Kruppa, **2004**  
available under [http://va.gdch.de/mv\\_zam/mv\\_online.asp](http://va.gdch.de/mv_zam/mv_online.asp)
- Gastdozenten als Experten, K. Agoston, C. Hirtreiter, M. Kruppa *Nachrichten aus der Chemie* **2003**, *9*, 1012.
- NADH Model Systems Functionalised with Zn(II)-Cyclen as Flavin Binding Site-Structure Dependence of the Redox Reaction within Reversible Aggregates  
Reichenbach-Klinke, R.; Kruppa, M.; König, B. *J. Am. Chem. Soc.* **2002**, *124*, 12999.

## Poster Presentations

- Kruppa, M.; Bonauer, C.; Mandl, C.; König, B. “Synthetic Receptors – Making Intermolecular Processes Intramolecular”, *IASOC`04 (Ischia Advanced School of Organic Chemistry)*, Ischia, Italy, 09/**2004**
- Kruppa, M.; Bonauer, C.; Mandl, C.; König, B. “Synthetic Receptors – Making Intermolecular Processes Intramolecular”, *ISBOMC`04 (International Symposium on Bioorganometallic Chemistry)*, Zurich, Switzerland, 07/**2004**
- Kruppa, M.; Bonauer, C.; Mandl, C.; König, B. “Synthetic Receptors – Making Intermolecular Processes Intramolecular”, *Reaction Mechanism VII*, Dublin Ireland, 07/**2004**
- Kruppa, M.; König, B. “Coordinative peptide Recognition – Design of modular connectable Receptor Units”, *Synthetic Receptors*, Lisbon, Portugal, 10/**2003**
- Kruppa, M.; König, B. “Coordinative peptide Recognition – Design of modular connectable Receptor Units”, *GDCh Annual Meeting*, Munich, Germany, 10/**2003**
- Subat, M.; Kruppa, M.; König, B. “Palladium-Catalysed Synthesis of Aryl-Bridged Bis-Tetraazamacrocycles”, *Molecular Catalysis*, Heidelberg, Germany, 06/**2003**

## Oral Presentation

- Kruppa, M. “Design of modular connectable Receptor Molecules for Molecular Recognition of Peptide Side Chains”, *Symposium of Molecular Recognition*, Prag, Czech Republic, 05/**2003**



## Curriculum Vitae

Name: Michael Christian Kruppa  
Date of birth: 17.02.1977  
Place of birth: Erlangen, Germany  
Nationality: German

### Education

09/1983 – 07/1984	Volksschule Laufach
09/1984 – 07/1986	Volksschule Plößberg
09/1987 – 06/1996	Gymnasium Neustadt an der Waldnaab
07/1996 – 04/1997	Military Service
11/1997 – 09/2002	Chemistry Studies, University of Regensburg
01/2002 – 09/2002	Diploma Thesis in organic Chemistry, University of Regensburg, Prof. Dr. B. König
10/2002 – 06/2005	PhD work in the research group of Prof. Dr. B. König
since 07/2003	Member of the Graduierten Kolleg GRK 760 Medicinal Chemistry

### Research Experience

01/2005 – 03/2005	Research collaboration with Prof. Dr. Dawei Ma, Shanghai Institute for Organic Chemistry, China <i>Project:</i> Natural Product Synthesis (Depsipeptides)
07/2001 – 08/2001	Research collaboration with Prof. Dr. Luisa DeCola, University of Amsterdam, Netherlands <i>Project:</i> Pico- and Femto-second Laser- Spectroscopy of Zn <sup>II</sup> -Cyclen compounds
02/2001 – 04/2001	Internship, Bayer AG Central Research (Life Science), Leverkusen, Germany <i>Project:</i> Building Block Synthesis for Combinatorial Chemistry

07/2000 – 08/2000	<p>Internship, SEKA (paper mill), Dalaman, Turkey</p> <p><i>Project:</i> Paper and Water Quality Control</p>
02/2000 – 03/2000	<p>Practical course in Medicinal Biochemistry, Regensburg University Hospital, Germany</p> <p><i>Project:</i> Basics of Biochemical Working Techniques</p>

### **Scholarships/Awards**

01/2005 – 03/2005	EU Scholarship for a Research Period in Shanghai
09/2004	Marie Curie Scholarship for Young Researchers
07/2004	Poster Award, Reaction Mechanism VII, Dublin
08/2003 – 08/2005	Graduiertenförderung des Freistaat Bayerns

## Summary

Focusing on interactions between Lewis acidic metal complexes and Lewis basic surfaces of proteins, I was able to outline the power of this concept by several projects.

An initial screening experiment in chapter 1 was used to find suitable metal complex – peptide side chain interactions. Based on potentiometric titration data it was possible to prove substrate-metal-complex interactions in aqueous solution. In addition to already known interactions of M(II)-IDA/M(II)-NTA and imidazole binding of imidazole to M(II)-cyclen was discovered. Cd(II)-cyclen showed imidazole binding and Zn(II)-cyclen binds to imidazole and phosphate. The newly identified metal complex to amino acid side chain functional group interactions, and the excluded interactions, may help to develop and optimise new IMAC polymers for protein purification.

To simplify the synthesis of a desired peptide receptor, a building block receptor synthesis was developed in chapter 2. The synthesis of C- and N-terminal receptor building blocks could be achieved by simple  $S_N2$  reactions of mono protected diamines and amino acids. The ligation of these building blocks was optimised using the active ester formed out of EDC/HOBt. Furthermore the synthesis of bidentate recognition units possessing an additional carboxylate for receptor ligation yielded the new receptor precursors **117**, **118**, **119** and **120**. The Zn(II) complex **122** synthesised by Boc-deprotection of **120** showed high affinity towards phenylphosphate which was examined by  $^{31}\text{P}$ -NMR and microcalorimetric titration.

In a first attempt a solid phase receptor synthesis was performed using a safety-catch resin. The resulting Ni(II)-NTA complex showed good affinities towards a pentapeptide containing a terminal histidine.

To create binding sites in the side chains of natural amino acids the functionalisation of tyrosine was used for cyclen ligation. The scope of the Negishi cross coupling reaction of organozinc compounds derived from chiral amino acids was extended to electron rich iodoanilines as coupling reagents. This now allows the direct modification of serine into phenylalanine derivatives bearing metal ion chelating ligand in their side chain.

The experiments in chapter 3 demonstrated that it is possible to restrict the conformation of a small flexible pentapeptide in DMSO solution by combining a Zn-NTA tether with a

heterocyclic peptide  $\beta$ -sheet binder. Intermolecular interactions of the MOPAS units with the pentapeptide in DMSO would be too weak to induce a conformational preference. The principle of “two-prong” binders is applicable to other peptide receptors, which suffer from competing solvent interactions. Exchanging Zn(II) in **142** by Cu(II) or Ni(II) leads to peptide-binding compounds with an affinity to H<sub>2</sub>N-His-Leu-Leu-Val-Phe-OMe in the lower micromolar range under aqueous physiological conditions.

Chapter 4 showed that the combination of an imidazole coordinating metal complex with a luminescent ammonium-binding crown ether resulted in a simple synthetic receptor with high affinity in buffered water for molecules bearing *both* functional groups. The emission response was triggered by the weak ammonium ion binding which only becomes possible intramolecularly within the assembly. The presence of just an ammonium group, even in large excess, does not trigger an optical output.

The final project, discussed in chapter 5, combined two different metal complexes within one receptor molecule. Targeting a terminal histidine and a phosphorylated serine or threonine, these receptors should be able to bind phosphorylated peptides containing terminal histidines with very high affinities.